HIGHWAY RESEARCH RECORD

Number 407

Pavement Technology

15 reports
prepared for the
51st Annual Meeting

Subject Areas

25 Pavement Design
26 Pavement Performance
62 Foundations (Soils)
63 Mechanics (Earth Mass)

HIGHWAY RESEARCH BOARD
DIVISION OF ENGINEERING NATIONAL RESEARCH COUNCIL
NATIONAL ACADEMY OF SCIENCES—NATIONAL ACADEMY OF ENGINEERING

Washington, D.C. 1972

NOTICE

The studies reported herein were not undertaken under the aegis of the National Academy of Sciences or the National Research Council. The papers report research work of the authors done at the institution named by the authors. The papers were offered to the Highway Research Board of the National Research Council for publication and are published herein in the interest of the dissemination of information from research, one of the major functions of the HRB.

Before publication, each paper was reviewed by members of the HRB committee named as its sponsor and was accepted as objective, useful, and suitable for publication by NRC. The members of the committee were selected for their individual scholarly competence and judgment, with due consideration for the balance and breadth of disciplines. Responsibility for the publication of these reports rests with the sponsoring committee; however, the opinions and conclusions expressed in the reports are those of the individual authors and not necessarily those of the sponsoring committee, the HRB, or the NRC.

Although these reports are not submitted for approval to the Academy membership or to the Council of the Academy, each report is reviewed and processed according to procedures established and monitored by the Academy's Report Review Committee.

ISBN 0-309-02079-4

Price: $6.00

Available from

Highway Research Board
National Academy of Sciences
2101 Constitution Avenue, N.W.
Washington, D.C. 20418

Contents

FOREWORD

The high cost of constructing and maintaining pavement systems makes it imperative that pavement design processes include a wide range of considerations in addition to initial cost and structural adequacy. The 15 papers in this RECORD cover field performance and evaluation, structural analysis, and design and maintenance strategies. They will be of interest to practicing engineers, researchers, and those involved in pavement investment decisions and pavement management.

Faulting of portland cement concrete pavements has long been of concern to the highway engineer. Spellman et al. report on a field investigation of the causes of faulting, including performance of experimental shoulder features and other design features that could have an effect on faulting. Reported also is a laboratory study that may lead to slip-form placing of lean concrete bases.

An analytical study by Abou-Ayyash et al. of the problem of transverse cracking in continuously reinforced concrete pavement showed that a significant drop in bending rigidity is encountered at crack locations. A procedure is outlined to simulate the effect and to specify the slab portion affected by the discontinuity.

The paper by Deen et al. presents a theoretical procedure based on multilayered elastic theory for designing flexible pavements. The use of a computer program permitted an extensive investigation of the effects of soil support properties, strength characteristics of the materials used, and component thickness. Curves describing the relations of various parameters are presented.

Han et al. describe a method of establishing the elastic moduli of individual pavement components in a soil-pavement system using plate load test data. Component moduli are determined by using both elastic theory and an axisymmetric finite-element approach. Field data were analyzed by using both methods, and the results are presented and compared and the influence of plate size and component thickness on the computed moduli discussed.

The object of the paper by Hajek and Haas was to develop a relation between field low-temperature performance of asphalt pavements and variables of significance for which data are commonly recorded by highway agencies. A mathematical model is presented that is capable of predicting cracking at various ages in the pavement life.

The design of flexible pavements by linear-elastic theory may be somewhat simplified by the use of existing tabulated results. However, a lengthy interpolation procedure is required to obtain results for variables other than those tabulated. Brown presents a computer program to carry out interpolation calculations on the three-layered system results tabulated by Jones in 1962. The program is considered to be more convenient than either the tables or the complex multilayer computer programs now available.

A proposed method for flexible pavement design for Minnesota requires the calculation of summation of equivalent 18,000-lb axle loads during a design period. Skok and Root report on the development of a computer program to calculate these equivalent loads by using total traffic volumes, vehicle-type distribution, and axle-load distribution data. The computer program is now usable for flexible pavement design.

The paper by Rao and Harnage presents a vibratory nondestructive evaluation procedure for rigid pavements based on a comparison between a measured deflection field around a loaded plate and a predicted deflection field computed by a finite-element program that uses elastic properties of layers. Methods are presented to correlate the results, and further studies are suggested to make the evaluation procedure a useful tool for solving practical problems.

A technique is described by Moore and Swift for observing the displacement vector field of motion of the points within the body of a pavement structure under the influence of the cyclic loading of a Dynaflect. The displacement fields are shown to have considerable similarity to fields computed for statically loaded, layered elastic structures.

This leads the authors to conclude that the development of a useful and practical mathematical model representing the displacement vector throughout a pavement structure should be possible.

In the paper by Pretorius and Monismith, an attempt is made to predict the formation and development of fatigue cracks in asphalt pavements with soil-cement bases. Pavement sections with transverse shrinkage cracks are analyzed by using the finite-element approach, and it is shown how load cracks propagate from shrinkage cracks. The variables that produce the crack pattern and rate of crack propagation are discussed, and these crack patterns are substantiated by field observations.

Fremond presents a theory to calculate stresses and deflections of concrete slabs resting on an elastic-layered system without making use of Winkler's hypothesis. Stresses and deflections are caused by static forces and temperature variations that cause sufficient warping so that the slab is only partially supported on its foundation. Numerical examples are presented and compared with experimental results.

Three papers are concerned with the systematic analysis of highway pavement systems. The paper by Kher et al. describes the equations and methods of solution that are required to perform the system analysis for rigid pavement systems. A computer program is presented to solve the mathematical models, which include a comprehensive economic analysis of various phases of design. Darter et al. report on a trial implementation of a flexible pavement design system. The paper describes how the uncertainty of estimation of variables, such as traffic or the highly variable deflections along the pavement, can be considered in a comprehensive design procedure to make it possible to determine design reliability. Haas et al. present the initial planning and development of a feedback data system for the systematic collection, storage, and retrieval of data essential to pavement performance evaluation. This activity is considered vital to the successful improvement and updating of any working system of pavement design and management.

One of the most important considerations in the management of a highway system is the cost of constructing and maintaining highway pavements to minimum desirable standards of service. Phang and Slocum use the present value of total costs during an analysis period as the means for cost comparisons of alternate flexible pavement design and maintenance strategies. The authors conclude that this approach offers a means of rationalizing flexible pavement design policies and a framework on which to base effective long-term planning and programming.

FAULTING OF PORTLAND CEMENT CONCRETE PAVEMENTS

D. L. Spellman, J. H. Woodstrom, and B. F. Neal, California Division of Highways

The findings from a previous field investigation of the causes of faulting of portland cement concrete pavements are summarized, and possible corrections are discussed. Details are given of a number of experimental shoulder features that have been incorporated into construction projects. Also reported is a laboratory study of lean concrete base (wet-lean cement-treated base). This material could be placed with a slip-form paver using internal vibration. Advantages would be the elimination of trimming of cement-treated bases and a superior abrasion resistance. Other experimental construction and design features that could have an effect on faulting are briefly covered.

•THE term faulting refers to the vertical displacement of concrete paving slabs at joints. As faulting progresses, riding quality is adversely affected, and cracking of the slabs may follow. Because "ride" is influenced by several factors, including vehicle wheelbase, suspension, and weight, there is some disagreement on the degree of faulting that seriously affects ridability. On a moderately faulted pavement (e.g., 0.12 to 0.25 in.), some vehicles may not be affected, but drivers of trucks and a number of the lighter-weight cars may feel considerable discomfort.

"Pumping" or "blowing" has long been considered to be associated with faulting. In 1946 California adopted the cement-treated base (CTB) for use under portland cement concrete (PCC) pavements. This greatly reduced pumping at joints, but it was not until about 1960, when the CTB was widened 1 ft on each side of the pavement, that edge pumping was virtually eliminated. Very little evidence of pumping is now seen, but some faulting is still occurring. In past years, faulting did not appear to be serious until pavements were about 12 to 15 years of age. More recently, a few projects were found to develop moderate faulting within 5 years after construction.

A limited statewide faulting survey of PCC pavements constructed since 1960 was made in early 1968. The survey consisted of selecting random locations on each project and measuring the vertical displacement, if any, at approximately ten consecutive joints. These are undoweled joints either at standard 15-ft spacing or at our current spacing of 13, 19, 18, and 12 ft. Because of traffic conditions in urban areas, measurements were made only on rural highways, although many of the urban freeways were driven and many conditions were observed.

Pavements in all areas of the state were found to be about equally subject to faulting. Generally, only the outside or truck-lane joints are faulted, with the greater magnitude at the outer edge and a lesser amount at the inner edge. There were a few exceptions noted, especially near urban areas where there are three or more lanes in each direction and a heavy concentration of truck traffic in all lanes. It was also noted that there was usually less faulting in urban areas. This may be attributable to the fact that better drainage is provided by curbs and gutters and more paved areas, thus decreasing the chance of water getting under the pavement.

Of the projects surveyed, 85 were in the age range of 3 to 8 years. Of these, 12 had experienced some faulting greater than 0.10 in., and four of the projects had some joints that were faulted 0.15 in. or more. It is reasonable to assume that faulting will continue to increase on these projects. To check on the progression of faulting and the

Sponsored by Committee on Rigid Pavement Design.

effect of seasonal changes, we established test sections throughout the state. Both new and old pavements were selected in areas that include the coastal, valley, mountain, and desert regions of California, and measurements are being made at 3- to 4-month intervals.

In 1968 and 1969, field investigations were carried out to determine the cause (or causes) of the faulting observed. The research was done with the cooperation of the Federal Highway Administration and the assistance of the Portland Cement Association in the form of manpower and specialized equipment. More detailed information on the 1968-69 investigation is given elsewhere (1).

A total of 14 openings were made at pavement joints in three different geographical regions: valley, coastal, and mountain. Ten of the joints were faulted in amounts varying from 0.10 to 0.30 in. At each site, a section of concrete 3 ft wide and approximately 3 ft on either side of the joint was removed. At each faulted joint, a buildup of granular material was found under the approach slab and, in some cases, under the leave slab as well, though to a lesser degree. ("Approach" and "leave" refer to the slabs on either side of transverse joints. If traffic is considered as moving from left to right, the approach slab is on the left and the leave slab is on the right). The buildup differential was approximately equal to the amount of the fault. There was no evident settlement or faulting of the cement-treated base.

At several locations, tracer sands were placed under slabs near the joints and under the shoulder pavement prior to removal of the 3- by 6-ft sections. Upon exposure, definite evidence of strong water action was found under the leave slab but less action under the approach slab. Small channels caused by rapid water movement were evident under the leave slab at some sites. At one location, there were indications that the water may have moved in a circular path or at least involved strong movement in a direction transverse to the centerline of the pavement in addition to longitudinal movement.

Various tests were made on the pavements and construction materials at the sites being investigated. These included strains, deflections, load transfer effectiveness across joints, joint openings and movements due to temperature changes, slab curl, compressive strength, and petrographic and chemical tests. Many of the test results have not been of particular value in determining the cause of faulting. By performing petrographic and chemical tests, however, the source of the buildup at two sites was identified. At one site, the source was the cement-treated base; at the other, it was the shoulder material. The shoulder is also suspected of being the source of the buildup at a third location. Unfortunately, on most of the projects investigated, the construction material used in the base and the shoulders was from the same source or was of similar appearance and composition; therefore, the source of the buildup could not easily be identified. The relatively high cement content (based on calcium oxide determinations) of the buildup material at most sites strongly suggests that the CTB is a major contributing source. A small amount of the material may also come through the joint from the pavement surface and possibly some from the joint interface due to the grinding action caused by slab movements.

Abrasion of the lower surface of the concrete slab is not considered a source of the buildup because in most instances the asphaltic curing seal was still intact on the slab bottom.

The effectiveness of load transfer across the undoweled transverse joints was found to be highly variable with changes in pavement temperature because of joint interlock. This indicates that, when the pavement is cooler such as in the winter months, the slabs are subject to more deflection from heavy wheel loads. Conditions that contribute to slab curl also result in higher deflections under loads.

When free water is available beneath the slabs in the vicinity of the joints, the water may be repeatedly moved in all directions under the downward deflection of the slabs caused by moving loads. As a load approaches a joint, water is moved in the leave direction relatively slowly, accumulating under the leave slab. Some water may also be forced into the shoulder area. As the load crosses the joint, there is a sudden rebound of the approach side of the joint creating suction and a sudden depression of the leave side of the joint creating pressure, which impart to the accumulated water great

force and, therefore, velocity in the direction of the approach side. As the wheel load continues past the joint, the water slowly returns to the leave side. The net effect is a series of low-velocity movements of water in the leave direction and a series of high-velocity water movements back toward the approach slab. Water in the shoulder may also reenter the space beneath the slabs. The high-velocity water movements would readily carry any available loose material backward, tending to deposit particles under the approach slab. This action, repeated over a period of time, eventually causes a buildup under the approach slab and thus creates a "faulted" joint.

The following conclusions were made:

1. Faulting of PCC pavement joints is caused by an accumulation or buildup of loose material under the slabs near the joints. This accumulation may occur only under the approach slab, or it may be a differential buildup under both slabs with the thicker layer under the approach side.
2. The buildup is caused by violent water action on available loose or erodible materials that are beneath or adjacent to the slabs. The water is moved backward (and probably transversely) by the fast depression of the curled or warped slabs under heavy wheel loads and by the suction caused by the release of load on the approach slab, which erodes and transports any loose material.
3. The major sources of the buildup are the untreated shoulder material and the surface layer of the cement-treated base. Minor amounts may come from abrasion of the concrete joint interface and from material on the pavement surface moving downward through the joints.

POSSIBLE SOLUTIONS

As a result of the findings from this investigation, numerous ideas were considered as possible solutions to the faulting problem. Among these were the following:

1. Use of continuous reinforcement.
2. Use of doweled joints to eliminate curl and to promote load transfer.
3. Use of shorter joint spacing—possibly 6 to 8 ft. Although this would not eliminate curl, it would reduce the distance through which curl acts and provide tighter joints with better interlock.
4. Construction of base and pavement monolithically. Possibly, the increased thickness, rigidity, and weight would reduce curling tendencies and result in less deflection.
5. Prevention or minimization of the entrance of water. This would involve maintaining seals of all joints and cracks.
6. Construction of free drainage to the outside for any water that gets under the slab. This would reduce the time that water is available to erode base or shoulder materials.
7. Use of more erosion-resistant base and shoulder materials. Lean concrete or asphalt concrete should serve satisfactorily for base and asphalt concrete for the outside shoulder adjacent to the slab. (The shoulder next to the median is not considered to be a contributing factor to the faulting problem.) An alternative to the use of erosion-resistant material in the shoulder is the placing of a membrane seal along the edge of the slab to prevent erodible materials from getting under the slab. Erosion of the CTB is believed to be due largely to poor recementing and recompaction of the surface after trimming to grade. Possibly, the elimination of the trimming operation would enhance the erosion resistance of the CTB.

In deciding on a course of action to solve the faulting problem, we had to consider several factors. One of the most important was the effect of any change on the contractor's operation and his production. In recent years, concrete pavement production rates have increased tremendously. With two large mixers and fast-charging equipment, a central batch plant can produce approximately 800 cu yd of concrete per hour, and a slip-form paver can place that concrete at a rate of up to 30 ft/min for conventional 24-ft wide and 0.70-ft thick pavement. The use of bottom dump trucks has increased the speed of concrete delivery such that production rates of up to 2 miles of

pavement in an 8- to 10-hour day are possible. These rates of production plus some changes in design and construction details are largely responsible for bid prices remaining about the same since 1956. Any construction or design change that would slow the high-speed operation would have a significantly adverse effect on bid prices. For example, on a recent project in California, it was found that, with the use of continuous reinforcement and concrete delivered from the side by belt, production rates in some cases were 50 percent lower than those of conventional pavement placing. Although production rates vary with the type and amount of placing equipment being used (and there are records of placing 2 miles of continuously reinforced concrete pavement per day), there is little doubt that, with the equipment and methods being used in California, placing costs are higher when side delivery is required. Preplaced dowels would result in similarly increased costs.

Maintaining sealed joints for the life of a pavement is considered impractical with currently available methods and materials. It was decided, therefore, that the most practical and economical solution to the faulting problem was to develop an erosion-resistant base and to prevent the movement of untreated material from the outer shoulder. Several experimental shoulder sections have been constructed and are now being monitored for performance.

EXPERIMENTAL SHOULDER SECTIONS

The following is a description of the experimental shoulder sections (outside shoulder only):

1. Four 1,000-ft sections were placed on I-880 near Sacramento. Section 1 used class 2 permeable base in lieu of the standard section of class 2 aggregate base. The shoulder was surfaced with 0.25-ft asphalt concrete (in all sections). The intent here is to reduce erodibility and to increase drainage of water from under the pavement. Section 2 is essentially the same as section 1, except that a seal of a fairly thick coating of 60- to 70-penetration asphalt was sprayed along the slab face and on the extra width of CTB before the base was placed. Section 3 is the same as section 2 except that a class 2 aggregate base was used. In section 4, asphalt concrete (AC) was placed at the full depth of the slab and the full width of the shoulder (10 ft).
2. One section was placed on I-5 near Willows in northern California. The aggregate base of the shoulder was replaced with permeable AC (very open graded) in a 1,000-ft section (Fig. 1).
3. Two 2,000-ft sections were placed on US-99 south of Sacramento. In section 1 a seal consisting of a fiberglass-reinforced plastic strip (2 ft wide) was placed along the edge of the slab and over the widened CTB in the shoulder. Aggregate base and AC were then placed as usual (Fig. 2). In section 2, the aggregate base was replaced by permeable AC (Fig. 3).
4. One 2,000-ft section was placed on I-205 south of Sacramento. A layered membrane of coal tar and fiberglass (2 ft wide) was placed along the slab and over the CTB extension as in the US-99 section.
5. Two 2,000-ft sections were placed on I-80 west of Sacramento. This was a partial shoulder replacement of a pavement that had been in service about 8 years and had moderate faulting. A 2-ft wide section of the outer shoulder adjacent to the slab was removed down to the bottom of the slab. Loose material was broomed away, a tack coat of asphalt emulsion was applied, and then 0.5-ft permeable AC and 0.25-ft dense-graded AC were used to complete the shoulder. A 2,000-ft section was replaced in both the eastbound and westbound lanes. The basic objective of this work was to eliminate erodible shoulder material from the areas adjacent to the slab to see if faulting could be arrested. In addition to providing erosion resistance, the permeable AC is expected to provide better drainage that may also help reduce faulting tendencies. Performance of the test sections will be compared to that of adjacent untreated areas (Fig. 4).

Because less than 10 percent of the aggregate passed the No. 4 sieve and 2 percent asphalt was used, there was some difficulty in compacting the permeable AC. After

some experience, it was found that cooler mix temperatures and lighter rollers (6 to 8 tons) provided better results. On the shoulder replacement test section, wheel rolling in the confined area was felt to be sufficient. A steel-wheeled roller was used on the dense-graded surface course. The cost of the permeable AC under the experimental conditions was 20 to 40 percent more than the dense-graded mix.

Some difficulty was also encountered in placing the membranes. Although an asphalt emulsion was satisfactory as an adhesive for the membranes on flat surfaces, it would not hold them for a sufficient time on vertical surfaces. As a result, it was necessary to hold the membrane against the slab by hand while the aggregate base was being placed against it. Finished placement proved to be satisfactory, at least for the plastic; the shoulder was examined about 8 months after placement. The material was found to be solidly stuck to the concrete and CTB and had conformed to all irregularities caused by excess concrete left on the edge during pavement construction (Fig. 5). The material cost for fiberglass-reinforced plastic was about $600 per mile, whereas the cost of the layered coal tar and fiberglass was about three times as much. The underground life of the plastic is unknown; however, if the theory of its use is correct, it would probably be sufficient to at least delay faulting for many years.

The sections with a 60- to 70-penetration asphalt membrane were also examined about a year after construction. Although the asphalt is readily visible, there does not appear to be sufficient thickness to be fully effective as a seal in preventing erosion.

The experimental shoulder sections are being monitored on a seasonal basis. To date, there has been no difference in performance noted between experimental and control sections.

Other possible solutions to prevent erosion of shoulder materials have been considered but not tried. One is the use of a membrane that could be sprayed on, such as plastic or polyurethane foam. Another is to place a small wedge of AC next to the slab and "wheel roll" with a motor grader. Either of these methods could reduce faulting potential by eliminating the availability of loose material adjacent to the bottom of the slab.

BASE MATERIALS

Although base settlement has long been suspected as a cause of faulting, there was no evidence found during the field investigation of any such settlement. (All pavements opened had cement-treated bases.) There was, however, positive evidence of erosion of the base surface under the leave slab. The evidence was in the form of rivulets caused by water movement, which might result in some lack of uniform support but would not allow the slab to be depressed (Fig. 6). The top portion of the CTB at many locations has been found to be loosely cemented and readily erodible. Although drying of the surface before curing may be responsible for part of the problem, much is felt to be due to the trimming operation used to conform to grading tolerances. Because a high base will result in thin pavement, for which a contractor is penalized, and a low base results in the use of excessive concrete, considerable effort is exerted in obtaining the proper grade. Trimming is usually done about an hour or more after original placement. The surface material, once loosened, is never fully rebonded and so does not form a monolithic erosion-resistant base.

To eliminate the need for trimming, a local paving machine manufacturer proposed the idea of placing CTB with a slip-form paver. By adding extra cement and water to form a "wet-lean" CTB or "lean concrete base" (LCB), the material could be vibrated internally and placed like concrete to final grade with no rolling or trimming needed. Although the manufacturer had done this in other countries, little was known of the properties of such material. A laboratory testing program was carried out to determine the advantages and disadvantages of LCB and to compare its properties with those of CTB.

Tests were performed using typical CTB aggregates from six sources. The aggregates from these sources had a representative range of characteristics such as durability, particle shape, and geological origin. The CTB specimens were fabricated by following routine procedures and by using the cement content necessary to obtain a

Figure 1. Permeable AC shoulder being placed on I-5.

Figure 2. Fiberglass-reinforced plastic placement, US-99.

Figure 3. Rolling of permeable AC, US-99.

Figure 4. Partial shoulder replacement, I-80.

Figure 5. Shoulder opening showing plastic conforming to irregularities.

Figure 6. Channels indicating water movement on CTB surface.

compressive strength of 750 psi at 7 days. Similar mixing procedures were used for LCB samples, but enough water was added such that the mixture resembled concrete with an approximate 2-in. slump. Cement contents of 6, 9, and 12 percent were used. The moisture content needed to produce the 2-in. slump was considered optimum, and other mixes were made using 1.5 percent less water and 1.5 percent more water. Aggregate gradings were also varied from the middle of the specification limits to both the fine and coarse sides of the limits. Internal vibration was used in compacting the LCB specimens.

Specimens of both materials were fabricated for comparison of the following properties: compressive strength, flexural strength, shrinkage, and abrasion loss. Tables 1 through 6 show how CTB compares to LCB made with 9 percent cement, medium grading, and optimum moisture content.

From these laboratory tests, it appears that a lean concrete mixture could be made having properties satisfactory for base. Superior abrasion resistance is a highly desirable property. Equivalent compressive strength can be achieved; LCB, however, requires approximately twice as much cement as does CTB. This increase in cost could be partially offset by the elimination of rolling and trimming equipment normally required. For some contractors, the immediate need for a central mixing plant and slip-form paver for concrete paving would be an added expense.

A few contractors have been contacted regarding a trial of LCB. Probably because of their prior planning and uncertainty, none has expressed interest in changing his method of operation.

Recently it has been noted that a few contractors are changing their CTB placing methods. They have changed to central mixing, whether required or not, and to placing with a slip-form paver. Instead of a wet mix and internal vibration, they use the regular dry mix and a vibrating screed behind the paver, followed by rollers. This results in a much harder appearing surface and trimming is seldom if ever, necessary. Unfortunately, there is no test method available for measuring the abrasion resistance of CTB in place. If the trend to the type of construction continues, our objection to CTB due to trimming may be overcome (Fig. 7).

OTHER BASE ALTERNATIVES

Asphalt Concrete

At several locations, PCC pavements have been constructed directly over old AC roadways or over AC on CTB used for detour purposes. Some of these pavements have exhibited very good performance with no apparent abrasion of the base taking place. A further trial of AC base has been planned for the near future. Cost data will be obtained, and performance will be compared to that of CTB sections and the use of CTB on the same project.

Monolithic Base and Pavement

A proposal now being considered is the construction of base and pavement in one layer, i.e., a nontreated base. As mentioned in the first faulting report, the increased thickness and weight of a monolithic slab should reduce curling and deflection. The thickness necessary to provide the desired features is now being studied. Also to be considered, however, is the effect that elimination of the widened CTB would have on pumping of the subgrade.

OTHER EXPERIMENTAL CONSTRUCTION

Continuously reinforced concrete pavement is considered as one solution to the faulting problem. Under another research project, approximately 10 miles of this type of pavement construction has been monitored. A report on construction details and comparative costs will be made at a later date. Other experimental features were incorporated into the same project, which might also be useful in preventing faulting.

Table 1. Cement and optimum moisture contents of CTB and LCB.

Sample Number	Cement Content (percent)		Moisture Content (percent)	
	CTB	LCB	CTB	LCB
70-1089	3.5	9.0	8.1	10.8
70-1097	4.5	9.0	8.0	13.7
70-1122	4.0	9.0	7.8	12.5
70-1127	5.5	9.0	8.1	13.5
70-1142	5.5	9.0	6.6	12.9
70-1308	3.2	9.0	6.6	11.6

Table 2. Compressive strengths of CTB and LCB.

Sample Number	After 7 Days (psi)		After 28 Days (psi)		After 90 Days (psi)	
	CTB	LCB	CTB	LCB	CTB	LCB
70-1089	842	765	1,055	1,119	–	–
70-1097	757	544	1,152	721	1,272	–
70-1122	738	350	541[a]	689	1,304	–
70-1127	812	450	871	692	1,131	938
70-1142	772	402	910	597	1,412	1,081
70-1308	825	640	773	1,230	884	1,437
Average	791	525	952	841	1,201	1,152

[a]Not included in average.

Table 3. Flexural strengths of CTB and LCB.

Sample Number	After 7 Days (psi)		After 28 Days (psi)	
	CTB	LCB	CTB	LCB
70-1089	50	168	89	251
70-1097	184	203	195	380
70-1122	106	56	171	231
70-1127	155	147	207	261
70-1142	154	133	207	246
70-1308	110	175	155	374
Average	126	147	171	290

Table 4. Seven-day surface abrasion losses.

Sample Number	CTB (grams)	LCB (grams)
70-1089	44.5	3.4
70-1097	16.7	0.5
70-1122	37.8	10.7
70-1127	15.4	5.0
70-1142	11.4	12.3
70-1308	4.0	1.5
Average	21.6	5.6

Table 5. Fifty-day shrinkage values.

Sample Number	CTB (percent)	LCB (percent)
70-1089	–	0.032
70-1097	0.111	0.138
70-1122	0.065	0.118
70-1127	0.042	0.053
70-1142	0.029	0.032
70-1308	0.026	0.023
Average	0.055	0.066

Table 6. Properties of LCB.

Characteristic	Cement Content (percent)			Moisture Content (percent)			Grading			Curing Period (days)		
	6	9	12	Optimum - 1.5	Optimum	Optimum + 1.5	Fine	Medium	Coarse	7	28	90
Compressive strength	I	I	I	D	D	D	I	I	I	I	I	I
Flexural strength	I	I	I	D	D	D	I	I	I	I	I	I
Abrasion losses	D	D	D	I	I	I	D	D	D	D	D	D
Shrinkage	SD	SD	SD	I	I	I	D	D	D	–	–	–
Workability	SI	SI	SI	I	I	I	D	D	D	–	–	–

Note: I = increase, D = decrease, SD = slight decrease, and SI = slight increase.

Figure 7. Placing CTB with slip-form paver.

Short-Joint Spacing

Two sections of pavement with short-joint spacing were constructed. Joints were skewed (4 ft in 24 ft counter clockwise) and sawed at repeat intervals of 8, 11, 7, and 5 ft. The length of the four slabs is about one-half that of our normal spacing. A check before shoulder construction indicated that more than 80 percent of the joints had cracked on at least one side of the centerline joint soon after construction. Performance will be monitored to determine if faulting tendencies are reduced as compared to normal joint construction.

Lean Concrete Base

This base should not be confused with the type previously referred to in this report. On this project, two experimental base sections were constructed with 4-sack concrete made with concrete aggregates. The base turned out to be stronger than anticipated, with a compressive strength of more than 3,000 psi in less than 28 days. No problems with surface abrasion are anticipated in these sections, and the test section should provide more positive evidence about intrusion of shoulder material if it occurs.

7.5-Sack Concrete

Although the job control concrete contained 5.5 sacks of cement, two experimental sections were constructed with concrete containing 7.5 sacks per cubic yard. The effect of extra strength concrete on performance characteristics such as curl and deflection will be studied.

Extra-Thick Pavement

These sections were constructed 0.95 ft in thickness over 0.45-ft CTB. Although constructed as "no-fatigue" sections, it was found that the extra thickness did not present any particular construction difficulties, and it, too, should provide some interesting data relative to deflection under load.

SUMMARY

To find solutions to the faulting problem, California has so far concentrated efforts toward preventing erosion and movement of materials of the base and the adjacent portion of the outside shoulder. Several experimental sections have been constructed, and others are being planned. Test sections are being monitored on a regular basis so that conclusions can be drawn as soon as possible. In the meantime, still other possible solutions are being actively considered. It is likely that any implementation will result in an initial increased pavement cost (which can be offset later in decreased maintenance); however, if such implementation can be made without adversely affecting paving production, then the increased cost will be much less.

ACKNOWLEDGMENTS

This project was performed in cooperation with the Federal Highway Administration. The opinions, findings, and conclusions expressed in this report are those of the authors and are not necessarily those of the Federal Highway Administration.

REFERENCES

1. California Pavement Faulting Study. California Division of Highways, Res. Rept. M&R 635167-1, Jan. 1970.
2. Spellman, D. L., Woodstrom, J. H., and Neal, B. F. Faulting of Portland Cement Concrete Pavements. California Division of Highways, Res. Rept. M&R 635167-2, Jan. 1972.

EFFECT OF CRACKS ON BENDING STIFFNESS IN CONTINUOUS PAVEMENTS

Adnan Abou-Ayyash, W. Ronald Hudson, and Harvey J. Treybig,
Center for Highway Research, University of Texas at Austin

Transverse contraction joints in rigid pavements were long considered essential to preventing pavement damage from volume-change stresses. Continuously reinforced concrete pavement handles these stresses in another way. It allows the pavement to develop a regular pattern of very fine random cracks. In previous analysis of such pavements, it has been extremely difficult to evaluate the effect of cracks on the load-carrying capacity and subsequent performance of the slab. This paper presents an analytical look at the problem of transverse cracking in continuously reinforced concrete pavements. The influence of these cracks on the longitudinal bending rigidity was studied by using basic moment-curvature relations. A relation was developed that expresses the average moment of inertia due to the effect of the crack as a function of material properties and slab geometric characteristics. Results showed that a significant drop of 80 to 90 percent in the bending rigidity is encountered at crack locations. Furthermore, the development length bond idea was used to specify the slab portion affected by the discontinuity. A procedure to simulate this effect by using the discrete-element method of slab analysis is outlined. The procedure is general and simple to use.

A GENERAL discrete-element method for solution of discontinuous plates and slabs has been developed by Hudson, Matlock, and Stelzer (1, 2). The method is based on a physical model representation of a plate or slab by bars, springs, and torsion bars that are grouped in a system of orthogonal beams. Computer programs developed for the aforementioned method are designated by the acronym SLAB. These programs have the ability to handle complex problems with combinations of load and a variety of discontinuities (cracks and joints) and support conditions.

In previous analyses of rigid pavements, it has been difficult to evaluate the effect of cracks on the bending stiffness and the load-carrying capacity of the slab. This paper describes the use of discrete-element SLAB methods to study the behavior of continuously reinforced concrete pavement (CRCP) including modeling of cracks and joints. The effect of cracks on slab bending stiffness was investigated in this study by using basic moment-curvature relations, which consequently made discrete-element modeling of the crack feasible.

THE PROBLEM AND THE APPROACH

CRCP may be defined as a concrete pavement in which the longitudinal reinforcing steel acts continuously for its length and no transverse joints other than occasional construction joints are installed. In actual practice, the continuity is sometimes interrupted by expansion joints at structures. Except for these, there is technically no limit to the length a CRCP can be.

Transverse contraction joints were long considered essential to preventing pavement damage from volume-change stresses. CRCP takes care of these stresses in another way. It allows the pavement to develop a regular pattern of very fine random transverse

Sponsored by Committee on Rigid Pavement Design.

cracks (Fig. 1). The design concept for this pavement type is to provide sufficient reinforcement to keep the cracks tightly closed and to provide adequate pavement thickness to carry the wheel loads across these tightly closed cracks (3).

Because of volume-change stresses, crack formation in the continuously reinforced pavement slab is inevitable until the expansive materials are perfected. Therefore, a thorough understanding of the behavior of a pavement structure with such discontinuities is needed. The real pavement system, including the cracks, must be analyzed. This can be approximated with reasonable confidence by using the SLAB programs.

Figure 2a shows a cracked portion of CRCP, and Figure 2b shows a variation in the moment of inertia in the cracked region. The exact shape of this curve is not clearly known because of the complexity of the problem. The discrete-element method was applied to the discrete CRCP by using basic moment-curvature relations. In these relations, an average moment of inertia, which simulates the effect of cracks on slab bending stiffness, was determined. Furthermore, the development length bond concept (4) was used to specify the slab portion over which the average inertia could realistically be applied.

ANALYSIS AND MODELING

Theoretical Background

Analytical solutions for two-dimensional plate problems have been discussed by others (5), who characterize three kinds of plate bending: thin plates with small deflections, thin plates with large deflections, and thick plates.

For thin plates with small deflections (i.e., in which the deflection is small in comparison with thickness), a satisfactory approximate theory of bending of a plate by lateral loads can be developed by making the following assumptions:

1. There is no deformation in the plate's middle plane;
2. Points of the plate, which initially lie "normal" to the middle surface of the plate, remain "normal" to the middle surface of the plate after bending; and
3. Normal stresses in the direction transverse to the plate can be disregarded.

With these assumptions, the deflected surface of an isotropic plate is described by the biharmonic equation

$$D[(\partial^4 w/\partial x^4) + 2(\partial^4 w/\partial x^2 \partial y^2) + (\partial^4 w/\partial y^4)] = q \qquad (1)$$

where

D = the bending stiffness of the plate,
w = the deflection (with positive upward), and
q = the lateral load.

A complete discussion of this equation is given elsewhere (5).

For a given set of boundary conditions, solution of this differential equation gives all the information necessary for calculating stresses at any point in the plate. Closed-form solutions of this equation are available for a number of special cases, including homogeneous isotropic plates, which are generally round with finite radii or with infinite dimensions in the x and y directions. The loading conditions in most closed-form solutions are either uniform over the entire plate or concentrated in the center of the plate. As the problem becomes complex, with various combinations of load, support, and stiffness conditions, closed-form solutions are generally not available, and a numerical method must be used to solve the problem. The discrete-element method is such a method.

Figure 3 shows the discrete-element model of the slab, as suggested by Stelzer and Hudson (2). The slab or the rigid pavement structure is replaced by an analogous mechanical model representing all stiffness and support properties of the actual slab. The joints of the model are connected by rigid bars that are in turn interconnected by torsion bars representing the plate twisting stiffness C. The flexible joint models the concentrated bending stiffness D and the effects of Poisson's ratio μ. The modulus of

subgrade support k is represented by independent elastic springs, i.e., the Winkler foundation (6). A problem involving almost any physical combination of loads and restraints applied to a slab, including lateral loads, in-place forces, and applied couples or moments, can be solved. Furthermore, slab discontinuities as well as partial subgrade support can be simulated on the model.

The deflection at each joint is the unknown. The basic equilibrium equations are derived from the free body of a slab joint with all appropriate internal and external forces and reactions. These equations sum the vertical forces at each joint and sum the moments about each individual bar. A complete derivation of these equations and the fourth-difference equations can be found elsewhere (2).

Crack Effect and Method of Attack

Because a discontinuity, such as a joint or crack, creates a change in the moment of inertia or stiffness (Fig. 2), it can be simulated on the discrete model with one of the following methods.

The first method requires a clear determination of stiffness variation in the crack region, which is then divided into increments sufficient to define the effect of the discontinuity. A disadvantage of this method is that it may not be possible to define the stiffness variation in the cracked region accurately enough to yield reasonable results. Furthermore, as the number of increments in either the x or y direction increases, computer time increases, making the solution impractical in some cases.

The second method, which was used in this study, deals with an average value of stiffness that considers the discontinuity effect. The derivation of this average value was solely based on basic moment-curvature relations and is independent of increment length. Hence, the whole structure can be divided into about 15 increments in each direction, and reasonable results can be obtained.

Derivation of Average Moment of Inertia $\overline{I}$

For the determination of average moment of inertia $\overline{I}$, the following assumptions are made:

1. A plane section remains plane before and after bending;
2. A straight-line neutral axis can be assumed to represent the average of the actual variable position of the neutral axis; and
3. At the fine crack location, very slight curvature is needed to bring the two parts of the slab in touch and hence allow the transfer of bending.

With these assumptions in mind, consider a 1-ft wide slab section, as shown in Figure 4 (after Winter et al., 4). Because of the cracks, the actual rigidity of the structure is variable along its length; it is largest between cracks where the tension in the concrete contributes to the rigidity and is smallest at the cracks. For the slab shown in Figure 4, we derive from the basic moment-curvature relation

$$1/\overline{\rho} = M_w/E\overline{I} \tag{2}$$

where

$\overline{\rho}$ = average radius of curvature,
M_w = working moment,
E = modulus of elasticity of concrete, and
$\overline{I}$ = average moment of inertia.

Furthermore, we derive from the strain diagram (Fig. 5)

$$1/\overline{\rho} = \overline{e}_s/[d(1 - K)] = \overline{f}_s/[E_s d(1 - K)] \tag{3}$$

where

$\bar{e}_s$ = average strain in reinforcement,
$\bar{f}_s$ = average stress in reinforcement,
E_s = modulus of elasticity of steel,
d = distance from top compression fiber to the centroid of steel, and

$$K = 2[\sqrt{Pn(1 + Pn)} - Pn] \tag{4}$$

in which

P = percentage of longitudinal reinforcement = (area of steel A_s/gross area of concrete b x t) x 100, and
n = E_s/E.

In Eq. 4, K is a fraction that, when multiplied by d, gives the distance to the neutral axis of the section (Fig. 5). This is based on the cracked transformed section (4). It is worthwhile to note that the area of concrete in the percentage of reinforcement term is the gross area of the section and not, as defined in the equations for reinforced concrete, the width of the section times the distance from extreme compression fiber to the centroid of the steel. In Eq. 4, P should be expressed as a ratio rather than as a percentage.

By combining Eqs. 2 and 3 and solving for $\bar{I}$, we get

$$\bar{I} = M_w nd(1 - K)/\bar{f}_s \tag{5}$$

To determine the average stress in the reinforcement, we must consider the contributing effect of the concrete in tension. Let the average tensile stress of concrete between cracks be expressed as

$$\bar{f}_t = k_1 f_r \tag{6}$$

where

f_r = flexural stress of concrete, and
k_1 = a reduction factor based on experimental results (7).

The part of the resisting moment corresponding to the average tensile stress of concrete $\bar{f}_t$, as shown in Figure 6 (after Yu and Winter, 8), is

$$M' = T_c\,(2t/3) \tag{7}$$

where

T_c = the tensile force in the concrete.

By substituting the value of T_c (Fig. 6) in Eq. 7, we get

$$M' = k_1 f_r bt(t - Kd)/3 \tag{8}$$

Further development of this equation is presented elsewhere (7), where the modulus of rupture (flexural stress at instant of cracking f_r) is expressed in terms of the compressive strength of concrete f_c' (8). In final form

$$M' = 0.1(f_c')^{2/3} bt(t - Kd) \tag{9}$$

Hence, the stress in the reinforcement f_s' corresponding to M' can be computed by

$$f_s' = M'/A_s jd \tag{10}$$

Figure 1. Continuously reinforced concrete pavement.

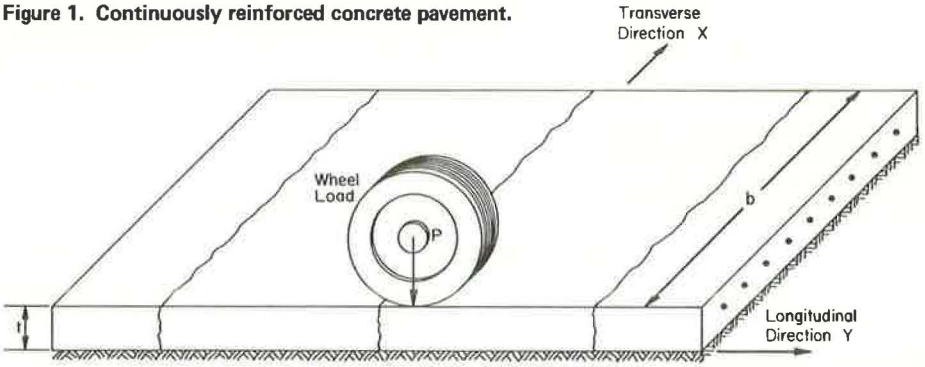

Figure 2. Effect of a discontinuity on the bending rigidity of the slab.

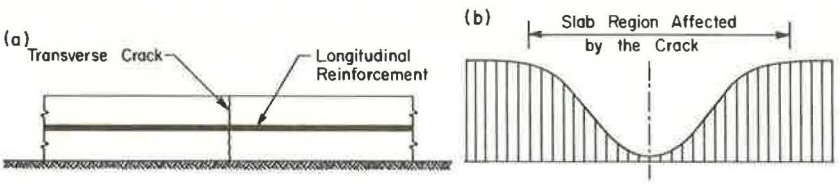

Figure 3. Discrete-element model of a plate or slab.

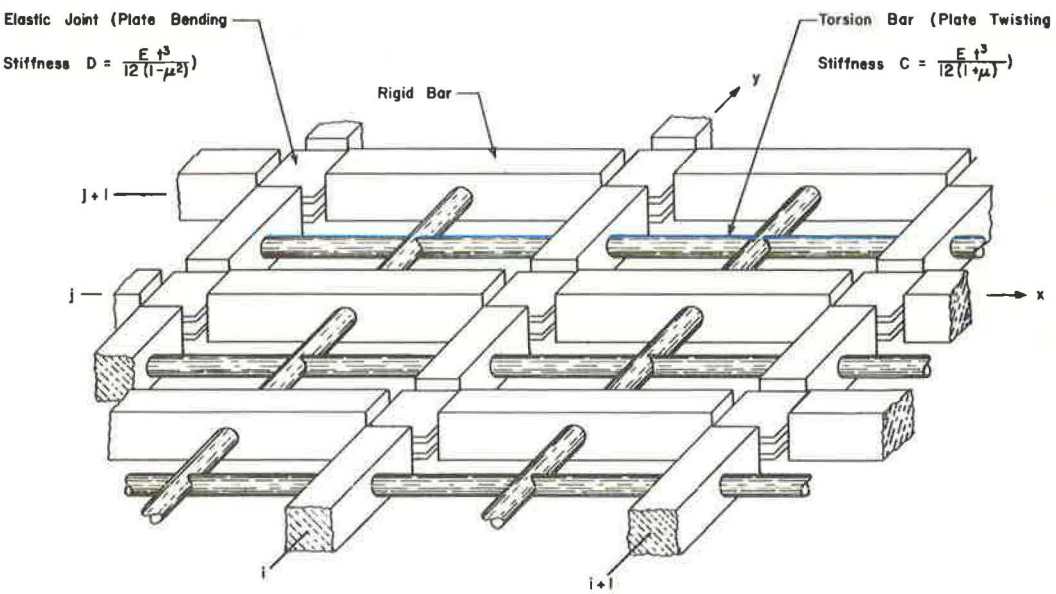

Figure 4. Cracked slab.

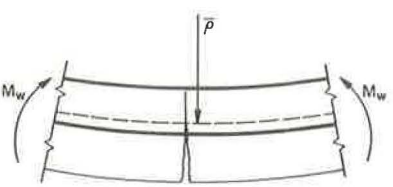

Figure 5. Strain distribution near crack location.

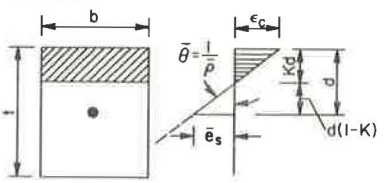

Figure 6. Stress distribution awa from crack location.

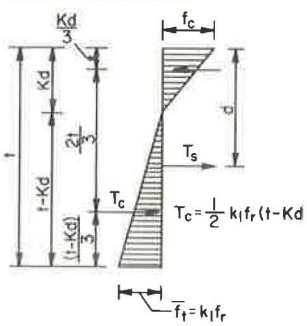

where

f_s' = tensile stress in the steel due to flexural stress in concrete at points away from crack, and
$j = 1 - (K/3)$

But at the cracked section, the steel stress f_s is

$$f_s = M_w/A_s jd \tag{11}$$

The value of the working moment M_w depends on whether the steel or the concrete stress governs (Fig. 7). If the former controls, we derive from Eq. 11

$$M_w = A_s f_s jd$$

where

f_s = the allowable stress in the steel.

On the other hand, if the concrete stress governs, then

$$M_w = f_c Kjbd^2/2 \tag{12}$$

where

f_c = the working compressive stress in the concrete.

By substituting the controlling value of M_w in Eq. 11, we derive the value of the steel stress at the crack and the actual average steel stress $\overline{f}_s$ at the instant of crack initiation:

$$\overline{f}_s = f_s - f_s'$$

Hence, the average moment of inertia is given by

$$\overline{I} = M_w nd(1 - K)/(f_s - f_s') \tag{13}$$

In this equation, the average moment of inertia $\overline{I}$ is expressed in terms of slab geometrical characteristics and material properties. By using the preceding analysis, we get the variation of the percentage of reduction in bending stiffness versus the percentage of reinforcement for different concrete compressive strength values (Fig. 8). Bending stiffness reduction ranged from 80 to 90 percent for the change encountered in the percentage of reinforcement. However, it is important to note the minor influence of the concrete compressive strength on stiffness reduction.

In the development of these curves, the allowable concrete compressive stress was $0.45\ f_c'$, and the allowable tensile steel stress was 0.75 of yield, which is equivalent to a safety factor of 1.33.

Several values of the yield stress, ranging from 40 to 70 psi, were tried. Fortunately, for the range and safety factor in the steel mentioned previously, the variation of the percentage of reduction in bending stiffness was independent of the yield stress. This is due to the fact that the working moment M_w, the lower of the values from Eqs. 11 and 12, was governed by the latter equation where the concrete stress controls. If a lower allowable steel stress is desired (i.e., $< 0.75 f_y$), Eq. 12 may need to be modified.

Region Affected by the Crack

Discontinuities in structural members not only cause severe localized bending stiffness reduction but also influence a certain amount of the area around them. Therefore, after determination of the average moment of inertia and the corresponding reduction in bending stiffness, one more step is required before the discrete-element model of the problem is performed. The length over which the original bending stiffness should be reduced to simulate the effect of the discontinuity must be determined.

A slab portion under the effect of transverse loading (Fig. 9a) is considered. Because the concrete does not resist any tension stresses at the crack, the compression force in the upper concrete fibers has to be balanced by a tensile steel force to maintain equilibrium at that section. In actuality, concrete fails to resist tensile stresses only at a crack. Between cracks, the concrete does resist moderate amounts of tensile stress; this reduces the tensile force in the steel (Fig. 9b), which creates a variable force in the bar. Because the bar must be in equilibrium, this change in bar force is resisted at the contact surface between steel and concrete by equal and opposite forces produced by the bond between steel and concrete. Figure 9c shows a distribution of the bond stress in the cracked region; it should be remembered that the bond development is the rate of change of tension. For the free body of a bar segment shown in Figure 9d, if U is the magnitude of the average bond force per unit length of bar, then $\Sigma F_x = 0$ yields

$$Udx + T - (T + dT) = 0$$

$$\therefore Udx = dT \tag{14}$$

By integrating over the required length, we get

$$U \int_0^a dx = \int_{T_1}^{T_2} dT$$

where

T_1 = tension in steel at some point between cracks, and
T_2 = tension in steel at crack.

Hence,

$$Ua = T_2 - T_1 = A_s f_s - 0$$

$$\therefore a = A_s f_s / U \tag{15}$$

Assuming that the bond force per unit length U is the resultant of shear-type bond stresses u uniformly distributed over the contact area, then

$$U = u\Sigma o \tag{16}$$

where

Σo = the perimeter of the bar(s).

By substituting the value of U in Eq. 15, we derive

$$a = A_s f_s / u\Sigma o \tag{17}$$

Hence, total affected length is as follows:

$$L = 2a \text{ and } L = 2(A_s f_s / u\Sigma o) \tag{18}$$

For the determination of the allowable bond stress u as well as f_s, the ACI 1963 code (Section 1301) specifies the following:

1. For tension bars, the allowable bond stress u is governed by

$$u = 3.4\sqrt{f'c}/\phi \leq 350 \text{ psi} \tag{19}$$

where

ϕ = the bar diameter; and

2. The allowable stress in the steel shall not exceed 24,000 psi.

Discrete-Element Modeling of the Crack Effect

By the previous analysis, the amount of reduction in bending stiffness, as well as the length over which it should be applied, has been determined. In this section, a method for modeling the effect is discussed.

In this method, there are two cases to be considered. In the first case, the region affected by the discontinuity extends over an even number of increments (Fig. 10a). If we assume, for example, that this region is two increments long (L = 2h), it is defined by three stations: two edge stations (i-1, j and i+1, j) and a middle station where the crack is located (i, j). Because the stiffness in the discrete-element model (Fig. 3) is lumped at the elastic joints or station locations in order to simulate the effect previously described, it is necessary to apply the total amount of the previously determined bending stiffness reduction at each middle station (in this case only one, i, j) and half of that amount at each of the boundary or edge stations, namely i-1, j and i+1, j. As an example, if the amount of reduction in bending stiffness is 90 percent of the original full value, 90 percent of the stiffness should be reduced at station i, j and 45 percent at each of the edge stations i-1, j and i+1, j.

In the second case, the area influenced by the crack extends over an odd number of increments, for example, three (L = 3h), as shown in Figure 10b. The main difference between the two cases is the relative position of the ends of the reduced stiffness region and station locations. When there is an even number of increments, a station is located at each of the boundaries or edges of the concerned region, which requires the half-value refinement discussed previously. When there is an odd number of increments, the edges of the reduced stiffness region lie midway between stations, and for modeling the total reduction in bending stiffness is applied at each station (i-1, j, i, j, and i+1, j), with no exception.

For the case where the number of increments is even, it was mentioned that a half value of the stiffness reduction should be applied at the edge stations. To test the sensitivity of the half reduction, we studied several examples. These covered a wide range of thicknesses, moduli of elasticity, crack spacings, and moduli of subgrade reaction. Without exception, neglect of the half-value reduction at the edge stations produced only negligible changes in deflections and principal stresses.

To validate this observation, we considered a problem involving a 20- by 40-ft pavement loaded with a 12-kip concentrated load placed 4 ft from the edge (Fig. 11). The thickness of the pavement was 8 in., and the modulus of subgrade reaction was 100 lb/in.^{3}. The reduction in bending stiffness was applied over a length of 12 in. at each transverse crack location. Figure 11 shows the change in deflection with the increase of the percentage of reduction in bending stiffness; as shown, the rate of change in deflection was almost negligible up to about 50 percent of the stiffness reduction, and then a significant increase was observed. Thus, the application of a half value of stiffness reduction at the edge stations produced almost negligible changes in stresses and deflections.

Therefore, it is recommended that the half bending stiffness reduction at the edge stations be neglected when there is an even number of increments, when the subgrade is not very weak, i.e., $k \approx > 40$ lb/in.^{3}, and when there is no loss in subgrade support.

Suggested Method and Sample Problem

The following step-by-step method is suggested for the application of SLAB programs in the analysis of discontinuities in CRCP:

1. Determine the physical characteristics of the concerned pavement, such as modulus of elasticity, thickness, and percentage of reinforcement;
2. Determine the percentage of reduction in bending stiffness to be applied at crack locations (from Eq. 13 or Fig. 8);

Figure 7. Stress distribution at crack location.

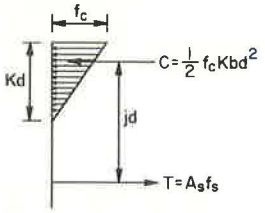

Figure 8. Percentage of reduction in bending stiffness at crack location and percentage of longitudinal reinforcement.

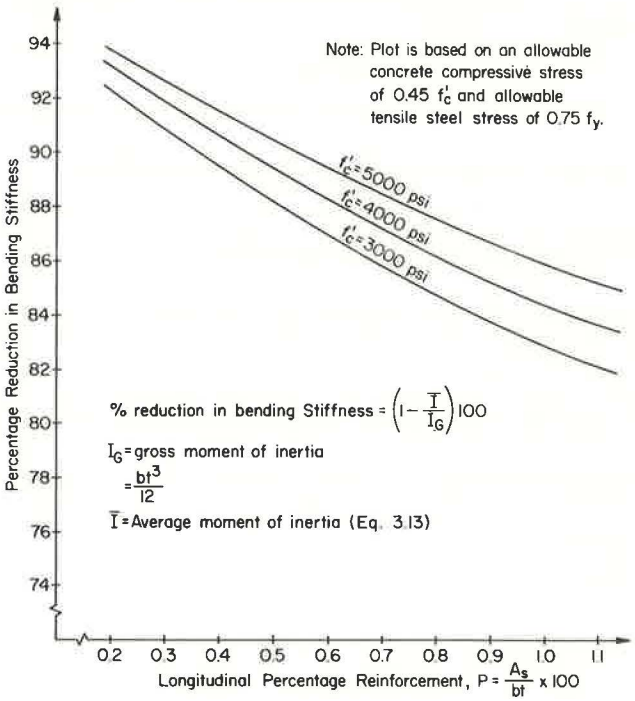

Figure 9. Region affected by the discontinuity.

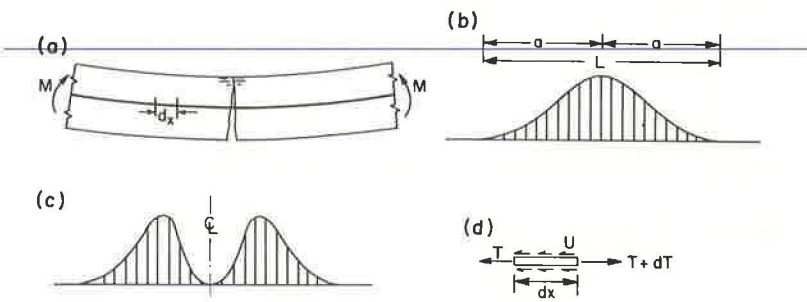

Figure 10. Discrete-element modeling of crack effect.

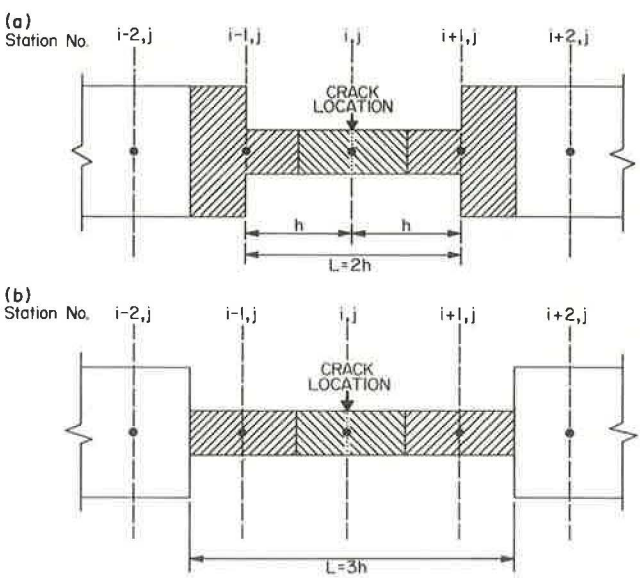

Figure 11. Effect of crack severity on deflection under a 12-kip wheel load.

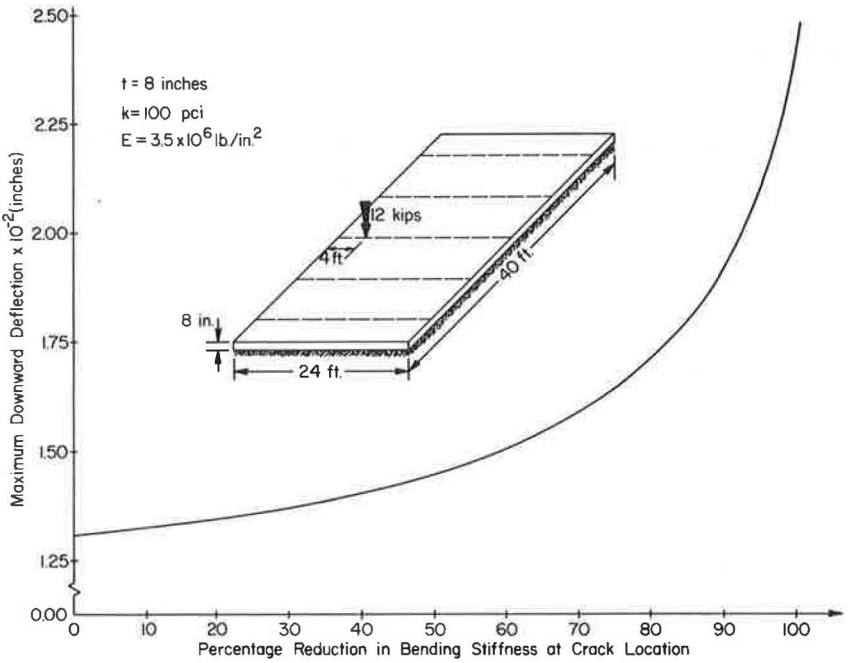

Figure 12. Influence of bending stiffness reduction at cracks on the deflection basin.

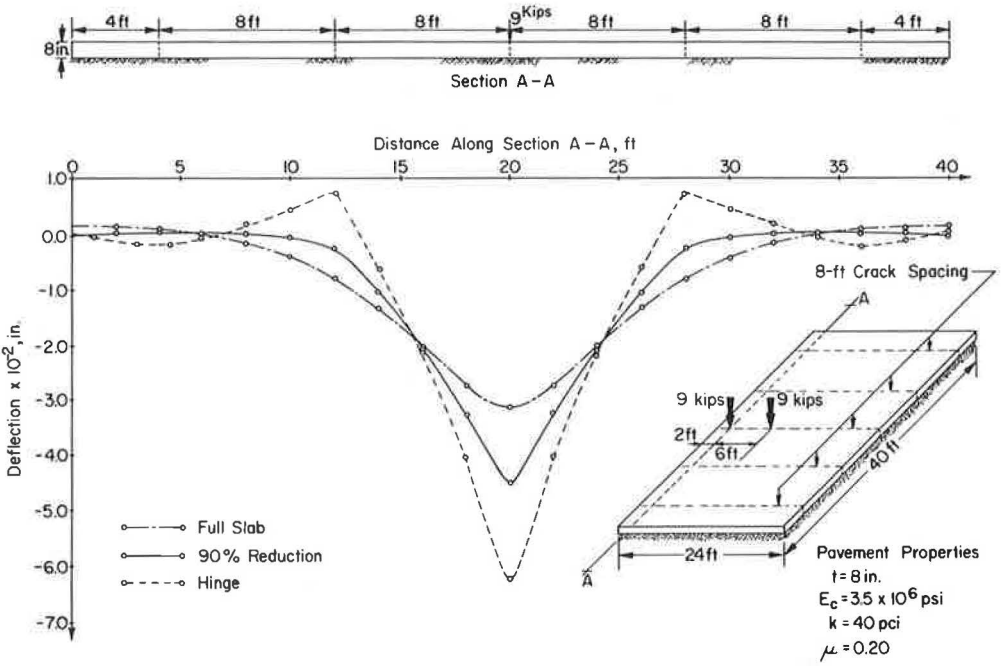

3. Determine the length affected by the discontinuity (from Eq. 18);
4. Decide on the increment length that best matches the slab geometry, as well as the length determined from step 3; and
5. Apply the percentage of stiffness reduction determined in step 2 at each crack location over the length from step 3.

This method is applied on the example problem shown in Figure 12. A 24- by 40-ft slab, loaded with 2, 9,000-lb wheel loads located at 2 and 8 ft from the edge was considered (Fig. 12), and the reduction in bending stiffness was 90 percent over a length of 12 in.

Besides the condition with 90 percent stiffness reduction at the crack location, two other conditions were studied: the hinged condition, where there is zero stiffness at the discontinuity, and the uncracked condition, where the full slab is treated as one piece. The variation in deflections for each of these cases is shown in Figure 12. The effect of the hairline cracks is clearly shown by the 30 percent deflection increase in the 90 percent reduction case over the uncracked case. Furthermore, a comparison of the hinge and the uncracked cases showed a 60 percent increase in maximum deflection for the hinged condition.

Implementation of Results

The development of the application of discrete-element analysis to the continuously reinforced pavement problem will enable designers to more confidently analyze design problems. The SLAB method should be used in a sensitivity analysis of the rigid pavement problem in general. Very specific design analyses can now be made of both jointed pavements and CRCP, which up to this time were approximated by still other techniques. This development will be implemented in the design process.

CONCLUSION

The problem of transverse cracking in CRCP and its influence on the bending rigidity of the slab in the longitudinal direction have been studied by using basic moment-curvature relations. A procedure to simulate this effect by using the discrete-element method is outlined.

The results of the study have indicated that the effect of cracks on the bending rigidity of the slab is highly significant. The reduction in bending stiffness varied from 80 to 90 percent of the original full value for the range of percentage of longitudinal reinforcement studied. Obviously, as the crack width increases, the bending reduction also increases, and ultimately a hinge exists as in the case in a jointed concrete pavement.

ACKNOWLEDGMENTS

This investigation was conducted at the Center for Highway Research, University of Texas at Austin. The authors wish to thank the sponsors, the Texas Highway Department and the Federal Highway Administration. The opinions, findings, and conclusions expressed in this publication are those of the authors and not necessarily those of the Federal Highway Administration.

REFERENCES

1. Hudson, W. R., and Matlock, H. Discontinuous Orthotropic Plates and Slabs. Center for Highway Research, Univ. of Texas at Austin, Res. Rept. 56-6, May 1966.
2. Stelzer, C. F., Jr., and Hudson, W. R. A Direct Computer Solution for Plates and Pavement Slabs. Center for Highway Research, Univ. of Texas at Austin, Res. Rept. 56-9, Oct. 1967.
3. McCullough, B. F. Design Manual for Continuously Reinforced Concrete Pavement. Aug. 1968.
4. Winter, G., Urquhart, L. C., O'Rouke, C. E., and Nilson, A. H. Design of Concrete Structures, 7th Ed. McGraw-Hill, New York, 1964.
5. Timoshenko, S., and Woinowsky-Krieger. Theory of Plates and Shells, 2nd Ed. McGraw-Hill, New York, 1967.

6. Winkler, E. Die Lehre von Elastegatat und Festigkeit. Prague, 1867.
7. Abou-Ayyash, A., and Hudson, W. R. Analysis of Bending Stiffness Variation at Cracks in Continuous Pavements. Center for Highway Research, Univ. of Texas at Austin, Res. Rept. 56-22, Aug. 1971.
8. Yu, Wei-Wen, and Winter, G. Instantaneous and Long-Time Deflections of Reinforced Concrete Beams Under Working Loads. Jour. American Concrete Institute, July 1960.

STRUCTURAL ANALYSIS OF BITUMINOUS CONCRETE PAVEMENTS

R. C. Deen, H. F. Southgate, and J. H. Havens,
Kentucky Department of Highways

•RATIONAL criteria for the structural analysis of pavements are emerging from classical theories equated to the observed behavior of real pavements. Pavement behavior is known to be affected by traffic, variations in soil support, and variations of component thicknesses and qualities. Considerable attention has been devoted to the mechanistic response of pavements to static and dynamic loads and to the development of theoretical analysis procedures that rely, in part, on the computation of certain critical stresses, strains, and deflections in the structure. A computer program (1) that permits the analysis of elastic multilayered pavement systems has made possible the extensive investigation of the effects of soil support properties, strength characteristics of the materials used in the pavement structure, and component thicknesses. In this study, the computer program was used to determine the patterns of stresses, strains, and deflections of the pavement system. The study also attempts to show the relation between these stresses, strains, and deflections and current and proposed design curves by using the fatigue concept [equivalent axle loads (EAL's)].

From the mechanistic point of view, load-deflection relations outwardly portray the composite stiffness or rigidity of pavement systems. Contrary to general impressions, surface deflection is not a discrete, limiting parameter. Stresses and strains in the subgrade soil and in the extreme fibers of the bituminous concrete layers may constitute overriding, fundamental limits. Therefore, thickness design criteria cannot be based directly on deflection spectra. In other words, two different pavements having equal, 18-kip deflections are not necessarily equal designs unless all accompanying stresses and strains are also equal.

COMPUTATIONS BASED ON THE ELASTIC THEORY

The Chevron Research Company furnished a "privileged" duplicate of its computer program for the elastic analysis of an n-layered pavement system to the Kentucky Department of Highways, Division of Research. This program is capable of handling the analysis of a 15-layered system and computes for any specified depth and distance from the axis of loading the stresses, strains, and deflections. In developing the Chevron program to make these computations, Michelow (1) assumed the following:

1. The asphalt pavement is a semi-infinite solid of n layers;
2. The elastic characteristics of one layer can be different from those of another;
3. The component layers are homogeneous and isotropic and are characterized by Young's modulus and Poisson's ratio;
4. A uniformly distributed load on a circular area is placed on and "normal" to the free surface of the pavement;
5. The interfaces between layers are rough, i.e., strains at the interface of two layers are identical; and
6. The bottom layer is a semi-infinite solid.

The determination of stresses, strains, and deflections by using the Chevron program requires the input of the elastic characteristics of the materials contained in the various layers of the pavement system. Values for the moduli of the subgrade E_3 investigated

Sponsored by Committee on Flexible Pavement Design.

ranged from 3,000 to 60,000 psi. For the convenience of plotting the results in terms of a "CBR scale," the relation developed by Heukelom and Foster (2) was used. The relation is not a precise measurement, but it suggests that the subgrade modulus (in psi) is approximately equal to the product of the California bearing ratio (CBR) and 1,500. A review of the literature (3) indicates that this relation is an acceptable approximation for evaluating subgrade moduli and provides a simple and practical approach to this estimation. Heukelom and Foster's relation is valid only for CBR values between 2.5 and 20, and the extrapolation of the relation into the range of CBR's above 20 is questionable but was done in this study only for the purpose of plotting results on a CBR scale. Thus, if an analysis is attempted involving CBR's greater than about 20, the CBR scale should first be converted to a modulus scale and the analysis then undertaken in terms of moduli.

Testing of pavements in place by Heukelom and Klomp (4) has shown that the effective elastic moduli of granular base courses E_2 tend to be related to the modulus of the underlying subgrade soil. The ratio of the base modulus to the subgrade modulus is a function of the thickness of the granular base, and in situ test results show that the range of this ratio is generally between 1.5 and 4. A value of 2.8 was selected in this study as being typical at a CBR of 7 (Fig. 1). Comparison of the analyses accomplished in this study with the 1958 design curves and field data (5) indicates that this assumption is reasonable. It was further assumed in Figure 1 that the ratio of E_2 to E_3 would be equal to 1 when $E_1 = E_2 = E_3$. The curves shown in Figure 1 were then obtained by assuming a straight-line relation on a log-log plot. A review of the literature (6, 7) indicates that Figure 1 gives reasonable values for good quality granular bases within a range of practical design situations (CBR value less than 20); and, therefore, this figure was used throughout the analysis to relate the modulus of the granular base to the subgrade support values. It is noted in Figure 1 that E_2 values are a function of E_1 and E_3 only.

The effective moduli of asphalt-bound layers depend on pavement temperature and time of loading. Subgrade strains are critical when the asphalt layer is warm and its modulus of elasticity is relatively low. On the other hand, strains in the asphalt layer are critical at lower temperatures when the modulus of the layer is relatively high. To investigate the effect of the modulus of the asphalt layer (E_1) on thickness requirements, we used a wide range of moduli (1,800,000 to 150,000 psi).

Dormon and Edwards (8) have reported that Poisson's ratio varies from 0.35 to 0.45. In this analysis, values of 0.40 for the asphalt concrete and dense-graded aggregate layers and 0.45 for the subgrade soil were used. An 18,000-lb axle load and a tire pressure of 80 psi were taken to represent the loading throughout the analysis.

Strain and deflection relations obtained from the computer output were plotted to show the effect of the variation of asphalt concrete and dense-graded aggregate thicknesses on (a) vertical compressive subgrade strains directly beneath the load, (b) pavement-surface deflections directly beneath the load, and (c) tangential strains at the bottom of the asphalt concrete layers and directly beneath the load for specified values of the moduli of the subgrade E_3 and of the asphalt-bound layer E_1. Data were read from this matrix of graphs and used to prepare graphs in which the axes were thickness of the asphalt-bound layer (ordinate) and log of the ratio of the asphalt concrete thickness to the total thickness (abscissa). From these graphs, total pavement thickness versus CBR plots were prepared for various asphalt concrete moduli and for given ratios of asphalt concrete thickness to total pavement thickness. By using these relations, we prepared nomographs for different ratios of asphalt concrete thickness to total pavement thickness (Fig. 2).

CONSTRUCTION OF DESIGN CURVES

The essential elements of design criteria involving predictive theory are (a) equations of static (or dynamic) equilibrium and (b) equations of failure. Elastic theory (represented here by a computer program capable of solving multilayered systems) is presumed to suffice as a first-order approximation of the equilibrium equations. Equations of failure are necessarily empirical or phenomenological; they bring into issue

all manner of experience, performance histories, and discrete test data, e. g., fatigue data. Failure equations are represented here by Kentucky's current design chart and other interpretative analyses of limiting strains or fatigue limits. Statements of equilibrium were equated to statements concerning failure and then graphically displayed.

Mixed Traffic Loadings

Standard weighting of the 1958-59 design curves (5) from the standpoint of deflection data would have positioned traffic curve X such that slightly greater thicknesses would have been required throughout. However, the final family of curves was tempered judiciously midway between the thicknesses required by earlier curves and the 1958-59 control points. Intuitively, then, it seemed that the curves should collapse toward the 100-CBR value and asymptotically approach infinite thickness toward the extremely low CBR's. It seemed also that doubling the equivalent wheel load (EWL) through each successive curve would require successively diminishing incremental thicknesses. A deflection of 0.017 in. (9-kip wheel load) was associated then with curve X at a CBR of 7 and a 23-in. pavement thickness, approximately one-third being asphalt concrete and the remainder being dense-graded aggregate. The present attempt to reconstitute the Kentucky curves theoretically began with the assumption that a mutual or coincident control point exists at a CBR of 7, total pavement thickness of 23 in., and a deflection of 0.015 in.

The remaining traffic curves were interpolated from this control point on the basis of a resolved proportional relation between various pavement structures and their respective 18-kip strains; soil strains were based on the ratio of the strain for an equivalent, single-axle load (or wheel load) corresponding to a given summation of EAL's to an 18-kip load strain.

The load equivalency (damage) factors, f, used in the AASHO method of summarizing mixed traffic can be described approximately by $f = a(1.25)^{P-18}$, where P = axle load (in kips) and a = 1 = first term of a geometric progression. The assumption of a constant ratio throughout the full range of AASHO load-equivalency factors is an operative license, which is real and valid only in the region of an 18-kip load but which permits computation of a hypothetical, equivalent single load. It may be mentioned that the real values of AASHO load-equivalency factors become inadequate, in this sense, in the range of extremely high axle loads. For instance, an incremental increase in load beyond 40 kip is proportionately less damaging than the same increment added to 30 kip. The preceding equation respects only the constant ratio of a geometric progression, which is clearly evident within a limited range about the 18-kip load level.

The computation of EAL's from mixed traffic data may be described as follows:

$$EAL_{(total)} = \Sigma_{All\ i's}\ EAL_i = \Sigma_{All\ i's}\ N_i(1.25)^{P_i}$$

where N_i = number of repetitions of axle load P_i (in kips). Hypothetically, any $EAL_{(total)}$ can be transformed to an equivalent number of repetitions of other base loads by the equation

$$EAL_{(total)} = N_i(1.25)^{P_i - 18}$$

where the base load is taken as 18 kip. If we let $N_i = 1$, P_i becomes an equivalent load that would, hypothetically, be as damaging as the number of EAL's.

Curve X was assigned a precise value of 256×10^6 EWL's. By custom, this has included two-directional traffic; thus, one-directional traffic for curve X would be 128×10^6 equivalent 5-kip wheel loads (or 10-kip axle loads). This had been equated to 8×10^6 18-kip equivalent axle loadings; that is,

$$N_K(\sqrt{2})^{P_K - 10} = 128 \times 10^6\ EWL's = N_{18}f_{18}$$

where N_K = number of wheel loads, P_K = wheel load (in kips, and $(\sqrt{2})^{P_K-10}$ = load equivalency factor used previously in the Kentucky design method. For an axle load of 18 kip, $f_{18} = (\sqrt{2})^{P_{18}-10} = 16$. Thus, $N_{18} = 8 \times 10^6$; or on the average AASHO EAL's = one-directional Kentucky EWL's/16. The equivalent, single-axle loads corresponding to the previously equated EWL's and EAL's are given in Table 1.

Limiting Subgrade Strains

It was observed from the computations and analysis that the vertical strain at the top of the subgrade ϵ_s for the control pavement was 2.400×10^{-4}. A review of other work (9, 10, 11) also indicated that an ϵ_s of 2.400×10^{-4} for traffic curve X (8×10^6 18-kip axles) would provide a high degree of assurance against rutting; this value was thus assigned to ϵ_{s9} at 8×10^6 repetitions and a wheel load of 9 kip.

An analysis of elastic theory computations relating the ratio of vertical strain in the subgrade ϵ_s at various impressed wheel loads to the strain under a basic wheel load of 9 kip ϵ_{s9} throughout a spectrum of pavement structures was made (Table 1). Such relations as given in Table 1 could be used to determine the limiting vertical strains at the top of the subgrade for various equivalent single wheel loads and thus for various values of accumulative EAL's. The results of this determination are also given in Table 1. The table is based on AASHO load-equivalency factors and thus alters the design curves based on Kentucky factors. The conversion from Kentucky to AASHO factors moderates the thicknesses of pavements required for traffic curves IA through IX and slightly increases the thicknesses for curves XI and XII.

Limiting Asphalt Concrete Strains

The criterion concerning limiting strains in the asphalt concrete was based on interpretative analyses of other work (11). Van Der Poel (12, 13) indicated that a safe limit for asphalt was in the order of 1×10^{-3} at 30 F. Because asphalt concrete consists of approximately 10 percent asphalt by volume, this fixes the safe strain level of asphalt concrete at 30 F in the order of magnitude of 1×10^{-4}. Others (3, 8, 10, 11) have established (by interpretative analyses of pavements and fatigue test data) that the magnitude of asphalt strain ϵ_a ensuring 1×10^6 repetitions at 50 F was 1.45×10^{-4}. Limiting values of strain (all at 50 F) as a function of number of repetitions of the base load as given by Dormon and Metcalf (10) can be represented by the equation $\log \epsilon_a = -3.84 - 0.199 (\log N - 6.0)$.

Some investigators suggest a fatigue diagram of the load-log N type. Fatigue theorists (14, 15, 16) have suggested and have shown in certain instances that a log load-log N plot is more realistic, and Pell (14) suggested an equation of the form $N = K'(1/\epsilon_a)^n$, where n is the slope of the log ϵ_a-log N plot and K′ is a constant. Pell (14), Deacon (16), and others have suggested that the value of n lies between 5.5 and 6.5 and is a function of the modulus of the asphalt concrete. Pell's work further suggested that the family of curves relating log ϵ_a to log N for different E_1 values is parallel. The use of such a relation in this study produced such inadequate results (as E_1 decreased, the total pavement thickness also decreased) that an alternative relation was sought.

By plotting (to a log-log scale) the 18-kip tensile strain versus the tensile stress at the bottom of the asphalt layer, we noted that, for a given E_1, the curves depicting structural influences appeared to converge at a single point near a strain of 2×10^{-3} (Fig. 3). By extrapolating Dormon and Metcalf's data, represented by the equation previously given, to a value of N = 1, we found the asphalt tensile strain to be 2.24×10^{-3}. This strain value was thus taken to be the limiting or critical asphalt tensile strain for a single application of a 9-kip wheel load. By constructing lines tangent to the strain versus stress curves at a strain of 2.24×10^{-3}, we obtained modulus lines that represent the limiting relations for asphalt strain versus stress—independent of structural influences. The stress-strain ratios read are in terms of bulk moduli ($E_1 = 0.6$ K).

For a total pavement thickness consisting of 33 percent of asphalt concrete (with a modulus of 480 ksi, typical of pavements in Kentucky), it was observed that the tensile strain at the bottom of the bound layer for a CBR of 7 and a total thickness of 23 in. was 1.490×10^{-4}. The traffic associated with this control point was 8×10^6 EAL's, as pre-

Figure 1. Relation between moduli of subgrade and moduli of granular base.

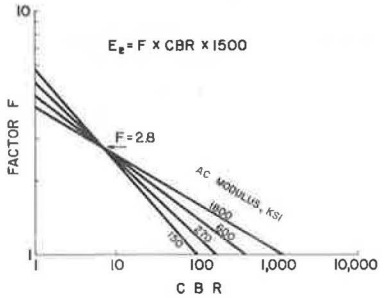

Figure 2. Nomographs for analysis of compressive and tensile strains.

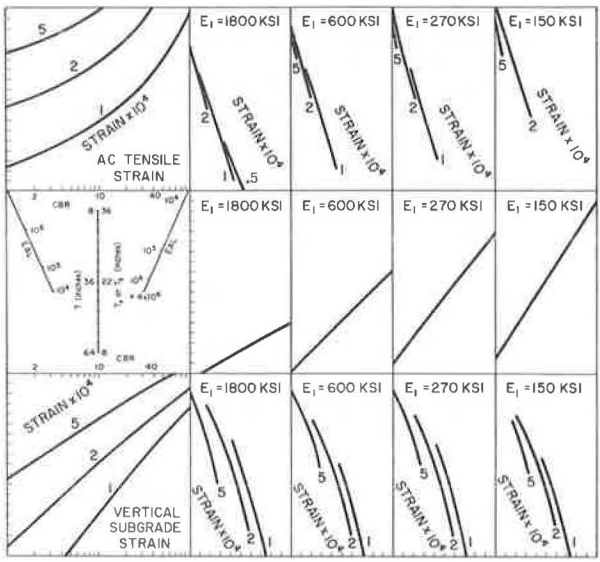

Table 1. Limiting subgrade strains.

Traffic Curve	Number of 18-kip Axle Loads	Wheel Load (kips)	$\epsilon_{aN}/\epsilon_{aS}$	ϵ_{aN} ($\times 10^{-4}$)
	5×10^3	25.5	2.837	6.809
IA	7.81×10^3	24.5	2.726	6.542
	1×10^4	24.0	2.664	6.394
I	1.56×10^4	23.0	2.553	6.127
II	3.12×10^4	21.4	2.381	5.714
	5×10^4	20.4	2.263	5.431
III	6.25×10^4	19.9	2.208	5.299
	1×10^5	18.8	2.091	5.018
IV	1.25×10^5	18.3	2.038	4.891
V	2.5×10^5	16.8	1.863	4.471
VI	5×10^5	15.2	1.690	4.056
VII	1×10^6	13.7	1.518	3.643
VIII	2×10^6	12.1	1.346	3.230
IX	4×10^6	10.6	1.172	2.813
	5×10^6	10.1	1.117	2.681
X	8×10^6	9.0	1.000	2.400
	1×10^7	8.5	0.944	2.266
XI	1.6×10^7	7.5	0.824	1.978
XII	3.2×10^7	5.9	0.654	1.570
	5×10^7	4.9	0.543	1.303
	1×10^8	3.3	0.371	0.890

Figure 3. Asphalt tensile strain-stress curves.

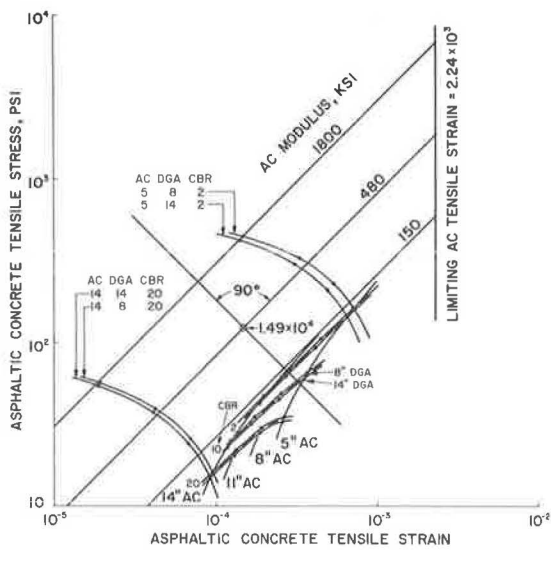

Figure 4. Effect of criterion of limiting strains.

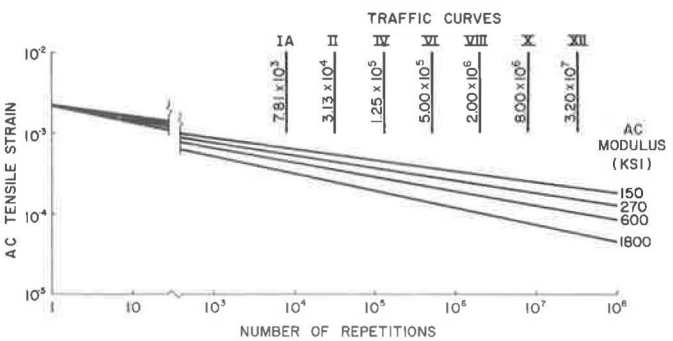

Figure 5. Application of strain-control criterion and stress-control criterion.

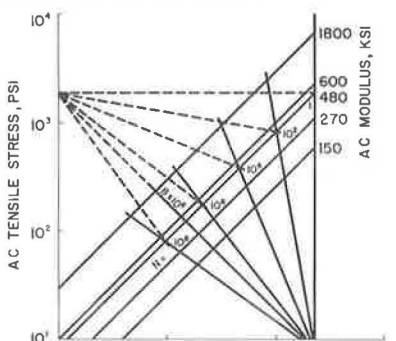

viously mentioned. In Figure 3, a line drawn perpendicular to the line for an asphalt concrete modulus of 480 ksi, as determined previously, at a strain of 1.490×10^{-4} intersected the other asphalt moduli lines at strains that were assumed to be critical strains at 8×10^6 EAL's. By assuming a straight-line variation between log ϵ_t and log N, we obtained the curves shown in Figure 4, which represent the critical asphalt concrete tensile strains.

Presumably, use of the criterion of limiting strains, which is shown in Figure 4 and given in Table 2, would prevent cracking and breakup; it does not allow a progressively increasing risk of failure of the lesser classes of roads. In the event that weighting in that way is desired, a pavement could be designed for a proportionately shorter life.

The limiting asphalt stress-strain curves are shown again in Figure 5. For any given modulus of asphalt concrete, the limiting strain for a single application of a catastrophic load is taken to be 2.24×10^{-3}. As shown in Figure 3, another known point of limiting strain falls on the line perpendicular to the stress-strain curves (a line of equal energy) for 8×10^6 repetitions. By assuming a logarithmic scale between these two points, we obtain the lines of equal numbers of repetitions shown in Figure 5. The limiting asphalt concrete tensile strain for any combination of number of repetitions and moduli of asphalt concrete is shown in Figure 5. Such values, of course, verify the limiting strains shown in Figure 4 and given in Table 2.

Figure 5 shows the condition in which the failure of the material involved is completely controlled by a strain criterion. If, however, it were desired to express the failure criterion in terms of a limiting stress, the relation shown by the dashed lines in Figure 5 might be obtained. The limiting stress value of 1.88 ksi is assumed to correspond to a single application of the catastrophic load (and a strain of 2.24×10^{-3} for a material with a modulus E_1 of 480 ksi). The other point on the scale is the stress at 8×10^6 applications of the basic load. Again if we assume a logarithmic scale between these two points, the lines of equal numbers of repetitions shown by the dashed lines in Figure 5 are obtained. Unfortunately, there are difficulties in respecting both a limiting stress and a limiting strain criterion in a pavement design problem. Relations between limiting stress and the modulus of the asphalt concrete are not so well known as relations involving strains. For the pavement designs reported herein, the criterion of failure for asphalt-bound materials of the pavement system respects only the limiting strains shown in Figure 4.

DISCUSSION OF RESULTS

Theory and Performance

Perhaps one of the significant findings of this study is that the 1958 design curves are very nearly parallel to the subgrade strain lines. In Kentucky designs, asphalt concrete has generally made up one-third of the total structural thickness. However, the apportionment of asphalt concrete was customarily increased when the lower order traffic curves were involved. In some instances, asphalt concrete content may have exceeded one-half of the total thickness. For this reason, it was not possible to reconstitute all of the 1958 design curves faithfully. In the region where extrapolation was made, the 1958 design curves also do not parallel deflection lines but cross them in a prominent manner.

Rutting of Subgrade

Rutting in pavements is objectionable from the standpoint of steerage, riding quality, and hydroplaning (skid resistance). The amount of rutting that is tolerable in designs remains conjectural. It seems impractical and uneconomical to design pavements having as relatively high a rut resistance for low classes of roads as for high classes of roads. Indeed, the rutting criterion is violable in some proportion to the level of service expected from the road.

The use of the limiting strains in terms of equivalent repetitions (Table 1) implies the prevention of rutting equally throughout the full spectrum of traffic. In one sense, it implies that a pavement designed by using curve IV, for example, would not rut to any

greater extent than a pavement designed by using curve X. Obviously, this is an extremely conservative approach. It was not possible, here, to assign tolerable rut-depths to EAL accumulations. Conceptually, at least, rut depths permitted in pavements in the class of curve IV, for example, should be somewhat greater than those permitted in pavements in the curve X class. A judicious weighting may be exercised by interpolating thickness designs between limiting subgrade strains and limiting strains in the asphalt concrete. Of course, for those combinations of variables giving a greater pavement thickness for the asphalt strain criterion than for the subgrade strain criterion, the rutting criterion is not applicable.

It has been judiciously presupposed that full control of rutting should be attempted in pavements associated with traffic curves IX, X, XI, and XII. On the other hand, it seemed that curve IA pavements might be allowed to rut in a completely uncontrolled manner. The intervening eight traffic curves were assumed to delineate nine zones for which different rutting criteria could be specified. Because curve III, for example, delineates the third of these "traffic-rutting" zones, the final design thickness should be increased over the thicknesses required by the asphalt strain criterion by one-third of the difference between the pavement thicknesses required by the subgrade strain criterion and the asphalt strain criterion. This weighting scheme can be used to adjust pavement thicknesses for curves I through VIII to permit progressively less rutting to occur as traffic increases. Such a weighting in relation to the traffic group is provided for in the supplemental nomograph shown in Figure 2 for those regions of the graphs where rutting criteria control (Fig. 6). It is suggested that this weighting be considered as advisory. It may be violated permissibly in either direction—provided that the fatigue limit of the asphalt layer is respected.

Pavement Temperatures

The effective modulus of the asphalt concrete layer depends on pavement temperatures. To gain insight into temperature distributions within the pavement systems in Kentucky, we analyzed the data reported by Kallas (17) for College Park, Maryland. Inasmuch as College Park is at the same approximate latitude as Kentucky, it seemed appropriate as a first approximation to accept the College Park temperature distribution as being applicable to Kentucky.

By plotting the average high pavement temperatures and the average low pavement temperatures for a given thickness of asphalt concrete (Fig. 7), we noted that a sinusoidal distribution is typical for a year. If we assume that the average high temperatures are representative of daytime design conditions, that the average low temperatures are representative of nighttime conditions, and that 75 percent of the travel consists of daytime traffic, an intermediate temperature curve can be used, which might be considered appropriate for design purposes. This cyclic temperature distribution, however, is difficult to handle in a design procedure. Thus a further attempt was made to resolve a single design temperature.

Kallas' data indicated that the average annual pavement temperature was 64 F. It was further noted that the average pavement temperature was above the mean $5\frac{1}{2}$ months out of the year. As shown in Figure 7, an equivalent square-wave temperature distribution can be found for those temperatures in excess of the 64 F annual mean. Weighting these excess step-temperature distributions for various thicknesses of asphalt concrete suggests that 76 F might be considered an equivalent design temperature. The deviation of the values for the various thicknesses of asphalt concrete was approximately ±1 F.

Designs having smaller proportions of asphalt concrete might be expected to be less sensitive to rutting of the asphalt concrete than full-depth designs. This reduced susceptibility might be considered as an increase in the effective modulus of elasticity of the asphalt concrete. To obtain an estimate of how temperature susceptibility to rutting varies, we noted first that there was an approximate coincidence between Kentucky's current design curves and theoretical solutions for an asphalt concrete modulus corresponding to 64 F and pavements that consist of one-third asphalt concrete. Correlating the mean pavement temperature with the modulus of elasticity of the asphalt con-

crete according to Southgate and Deen (18), the moduli corresponding to 64 F and 76 F can be determined and plotted on Figure 8. If we assume a straight-line relation, Figure 8 then describes the change in asphalt concrete modulus as the temperature sensitivity to rutting varies. Designs obtained by using modulus values shown in Figure 8 would surely perform at least as well as current designs (employing usual proportions of dense-graded aggregate base and asphalt concrete surface courses). Other more refined weightings should be regarded as admissible.

Comparison With AASHO Design Guides

It has been reported (19, 20) that the performance of flexible pavements at the AASHO Road Test could be described by the equation

$$\log EAL = 9.36 \log (\overline{SN} + 1) - 0.20 + G_t/[(0.40 + 1{,}094/(\overline{SN} + 1)^{5.19}]$$

where EAL = number of 18-kip axle load applications, $\overline{SN}$ = structural number, and G_t = a function of the ratio of loss in serviceability to the potential loss to a time when the serviceability index is 1.5. This equation is specific only for soil and climatic conditions similar to those found at the AASHO Road Test site. To develop design charts for other soil support conditions, we found it necessary to establish a soil support scale. The starting point for this scale was a soil support value of 3.0, representing the load-carrying capability of the roadbed soils at the test site. A second point was based on the performance of pavement structures on an aggregate base sufficiently thick to minimize the effect of the subgrade soil. This point was given a value of 10.0 on the soil support scale. A linear scaling was assumed between the points of 3.0 and 10.0, suggesting that an additional term be added to the preceding equation to account for variable soil support conditions. The modified design equation would then become

$$\log EAL = 9.36 \log (\overline{SN} + 1) - 0.20 + G_t/[(0.40 + 1{,}094/(\overline{SN} + 1)^{5.19}] + k(S - 3.0)$$

where k = a coefficient and S = soil support value.

By using the correlation between soil support value and the Kentucky CBR reported by Hopkins (21), we can observe that there is essentially a linear relation between the soil support value and the log CBR, except for very high CBR values. To verify the preceding equation, we used design nomographs similar to the ones shown in Figure 2 to determine the relation between EAL's and the CBR. The result is shown in Figure 9. Figure 9 suggests that the relation between the EAL and the supporting capacity of the subgrade soil can be given by $\log EAL = A_0 + A_1 \log CBR$, where A_0 and A_1 are coefficients. For CBR's of less than 20, it was determined that the squares of correlation coefficients for the relations shown in Figure 9 ranged between 0.957 and 1.000 with a typical value of 0.987.

Figure 9 shows that the coefficients A_0 and A_1 are functions of pavement thickness, stiffness of the asphalt concrete, and ratio of asphalt concrete thickness to total pavement thickness. The structural number is a measure of these variables. Comparison of the two equations indicates that $A_0 = 9.36 \log (\overline{SN} + 1) - 0.20 + G_t/[(0.40 + 1{,}094)/(\overline{SN} + 1)^{5.19}]$ and $A_1 = f(k) = f(\overline{SN})$. It should be pointed out that the relation between the soil support value and the CBR (21) is an average correlation. Further analysis of the data relating soil support value to the Kentucky CBR suggested that the scatter of data could be accounted for (to a large degree) by variations in ratio of asphalt concrete thickness to total pavement thickness, verifying the possible dependency of A_0 and A_1 (or k) on structural number.

Other Considerations

In Figure 3 there appears to be some level of asphalt concrete tensile strain and stress at which the effect of the CBR is no longer significant. Selected curves are shown in Figure 3, which indicate the convergence of CBR lines at some low level of stress and strain. This pattern was noted over the entire range of values. An additional pattern of lines (Fig. 3) shows the relation between asphalt concrete tensile strain

Table 2. Limiting asphalt concrete tensile strains.

Traffic Curve	Number of 18-kip Axle Loads	Asphalt Concrete Modulus ($\times 10^{-4}$) 1,800 ksi	600 ksi	270 ksi	150 ksi
	5×10^3	3.69	4.92	6.03	7.03
IA	7.81×10^3	3.37	4.55	5.64	6.62
	1×10^4	3.20	4.36	5.43	6.40
I	1.56×10^4	2.91	4.03	5.08	6.03
II	3.12×10^4	2.50	3.57	4.58	5.50
	5×10^4	2.27	3.28	4.26	5.17
III	6.25×10^4	2.17	3.14	4.11	5.00
	1×10^5	1.96	2.89	3.82	4.70
IV	1.25×10^5	1.87	2.78	3.69	4.56
V	2.5×10^5	1.62	2.46	3.22	4.17
VI	5×10^5	1.40	2.18	3.00	3.81
VII	1×10^6	1.22	1.94	2.71	3.48
VIII	2×10^6	1.05	1.72	2.45	3.18
IX	4×10^6	0.91	1.52	2.20	2.89
	5×10^6	0.87	1.46	2.12	2.80
X	8×10^6	0.79	1.35	1.97	2.63
	1×10^7	0.75	1.29	1.91	2.56
XI	1.6×10^7	0.68	1.19	1.78	2.41
XII	3.2×10^7	0.59	1.06	1.61	2.20
	5×10^7	0.56	0.98	1.50	2.07
	1×10^8	0.46	0.87	1.36	1.90

Figure 6. Nomograph used to adjust design thicknesses for rutting criterion.

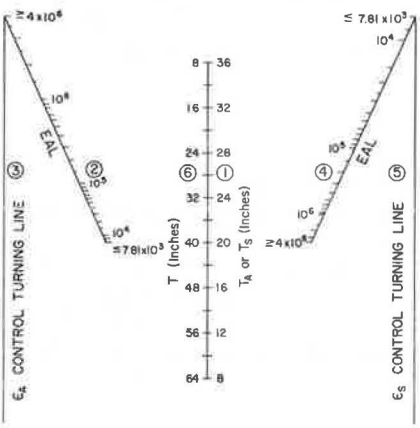

Figure 7. Pavement temperatures as a function of time.

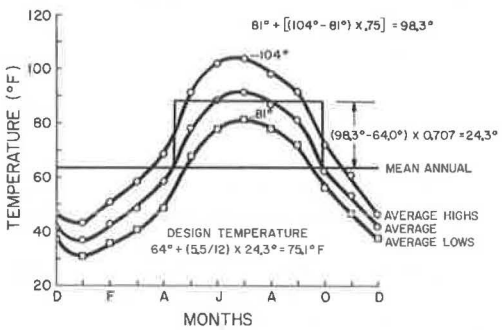

Figure 8. Weighting of asphalt concrete modulus.

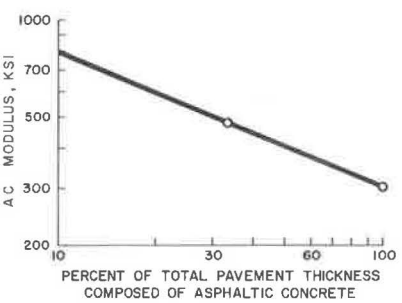

Figure 9. Relations between CBR's and EAL's.

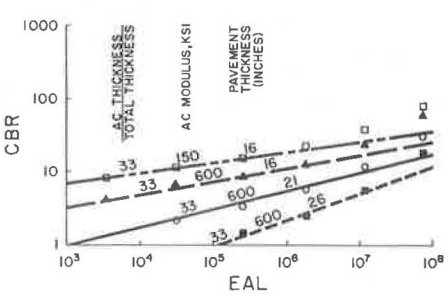

and stress when all variables are kept constant except the stiffnesses of the asphalt concrete and the aggregate base.

Conclusions

In order to determine pavement thicknesses from nomographs similar to the ones shown in Figure 2, we must know EAL's, the CBR of the subgrade soil, and the modulus of elasticity of the bituminous concrete. Such a set of nomographs permits selection of pavement structures employing alternative proportions of bituminous concrete and crushed stone base. Total thickness varies according to the proportion chosen. However, the choice may not be made arbitrarily. It is implicitly intended that the final selection be based on engineering considerations such as estimates of comparative construction costs, compatibility of cross sectional template and shoulder designs, uniformity of standardization of design practices, highway system classifications, engineering precedence, and utilization of indigenous resources. Designs based on 33 percent and 67 percent proportions of bituminous concrete (AC modulus of 480 ksi) and crushed rock base respectively conform to the department's current design chart, which shows current, conventional, or precedential design. The nomographs represent theoretical extensions of conventional designs and, from a theoretical standpoint, provide equally competent structures. However, they may not yet be employed with the same degree of confidence attributed to conventional designs.

REFERENCES

1. Michelow, J. Analysis of Stresses and Displacements in an N-Layered Elastic System Under a Load Uniformly Distributed on a Circular Area. Unpublished, Sept. 24, 1963.
2. Heukelom, W., and Foster, C. R. Dynamic Testing of Pavements. Jour. Structural Division, ASCE, No. ST1, Feb. 1960.
3. Lettier, J. A., and Metcalf, C. T. Application of Design Calculations to "Black Base" Pavements. Proc. AAPT, Vol. 33, 1964, pp. 221-234.
4. Heukelom, W., and Klomp, A. J. G. Dynamic Testing as a Means of Controlling Pavements During and After Construction. Proc., Internat. Conf. on Structural Design of Asphalt Pavements, Univ. of Michigan, 1962, pp. 667-697.
5. Drake, W. B., and Havens, J. H. Kentucky Flexible Pavement Design Studies. Univ. of Kentucky, Eng. Exp. Stat., Bull 52, 1959.
6. Proc., 2nd Internat. Conf. on Structural Design of Asphalt Pavements, Univ. of Michigan, 1967.
7. Seed, H. B., Mitry, F. G., Monismith, C. L., and Chan, C. K. Prediction of Flexible Pavement Deflections From Laboratory Repeated-Load Tests. NCHRP Rept. 35, 1967, p. 35.
8. Dormon, G. M., and Edwards, J. M. Developments in the Application in Practice of a Fundamental Procedure for the Design of Flexible Pavements. Proc., 2nd Internat. Conf. on Structural Design of Asphalt Pavements, Univ. of Michigan, 1967, pp. 99-108.
9. Dormon, G. M. The Extension to Practice of a Fundamental Procedure for the Design of Flexible Pavements. Proc., Internat. Conf. on Structural Design of Asphalt Pavements, Univ. of Michigan, 1962, pp. 785-793.
10. Dormon, G. M., and Metcalf, C. T. Design Curves for Flexible Pavements Based on Layered Systems Theory. Highway Research Record 71, 1965, pp. 69-84.
11. Mitchell, J. K., and Shen, C. K. Soil-Cement Properties Determined by Repeated Loading in Relation to Bases for Flexible Pavements. Proc., 2nd Internat. Conf. on Structural Design of Asphalt Pavements, Univ. of Michigan, 1967, pp. 427-452.
12. Van Der Poel, C. Chapter IX: Road Asphalt. In Building Materials (Reiner, M., ed.) Interscience Publishers, 1954, pp. 361-413.
13. Van Der Poel, C. Time and Temperature Effects on the Deflection of Asphaltic Bitumens and Bitumen-Mineral Mixtures. Jour., Society of Plastics Engineers, Vol. 11, No. 7, Sept. 1955, pp. 47-53.

14. Pell, P. S. Fatigue of Asphalt Pavement Mixes. Proc., 2nd Internat. Conf. on Structural Design of Asphalt Pavements, Univ. of Michigan, 1967, pp. 577-593.
15. Kasianchuk, D. A. Fatigue Considerations in the Design of Asphalt Concrete Pavements. Univ. of California, Berkeley, PhD dissertation, 1968.
16. Deacon, J. A. Fatigue of Asphalt Concrete. Univ. of California, Berkeley, DEng dissertation, 1965.
17. Kallas, B. F. Asphalt Pavement Temperatures. Highway Research Record 150, 1966, pp. 1-11.
18. Southgate, H. F., and Deen, R. C. Temperature Distribution Within Asphalt Pavements and Its Relationship to Pavement Deflection. Highway Research Record 291, 1969, pp. 116-128.
19. AASHO Interim Guide for the Design of Flexible Pavement Structures. Oct. 1961.
20. Langsner, G., Huff, T. S., and Liddle, W. J. Use of Road Test Findings by AASHO Design Committee. HRB Spec. Rept. 73, 1962, pp. 393-414.
21. Hopkins, T. C. Relationship Between Soil Support Value and Kentucky CBR. Division of Research, Kentucky Department of Highways, 1970.

DISCUSSION

R. L. Davis, Koppers Co., Inc.

The paper by R. C. Deen, H. F. Southgate, and J. H. Havens represents a laudable attempt to develop a general pavement design procedure based on rational criteria. The report undoubtedly represents a considerable effort on the part of the authors and the Kentucky Department of Highways, and congratulations are extended on the result of this effort. Furthermore, it appears to me that, in general, the approach is sound and in accord with some of the more widely accepted theories of pavement design. However, there are two things in the paper that cause me some uneasiness.

First, the modulus for the aggregate base E_2, shown in Figure 1, is entirely dependent on the CBR of the subgrade and the modulus of the asphalt concrete and is entirely independent of the quality of the aggregate itself. Although it can be readily admitted that both the CBR of the subgrade and the modulus of the asphalt concrete do influence the modulus of the granular base, it does not seem realistic to totally ignore the effect of the aggregate base material itself.

Second, the integration and weighting of the various factors that go into the calculation of EAL's to failure disturb me. Temperature is of particular concern because, if the temperature becomes low enough, the pavement may crack extensively without a single load passing over it; and, if the temperature becomes very high, relatively few traffic loads will cause excessive deformations. The resolution of these extremes into a single design temperature, especially when the extremes are so much more important to the design than the temperatures that lie between them, is a very difficult matter.

Nevertheless, I think that the design method outlined in this paper is an interesting approach to a general asphalt pavement design procedure, and I hope that properly instrumented test sections will be built to properly evaluate it.

R. G. Ahlvin and Y. T. Chou, U. S. Army Engineer Waterways Experiment Station, Vicksburg, Mississippi

The authors have presented a thorough and scholarly paper on the design of flexible pavements; it is a great step toward the application of theory to practice. A similar study has been conducted by the Corps of Engineers at the Waterways Experiment Station (WES) to develop a design procedure that combines theory with observed performance of numerous field test sections subject to aircraft loadings. In the WES analysis, the ratios of the elastic moduli of granular material to that of subgrade soil were evaluated by the use of the CBR equation. The results agree very well with the values used by the authors in analyzing pavement behaviors in Kentucky.

Formulation of the CBR equation was based on results of numerous full-scale accelerated traffic tests, which represented reliable data and extensive observations accumulated by the Corps of Engineers. A pavement designed by using the CBR equation has a thickness sufficient to prevent shear failure in the subgrade soil. Consequently, two pavements designed by using the CBR equation for the same coverage level would experience approximately equal shearing strain at the surface of the subgrade soils. Based on this principle, the elastic moduli of various pavement materials of conventional airfield flexible pavements were evaluated.

For subgrade soils of different CBR values, pavement thickness designed at capacity operation (5,000 coverages) for different single-wheel loads were computed by using the CBR equation (22).

$$t = \sqrt{P/8.1\ CBR - (A/\pi)}$$

where P is the wheel load and A is the contact area.

By considering the total pavement thickness as a single layer, i.e., neglecting the differences in the structural rigidity of the surface, base, and subbase materials, we computed the maximum shearing strains at the surface of the subgrade soil for different CBR ratios. For instance, for a 4-CBR subgrade soil, four different computations were carried out with the CBR values of the pavement structure above the subgrade being 8, 20, 32, and 40, which corresponded to ratios of 2, 5, 8, and 10 respectively. The computations were made by the Chevron program (1), which is based on Burmister's layered elastic theory. To convert CBR into elastic modulus E for use in the computer program, we used the relation E = 1,500 CBR.

The computed results are shown in Figure 10. It is seen that the computed values all plot along a smooth curve, indicating that pavements designed by the CBR equation yield equal computed maximum shearing strain at the surface of the subgrade soil when the computations are carried out for selected modulus ratios. With a ratio of 3, for instance, the maximum shearing strain γ_{max} at the surface of a 4-CBR subgrade soil subject to a 10-kip load is equal to γ_{max} at the surface of a 20-CBR subgrade soil subject to a 30-kip load (if 12 and 60 CBR are assigned respectively to the layers above the subgrade in the computations for these two pavements). Similarly, when the same loadings and a ratio of 5 are used, the maximum shearing strains would also be equal if 20 and 100 CBR were assigned respectively to layers above the subgrade. The same principle is applicable to other ratios. It should be pointed out here that the shearing strains so obtained are merely computed values, and their physical meanings are not specified.

The differences in the structural rigidities of component layers are considered in the layered analysis. The thicknesses of asphalt concrete and base course (well-compacted crushed stone) under different wheel loads were determined by Corps of Engineers standard flexible pavement design procedure. For all the pavements designed, the minimum thickness of subbase layer (sandy gravel) was 4 in.

In computations, the CBR value of the asphalt concrete was assumed to increase with increasing thickness of the layer because of its temperature-dependent nature. The thickness-CBR (or elastic modulus) relation used follows that developed by the Shell group (23), in which the CBR is exactly 100 at a thickness of 3 in. The CBR value of the base course material was assumed to be 1.5 times greater than the subbase material. In the case of strong subgrade soils, when the CBR value of the base course exceeded that of the asphalt concrete layer, the latter was arbitrarily increased to be equal to that of the former.

Figure 11 shows the result of layered analysis plotted in a manner similar to Figure 10. For a given wheel load, computations were carried out for several pavements with subgrade soils of different strengths; it was found that computed values could all be plotted along a smooth curve with almost no scattering. Each curve shown in Figure 11 represents the average of computed values for several pavements.

The results shown in Figure 11 indicate some very significant facts about the behavior of flexible pavements under aircraft loads. First, the thickness of the granular layer has no significant effect on its effective elastic modulus (or CBR value). Second,

Figure 10.

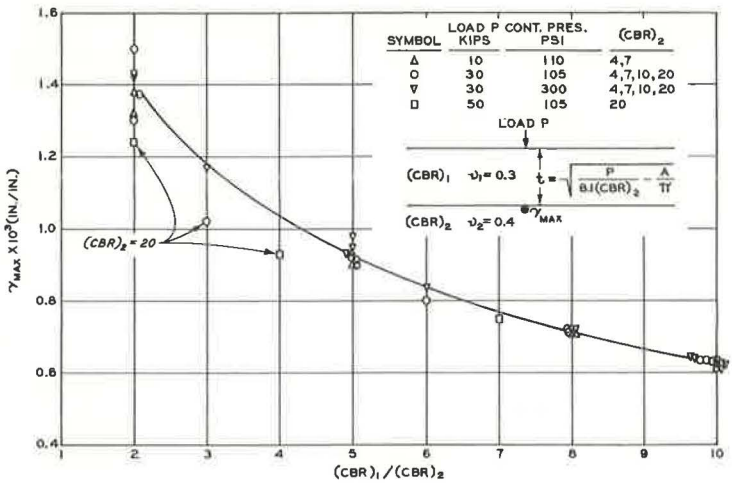

Figure 11.

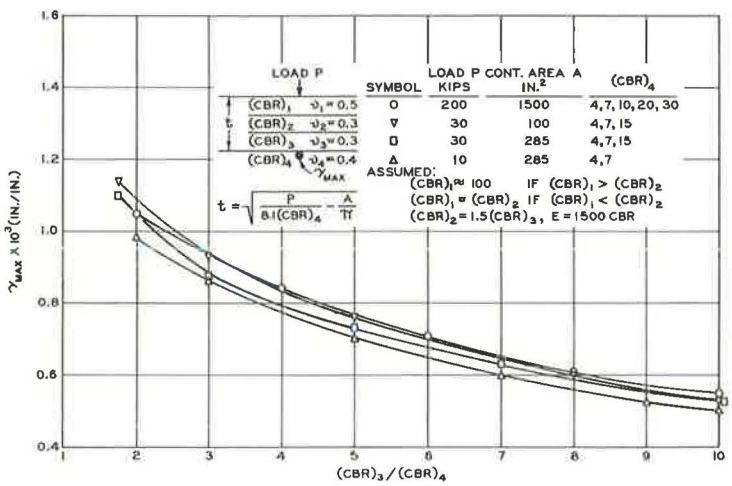

the effective modulus of granular material is not a constant but depends on the modulus of underlying materials. Also, equal maximum shearing strain at the surface of the subgrade soils can be obtained for two pavements designed by the CBR equation if the computations are carried out for the same modulus ratio, such as 2.8 used by the Kentucky Department of Highways. It should be pointed out that in Figure 1, for the straight line E = 1,800 ksi and for subgrade CBR's varying from 4 to 20, the modulus ratio varies only from 2.4 to 3.1; a value of 2.8 or 3 is actually a good average value for design purpose. Study conducted at WES (24) has shown that, with a modulus ratio of 3, good correlations were obtained when the observed performance of field test sections was plotted against the computed maximum shearing strain.

The significance of the elastic modulus ratio of the base material to the subbase material is discussed elsewhere (24).

References

22. Turnbull, W. J., and Ahlvin, R. G. Mathematical Expression of the CBR (California Bearing Ratio) Relations. Proc., 4th Internat. Conf. on Soil Mechanics and Foundation Engineering, 1957.
23. Izatt, J. O., Lettie, J. A., and Taylor, C. A. The Shell Group Methods for Thickness Design of Asphalt Pavements. Paper prepared for presentation to the Annual Meeting of the National Asphalt Paving Association, 1967.
24. Chou, Y. T., and Ledbetter, R. H. The Behavior of Airfield Flexible Pavements Under Loads—Theory and Experiments. U. S. Army Engineer Waterways Experiment Station, CE, Vicksburg, Mississippi, unpublished tech. rept.

AUTHORS' CLOSURE

It is acknowledged that the design curves presented in the paper do not allow for a variation in the quality of the aggregate used in the base course layer. As shown in Figure 1, the modulus of the aggregate base course is dependent on the CBR of the subgrade and the modulus of the asphalt concrete. It should be noted that the values represented by the intersection point of the curves shown in Figure 1 (CBR of 7 and a factor of 2.8) are based on 40 years of field experience in Kentucky. This intersection point represents the same control point relating experience with theoretical calculations used throughout the report. Thus, the relations shown in Figure 1 are related to aggregates typically used in base courses in Kentucky. Generally, dense-graded aggregates used in Kentucky are high-quality materials. It should be further noted that the straight-line relation of log F versus log CBR is an assumption, as is the value of CBR at factor value of 1. Strong implications can be derived from literature that suggests that confinement of an unbound granular base course is a very significant factor in the load-carrying capabilities of that layer. In this study, the confinement of the aggregate base course was represented by the modulus of elasticity of the asphalt concrete and the modulus of elasticity of the subgrade. The applicability to pavement design concepts of the ratio of elastic modulus of granular base material to that of the subgrade is also illustrated by work done at the Waterways Experiment Station. It is reassuring to note that field experience at the Waterways Experiment Station in full-scale tests and on Kentucky highways suggests essentially the same values for this ratio.

It should be realized that any attempt to prepare design guides will involve certain simplifications to put the design procedure within the scope of the practicing engineer. The resolution of a broad temperature regime into a single design temperature represents just such an effort. It would seem that the use of a single value for the modulus of elasticity of the asphalt concrete is probably no more serious than the assumption of a single CBR value for the life of the pavement. It is recognized that subgrade support varies over a broad range as environmental changes in moisture and temperature occur. These varying characteristics of the subgrade and asphalt concrete may be compensating to a degree. When design procedures based on single values of input parameters are used, engineering judgment must consider the possible effects of extreme environmental variations occurring during the life of the pavement.

DETERMINATION OF THE ELASTIC MODULI OF FLEXIBLE PAVEMENT COMPONENTS

H. C. S. Han, T. J. Hirst, and H. Y. Fang, Lehigh University

ABRIDGMENT

•AN extensive investigation of the applicability of the AASHO Road Test design equations to conditions in Pennsylvania has included field evaluation of the elastic moduli of a number of flexible pavement components. These moduli have been used to develop improved structural coefficients for each component studied.

The field tests were conducted in the eastern part of Pennsylvania during the summers of 1969 and 1970. Each flexible pavement that was studied consisted of the same asphalt concrete surface layer, one of five base types (aggregate bituminous, aggregate cement, aggregate lime pozzolan, bituminous concrete, or crushed aggregate), and a crushed aggregate subbase. The pavement sections were supported on subgrade soils having a range of supporting capacities.

Each field test site included a 1,000-ft section of the pavement. At a randomly selected location in the outer wheelpath of each test section, plate load deflections were measured on the surface of each layer of the pavement. On each layer, three different unit plate pressures were repeatedly applied and released, and the resulting deflection and rebound movements of the plates were recorded.

The elastic moduli for each layer were computed by two methods. Burmister's (1) two-layer elastic theory was applied to the problem by considering the deflection of each layer as being comprised of the deflection due to the layer immediately below the plate plus a composite deflection due to all of the layers beneath the upper one. By starting with the subgrade modulus determined directly from plate load deflections on the subgrade, we computed the modulus of each layer above the subgrade from knowledge of the deflections on that layer and a composite modulus of all layers underneath.

A second approach utilized an axisymmetric finite element program (2). The pavement was modeled as a four-layered linearly elastic system with each layer having its own elastic modulus. The system was divided into a series of triangular elements, and an "overrelaxation" technique was used to solve the simultaneous displacement equations resulting from the element formulation. An iterative procedure was introduced to develop individual layer moduli that provide computed deflections matching those measured in the field plate loading tests.

A comparison of the results obtained by each method is shown in Figure 1 where the subgrade moduli determined from both Burmister's theory and the finite element analysis for 12-in. diameter plates subjected to various applied unit pressures are shown. It may be seen that the variation of subgrade moduli between those obtained from Burmister's theory and those from the finite element analysis is small.

Figure 2 shows the variation of subbase modulus with thickness for both the equivalent two-layered system and the finite element method. It may be seen that, within the range of subbase thicknesses from 6 to 9 in., the variation of modulus with thickness is much more pronounced than for thicknesses outside this range. When the thickness of subbase is less than the radius, or exceeds approximately 1.5 times the radius of the loaded area, the subbase modulus is independent of its thickness. This range may be defined as an "effective thickness." It is important to note that the range of effective thickness depends on the type of subbase material in use as well as on the area of

Sponsored by Committee on Strength and Deformation Characteristics of Pavement Sections.

Figure 1. Deflection versus subgrade modulus.

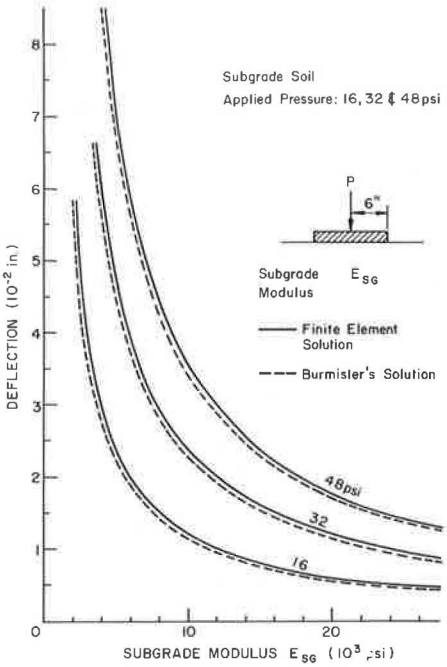

Figure 2. Variation of subbase moduli with thickness.

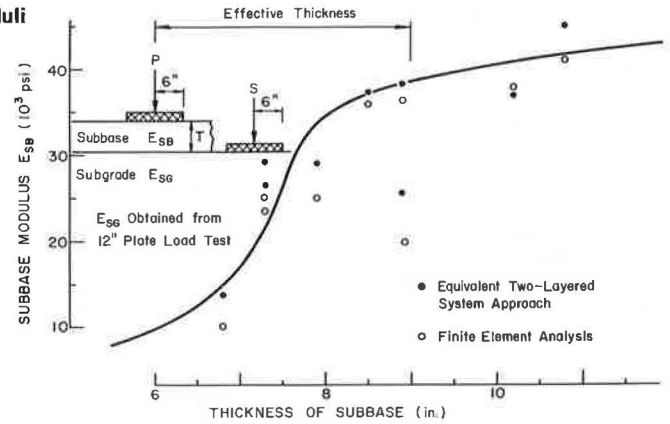

Figure 3. Variation of base moduli with thickness.

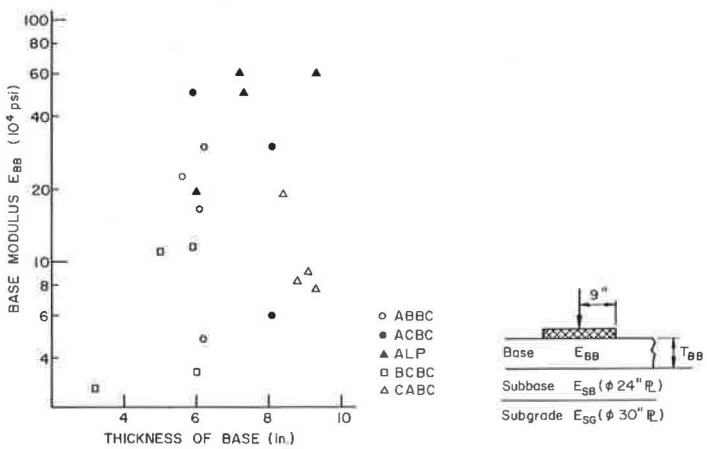

loading. The subbase material analyzed in this study is a crushed aggregate having laboratory CBR values ranging from 89 to 144 percent.

The moduli of the five base types computed from the finite element analysis are shown in Figure 3. Considerable scatter in the computed moduli is apparent. However, certain trends in behavior may be noted. The magnitudes of the elastic response of each of the five base types are significantly different, extending over a range of more than one order of magnitude. The aggregate lime pozzolan exhibits the highest moduli, and the crushed aggregate and the bituminous concrete have similarly low moduli. No conclusions regarding the influence of thickness of base course on the moduli can be made because of the restricted range of thicknesses present in the pavement sections studied.

All pavement sections studied were constructed of the same asphalt concrete surface course, each having essentially the same thickness. The elastic moduli determined for each pavement were relatively constant; the average value was 143,000 psi.

It is concluded that there is good agreement between the subgrade modulus determined from Burmister's theory and that computed by using the finite element formulation. For the unstabilized crushed aggregate subbase studied, there is an effective thickness for which the modulus increases effectively with increase in thickness. Outside of the range of the effective thickness, the modulus remains approximately constant. Although there is considerable scatter in the computed base moduli, certain trends in behavior are evident. In particular, an order of magnitude change in the modulus is evident over the range of base types studied. This suggests that the careful selection of base course material is necessary to ensure satisfactory load-deflection performance of a pavement system.

A pavement is designed to perform at loads that are presumably well below the system failure loads. Structural coefficients that are used to characterize the load-carrying ability of the pavement components should reflect the stress-strain response of the system in this loading range. Field determined elastic moduli represent useful in-service parameters that permit realistic comparative evaluation of pavement materials and hence their structural coefficients.

ACKNOWLEDGMENTS

The work reported here was sponsored by the Pennsylvania Department of Transportation and the Federal Highway Administration. The authors would like to express their sincere appreciation to W. G. Weber, Jr., and Gaylord Cumberledge of the Pennsylvania Department of Transportation for their advice and assistance. The opinions, findings, and conclusions expressed in this publication are those of the authors and not necessarily those of the sponsors.

REFERENCES

1. Burmister, D. C. The Theory of Stresses and Displacements in Layered Systems and Applications to Design of Airport Runways. HRB Proc., Vol. 23, 1943, pp. 126-144.
2. Ducan, J. M., Monismith, C. L., and Wilson, E. L. Finite Element Analysis of Pavements. Highway Research Record 228, 1968, pp. 18-33.

PREDICTING LOW-TEMPERATURE CRACKING FREQUENCY OF ASPHALT CONCRETE PAVEMENTS

J. J. Hajek, Department of Transportation and Communications of Ontario; and
R. C. G. Haas, University of Waterloo, Ontario

Low-temperature shrinkage cracking of asphalt pavements is a serious and costly problem throughout much of Canada and the northern United States. The large amount of effort devoted to the problem has provided several design approaches. This paper describes the latest and most comprehensive of such a design approach. A mathematical model based on field observations has been developed and is capable of predicting the frequency of cracking at various ages in the pavement life. The variables used involve stiffness of the original asphalt cement, winter design temperature, subgrade soil type, thickness of the asphalt concrete, and age of the pavement. Data for the variables are commonly recorded by highway agencies. The model provides a very powerful design approach in that serviceability losses and maintenance costs are directly related to degree of cracking. If these are intolerable, new designs can be generated and very quickly and easily tested by the model. The paper provides a numerical example, including a nomograph for solving the model. The model is "reasonable" in its use of the variables, and the degree of error involved is acceptable.

•NONTRAFFIC load associated cracking forms one of the three principal pavement design subsystems recognized by several authorities including The Asphalt Institute (1). In Canada and in the northern United States, this cracking of flexible pavements is primarily caused by low winter temperatures that induce tensile forces in the asphalt concrete. If the induced tensile forces exceed the tensile strength of the material, cracks are formed. Because the pavement cannot predominantly contract in the longitudinal direction, most low-temperature cracks are formed in the transverse direction to the highway route. These cracks are an annual multimillion dollar damage problem in Canada alone (2).

Various agencies and individuals have devoted considerable research effort to the problem. These investigations, both field- and laboratory-oriented, have led to the following design concepts for controlling or eliminating low-temperature cracking:

1. Limiting penetration and viscosity requirements on the asphalt cements;
2. Limiting strain or stiffness of the asphalt concrete (3, 4); and
3. Calculating fracture temperature [i. e., temperature at which the cracks are likely to be formed (5, 12)].

Although these concepts provide some very useful quantitative guidelines, they take into account only some of the variables that influence low-temperature cracking. Moreover, they do not allow predictions to be made of losses in pavement serviceability due to cracking during the pavement life.

The major objective of the study described in this paper was to develop a relation between field low-temperature pavement performance of asphalt pavements, in terms of low-temperature transverse cracking frequency, and variables of recognized significance on this frequency, which are usually recorded by highway agencies. Such a

Sponsored by Committee on Flexible Pavement Design.

relation should make it possible to predict the low-temperature cracking frequency of newly planned highways at various ages. In turn, this will allow estimates to be made of the loss of pavement serviceability plus maintenance costs, due to cracking, in future years. If the estimates are considered to be excessive, a new design may be generated and again evaluated.

VARIABLES INFLUENCING LOW-TEMPERATURE CRACKING FREQUENCY

Variables influencing low-temperature cracking frequency and methods for their measurement have been presented elsewhere (6). In the following discussion, only factors of recognized significance in low-temperature cracking, which are generally recorded by highway departments and which will be subsequently used for the transverse pavement cracking prediction model, are considered.

Stiffness of Asphalt Cement or Mix

The influence of stiffness of the asphalt cement on low-temperature cracking has been reported and demonstrated by many investigators (3, 7). The major difficulty encountered here was the selection of the method to be used for obtaining asphalt and/or mix stiffness at temperatures when the cracks are likely to be formed. The methods for stiffness determination of bituminous materials at low temperatures may be classified as follows. Direct methods, based on direct testing of the materials; and indirect methods that estimate the stiffness modulus of bituminous materials by using their rheological properties at higher temperatures assessed by direct standard tests. Several various direct and indirect methods have been proposed and used.

A recent statistically designed experiment (8) showed that the efficient, indirect methods appear to estimate stiffness to a reasonably satisfactory degree necessary for prediction of low-temperature cracking frequency. As the best indirect method for the given purpose, a slightly modified version of McLeod's method was recommended. The selection of this method of stiffness determination has been made on the basis of 43 field observations (Tables 1 and 2) according to a statistical relation between stiffness moduli determined by various indirect methods and the appropriate low-temperature cracking frequency. The analysis also showed that the stiffness modulus of the original asphalt cement generally exhibits a greater degree of association with the cracking frequency than the stiffness moduli of field-aged asphalt cements and asphalt concretes (8). The use of stiffness of original asphalt cement has further advantages in that its value can be forecast on the basis of historical data.

Calculation of Stiffness

The stiffness of asphalt cement is calculated for a loading time of 20,000 sec and a temperature equal to a minimum ambient temperature chosen on a probabilistic basis of frequency and length of occurrence. Only the knowledge of penetration of the asphalt cement at 77 F and its viscosity at 275 F is required. From these two values, the penetration index (PI) may be determined, using Figure 1, based on the method recommended by McLeod (3). If the PI of the asphalt cement is known, we can use the nomograph shown in Figure 2 to calculate the value of the base temperature, which corresponds to the temperature of $T_{R\&D}$. In the final step, the stiffness modulus is estimated by using the nomograph shown in Figure 3.

Climatic Conditions

The results of Ste. Anne Test Road (7) demonstrated that most low-temperature transverse pavement cracks were initiated when the temperature decreased to a certain level for a certain time period. This shows that the formation of low-temperature cracks depends on overall winter climatic conditions. Thus, if we want to obtain a linear relation between cracking frequency and stiffness of asphalt cement (or mix), the ambient temperature that prevails most when cracks are initiated should be used for calculation of stiffness.

Because of the foregoing, a winter design temperature, defined as the lowest temperature at or below which only 1 percent of the hourly ambient air temperatures in January occur for the severest winter during a 10-year period, has been established in this study. This temperature was used to calculate stiffness moduli. The empirical relation between air freezing index (40-year average) and the winter design temperature developed on the basis of limited data for Ontario and southern Manitoba is shown in Figure 4. This relation can be modified as more data are available. In the meantime, it can serve as a guide for estimating winter design temperatures when only freezing indexes are known.

Age of Pavement

Results of transverse crack frequency surveys, involving more than 1,900 miles of paved highways in Alberta (10), showed an increase of cracking frequency with pavement age. The increase of low-temperature cracking frequency can be caused both by increase of stiffness of asphalt mix and by increase of the probability of occurrence of more extreme low temperatures, which increases with pavement age.

Thickness of Asphalt Concrete Layer

The Ste. Anne Test Road (7) showed that increase of the thickness of asphalt concrete layer (from 4 to 10 in.) results in only half of the low-temperature cracking frequency when all other variables were the same. This difference in pavement performance may be explained by the relatively good insulating properties of asphalt concrete (8).

Pavement Foundations

It has been reported several times that the transverse cracking frequency for pavements placed over sand subgrades is considerably higher than for pavements placed over clay subgrades, all other variables being constant (6, 7). A similar effect on pavement performance caused by a 16-in. thick granular base was reported by McLeod (11).

MATHEMATICAL MODEL

Purpose of Mathematical Model

The foregoing discussion showed that low-temperature cracking frequency depends on many variables, some of which interact with one another. A mathematical model enables one to produce an overall functional relation when one variable, in this case cracking frequency, is a multivariable function of a large number of independent variables, i. e., stiffness of asphalt concrete, age and thickness of asphalt concrete layers, winter design temperature, and type of subgrade.

Description of Data Used

From the practical point of view, the aim of the mathematical model is to predict the low-temperature cracking frequency of future asphalt concrete pavements on the basis of past experience, that is, to make generalizations from observed data in space and time. To increase the scope of generalization as well as to provide unbiased estimates within this scope, one should choose the observations used for construction of a mathematical model in a random manner from all possible observations in the space where the future predictions are to be made. Because this requirement could not be satisfied, we decided to use all available observations that satisfied given requirements to eliminate a personal bias. It was assumed that the observations that would become available during the course of the work, or later on, could be used for checking purposes.

The observations used in this study, most of which were obtained through the courtesy of the Department of Transportation and Communications of Ontario (DTCO), are summarized in Table 1. The DTCO data were collected from subobservations by using an arithmetic mean. The observations based on the results of the Ste. Anne Test Road were extracted in a similar manner from tables given elsewhere (7).

Table 1. Transverse pavement cracking data.

Observation Number (1)	Source (2)	Locality and/or DTCO Contract Number (3)	Transverse Cracks per 500 ft W (4)	X (5)	Y (6)	Z (7)	CI (8)	Original Asphalt Pen. at 77 F (9)	Vis. at 275 F (cs) (10)	PI (11)	AC Stiffness (kg/cm²) (12)	FI (degree-days) (13)	WDT (deg C) (14)	AC Thickness (in.) (15)
1	D	Arkona A	1	10	21	36	21	98	151	-1.8	80	650	-20	3.7
2	D	Arkona B	0	0	1	9	1	91	368	-0.6	25	650	-20	3.7
3	D	Arkona C	0	1	0	2	1	95	427	-0.3	22	650	-20	3.9
4	D	63088, Grand Bend	0	0	0	0	0	87	338	-0.7	31	650	-20	2.2
5	D	61078, Highway 11	0	7	3	10	9	84	425	-0.3	301	1,850	-30	4.6
6	D	61025, South River	2	17	5	10	22	87	208	-1.4	630	1,880	-30	4.2
7	D	60102, Highway 11	0	10	10	54	15	171	141	-1.3	170	1,900	-30	4.0
8	D	Sault Ste. Marie to Heyden	0	3	3	5	5	89	331	-0.7	230	1,650	-28	5.5
9	D	Heyden to Haviland Bay	2	10	18	18	20	96	211	-1.3	400	1,750	-28	3.2
10	D	Agawa	0	1	0	0	1	161	256	-0.3	220	2,650	-35	4.5
11	D	60041, Highway 17	0	1	0	1	1	145	222	-0.7	370	2,650	-35	3.1
12	D	Orangeville A	0	10	37	61	23	84	205	-1.4	320	1,450	-26	3.2
13	D	Orangeville B	0	1	10	6	6	157	142	-1.3	66	1,450	-26	3.1
14	D	58277, Highway 17	0	2	1	4	3	175	270	-0.8	60	1,650	-28	3.4
15	D	Val Albert easterly	0	10	43	22	33	153	226	-0.6	900	3,450	-40	2.1
16	D	Val Albert	0	1	2	7	2	153	223	-0.7	1,000	3,450	-40	2.0
17	D	62065, Madoc-Ivanhoe	0	0	0	0	0	85	420	-0.3	125	1,400	-26	2.3
18	D	56384, Highway 28	0	1	1	0	2	176	252	-0.2	61	1,550	-27	5.3
19	D	62185, Highway 62	0	0	0	0	1	151	250	-0.5	51	1,550	-27	2.5
20	D	61124, Highway 69	0	6	17	19	15	87	382	-0.5	150	1,480	-26	4.6
21	D	61113, Parry Sound	0	1	13	27	8	85	450	-0.3	125	1,480	-26	3.0
22	D	62609, Highway 12 Orillia	0	6	5	13	8	83	216	-1.4	360	1,500	-26	5.0
23	D	60183, Highway 62	0	4	1	1	5	168	226	-0.5	80	1,900	-30	3.7
24	D	61052, Highway 62	0	2	0	0	2	168	243	-0.3	85	1,880	-30	3.7
25	D	60131, Highway 41 Caledon	0	0	0	3	0	154	203	-0.8	60	1,500	-27	3.3
26	7	Ste. Anne Road Test	-	62	0	-	63	192	110	-1.6	1,850	3,250	-40	4.0
27	7	Ste. Anne Road Test	-	-	-	-	0	159	225	-0.5	680	3,250	-40	4.0
28	7	Ste. Anne Road Test	-	-	-	-	0	313	86	-1.4	540	3,250	-40	4.0
29	7	Ste. Anne Road Test	0	25	0	0	25	192	110	-1.6	1,850	3,250	-40	4.0
30	7	Ste. Anne Road Test	-	-	-	-	0	159	225	-0.5	680	3,250	-40	4.0
31	7	Ste. Anne Road Test	0	8	0	0	8	313	86	-1.4	540	3,250	-40	4.0
32	7	Ste. Anne Road Test	0	10	1	0	10	192	110	-1.6	1,850	3,250	-40	9.9

Note: Original asphalt properties of observations 1 and 2 are those given by Gulf Oil Canada Ltd. In column 2, D = DTCO, and 7 is reference number. In columns, 4, 5, 6, and 7, W = multiple, X = full, Y = half, and Z = partial. In column 8, CI = cracking index. In column 9, penetration of 100 grams for 5 sec. In column 13, freezing index is based on a 40-year average. Winter design temperatures given in column 14 are derived from column 13 according to Figure 4. In column 19, 12 and 7 are reference numbers, and P = estimated by using a pedologic map.

Table 2. Check on model.

Observation Number	Locality and/or DTCO Contract Number	Original Asphalt Pen. at 77 F	Original Asphalt Vis. at 275 F (cs)	Climate FI (degree-days)	Climate WDT (deg C)	AC Stiffness (kg/cm²)	AC Thickness (in.)	Age (years)	Subgrade Description	Subgrade Method
33	60181, Highway 17, Black River	183	171	2,650	-35	270	1.9	6	Lacustrine deposits	G[a]
34	59177, Highway 11, New Liskeard	170	139	2,800	-36	720	5.0	7	Silty clay loam	P[b]
35	60138, Highway 11, Earlton	144	277	2,830	-36	350	3.1	5	Clay	P
36	62030, Highway 11, Englehart	180	313	2,850	-36	120	3.1	3	Mostly silt and loam	P
37	53023	90	350	1,450	-26	155	4.1	13	Unknown	-
38	57121, Highway 17, Iron Bridge	180	306	1,650	-28	25	3.1	9	Varved or massive clay and silt	G
39	52080	90	350	1,150	-24	115	3.9	14	Unknown	-
40	59038, Highway 17, North Bay	164	259	2,000	-30	80	3.6	8	Mostly sandy till	G
41	Brampton, test road, sections 16, 18, 35, 36	89	312	700	-20	25	5.5	6	Clay	D[c]
42	60122, Highway 17, North Bay	159	139	2,000	-30	215	3.0	7	Mostly sandy till	G
43	Saskatoon Airport, Taxi A	158	315	4,000	-42	420	6.0	9	Silty clay	T[d]

Note: For an explanation of abbreviations, see Table 1.

[a]G = map of surficial geology. [b]P = pedologic map. [c]D = DTCO. [d]T = Canadian Department of Transport.

Age (years) (16)	Subgrade			No. Sub-obser-vations (20)	Obser-vation Num-ber (1)
	Description (17)	Code (18)	Method (19)		
6	Clay	2	12	10	1
6	Clay	2	12	9	2
6	Clay	2	12	7	3
3	Sand	5	P	2	4
5	Sandy loam	3	P	8	5
4	Sandy loam	3	P	6	6
6	Sandy loam	3	P	2	7
5	Clean granular	5	12	6	8
6	Clean granular	5	12	8	9
6	Sandy loam	3	12	3	10
6	-	-	-	3	11
6	Silty sand	3	12	3	12
6	Silty sand	3	12	3	13
8	Sandy loam	3	P	3	14
3	Deep sand fill	5	12	5	15
3	Clayey sand	2	12	7	16
5	Clayey loam	2	P	3	17
11	Sandy loam	3	P	3	18
5	Gravelly sandy loam	3	P	2	19
5	Sandy loam	3	P	6	20
6	Sandy loam	3	P	4	21
5	Sandy loam	3	P	6	22
7	Sandy loam	3	P	6	23
6	Sandy loam	3	P	4	24
7	Sandy loam, rocky phase	3	P	3	25
2	Sand	5	7	-	26
2	Sand	5	7	-	27
2	Sand	5	7	-	28
2	Clay	2	7	-	29
2	Clay	2	7	-	30
2	Clay	2	7	-	31
2	Clay	2	7	-	32

Figure 1. Modification of McLeod's graph for estimation of penetration index.

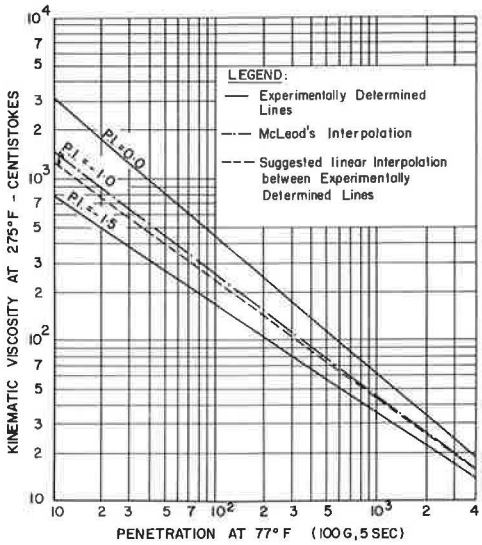

Cracking Index

CI for Subob-servations	Estimated			Agree-ment	Obser-vation Number
	Sand	Loam	Clay		
11, 4, 4	6.2	6.9	6.1	Yes	33
16, 40	-	21.6	16.1	Yes	34
4, 6, 25, 48	-	-	4.5	?	35
5, 1, 2, 1	0	0	0	Yes	36
14, 13	18.3	20.5	21.0	Yes	37
2, 7, 2, 2, 1, 9	-	0	0	Yes	38
0, 4, 6, 12, 17, 20	18.0	20.7	21.7	?	39
0, 1, 0, 0, 2, 2	0	1.7	-	Yes	40
0	-	-	2.5	Yes	41
17, 18, 24	9.3	10.7	-	No	42
0, 1	-	-	2	Yes	43

Figure 2. Pfeiffer's and Van Doormaal's nomograph for determination of penetration index.

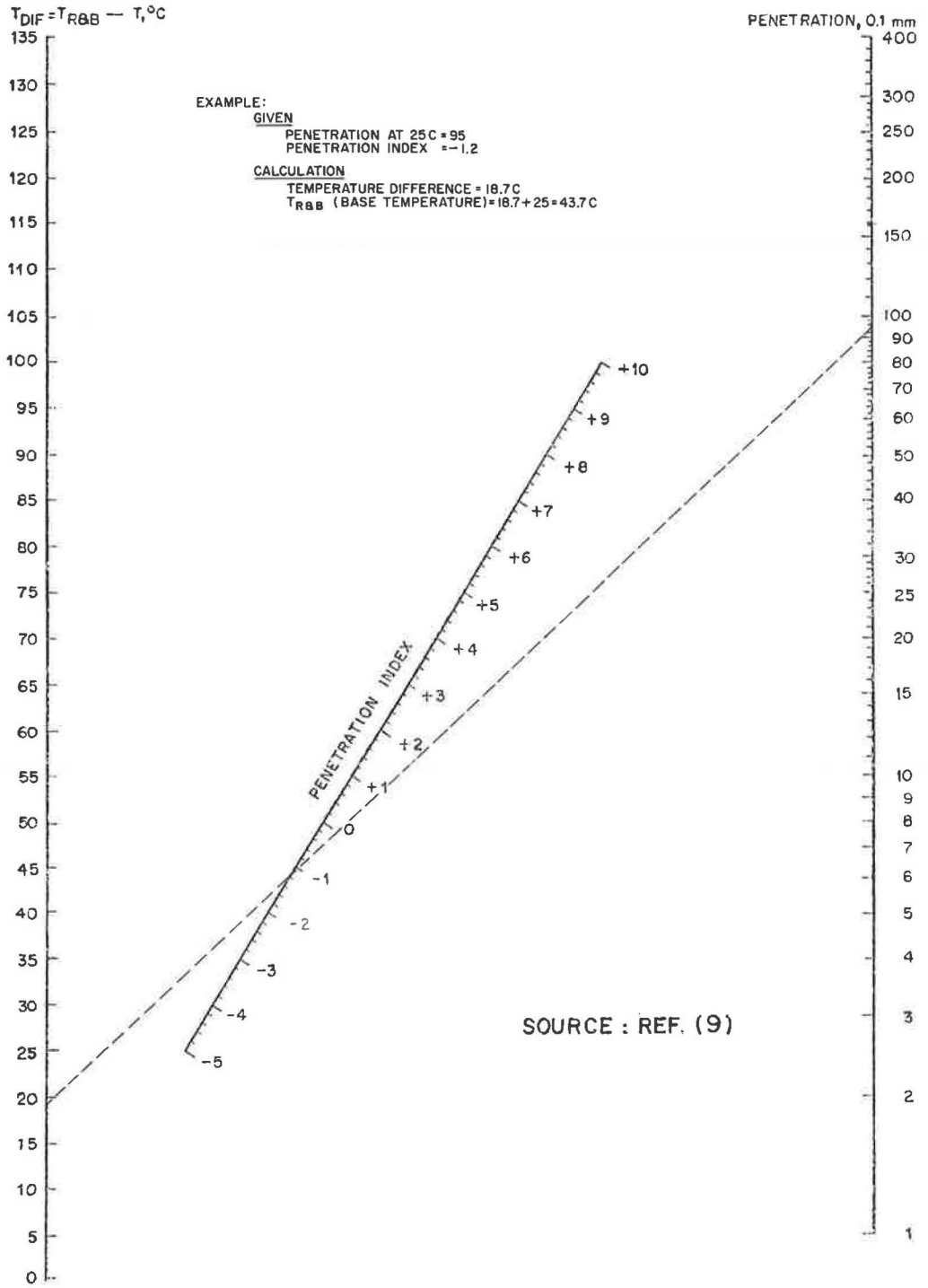

Figure 3. Van Der Poel's nomograph for determination of stiffness modulus of bitumens.

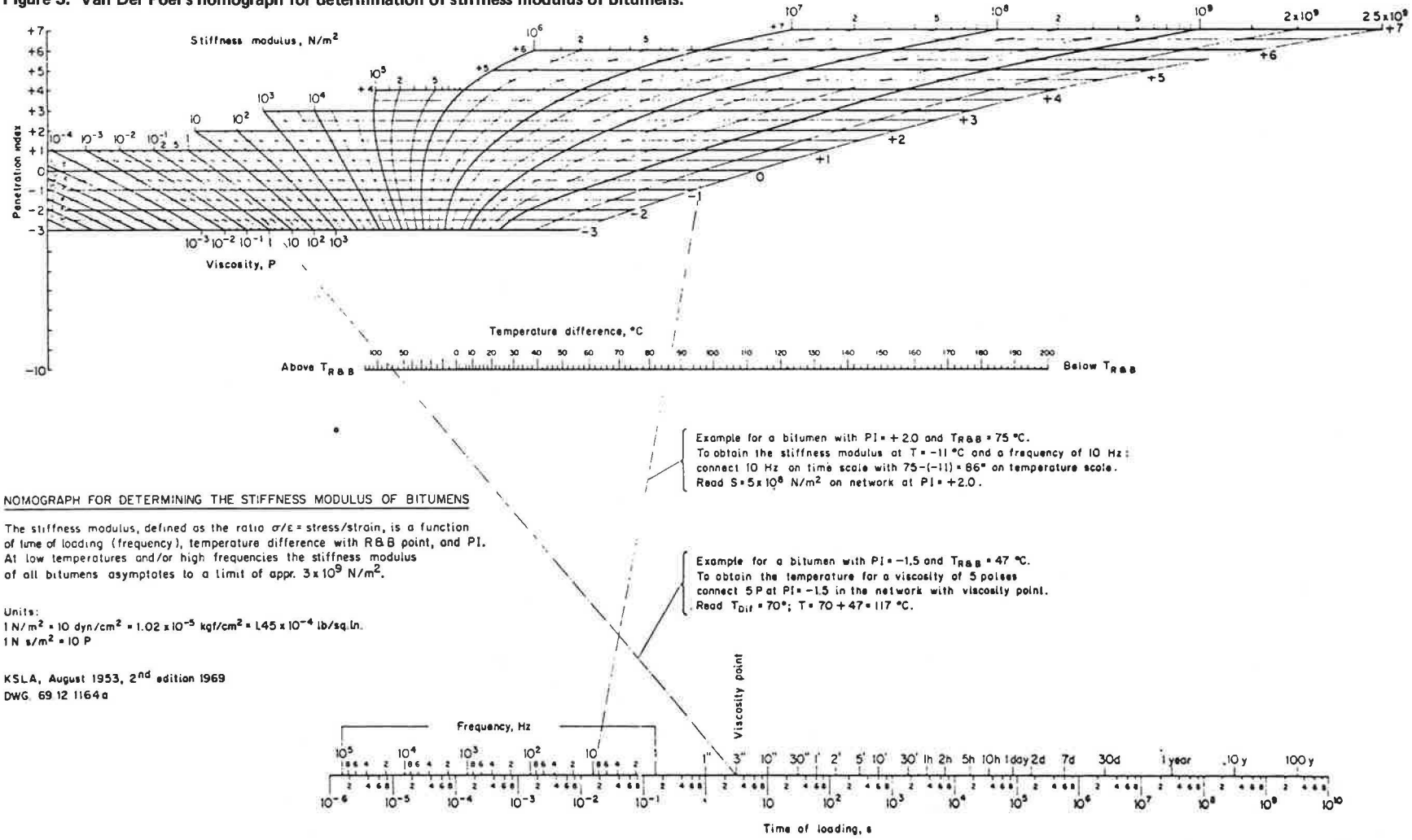

NOMOGRAPH FOR DETERMINING THE STIFFNESS MODULUS OF BITUMENS

The stiffness modulus, defined as the ratio σ/ε = stress/strain, is a function of time of loading (frequency), temperature difference with R&B point, and PI. At low temperatures and/or high frequencies the stiffness modulus of all bitumens asymptotes to a limit of appr. 3×10^9 N/m².

Units:
1 N/m² = 10 dyn/cm² = 1.02×10^{-5} kgf/cm² = 1.45×10^{-4} lb/sq.in.
1 N s/m² = 10 P

KSLA, August 1953, 2nd edition 1969
DWG. 69 12 1164a

Dependent Variable—Definition of Cracking Index

The cracking index, introduced by the DTCO and defined as the number of full and half transverse cracks per 500-ft section of two-lane highway, does not include transverse cracks less than one-half of roadway width. The assumption is that such cracks usually occur subsequent to the formation of half and full cracks, and therefore they are not a primary manifestation of low-temperature pavement cracking (12). It should be pointed out that the values of cracking indexes given in Table 1 are based on field counts. Thus, they refer to transverse pavement cracking frequency (13) rather than to the low-temperature cracking frequency per se.

Selection of Independent Variables

The stiffness of original asphalt cement, determined by the modified McLeod method, was selected as the sole representative of asphalt and/or mixture properties related to low-temperature cracking frequency. In addition to the reasons behind this decision given previously, the use of the stiffness modulus has the advantage of combining several variables into one and thus reducing the complexity of the mathematical model. It was felt that the addition of variables not included in the model (i. e., aggregate absorption, coefficient of thermal expansion of aggregate, and thickness of granular material forming the subbase) might result in improvement of both statistical validity and applicability of the model, but values of these variables were not available.

Construction of Mathematical Model

Construction of the model consisted of finding a function that relates the cracking index, I, to other variables, that is, to find

$$I = f(s, t, a, m, d)$$

where

I = cracking index, $I \geq 0$;
s = stiffness of original asphalt cement determined for temperature m and loading time of 20,000 sec by modified McLeod method, $(kg/cm^2) \times 10^{-1}$;
t = thickness of all asphalt concrete layers, in.;
a = age of asphalt concrete layers, years;
d = type of subgrade (dimensionless code: 2 is clay, 3 is loam, and 5 is sand); and
m = winter design temperature, deg C × -0.10.

The determination of the function could not be deduced solely on the basis of theoretical mathematical considerations and past experience. Only the following limiting conditions could be set forth:

1. Whenever the modulus of stiffness equals zero, the function must give zero as a value. The same requirement may be set for age, but it can be assumed that, whenever this variable is equal to zero, the modulus of stiffness is inevitably equal to zero as well because of the interaction of variables.
2. With increase of stiffness and/or age, the cracking index should increase when all other variables are fixed.
3. With unlimited increase of thickness, the cracking index should decrease without limit if all other variables remain constant.

The following suggested model was arrived at by testing and evaluating more than 20 various functions:

$$10^{I} = c_1 \times s^{(c_2 + c_3 t + c_4 a)} \times c_5^{d} \times c_6^{m} \times d^{c_7 s} \qquad (1)$$

where I, s, t, a, m, and d are the original dependent and independent variables defined previously; and $c_1, c_2, \ldots, c_7$ are constants of the model.

Estimation of constants in the model has been done in two steps:

1. The model represented by Eq. 1 was linearized by taking logarithms of both sides of the equation as follows:

$$I = \log c_1 + c_2 \log s + c_3 t \log s + c_4 a \log s + \log c_5 d + \log c_6 m + c_7 s \log d \qquad (2)$$

where $\log c_1$, c_2, c_3, ..., c_7 are partial regression coefficients, and log s, t log s, a log s, ..., log d are transformed independent variables.

2. The constants of the linearized model (regression equation) were calculated by using the least squares method and a stepwise regression computer program. The sequence of transformed independent variables added to the regression equation, and their contribution to the increase of the proportion of the total variance explained by the regression equation is given in Table 3. The abbreviated printout for the last step is interpreted in Tables 4 and 5.

By substituting the calculated constants given in Tables 4 and 5 into Eq. 1 and taking appropriate antilogs where necessary, we get the suggested mathematical model for prediction of low-temperature cracking frequency of asphalt concrete pavements in the following form:

$$10^I = 2.497 \times 10^{30} \times s^{(6.7966 - 0.8740\,t + 1.3388\,a)} \times (7.054 \times 10^{-3})^d \times (3.193 \times 10^{-13})^m \times d^{0.6026\,s} \qquad (3)$$

Equation 3 shows that the model satisfies the limiting conditions, provided that stiffness of asphalt cement is equal to or greater than 1.0 kg/cm^2.

EVALUATION OF THE MODEL

The model was evaluated in terms of its statistical significance, rational behavior, and relation to observed data. Also, limitations of the model were outlined.

Statistical Evaluation

The two biggest values of the simple regression coefficients given in Table 6, $r_{5,6}$ and $r_{6,7}$, suggest that there is a degree of association between the pairs of transformed independent variables 5,6 and 6,7. Because the dependencies between these pairs of independent variables are nonlinear, they can be included in the regression equation (14).

The significance of the multiple correlation coefficient of the model, R = 0.91, can be judged by the method developed by Fisher (15). We can say, according to the method, that the true correlation is at least 0.81 in the universe from which the sample was drawn, with 1 change in 20 being wrong on the average. Table 3 shows that 82.2 percent of the total variance is explained by the regression equation. The standard error of estimate is 6.2 of the cracking index. By comparing this standard error of estimate with the average observed standard deviation of the cracking index (calculated for DTCO observations aggregated from more than two subobservations), which is 3.61, we can conclude that the standard error of estimate of 6.2 of the cracking index is comparable. For example, the observed standard deviation of the cracking index for the Arkona Test Road, section A, is 4.4. Statistical significance of the partial regression coefficients of the transformed independent variables is given in Table 5.

Rational Behavior of the Model

The behavior of the model and the isolated effects of the independent variables may be best demonstrated by means of a graphic presentation. The model has five original independent variables. If values are assigned to any four of these, the resulting equation may be plotted in the form of a two-dimensional graph (dependent variable versus original independent variable), which represents a 2-variable trace of the multidimensional space defined by the model.

Figure 4. Relation between freezing index and winter design temperature.

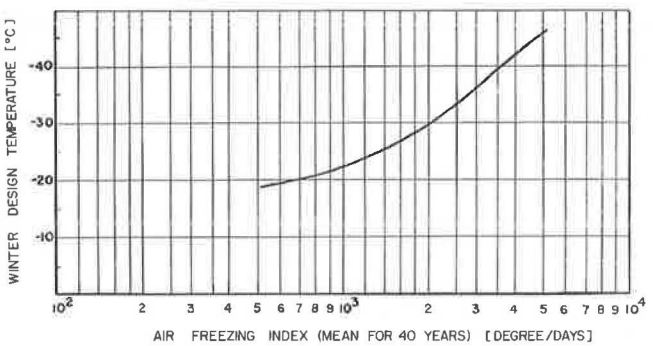

Table 3. Summary of stepwise regression analysis.

Step Number (1)	Transformed Independent Variable Included (2)	Multiple Correlation Coefficient R (3)	Multiple Correlation Coefficient R^2 (4)	Increase in R^2 (5)	F-Value to Enter the Equation (6)	Significance of Addition (percent) (7)	Standard Error of Estimate (cracking index) (8)
1	s log d	0.7570	0.5730	0.5730	40.2562	0.5	8.8228
2	m	0.8491	0.7210	0.1480	15.3814	0.5	7.2538
3	a log s	0.8787	0.7721	0.0511	6.2750	2.5	6.6723
4	d	0.8906	0.7931	0.0210	2.7469	20	6.4734
5	t log s	0.9021	0.8138	0.0207	2.8695	20	6.2582
6	log s	0.9068	0.8222	0.0084	1.1868	30	6.2358

Note: In column 1, step number equals the number of transformed independent variables included in regression equation. In column 4, R^2 multiplied by 100 gives the percentage of the total variance explained by the regression equation in a given step. In columns 6 and 7, 6.2750, for example, means that by adding variable a log s to the previous two variables already in the equation, statistical effect of this addition measured by F-test is equal to 6.2750. For the appropriate degrees of freedom ($n_1 = 1$ and $n_2 = 28$), 6.2750 is significant at 2.5 percent probability level (column 7). We can conclude that the addition of the third variable a log s results in a significant improvement of the equation with only two independent variables having 2.5 percent probability of being wrong.

Table 4. Analysis of variance.

Variance	Degrees of Freedom	Sum of Squares	Mean Square	F Ratio	Level of Significance (percent)
Due to regression	6	4,496.723	749.454	19.273	0.1
Residual	25	972.130	38.885	-	-
Total	31	5,468.853	176.414	-	-

Note: Multiple correlation coefficient = 0.9068. Standard error of estimate = 6.2358.

Table 5. Partial regression coefficients.

Transformed Independent Variable	Partial Regression Coefficient	Standard Error	Value of Student t Test	Level of Significance[a] (percent)
s log d	0.6026	0.0836	7.18	0.1
m	-12.4958	3.3902	3.68	0.5
a log s	1.3388	0.6570	2.03	10.0
d	-2.1316	1.1808	1.80	10.0
t log s	-0.8740	0.4340	2.02	10.0
log s	6.7966	6.2387	1.09	25.0

Note: Constant term of regression equation = 30.3974.

[a]Refers to the 2-sided test for zero hypothesis.

Table 6. Correlation matrix of linearized model.

	Variable						
Variable	i	t log s	a log s	d	m	log s	s log d
i	1.000	0.265	0.150	0.233	0.240	0.502	0.757
t log s		1.000	0.059	-0.012	0.580	0.726	0.560
a log s			1.000	0.128	-0.012	0.192	-0.072
d				1.000	0.172	0.156	0.374
m					1.000	0.852	0.687
log s						1.000	0.782
s log d							1.000

This has been done in Figures 5 through 9 for observations 1, 2, 6, and 29 given in Table 1. The assumption is that the original independent variable, for which the 2-variable trace is plotted, can obtain any value (in the range used for the construction of the model), whereas values of all remaining original independent variables, for the given observation, are fixed.

Thickness of Asphalt Concrete Layers

The isolated effect of thickness of asphalt concrete layer on the cracking index is shown in Figure 5. The increase of thickness of asphalt concrete layer results in a decrease of low-temperature cracking frequency. The decrease is not constant for different highway sections. This is quite rational because we cannot expect a low cracking index, observed after several years of pavement service, to be decreased by the assumed increase of thickness to the same degree as a considerably high cracking index, particularly if the latter one was observed for an area with lower winter design temperature.

Age of Asphalt Concrete Layers

The separated effect of age of asphalt concrete pavements on the cracking index (Fig. 6) is in many respects similar to the effect of thickness. In this case, however, the index increases with an increased pavement age. Again, we cannot expect that the same increase of cracking index will result for different highway sections.

Type of Subgrade

Figure 7 shows the isolated effect of type of subgrade, identified by the given code, on the cracking index. With a change of subgrade from clay to sand, the cracking index for the observations with extremely low winter design temperatures (i. e., -40 C) significantly increases. For observations of (-20 C) winter design temperatures, type of subgrade does not exhibit a significant effect. This behavior of the model may be considered rational on the basis of the following explanation.

The initial decrease of temperature below the freezing point results in formation of ice crystals, which may be accompanied by an increase in the volume of soil. This increase is probably more pronounced in the case of sandy soils because practically all their water becomes frozen. At the same time, the decrease of temperature causes contraction of the soil particles. According to the model, the effect of the initial increase of volume of sandy soils, caused by formation of ice crystals, is overcome by shrinkage induced by further temperature decrease at a winter design temperature of approximately -30 C. The quite different effect of clay and sand subgrade on the cracking index at this and lower temperatures was explained by Hajek (8), who used a soil-water retention theory.

Stiffness of Original Asphalt Cement

The isolated effect of the stiffness modulus of original asphalt cement on the cracking index is shown in Figure 8. As stiffness increases, the cracking index increases.

Winter Design Temperature

Figure 9 shows that, when winter design temperature decreases, the cracking index decreases as well. This is quite rational because the winter design temperature was used for calculation of stiffness. For example, in the case of observation 29, the model predicts a cracking index of 23.3 for a winter design temperature that is equal to -40 C. The observed cracking index for this condition was 25. If the four other original variables of the model (thickness, age, stiffness, and type of subgrade) are held constant and the winter design temperature is assumed to be equal to -30 C, the predicted cracking index equals 35.8. This is logical because stiffness calculated for the temperature of -40 C is assumed to be the same as stiffness calculated for the temperature of -20 C.

Figure 5. Predicted effect of thickness on cracking index.

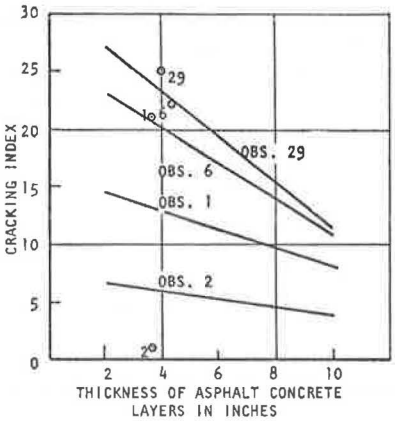

Figure 6. Predicted effect of age on cracking index.

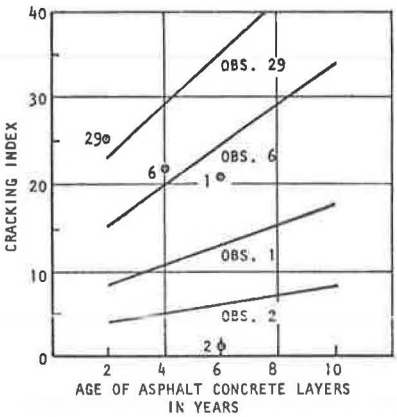

Figure 7. Predicted effect of type of subgrade on cracking index.

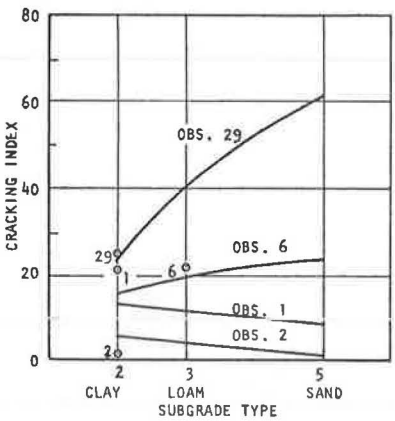

Figure 8. Predicted effect of stiffness modulus on cracking index.

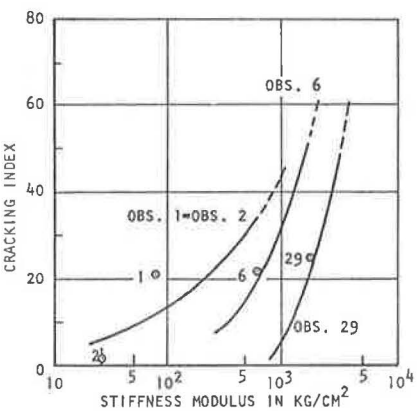

Figure 9. Predicted effect of winter design temperature on cracking index.

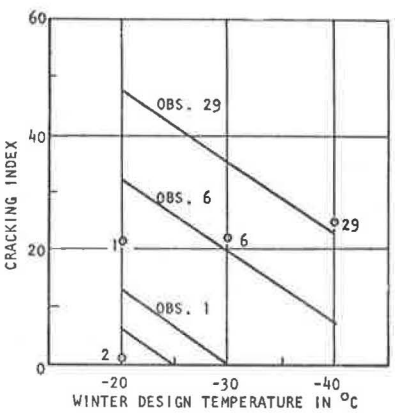

Relation to Observed Data

The observed values of the cracking index are plotted against values estimated by the model shown in Figure 10. Generally, a good agreement may be noted; nevertheless, for several observations a considerable difference between estimated and observed values of the cracking index was obtained. Several explanations of this fact can be offered, and some of them are discussed in the section devoted to limitations of the model.

Testing of the Model

The model was tested using all additional observations that had become available. Some of these observations were not used for construction of the model because of the uncertainty encountered in determining subgrade type. The result of the check, given in Table 2, suggests that the model can be used for design purposes with a reasonably high degree of confidence.

Limitations of the Model

The most significant limitation, imposed by the regression analysis used for the calculation of constants and the statistical evaluation of the model, was the assumption that all independent variables are measurable on interval or ratio scales, which was not the case for the variable type of subgrade. On the other hand, Hajek (8) in an extensive discussion showed that the use of a different code for expressing the effect of subgrade type (i.e., 1 is sand, 2 is loam, and 3 is clay) would result in a very similar prediction model as far as its statistical significance and rational behavior are concerned. The present difficulties encountered in developing the interval scale for measuring the effect of type of subgrade on low-temperature cracking frequency may be overcome by developing separate prediction equations for different subgrade types—on the condition that enough observations are available (8).

The additional limitations inherent in the model are as follows:

1. The suggested model may not represent the "true law" that governs low-temperature transverse cracking frequency. Moveover, the 32 observations used for construction of the model are not usable (so far as their number and selection are concerned) as a basis for establishing such a "true law."
2. Extrapolation outside the range of values of the original variables used is "risky."
3. The least squares solution provided by the regression analysis is valid for the linearized model (Eq. 2) but not for the original model (Eqs. 1 and 2).
4. The model was constructed to fit the cracking index, but the model predicts the low-temperature transverse cracking frequency, assuming as was demonstrated (7) that most of the transverse pavement cracks in the region investigated are low-temperature cracks. The model does not have, for example, any provision for including transverse cracks caused by shrinkage associated with absorptive aggregates (16), reflection transverse pavement cracks through overlays, and so forth.

Example Application

The major significance of the suggested model is seen in its immediate capacity to provide an engineering solution to the problem of minimizing low-temperature transverse pavement cracking in North America. For an illustration of the procedure involved, the following numerical example is provided.

Let us assume that we want to predict the low-temperature transverse cracking frequency of a newly planned asphalt concrete pavement throughout its service life. The following variables are known:

1. The ambient freezing index (40-year average) is estimated as equal to 1,650 degree-days;
2. Thickness of asphalt concrete pavement is 4 in.;
3. Reference to pedological and topographical maps reveals that we can expect poorly graded sands with some fines as a subgrade type; and

Figure 10. Observed cracking index versus cracking index estimated by model.

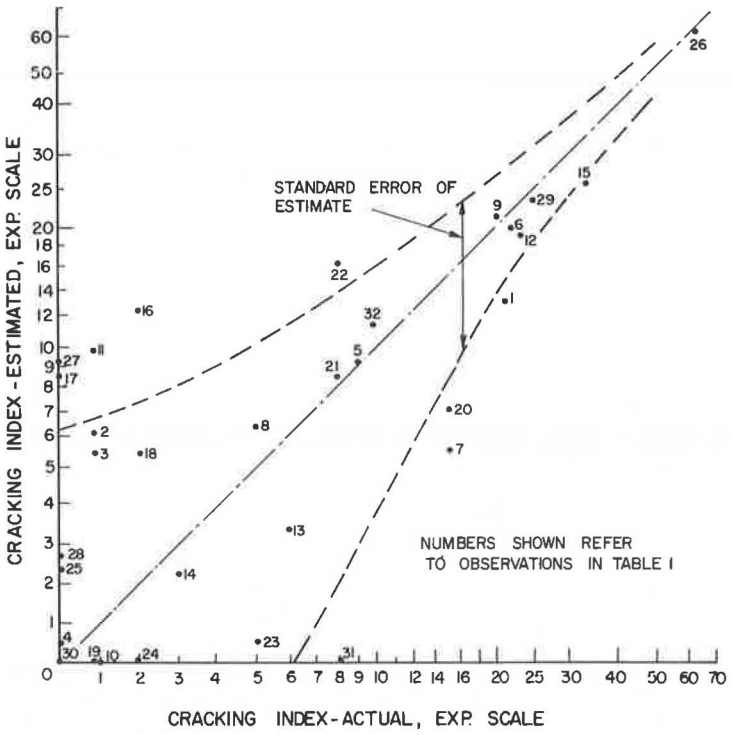

Figure 11. Nomograph for predicting low-temperature cracking frequency of asphalt pavements.

MODEL : $10^{I} = 2{\cdot}4970 \times 10^{30} \cdot s^{(6{\cdot}79660 - 0{\cdot}87403t + 1{\cdot}33884a)} \cdot (7{\cdot}0539 \times 10^{-3})^{d} \cdot (3{\cdot}1928 \times 10^{-13})^{m} \cdot d^{0{\cdot}60263s}$

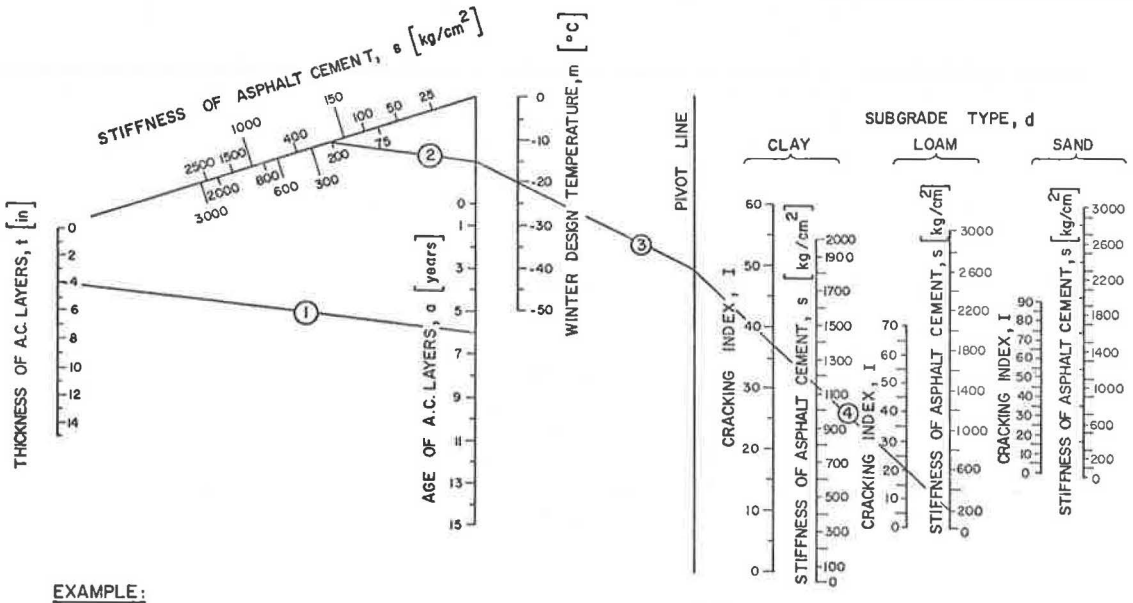

EXAMPLE:

thickness = 4 inches
age = 6 years
stiffness of original asphalt cement = 200 kg/cm²*
winter design temperature = -20°C
subgrade type = loam

*for temp. = m and time = 20000 sec.

NOTE:

A) lines ① and ② are parallels
B) in step ④ select scales for the appropriate subgrade type

RESULT: cracking index = 20 at 6 years

4. The asphalt cement to be employed has the following original properties—penetration at 77 F, 100 gram, 5 sec = 95 and viscosity at 275 F = 210 cs.

The computation procedure consists of the following steps:

1. The expected minimum ambient temperature, equal to -27 C, is derived from the freezing index (Fig. 4);
2. Penetration index of asphalt cement, equal to -1.2, is obtained by means of Figure 1;
3. Ring and ball temperature, equal to 43.7 C, is determined by using the nomograph shown in Figure 2;
4. Modulus of stiffness of original asphalt cement is estimated by using the nomograph shown in Figure 3. [For a temperature -27 C (see step 1) and for a loading time of 20,000 sec, stiffness modulus of asphalt cement is equal to 205 kg/cm^2];
5. On the basis of the ordinal scale described (5 is sand, 3 is loam, and 2 is clay), it was decided to use code 5 for the type of subgrade; and
6. By substituting all required variables into Eq. 3 and solving for the cracking index (or by using the nomograph shown in Fig. 11), we get a cracking index of 7.7 for an age of 5 years and 16.5 for 10 years.

The standard error of the estimate is 6.2. Finally, if the designer concludes that the loss of pavement serviceability due to cracking may be too high for the particular conditions (subgrade type and thickness of asphalt concrete layer), he may use an asphalt cement with a lower modulus of stiffness by using softer asphalt cement and/or less temperature-susceptible asphalt cement (e.g., a 150- to 200-penetration asphalt of the same source). If all other variables remain equal, then a significantly lower cracking index would result. If such a change does not violate any other constraints (i.e., mix stability, fatigue life requirements, and so forth), the softer asphalt cement should be employed as a new design.

Additional Comments on the Modeling Approach Used

This paper has demonstrated only that a quite reasonable design model for predicting low-temperature cracking frequency of asphalt pavements can be developed from easily obtainable data. It must be emphasized though that this is not necessarily the best or the only model possible. Certainly, more data on additional variables and from more sections would be desirable.

It must also be emphasized that, because the model uses indirectly determined stiffness values, this does not necessarily imply that stiffness determination is most reliable from such methods. The available data only permitted the indirect type of analysis. For control or specification purposes, the use of direct, fundamental methods of stiffness determination has been recommended (1).

CONCLUSIONS

Low-temperature transverse cracking of asphalt pavements is a serious and costly problem in many parts of North America. Considerable effort has been devoted to investigating the problem and finding solutions.

This paper demonstrates that it is now possible to develop a model for predicting the frequency of such cracking. A very powerful design tool is thereby provided in that serviceability losses and maintenance costs can be related to degree of cracking.

The model presented in this paper is considered to be "reasonable" and to have an acceptable limit to the error involved. Moreover, only easily obtainable data are required, and the use of the model in design is very simple and quick.

ACKNOWLEDGMENTS

The study upon which this paper is based was funded primarily by the National Research Council of Canada and Gulf Oil Canada Ltd. The assistance and cooperation of the Department of Transportation and Communications of Ontario in supplying data are gratefully acknowledged. In particular, we thank W. Phang, H. Fromm, and A. Rutka.

REFERENCES

1. Kasianchuk, D. A., Terrel, R. L., and Haas, R. C. G. A Design System for Minimizing Fatigue, Permanent Deformation and Shrinkage Fracture Distress of Asphalt Pavements. Proc. Third Internat. Conf. on Structural Design of Asphalt Pavements, London, Sept. 1972.
2. Haas, R. C. G. The Performance and Behaviour of Flexible Pavement Surfaces at Low Temperatures. Proc., Canadian Tech. Asphalt Assn., 1968.
3. McLeod, N. W. Prepared Discussion on Ste. Anne Test Road. Proc. Canadian Tech. Asphalt Assn., 1969.
4. Anderson, K. O., and Hahn, W. P. Design and Evaluation of Asphalt Concrete With Respect to Thermal Cracking. Proc. AAPT, Vol. 37, 1968.
5. Burgess, R. A., Kopvillem, O., and Young, F. D. Ste. Anne Test Road—Relationships Between Predicted Fracture Temperatures and Low Temperature Field Performance. Proc. AAPT, 1971.
6. Hajek, J. J., and Haas, R. C. G. Some Factors Influencing Low-Temperature Cracking of Flexible Pavements and Their Measurement. Proc., Canadian Tech. Asphalt Assn., 1971.
7. Young, F. D., Deme, I., Burgess, R. A., and Kopvillem, O. Ste. Anne Test Road: Construction Summary and Performance After Two Years Service. Proc., Canadian Tech. Asphalt Assn., 1969.
8. Hajek, J. J. A Comprehensive System for Estimation of Low-Temperature Cracking Frequency of Flexible Pavements. University of Waterloo, Ontario, Transport Group Report, 1971.
9. Kopvillem, O., and Heukelom, W. The Effect of Temperature on the Mechanical Behaviour of Some Canadian Asphalts as Shown by a Test Data Chart. Proc., Canadian Tech. Asphalt Assn., 1969.
10. Shields, B. P., Anderson, K. O., and Dacyszyn, J. M. An Investigation of Low-Temperature Cracking of Flexible Pavements. Proc., Canadian Good Roads Assn., 1969.
11. McLeod, N. W. Transverse Pavement Cracking Related to Hardness of the Asphalt Cement. Proc., Canadian Tech. Asphalt Assn., 1968.
12. Haas, R. C. G., and Phang, W. A. Case Studies of Pavement Shrinkage Cracking as Feedback for a Design Subsystem. Highway Research Record 313, 1970, pp. 32-43.
13. Standard Nomenclature and Definitions for Pavement Components and Deficiencies. HRB Spec. Rept. 113, 1970, 29 pp.
14. Irick, P. E., et al. The Use of Multiple Regression and Correlation in Test Road Data. HRB Proc., Vol. 35, 1956, pp. 268-298.
15. Ezekiel, M., and Fox, K. A. Methods of Correlation and Regression Analysis, 3rd Ed. John Wiley and Sons, Inc., 1959.
16. Tuckett, G. M., Jones, G. M., and Littlefield, G. The Effects of Mixture Variables on Thermally Induced Stresses in Asphaltic Concrete. Proc. AAPT, 1970.

COMPUTATION OF STRESSES AND STRAINS FOR THE DESIGN OF FLEXIBLE PAVEMENTS

S. F. Brown, University of Nottingham, England

The development of improved design methods for flexible pavements requires an analytic tool that is relatively simple and cheap for use in routine design. Currently linear-elastic theory is considered the most satisfactory for this purpose, but the various solutions available are themselves rather inconvenient to use. Tabulated results for three-layer systems require a lengthy interpolation procedure to obtain results for variables other than those tabulated. On the other hand, the powerful and flexible multilayer computer programs require a large, fast computer and can thus be expensive to run. A computer program called "Interpolation" has been developed to carry out interpolation calculations on the three-layer elastic-layered system results tabulated by Jones in 1962. The object of this program is to provide a pavement design tool, considered to be more convenient than either the tables themselves or the complex multilayer computer programs now available. The interpolation procedure is based on fitting a curve to the log-log plot of stress function against each of the dependent variables used by Jones, which specify the system. The results have the same restrictions as Jones' tables, namely that all layers have a value of 0.5 for Poisson's ratio, and results are produced on the centerline of a single wheel load at the two interfaces. From a design point of view, this latter restriction is not likely to be important. The "Bistro" multilayer computer program was used to check the accuracy of results, and this appears satisfactory for design purposes. The Interpolation program has been incorporated in a simplified pavement design program in which an approximate nonlinear analysis may be used if required.

•ONE of the main objects of current highway research is the development of improved design methods for flexible pavements. The need for such research results from the recognition that current methods of design rely heavily on empirical rules that cannot be used with confidence in the heavy-load situations that are likely to exist in the future or under unusual environmental conditions.

The development of a structural design approach, which has been sometimes termed the "rational" approach, aims to reduce empiricism and establish pavement design on a reliable theoretical base. This approach is analogous to that used in other fields of civil engineering design, and it has been outlined in several papers (1, 2, 3).

There are many problems to be solved before the structural design method can be used with confidence for general design work. Many of these problems are associated with the behavior of paving materials (4) and with the correlation of laboratory-determined results and field performance (5).

The availability of high-speed digital computers has helped the development of pavement design during recent years. It has given impetus in particular to the solution of analytic problems concerned with the behavior of layered systems. Linear-elastic analysis (6, 7), viscoelastic analysis (8), and the use of finite-element techniques (9, 10) have all been made possible by the availability of computers.

The application of systems analysis to the problem of pavement design has also arisen because of the increasing use of computers, and several systems and subsystems have been proposed (11, 12).

Sponsored by Committee on Flexible Pavement Design.

The long-term aim of developing improved pavement design procedures may well be toward a complete pavement design computer program dealing with all aspects of the design problem. In the meantime, increasing use is being made of available programs for analyzing pavement structure, whereas the remainder of the design process is carried out manually. To increase interest in this approach and to help in the development of a complete design program, we need to develop an analytic technique that is simple, fast, and accurate.

Currently, the most widely used analytic procedures are those based on linear-elastic theory. The computer programs developed by the Shell (6) and Chevron (7) organizations allow computation of stresses, strains, and deformations in multilayered pavement systems at any depth and radius relative to the applied surface load. There is complete freedom of choice of elastic constants for the layers and geometry of the system. These programs have a capability beyond routine design requirements and are hence mainly of use as research tools. In addition, they require large high-speed computers and are not ideal for building into a complete pavement design program.

The only alternatives available for design computations, where precise accuracy and comprehensive stress distributions are not necessary, are tabulated stress functions for three-layer systems. The most comprehensive of these were produced by Jones (13), but in practice there are a number of restrictions that make their use time-consuming and tedious.

There was a need, therefore, for an analytic procedure that fell between these two where the emphasis was on design use, which implies speed, convenience, and reasonable accuracy. The program "Interpolation" described herein is an attempt to fulfill this need.

ANALYTICAL REQUIREMENTS FOR PAVEMENT DESIGN

The three-layer linear-elastic system (Fig. 1) is thought to be a reasonable approximation of a flexible pavement structure (14). The top layer embraces all asphalt-bound layers, the second layer includes the unbound materials, and the subgrade forms the third, semi-infinite layer.

The maximum stresses and strains are the ones that require computation for design purposes. In a pavement, they generally occur on the centerline of the load and either just above or just below the interfaces.

With the current state of knowledge of material behavior, it is not possible to stipulate the elastic constants needed for analysis with great accuracy. Research has shown that soils and unbound materials behave in a nonlinear-elastic manner when subjected to dynamic loading, though for pavements with a thick asphalt layer the effect of this has been shown to be small (10). A successive approximation procedure has been used to cope with this problem while still using basically linear analysis (15). The finite-element analyses (9, 10) are based on this procedure. It can only be followed, however, if appropriate laboratory tests have been carried out to specify the nonlinearity. Hence, a single value of modulus is generally used for each layer.

Both the powerful multilayer computer programs and the tabulated stress functions for three-layer systems have disadvantages. The former requires access to large high-speed computers, and the computing time involved in solving a particular problem is relatively high. Because of their flexibility, a large number of data cards are required for each system in order to specify elastic constants, loads, geometry, and coordinates of the points where solutions are required.

The tables produced by Jones (13) allow the vertical and radial stresses and strains just above and below the interfaces of a three-layer system to be obtained on the axis of the load (Fig. 1). Poisson's ratio for all layers was taken as 0.5, and stress functions were tabulated for four variables, which were as follows:

$$k_1 = E_1/E_2;\ k_2 = E_2/E_3;\ H = h_1/h_2;\ a_1 = a/h_2$$

where

E_1, E_2, and E_3 = elastic modulus of each layer,
h_1 and h_2 = thickness of the two upper layers, and
a = radius of the loaded area.

The tables were produced for all combinations of four values of k_1 and k_2, seven values of H, and six values of a_1. For each of these, six stress functions were produced, which was the minimum number required to give the stresses and strains at the four positions involved. The stress functions (where σ_r is the horizontal, radial stress) were for a unit contact pressure and are as follows:

1. σ_{z1} = vertical stress at the first interface;
2. $(\sigma_{z1}-\sigma_{r1})$ and $(\sigma_{z1}-\sigma_{r2})$ = stress differences just above and below the first interface;
3. σ_{z2} = vertical stress at the second interface; and
4. $(\sigma_{z2}-\sigma_{r2})$ and $(\sigma_{z2}-\sigma_{r3})$ = stress differences just above and below the second interface.

In solving a particular problem, these tables are fairly satisfactory if the problem fits the tabulated values in terms of the four variables used. Interpolation is a long and not particularly accurate process. This can be shortened by the use of graphs produced in a companion paper by Peattie (16). The computation of strains from the tabulated stresses also requires time and care. Hence, for reasonably quick answers, the problem has to be adjusted to fit the solution, which is clearly unsatisfactory if any accuracy is required. The whole process is, in any event, a manual one that is not in keeping with the idea of a computerized design procedure.

The Interpolation program uses Jones' tables as basic data and carries out interpolation computations to produce stress functions for any reasonable values of the four tabulated variables. It thus overcomes the problem of hand or graphic interpolation and also produces the results in a more useful form. All the vertical and radial stresses and strains just above and below the two interfaces of the three-layer system are printed out for the actual contact pressure required. The input data consist of the thicknesses and elastic moduli of each layer plus the contact pressure and radius of loaded area; therefore, it is not necessary to calculate the four variables used in the tables. The program has been fitted in a simplified design program (17) discussed in a later section.

BASIS OF INTERPOLATION

A study of the charts produced from Jones' tables (13) by Peattie (16) indicates that, when plotted on a log-log base, the variations of stress function with each of the four basic variables are nearly linear. In view of this, it was thought originally that a linear procedure could accurately interpolate the tabulated variables. Early tests with the program indicated that this was not true, and a more accurate procedure was tried. The simplest curve mathematically is the quadratic, so this was used as the basic curve. For linear interpolation, only two points are needed on either side of the value required; for a quadratic curve, at least three points are necessary to specify the curve and to do the interpolation. The basic arrangement is shown in Figure 2, which illustrates a typical single interpolation calculation. In order to cope with curvatures and slopes of various sizes and magnitudes, we chose the circle having a curve of the form

$$x^2 + y^2 = ax + by + c$$

where x represents values of log (k_1, k_2, H, or a_1), y represents values of log (stress function), and a, b, and c are coefficients. The three points are chosen so as to include in their range the required value. Their coordinates are fed into the preceding equation in turn, thus producing three simulataneous equations from which the values of a, b, and c are calculated. The equation of the curve for the chosen points is thus established, and by substituting log (required value) for x the corresponding value of y is computed. This computation includes a procedure for selecting the required root of the equation from the two that are possible.

In general, to compute one of the six tabulated stress functions, we must interpolate at four levels, i.e., for k_1, k_2, H, and a_1. In practice this involves forty interpolation calculations such as the one shown in Figure 2. Hence, to compute all stresses, 240 interpolations are required.

DETAILS OF COMPUTATION

There are six basic stages in Interpolation, and these are shown in Figure 3. Each stage is discussed in the following sections.

Read in Basic Data

Jones' tables include stress functions for a wide range of values of the four basic variables. This extends beyond the practical range of values. In deciding on the basic data for Interpolation, which consists of values from Jones' tables, it was possible to exclude many of his values to reduce the amount of computer store necessary while ensuring that normal practical values were included.

All combinations of the following values of k_1 and k_2 were used: k_1 = 2, 20, and 200; and k_2 = 0.2, 2, 20, and 200. The combinations of H and a_1 values (totaling 27) used are shown in Figure 4. Hence, for each stress function, there are 324 items of data (3 x 4 x 27). There are six tabulated stress functions; so the full set of basic data includes 1,944 numbers (6 x 324).

In the program, the data are identified as A, B, C, D, E, F(I, J, K, L) where A to F are the stress functions tabulated; i.e., σ_{z1} ($\sigma_{z1} - \sigma_{r1}$) and ($\sigma_{z1} - \sigma_{r2}$), σ_{z2} ($\sigma_{z2} - \sigma_{r2}$) and ($\sigma_{z2} - \sigma_{r3}$), and I to L represent the matrix positions for the values of k_1, k_2, H, and a_1. Hence I = 1 or 2 or 3 for k_1 = 2 or 20 or 200, etc. These variables can have the following values: I, 1 to 3; J, 1 to 4; K, 1 to 7; and L, 1 to 6. It can be seen from Figure 4 that not all combinations of these values occur because of the economies effected by omitting some of Jones' basic data, even within the restricted ranges chosen. Subsequently, tests with the completed program have indicated that some additional values could be usefully included, particularly for high values of a_1 at low values of H (Fig. 4). This could be done at the expense of values for k_2 = 200. Stress functions for k_2 = 0.2 were included at a late stage in the development to accommodate nonlinear analysis (17), which often resulted in values of $k_2 < 2$.

Read in System Details

This short section of the program reads in the specification of the three-layer system including the contact pressure and the radius of the load. The values of k_1, k_2, H, and a_1 are then calculated. Any number of systems may be dealt with in one run on the computer, so the foregoing information is repeated for each system and is preceded by the number of systems.

Calculate Appropriate Gaps

The values of the four basic variables computed in the previous section will in general fall between two tabulated values. The purpose of this part of the program is to find the tabulated values immediately below the one required. This is done by calculating the values of I, J, K, and L for the system. This is done for each of these in turn by using a procedure called "gap."

Check System

Prior to preparing the data cards that specify the systems to be calcualted, a check should be made to ensure that the values of k_1, k_2, H, and a_1 fall within the limits of the program's capability as previously specified. For k_1, this simply means values between 2 and 200 and for k_2 between 0.2 and 200; however, for H and a_1, reference should be made to Figure 4 because there are some gaps in the matrix. In case this check is overlooked, the computer carries it out and indicates by a statement an unacceptable system; i.e., it gives the system number and the message "This system is outside the limits of the program." This check has been included so as to allow the program to continue with other systems, if any, whereas it would fail if calculations were tried with a system outside the limits.

Figure 1. The three-layer system.

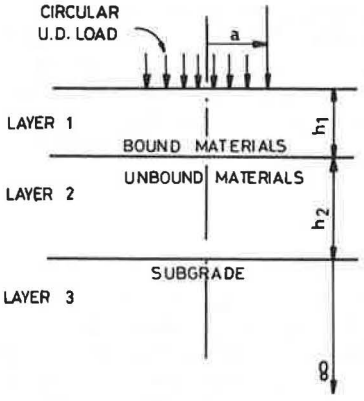

Figure 2. Basis of Interpolation.

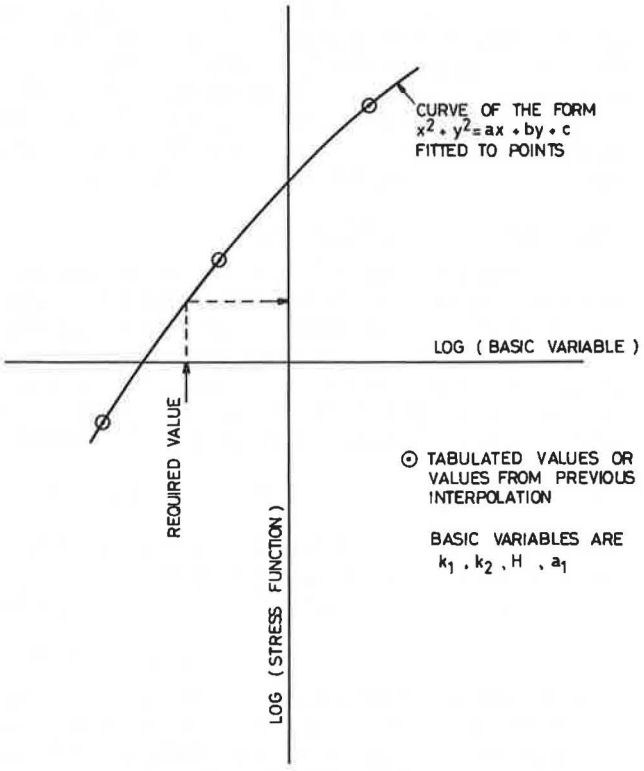

Figure 3. The main stages of program Interpolation.

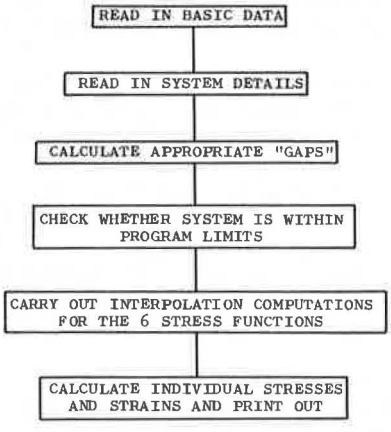

Interpolation Computations

This is the main part of the program and is carried out by using procedure "inter," which is called in for each of the six stress functions in turn. The individual interpolation calculations required are shown in Figure 5. The first part of "inter" carries out interpolations at the a_1 level of which there are 27. The next part carries out the remaining interpolations at the other three levels. Each successive level uses results from the previous one. Hence interpolation for H uses the results from interpolating for a_1, k_2 from interpolating H and k_1 from k_2.

Calculate and Print Out Results

After the six calls to "inter" are made, the six interpolated values of the stress functions are stored. Before the individual stresses and strains from these values are calculated and printed out, the system specification details are printed. The vertical and radial stresses are easily computed from the stress functions, which are themselves simple functions of these, i.e., $\sigma_{z1}(\sigma_{z1} - \sigma_{r1})$, etc. At this stage the stress for unit contact pressure, which is the basis of Jones' values, is multiplied by the actual contact pressure. Strains are calculated as follows:

$$\epsilon_z = 1/E\,(\sigma_z - \sigma_r) \text{ and } \epsilon_r = (1/2E)\,(\sigma_z - \sigma_r)$$

Since Poisson's ratio is 0.5 and the two horizontal stresses are equal to σ_r, E is the value of modulus for the layer in question.

Typical output is shown in Figure 6 and explained in the Appendix.

ACCURACY AND SPEED OF COMPUTATIONS

The "Bistro" computer program (6) was used as the standard against which to check the accuracy of results obtained from Interpolation. Sixteen systems covering a wide range of the basic variables were computed for this purpose.

The average error was ±2 percent, and the highest individual stress errors were -13 percent and +7 percent. Strain errors were more uniform, not exceeding ±5 percent. The reason for this may be that strains and vertical stresses, which had comparable accuracies, are calculated from just one of the stress functions, whereas radial stresses, which were less accurate, are derived from two such functions. In determining the percentage of errors, stresses less than 1 lbf/in.^{2} were not considered because the results could have been misleading.

A more stringent test of accuracy was carried out by comparing calculations from Interpolation with those from Bistro, wherein the value of Poisson's ratio was not constrained to 0.5. Eight practical structures covering a wide range of conditions were chosen, and the values of Poisson's ratio for each layer were selected from a knowledge of material properties (4). As may be expected, the accuracy was generally poorer, though a slight majority of the results were within ±10 percent of Bistro. Of the stresses and strains that are considered of most importance for design (i.e., vertical stress and strain on the subgrade and horizontal stress and strain at the bottom of the asphalt layer), all values except one were within 10 percent of Bistro. The exception was vertical strain on the subgrade, which was consistently low by an average of 24 percent.

An exact comparison of the computing time required for Bistro and Interpolation is not possible because of the very different natures of the two programs. The length of time for Bistro to produce comparable results at the same four positions as Interpolation depends on the structure geometry and the elastic constants of the layers. In addition, it may depend on the particular computer available. For a range of structures using a KDF9 computer, Interpolation was an average of four times as fast as Bistro.

APPLICATION TO DESIGN PROBLEMS

As a first step toward evolving a computer program for pavement design, a simplified program has been developed incorporating Interpolation as the basic analytic

Figure 4. Combinations of H and a_1 values used in program Interpolation.

H \ a_1	0.1	0.2	0.4	0.8	1.6	3.2
.125	x	x	x			
.25	x	x	x			
.5	x	x	x	x		
1		x	x	x	x	x
2		x	x	x	x	x
4			x	x	x	x
8				x	x	x

For all combinations of:-

k_1 = 2, 20, 200

and

k_2 = .2, 2, 20, 200

x Data in program

● Gaps which may be used

Figure 5. Interpolations required for each stress function.

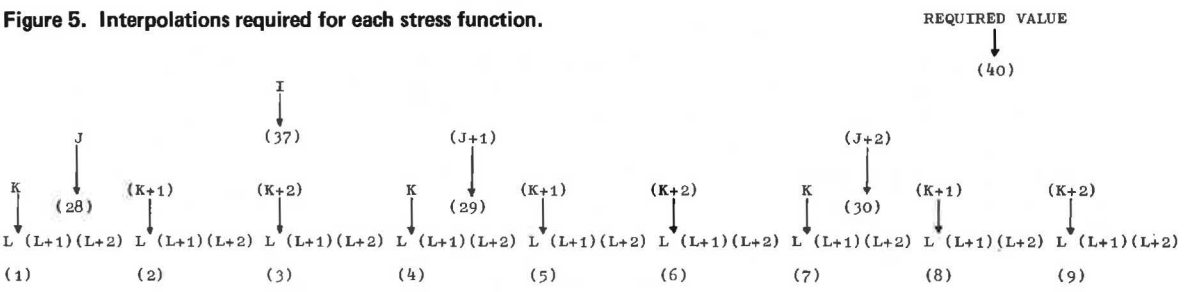

4 LEVELS OF INTERPOLATION, FROM a_1 TO k_1, L, K, J AND I ABOVE

3 POINTS FOR EACH INTERPOLATION, e.g. L, (L+1), (L+2)

40 INTERPOLATIONS IN ALL, NUMBERED ABOVE THUS - (29) IN ORDER

ONLY A THIRD OF THE DETAILS ARE SHOWN ABOVE - THE PATTERN IS REPEATED FOR (I+1) AND (I+2)

Figure 6. Typical output from program Interpolation.

SYSTEM NO. 1

LAYER	MODULUS	THICKNESS
ONE	200000	6.0
TWO	9000	18.0
THREE	3000	
CONTACT PRESSURE		80.0
LOAD RADIUS		6.0

VERSTRS	RADSTRS	RADSTRS	VERSTRS	RADSTRS	RADSTRS	VERSTRN	RADSTRN	VERSTRN	RADSTRN
14.7	-196.4	5.2	2.7	-4.3	0.4	1056	-528	778	-389

procedure (17). This program also incorporates an approximate procedure to deal with nonlinear material behavior such that the final design can be based on either a linear or nonlinear analysis of the structure. The design is based on the following three criteria that are thought to be of importance:

1. Tensile strain at the bottom of the asphalt layer. This is limited to prevent fatigue cracking.
2. Tensile stress at the bottom of the granular layer. This recognizes the fact that the unbound layer can only take a limited amount of tension (18).
3. Vertical strain at the top of the subgrade. This has been suggested (14) as the criterion to prevent excessive permanent deformation of the pavement.

The procedure involves adjustment to layer thicknesses of an initial, estimated structure in order to satisfy the three design criteria. The analysis of adjusted structures during each iteration may be carried out by either the linear or approximate nonlinear procedures.

The simplified nonlinear analysis included in the design program used relations between modulus and stress obtained from laboratory tests while assuming the asphalt layer to be linear-elastic. This procedure is based on the method used by Monismith et al. (15).

DISCUSSION AND SUMMARY

The program Interpolation was developed in an attempt to provide an analytic tool for the structural design of flexible pavements, which was easier to use than those previously available. This was thought necessary if the ideas and research developments taking place in this field are to be extended to use in practice. With the current state of knowledge great accuracy is not considered necessary in analyzing layered systems, since the theory does not model the real situation accurately and the material properties cannot be defined exactly.

Although the direct check of Interpolation against Bistro showed the former to be quite accurate, the more practical check discussed subsequently is the more realistic in terms of design, and in this case the accuracy was less impressive. The reason for this is that the basic data on which Interpolation operates are based on Poisson's ratio of 0.5 throughout the structure. In practice the asphalt layer has values between 0.35 and 0.5, depending on temperature; granular materials have values from 0.25 to 0.4; and cohesive soils have a value of about 0.4 (4). If new basic data were generated by using Bistro (with values of Poisson's ratio of, for example, 0.4, 0.3, and 0.4 for the three layers respectively), the resulting Interpolation values would be more accurate than at present.

A similar interpolation program could be developed to calculate surface deflection based on the tabulated values of Jones and Peattie (19). In this case, the value of Poisson's ratio is 0.35, which is a more realistic average value than the 0.5 used previously by Jones (13).

During the development of Interpolation, consideration was given to inserting chosen values of Poisson's ratio into the calculation of strains from stresses. Because of the horizontal strain compatibility condition built into Jones' original stress calculations, any values of Poisson's ratio other than 0.5 will destroy this compatibility in the final strain results. Though the comparison with Bistro using the practical range of structures was nearly as good as for $\nu = 0.5$, it was felt that the results were rather unrealistic, and this approach was abandoned.

CONCLUSIONS

The data given in this paper support the following conclusions:

1. The computer program Interporlation produces values of stress and strain in a three-layer elastic system, which may be of use for design purpose;
2. It extends the usefulness of Jones' tabulated values by allowing the solution to fit the problem rather than vice versa;

3. It requires approximately a quarter of the computing time taken by the multilayer Bistro program and is more convenient to use;
4. Interpolation can conveniently be fitted into a full pavement design program and can deal approximately with nonlinear behavior;
5. Direct comparison with Bistro indicates that the average accuracy of Interpolation is ±2 percent;
6. When realistic values of Poisson's ratio other than 0.5 are used, the accuracy of Interpolation is poorer than Bistro's, but the majority of stresses and strains are within 10 percent;
7. The accuracy of Interpolation could be improved by generating new basic data that use more realistic values of Poisson's ratio; and
8. A program similar to Interpolation could be developed to calculate surface deflection.

ACKNOWLEDGMENTS

The author wishes to express his thanks to R. C. Coates, for providing the facilities for this research. The computer programs were developed on the KDF9 computer at the University's Cripps Computing Centre, and some of the programming was done by W. Luty.

REFERENCES

1. Brown, S. F., and Pell, P. S. A Fundamental Structural Design Procedure for Flexible Pavements. Proc. 3rd Internat. Conf. on Structural Design of Asphalt Pavements, Vol. 1, London, 1972.
2. Peattie, K. R. A Fundamental Approach to the Design of Flexible Pavements. Proc. Internat. Conf. on Structural Design of Asphalt Pavements, 1962, pp. 403-411.
3. Monismith, C. L. Design Considerations for Asphalt Pavements. Proc. Conf. on Asphalt Pavements for Southern Africa, Durban, 1969.
4. Pell, P. S., and Brown, S. F. The Characteristics of Materials for the Design of Flexible Pavement Structures. Proc. 3rd Internat. Conf. on Structural Design of Asphalt Pavements, Vol. 1, London, 1972.
5. Hicks, R. G., and Finn, F. N. Analysis of Results From the Dynamic Measurements Program on the San Diego Test Road. Proc. AAPT, Vol. 39, 1970, pp. 153-184.
6. Peutz, M. G. F., van Kempen, H. P. M., and Jones, A. Layered Systems Under Normal Surface Loads. Highway Research Record 228, 1968, pp. 34-45.
7. Warren, H., and Dickmann, W. L. Numerical Computation of Stresses and Strains in a Multiple-Layer Asphalt Pavement System. Chevron Research Company, Unpublished Rept, 1963.
8. Barksdale, R. D. A Nonlinear Theory for Predicting the Performance of Flexible Highway Pavements. Highway Research Record 337, 1970, pp. 22-39.
9. Duncan, J. M., Monismith, C. L., and Wilson, E. L. Finite Element Analyses of Pavements. Highway Research Record 228, 1968, pp. 18-33.
10. Dehlen, G. L., and Monismith, C. L. Effect of Nonlinear Material Response on the Behavior of Pavements Under Traffic. Highway Research Record 310, 1970, pp. 1-16.
11. Hudson, W. R., Finn, F. N., McCullough, B. F., Nair, K., and Vallerga, B. A. Systems Approach to Pavement Design. Materials Research and Development Inc., NCHRP Interim Rept. on Project I-10, 1968.
12. Kasianchuk, D. A., Monismith, C. L., and Garrison, W. A. Asphalt Concrete Pavement Design—A Subsystem to Consider the Fatigue Mode of Distress. Highway Research Record 291, 1969, pp. 159-172.
13. Jones, A. Tables of Stresses in Three-Layer Elastic Systems. HRB Bull. 342, 1962, pp. 176-214.
14. Dormon, G. M., and Metcalf, C. T. Design Curves for Flexible Pavements Based on Layered System Theory. Highway Research Record 71, 1964, pp. 69-84.

15. Monismith, C. L., Seed, H. B., Mitry, F. G., and Chan, C. K. Prediction of Pavement Deflections From Laboratory Repeated Load Tests. Proc. 2nd Internat. Conf. on Structural Design of Asphalt Pavements, 1967, pp. 109-140.
16. Peattie, K. R. Stress and Strain Factors in Three-Layer Elastic Systems. HRB Bull. 342, 1962, pp. 215-253.
17. Luty, W. Effect on Non-Linearity on Pavement Design. Univ. of Nottingham, B.Sc. thesis, 1971.
18. Heukelom, W., and Klomp, A. J. G. Dynamic Testing as a Means of Controlling Pavements During and After Construction. Proc. Internat. Conf. on Structural Design of Asphalt Pavements, 1962, pp. 667-679.
19. Jones, A., and Peattie, K. R. Surface Deflection on Road Structures. Symposium on Road Tests for Pavement Design, Lisbon, 1962.

APPENDIX

INPUT AND OUTPUT DETAILS

Input

The following information (all of which is repeated for each system except for number of systems) is required on the input data cards:

1. Number of systems,
2. Modulus of elasticity for layer No. 1,
3. Modulus of elasticity for layer No. 2,
4. Modulus of elasticity for layer No. 3,
5. Thickness of layer No. 1,
6. Thickness of layer No. 2,
7. Radius of loaded area, and
8. Contact pressure.

The elastic moduli and contact pressure should all be in the same units, and these will be the units of the calculated stresses. The layer thicknesses and radius of loaded area must all be in the same units.

Output

Typical output is shown in Figure 6. Reading from left to right the tabulated results are as follows:

1. Vertical stress at the first interface,
2. Radial stress above the first interface,
3. Radial stress below the first interface,
4. Vertical stress at the second interface,
5. Radial stress above the second interface,
6. Radial stress below the second interface,
7. Vertical strain at the first interface,
8. Radial strain at the first interface,
9. Vertical strain at the second interface, and
10. Radial strain at the second interface.

It should be noted that, at a particular interface, the following effects are equal just above and below the interface:

1. Vertical stress—for equilibrium,
2. Radial strain—for compatibility as the interface is considered "rough," and
3. Vertical strain—because Poisson's ratio is 0.5.

USE OF TRAFFIC DATA FOR CALCULATING EQUIVALENT 18,000-LB SINGLE-AXLE LOADS

Eugene L. Skok, Jr., University of Minnesota; and
Richard E. Root, The Asphalt Institute

A method for flexible pavement thickness design has been proposed for use in Minnesota. It requires the calculation of summation of equivalent 18,000-lb axle loads during a design period. To calculate equivalent loads requires a knowledge of equivalency factors for various axle loads and configurations, total traffic, vehicle-type distribution, and axle-load distribution within each vehicle type. The load distribution for each type of vehicle is laid out in the format of a standard W-4 table, and the average effect is determined and called an N-18 factor for each type of vehicle. Axle-load equivalencies, taken from the AASHO Road Test, are dependent on thickness index and terminal serviceability index. Based on a traffic-load and vehicle-type distribution study on 40 Minnesota test sections, it was found that design thicknesses can vary by 2 to 3 in. of granular equivalent for variations in vehicle-type distribution and up to 10 in. for typical variations in vehicle-weight distribution. A computer program, which can be used on either the IBM 360 or the CDC 6600, has been developed to calculate equivalent 18,000-lb axle loads by using total volume, vehicle-type distribution, and axle-load distribution data. Generally, volume and vehicle-type distribution data are available from highway department traffic sections. However, load distribution data are not usually available except on a statewide basis. Histograms are presented showing variations in the average effect of various types of vehicles in terms of average number of equivalent 18,000-lb axle loads per passage of that type of vehicle. The computer program is now usable for flexible pavement design.

•A REVISED method for designing flexible pavements in Minnesota has been proposed for use. It is based on the performance of 49 in-service test sections throughout the state. This method has been reported on elsewhere (1).

One of the parameters required to use this procedure is the traffic factor in terms of the total number of equivalent 18,000-lb single-axle loads over a proposed pavement section during a given design period. This factor and the embankment strength in terms of a stabilimeter R-value are used to establish a pavement section thickness factor called the granular equivalent. The equivalent load concept makes it possible to calculate the destructive effect of various axle loads relative to a base or standard axle load (18,000 lb). The relation between the base axle load and the respective axle loads are called "equivalency factors." It is possible to calculate the average effect of each type of vehicle in terms of equivalent 18,000-lb axle loads by multiplying the axle loads by their respective equivalency factors. The summation of effects divided by the number of vehicles used for determining the effect is called the N-18 factor. This factor can vary with location and time. For design purposes, the total number of equivalent loads for a given year is calculated by multiplying the N-18 factors for each type of vehicle by the number of vehicles in that category and then summing these

Sponsored by Committee on Flexible Pavement Design.

values for all vehicle types. The same procedure is followed for each year of the design period, and the total summation of equivalent loads is derived.

In this paper, a method is proposed for determining the summation of equivalent 18,000-lb single-axle loads. The method requires information about the number, distribution, and weight of the vehicles using the highway at the point of interest and the variation of these values with time. The current and future number and distribution of vehicles can be determined by the traffic section of the highway department. A method of estimating the N-18 factors for each type of vehicle is also presented. Appropriate annual increases in the N-18 factors based on statewide data during the last 15 years are also presented.

A computer program was developed to calculate the summation of equivalent 18,000-lb single-axle loads for each year of the design period and is used to check the sensitivity of the pavement thickness to changes in the input parameters.

CONVERSION OF MIXED TRAFFIC DATA

The three factors that are used to calculate the summation of equivalent 18,000-lb single-axle loads from mixed traffic data are as follows: total volume, vehicle-type distribution, and vehicle-weight distribution. The variation of these with time and location is studied to determine the change in the summation of equivalent loads when the effect of these variations is taken into account. The CDC 6600 and IBM 360 computers have been used to study these changes.

DETERMINATION OF TOTAL NUMBER OF VEHICLES

A great deal of work has been done to determine the number of vehicles using a section of highway. These data are used for both geometric and thickness design of highways. The volume data are generally defined as the annual average daily traffic (AADT). The AADT, which represents the number of vehicles in both directions, is determined for highways by the projection of traffic counts made at selective locations at certain times of the year. For use in the structural design of pavements, the number of vehicles in the design lane of interest is determined. A value of AADT is needed for each year of the design period.

Currently, AADT data for a specific design section are obtained from a traffic flow map, a vehicle count at the proposed location, or an estimate made from a general knowledge of the area.

Predictions of future AADT data can be obtained from the traffic section of a highway department. These data are predicted from past trends and furture expectations of traffic in the given area. The AADT data are predicted for all the highways in the state every 5 or 6 years and cover at least 20 years in the future.

For the method of calculating equivalent loads presented in this paper, current and future AADT values are used along with the years for which these values are predicted. A linear relation between the two predicted values is used to calculate the values for the intervening years. More than one future AADT value may be used to improve the prediction.

EFFECT OF VEHICLE-TYPE DISTRIBUTION VARIATION ON SUMMATION OF EQUIVALENT LOADS

The second factor used for calculating equivalent loads is the vehicle-type distribution. This factor is used to divide the AADT data into vehicle types for use with the weight distribution data. These data are commonly called the distribution data and consist of the percentages of the total number of vehicles represented in each vehicle category. The volume data in Minnesota are divided into ten vehicle types (Table 1).

The vehicle-type distribution is considered variable with location by most procedures used for calculating the summation of equivalent loads. None of the current methods of calculating equivalent loads considers the distribution data to vary with time (2, 3, 4, 5).

The data from a traffic study conducted by the Minnesota Highway Department and the Civil Engineering Department at the University of Minnesota in 1964 have been

analyzed to determine if the distribution data vary significantly with time and location and how this variation affects a prediction of the summation of equivalent loads (6). The data include the percentage of vehicles in each of the ten vehicle types and the statewide average distribution data for 1964.

The effect of vehicle-type distribution variations can be shown by considering the percentage of equivalent loads of vehicle type 8. The range of distribution values for this type of vehicle is from 0 to 11.7 percent for the sections studied compared to 3.3 percent for the statewide data. The summation of equivalent 18,000-lb single-axle loads has been calculated for the statewide data and for the data from sections 1, 6, 26, 38, 43, and 47 of the Minnesota Satellite Study (6). These sections were chosen based on the percentage of type 8 vehicles: Sections 1 and 6 represent a high percentage of type 8 vehicles, sections 38 and 47 are similar to the statewide data, and sections 26 and 43 represent a low percentage. Calculations of equivalent loads were made in which only the percentage of vehicles was varied. The results of these calculations are given in Table 2. The results for the two sections, which have approximately the same percentage of type 8 vehicles as the statewide data, agree quite well with the number of loads predicted for the statewide data. The values for two high-percentage sections are 217 and 229 percent of the statewide value. The values for the two sections with a low percentage of type 8 vehicles are 18 and 37 percent of the statewide value.

If the variation in design summation of equivalent loads is assumed to be the same as the variation found for the summation of equivalent loads for 1964, it is possible to compare the pavement thicknesses required for each section. The comparison was made by using the calculated granular equivalent for each set of data (Table 3). The granular equivalent for a pavement section in Minnesota is calculated by using Eq. 1 (1):

$$GE = a_1D_1 + a_2D_2 + a_3D_3 \ldots \quad (1)$$

where

GE = granular equivalent thickness, in.;
a_1, a_2, a_3, ... = constants that define the relative effect of the given layer; and
D_1, D_2, D_3, ... = thickness of individual layers, in.

The design summation of equivalent loads given in Table 3 was converted to granular equivalents by using a design chart given elsewhere (1). The variations in granular equivalent thicknesses for these various traffic values and an R-value of 20 for the embankment are given in Table 3. A difference in granular equivalent of 5 in. between the statewide data and the two sections with the high percentage of type 8 vehicles and a difference of 10 in. in granular equivalent between the statewide data and the low percentage sections are indicated. It is felt that this variation is of sufficient magnitude to require that the distribution data be varied with location.

The statewide distribution histories for vehicle types 6, 7, and 8 are shown in Figure 1 for 1952 through 1968. Vehicle type 8 has shown a steady increase of 0.25 percent per year, whereas the percentages of types 6 and 7 vehicles have decreased. This shows that the vehicle-type distribution is not necessarily constant over the design life of a road. An analysis was made to determine whether the summation of equivalent loads predicted by using variable distribution data was significantly different from the summation of equivalent loads predicted by using constant distribution data for the design period of a given section. The 1952 statewide distribution data were used for constant data for a design life of 17 years, and the 1952 through 1968 statewide distribution data were used as an example for variable distribution data.

For this example, the summation of equivalent loads using a constant distribution is 462,000; the summation of equivalent loads for the section with the variable distribution is 608,000. This latter value is 32 percent higher in equivalent loads. When using the same procedure to calculate the difference in granular equivalent as previously summarized, the difference is approximately 2 in. This is the same as saying that constant distribution data would yield a design that would require maintenance at 462,000 equivalent loads that hypothetically would take place in mid-1964 instead of the end of 1968 according to the variable data.

Current and future vehicle-type distribution data can be obtained from the traffic section of a highway department along with the volume data. The distribution data are generally predicted for the same years as the volume data. For the method proposed, the distribution values for the years between those given specific values are calculated by using a linear relation between the two data points entered. By using this method it is possible to account for possible changes in types of vehicles using a highway during the design period.

EFFECT OF VEHICLE-WEIGHT DISTRIBUTION VARIATION ON SUMMATION OF EQUIVALENT LOADS

The third factor used to calculate the summation of equivalent 18,000-lb axle loads is the distribution of axle loads within each type of vehicle. California, Idaho, and The Asphalt Institute use statewide loadometer data obtained from yearly W-tables to determine the average effect of traffic weights on a road (2, 3, 4). Recent studies in Minnesota and Kentucky have shown that weight distributions at various locations throughout the states differ to a great extent from the statewide averages (5, 6). It has also been found in Minnesota and Idaho that the weight data for individual vehicle types are not constant for the design period as assumed by some procedures (4, 6). Therefore, the proposed procedure allows for the variation of weight data with location and time. The weight distribution for each of the 10 types of vehicles listed previously has been studied invididually to determine the average load effect of each vehicle type. This term is called the N-18 factor.

To calculate the N-18 factor, we divide the weight data for each vehicle type into 32 weight categories, which coincide with the weight categories in standard W-4 tables. Each weight category has an equivalency factor calculated from the AASHO equations for the average weight of that category (7). The weight categories along with a set of equivalency factors are given in Table 4. The number of axles within each weight category is multiplied by the appropriate equivalency factor and summed for the 32 weight catagories. This value gives a total summation of equivalent 18,000-lb single-axle loads for the vehicles of that type. This value is then divided by the number of vehicles weighed to give the average load effect of the vehicle type in terms of equivalent 18,000-lb single-axle loads.

This method was used to calculate N-18 factors for each type of vehicle on the 49 Minnesota test sections. The data were gathered by setting up portable weighing stations at each of 40 locations for the 49 test sections during the summer and fall of 1964 and the spring of 1965. N-18 factors were calculated for each of the three seasons. The summer values represent both summer and winter and thus 7 months of the year, the fall values represent 3 months of the year, and the spring values represent 2 months of the year. The N-18 factors for each season are weighted according to the time periods. The 10 combined weighted N-18 factors are used to represent the average load effect of each of the 10 vehicle types on that location for 1964.

The 1964 N-18 factors for the 49 test sections and the 1964 statewide N-18 factors are presented elsewhere (8). These values show the wide range of average vehicle effect on the Minnesota highway system. Two sections have been chosen to study the effect of this variation. Section 47 with high N-18 factors and section 19 with low N-18 factors are used to compare the difference in the design summation of equivalent loads. The calculations have been made with the assumption that the volume and distribution data are constant for the design period of the section. The 1964 statewide vehicle-type distribution along with an AADT value of 1,000 was used for the calculation. The results of these computations are given in Table 5. A range of granular equivalent of more than 7 in. between the sections of high and low N-18 factors results. The statewide data indicate a granular equivalent thickness of 3 in. greater than the section with low N-18 factors and 4½ in. less than the section with the high N-18 factors. These variations are of sufficient magnitude to justify varying the weight data with location.

The N-18 factors calculated for the statewide data from 1952 through 1968 are plotted semilogarithmically to show the trends in N-18 factor for the various vehicle types. As shown in Figure 2, the N-18 factors for vehicle types 3 through 8 have increased generally at a uniform rate except for the 1968 values. Vehicle type 1 is considered constant

Table 1. Types of vehicles.

Vehicle Type	Vehicle Description
1	Passenger car
2	Panel and pickup (under 1 ton)
3	Single unit, 2-axle, 4-tired
4	Single unit, 2-axle, 6-tired
5	Single unit, 3-axle, 6-tired
6	Tractor semitrailer combination, 3-axle
7	Tractor semitrailer combination, 4-axle
8	Tractor semitrailer combination, 5-axle
9	Tractor semitrailer combination, 6-axle
10	Truck and trailer combination and bus

Table 2. Summation of equivalent 18,000-lb single-axle loads for 1964.

Location	Percentage of Type 8 Vehicles	Equivalent Loads for 1964	Percentage of Statewide Data
Statewide	3.3	14,263	100
Section 1	8.8	31,010	217
Section 6	11.7	32,673	229
Section 26	0.0	5,238	37
Section 38	3.4	15,453	108
Section 43	0.0	2,633	18
Section 47	3.0	14,348	101

Note: Volume data = 500 AADT; weight data derived from 1964 Minnesota statewide average (W-4 table).

Table 3. Comparison of granular equivalents for variations in vehicle-type distribution.

Location	Design Summation of Equivalent Loads	Granular Equivalents
Statewide	1,000,000	25.8
Section 1	2,170,000	30.5
Section 6	2,290,000	30.8
Section 26	370,000	20.0
Section 38	1,080,000	26.3
Section 43	180,000	15.7
Section 47	1,010,000	26.0

Note: The designs are based on an assumption of 1,000,000 equivalent loads for statewide data.

Figure 1. Variation of statewide vehicle-type distribution data with time.

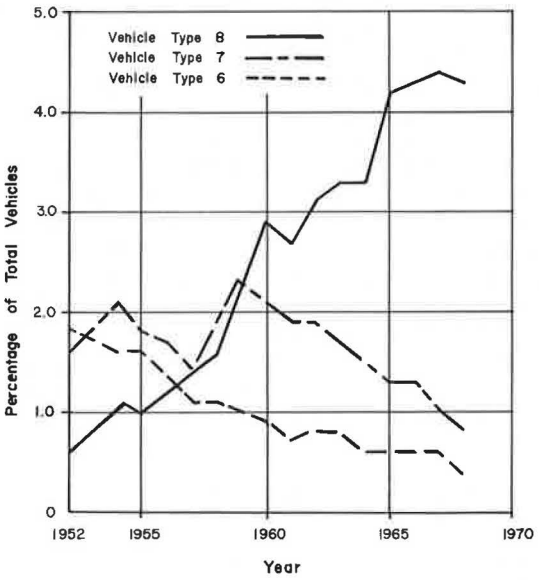

Table 4. Weight category used for determination of average load effect.

Category Number	Weight Category	Equivalency Factor[a]
1	1-2,999[b]	0.0002
2	3,000-6,999	0.005
3	7,000-7,999	0.03
4	8,000-11,999	0.09
5	12,000-15,999	0.36
6	16,000-17,999	0.80
7	18,000-19,999	1.24
8	20,000-21,999	1.83
9	22,000-23,999	2.58
10	24,000-25,999	3.53
11	26,000-29,999	5.39
12	30,000-34,999	9.42
13	35,000-39,999	16.33
14	40,000-44,999	26.90
15	1-5,999	0.01
16	6,000-11,999	0.01
17	12,000-17,999	0.04
18	18,000-23,999	0.15
19	24,000-29,999	0.43
20	30,000-31,999	0.75
21	32,000-33,999	0.97
22	34,000-35,999	1.23
23	36,000-37,999	1.53
24	38,000-39,999	1.89
25	40,000-41,999	2.29
26	42,000-43,999	2.75
27	44,000-45,999	3.27
28	46,000-49,999	4.17
29	50,000-54,999	5.83
30	55,000-59,999	8.18
31	60,000-64,999	11.17
32	65,000-69,999	14.95

[a]SN = 5.0 and terminal serviceability = 2.50.
[b]Single axle.
[c]Tandem axle.

over the design life of the section because this category is composed of passenger cars. At this time there is insufficient data on vehicle types 9 and 10 to show any trends. Therefore, these vehicle types are assumed to be constant over a given design period.

A best-fit line has been calculated for the data shown in Figure 2 for each vehicle type. The antilogarithm of the slopes of the lines through the data represents the percentage of increase in the statewide N-18 factor for each year. The slopes and percentage of increase from these analyses of the statewide data from 1952 to 1967 and also from 1952 through 1968 are given in Table 6. These percentages can be used to project future values of the N-18 factors.

By using the percentages of increase from the 1952-to-1967 analysis, which are slightly higher than those from the 1952-to-1968 analysis, we can compare the summation of equivalent loads predicted from constant weight data and time-dependent weight data. The values of the volume data and distribution data were held constant for these comparisons. An AADT value of 1,000 was used, and the distribution data were the average 1964 statewide distribution. The predictions were made by using the statewide weight data for 1964 from the W-4 tables and the 1964 weight data from sections 19 and 47.

The values for the 1964-through-1979 summation of equivalent loads (Table 7) show that the data using variable N-18 factors are about 66 percent higher than the data using constant N-18 factors. This difference represents about 3.2 in. of granular equivalent. It is felt that this variation warrants the use of a procedure in which the variation of N-18 factor with time can be accounted for. The data used to predict the increase in N-18 factors with time currently come from statewide loadometer studies that have been shown to underestimate the actual loading highways (6). Therefore, it may be possible that an even greater increase in N-18 factors could be taking place on individual sections.

When working with trends and percentages of increase for the N-18 factors, it is possible to predict N-18 factor values that exceed the maximum possible load a vehicle can haul. In order to prevent this, maximum values of N-18 factors have been determined individually for types 2 through 8 vehicles. The highest values of the measured N-18 factors in the 1964 weight study for each vehicle type (except types 2 and 4) were increased by 25 percent and were used as the maximum value possible for N-18 factors. In the case of types 2 and 4, the highest value was disregarded because it is more than twice the next largest value and only a few vehicles were weighed. The maximum assumed values for N-18 factors are given in Table 8.

There are two types of weight data that can be used with the developed computer program for calculating equivalent loads. It is possible to obtain the necessary data from a weight study at the proposed location of the highway. These data are put into the form of a W-4 table. The other form of data that can be used consists of a set of N-18 factors that have already been calculated from loadometer data. These N-18 factors would represent factors calculated for a similar section of highway. They are used when it is not possible to conduct a weight study at the proposed location. If no sections in the area are similar to the proposed section, it is possible to predict assumed values of N-18 factors from histograms plotted from the 1964 traffic study (9). The histograms (Figs. 3 through 6) indicate the distribution of N-18 factors for vehicle types 2 through 8 and type 10. The histograms represent the number of observations within a given range of N-18 factors for the respective vehicle types. It can be seen that there is a wide variation in these factors and that some thought must be given to the choice of an appropriate N-18 factor.

COMPUTER PROGRAM FOR CALCULATING SUMMATION OF EQUIVALENT 18,000-LB SINGLE-AXLE LOADS

A method that makes it possible to calculate equivalent 18,000-lb single-axle loads has been presented. The method developed utilizes the AADT, vehicle-type distribution, and axle-weight distribution within the various vehicle types for the prediction of equivalent 18,000-lb single-axle loads over a given design period. It has been shown that it is appropriate, in terms of design thickness variations, to allow these factors to vary

Table 5. Difference in computed granular equivalent thickness.

Location	Summation of Equivalent Loads, 20-Year Design	Granular Equivalent Thickness[a]	Difference From Statewide Granular Equivalent Thickness
Statewide	584,892	22.7	—
Section 19	361,845	19.8	2.9
Section 47	1,239,533	27.2	4.5

[a]From design chart in Ref. 1; assumed R-value = 20.

Figure 2. Variation of statewide N-18 factors with time.

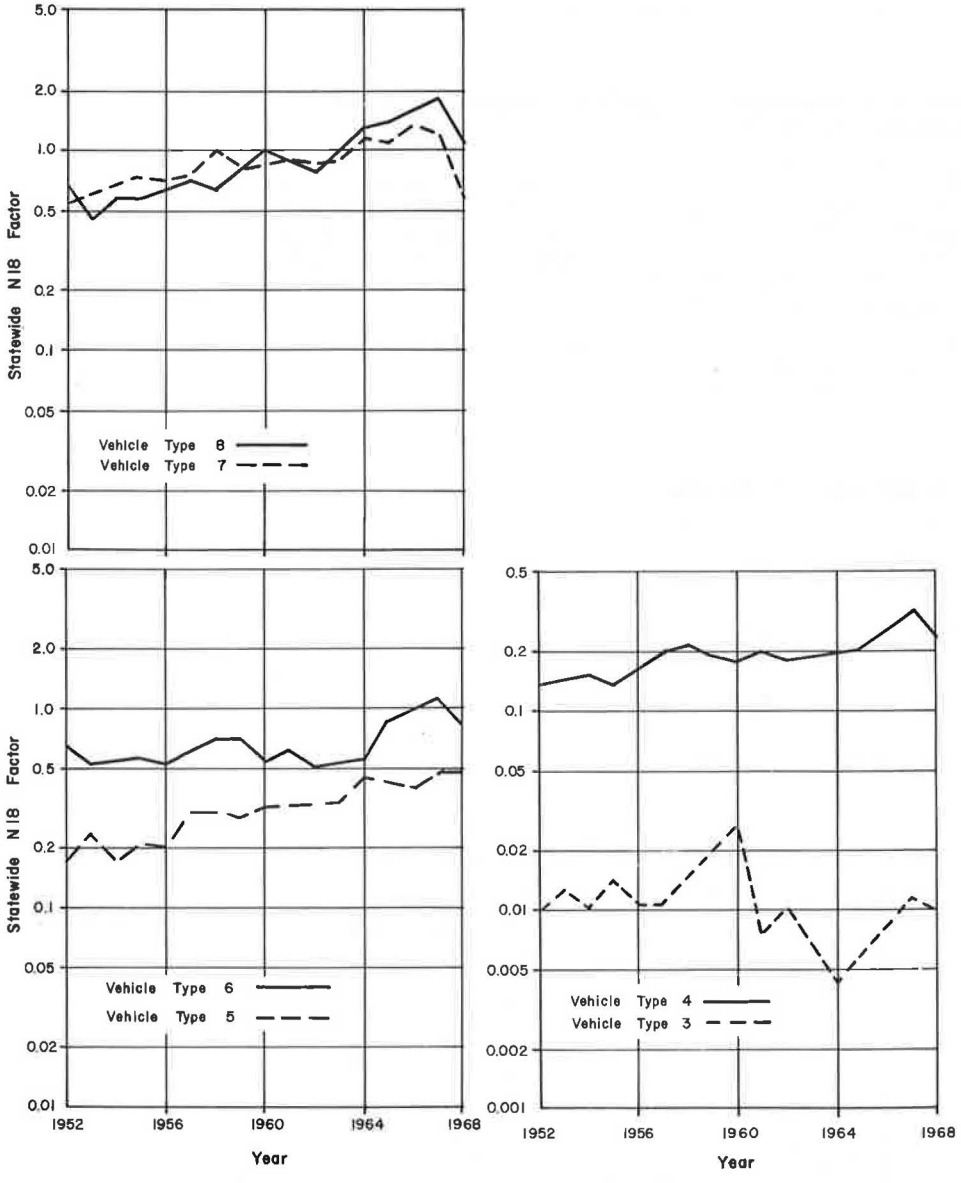

Table 6. Least squares regression analysis of Minnesota statewide N-18 factors with time.

Vehicle Type	1952-1967 Slope	1952-1967 Percentage of Increase Per Year	1952-1967 Standard Error	1952-1968 Slope	1952-1968 Percentage of Increase Per Year	1952-1968 Standard Error
2	0.00158	0.36	0.0858	0.00191	0.44	0.0830
3	0.01837	4.32	0.1999	-0.01509	-3.42	0.1969
4	0.1626	3.82	0.0537	0.01544	3.62	0.0528
5	0.02698	6.41	0.0517	0.02643	6.28	0.0503
6	0.01198	2.80	0.0782	0.01143	2.67	0.0759
7	0.02101	4.96	0.0415	0.01461	3.42	0.0847
8	0.03242	7.75	0.0597	0.02961	7.07	0.0663

Table 7. Variation in the summation of equivalent loads caused by varying the weight-distribution data with time.

Type of Data	Statewide	Section 19	Section 47
Summation of equivalent loads, 1964-1968			
Variable N-18F	147,382	90,868	311,890
Constant N-18F	128,391	79,429	272,093
Percentage of increase when using variable data	15	14	15
Summation of equivalent loads, 1964-1979			
Variable N-18F	737,926	453,161	—
Constant N-18F	442,236	273,590	—
Percentage of increase when using variable data	67	66	—

Table 8. Maximum assumed N-18 factors.

Vehicle Type	Maximum N-18 Factor, Table Measured	Maximum Assumed N-18 Factor
2	0.008	0.012
3	0.04	0.05
4	0.46	0.58
5	0.68	0.85
6	1.94	2.42
7	3.13	3.91
8	3.19	3.99

Figure 3. Histograms of number of N-18 factors for vehicle types 2 and 3.

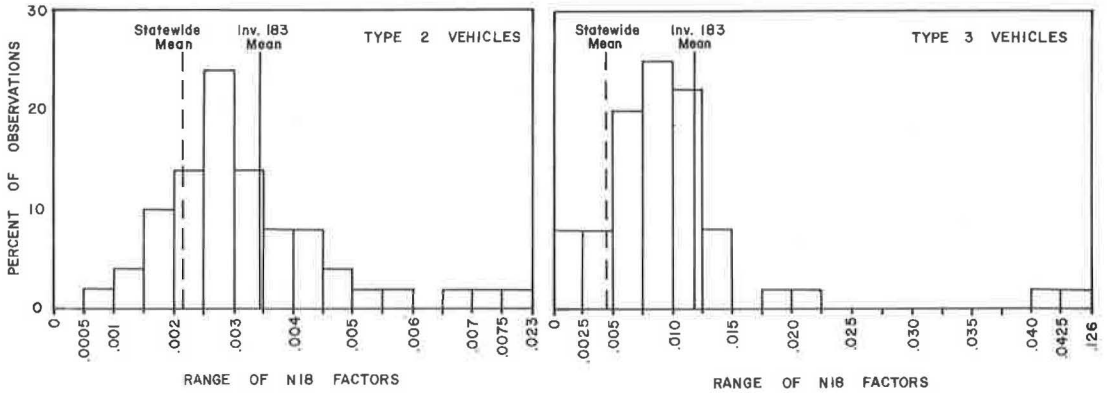

Figure 4. Histograms of number of N-18 factors for vehicle types 4 and 5.

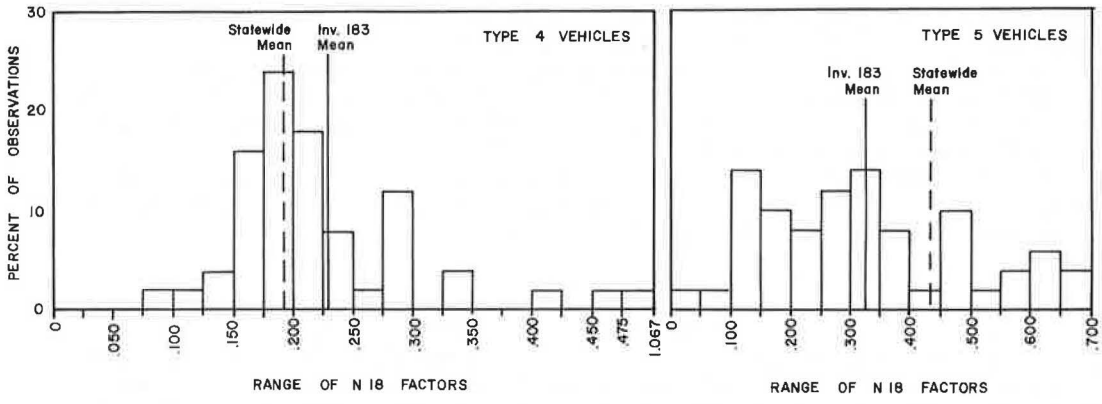

Figure 5. Histograms of number of N-18 factors for vehicle types 6 and 7.

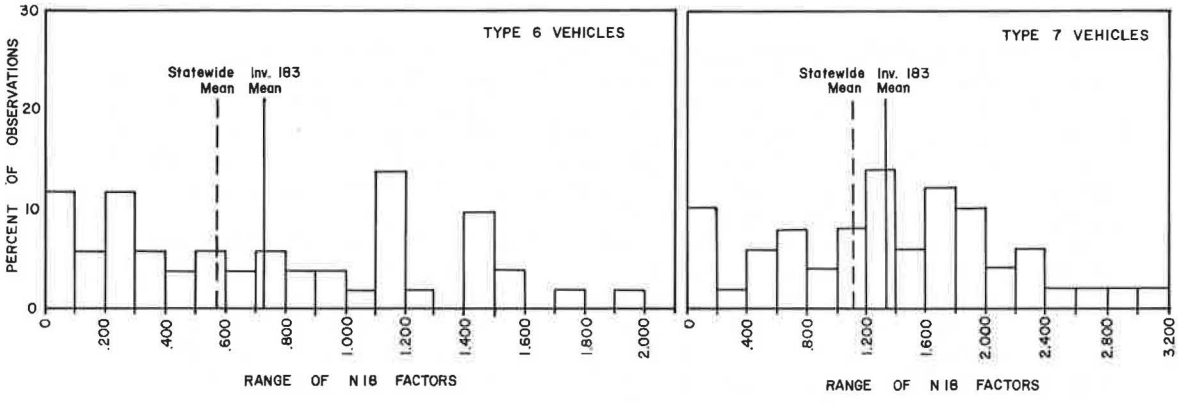

Figure 6. Histograms of number of N-18 factors for vehicle types 8 and 10.

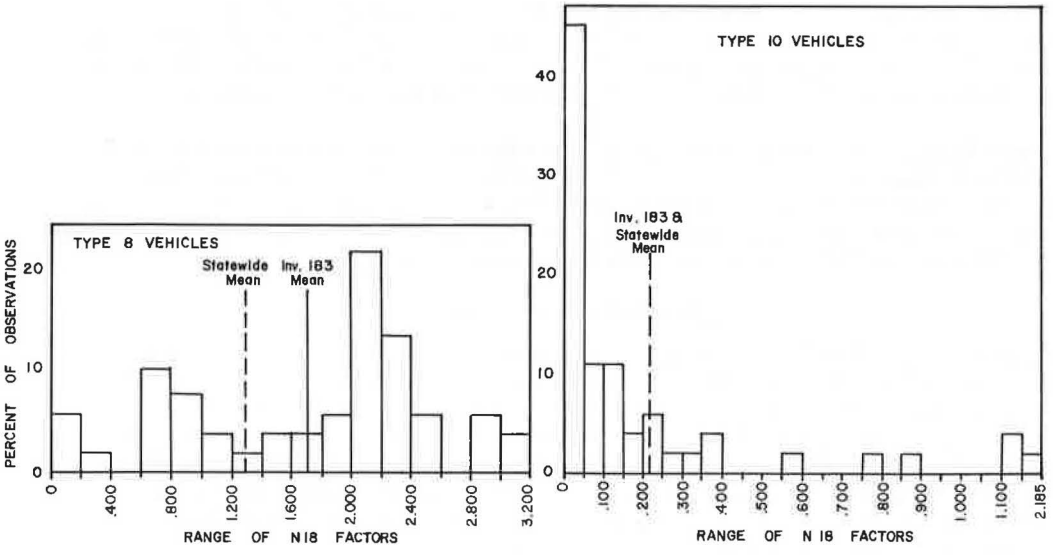

with both time and location. It would not be practical to use this method and make the calculations without a computer. Therefore, all the calculations have been programmed in FORTRAN for the CDC 6600 and IBM 360 computers.

The program developed has the capabilities of calculating the number of equivalent loads for past and/or future traffic. The input data required include total vehicle volume, vehicle-type distribution, and weight-distribution data along with some general information about the proposed highway sections. The future summation of the equivalent 18,000-lb axle loads is calculated by using predicted values of volume and vehicle-type distribution for future years along with assumed percentages of increase in N-18 factors based on the statewide trends from past years.

CONCLUSIONS

The design of an asphalt pavement requires an estimate of the loading anticipated on the pavement during its design life. It has been shown by others that this loading can be expressed in terms of the summation of equivalent 18,000-lb axle loads. A computer program was developed and used to check the variation of the pavement thickness due to variations of the input values with time and location. The three main input variables were defined as the annual average daily traffic, vehicle-type distribution, and the axle-weight distribution. The thickness variations found as a result of this study are as follows:

1. Variation of distribution data with location. A comparison was made between the summation of equivalent loads for sections of high and low percentages of 5-axle vehicles and the statewide value. It was found that the required granular equivalent thickness by a particular design method indicated a difference of 15 in. in granular equivalent between the sections with high and low percentages of 5-axle vehicles. The granular equivalent for the statewide distribution data was 10 in. higher than the low percentage section and 5 in. lower than the high percentage section.
2. Variation of distribution data with time. The statewide vehicle-type distribution percentages were calculated from 1952 through 1968. These values were used to show that there is a significant variation of distribution data with time. An analysis was made to determine the difference in granular equivalent thicknesses for a section of constant distribution data and one with variable distribution data (assuming all other data are constant). The analysis shows that the variable data result in a granular equivalent of 2 in. thicker than the constant data.
3. Variation of axle-weight distribution data with location. The weight data from the 1964 traffic study on the Minnesota test sections were used to analyze the effect of varying this information with location. N-18 factors were calculated for each of the sections and also for the 1964 statewide data. High, low, and statewide N-18 factors were used to calculate the granular equivalent thickness, again holding all other data constant. The range of granular equivalent was 7.5 in. from low to high N-18 factors. The statewide values for the N-18 factor resulted in a design in the middle of this range.
4. Variation of axle-weight distribution data with time. Statewide loadometer data were analyzed from 1952 through 1968. The results of the analysis showed that all vehicle types except single unit trucks (2-axle, 4-tired) have increasing N-18 factors with time. The difference in granular equivalent thickness was 3.2 in. between the section with constant N-18 factors and one with variable N-18 factors.

ACKNOWLEDGMENTS

The study reported in this paper is part of a research project that was a cooperative venture between the Minnesota Department of Highways and the Civil Engineering Department of the University of Minnesota. The project was conducted under the Highway Planning and Research Program financed jointly with federal-aid funds of the Federal Highway Administration and with state funds of the Minnesota Department of Highways. However, the opinions, findings, and conclusions expressed in this paper are those of the authors and not necessarily those of the Minnesota Department of Highways or the Federal Highway Administration.

REFERENCES

1. Fredrickson, F. C., Diethelm, P. J., and Zwiers, D. M. Minnesota Department of Highways Flexible Pavement Design—1969. Highway Research Record 329, 1970, pp. 55-64.
2. Hveem, F. N., and Sherman, G. B. Thickness of Flexible Pavements by the California Formula Compared to AASHO Road Test Data. Highway Research Record 13, 1963, pp. 142-166.
3. Thickness Design-Asphalt Pavement Structures for Highways and Streets. The Asphalt Institute, Manual Series 1, March 1964.
4. Erickson, L. F. An Evaluation of Flexible Pavement Design Methods. Research Division, Idaho Department of Highways, May 1964.
5. Deacon, J. A., and Lynch, R. L. Determination of Traffic Parameters for the Prediction, Projection and Computation of EWL's. Division of Research, Kentucky Department of Highways, Aug. 1968.
6. Kersten, M. S., and Skok, E. L., Jr. Application of AASHO Road Test Results to Design of Flexible Pavements in Minnesota. Minnesota Department of Highways Investigation 183, Summary Rept., June 30, 1968.
7. AASHO Interim Guide for the Design of Flexible Pavement Structures. American Association of State Highway Officials, Oct. 1961.
8. Root, R. E. Development of a Traffic Factor for the Design and Evaluation of Flexible Pavements. Thesis, March 1970.
9. Skok, E. L., Jr., and Root, R. E. Use of Traffic Data for Calculating Equivalent 18,000-lb Single Axle Loads. Minnesota Department of Highways Investigation 183, Interim Rept., 1970.

EVALUATION OF RIGID PAVEMENTS BY NONDESTRUCTIVE TESTS

H. A. Balakrishna Rao, University of New Mexico; and
D. Harnage, U.S. Air Force Weapons Laboratory

This paper presents a vibratory nondestructive evaluation procedure as applied to rigid pavements. It is restricted, however, to a comparison between a measured deflection field around a loaded plate and a predicted deflection field obtained by using elastic properties of layers (gathered by nondestructive tests) in a radial symmetric finite-element program on a test section. Because these two deflection fields do not agree in their magnitudes due to the low strain level created by the vibrator during the determination of the elastic properties of the layers, two methods to correct the modulus of the subgrade material (determined by low-intensity vibration tests) were investigated. The first method uses the information obtained by a plate load test; the second method uses laboratory repeated load test results (developed by the University of Kentucky). These methods were applied in a simplified form to a test section. By utilizing the finite-element method, the predicted deflection field with the corrected modulus was compared with the measured deflection field. Further studies required to make this evaluation procedure a useful tool in solving practical problems are outlined.

•THERE are several hundred airfields in the United States that are being used extensively by military and commercial aircraft. Most of these airfields have been in existence for quite some time. Some of these airfields require strengthening because of the heavy gear loads of the latest aircraft. Determination of airfield strengthening requirements is made by studying the current condition of the airfield and evaluating its load-carrying capacity. Thus, pavement evaluation can be defined as a study to determine the suitability of the pavement to support repeated loads of known magnitude.

There are several types of pavement evaluation. Grouped into four categories, they are as follows:

1. Visual evaluation—detect cracks, pumping, soft spots, and so forth;
2. Surface evaluation—skid resistance, drainage, and so forth;
3. Strength evaluation—study the load-carrying capacity; and
4. Environment effects and repeated load effects.

This paper is restricted to the study of strength evaluation only.

Currently, there are semi-empirical methods for evaluating a pavement. For instance, according to the Bureau of Yards and Docks, the load required to cause a 0.15-in. deflection would be the limiting load that could be applied on a flexible pavement (1), or if the stresses, computed by Westergaard's analysis, in a rigid pavement are less than the permissible stresses for concrete, the pavement would be safe to carry that load. Similar criteria on limiting radius of curvature are also available in the literature (2). However, in order to use these methods, support tests (determination of CBR or coefficient of subgrade reaction or plate load tests, etc.) are required. This, in turn, would result in closing down the runway or taxiway for a considerable

Sponsored by Committee on Pavement Condition Evaluation.

period of time. Hence, a rapid method of evaluating the pavement by nondestructive methods is urgently needed. This paper explores one such method, namely, the vibratory nondestructive procedure.

When a vibrator operates on the surface of a layered system, it generates elastic waves that travel as surface, compression, and shear waves. A major portion of the energy is transmitted as a surface wave. Dispersion curves can be obtained for the medium by determining the velocity of this surface wave and by studying its change with the frequency of the vibrator. This paper is concerned with the dispersion of the surface Rayleigh waves. By studying the dispersion phenomenon, it is possible to obtain the elastic properties of the various layers (3).

The objectives of this study were as follows:

1. Estimate the elastic properties of layered systems by steady-state vibration testing;
2. Predict the deflection basin under a statically loaded plate by using the estimated layer properties;
3. Compare the predicted deflection basin with an experimentally measured deflection basin; and
4. If the measured deflection basin and the predicted deflection basin are radically different from each other, state the causes for disagreement and suggest procedures for correcting the properties of layered systems to make the deflection basins agree.

These objectives serve to develop a method of predicting the deflection basin under a given load, which is the first step in developing a rational method of pavement evaluation.

EXPERIMENTAL PROCEDURE

A low-intensity dynamic force was generated with an electrodynamic vibration generator by means of a power amplifier driven by an oscillator. The vibration generator operates between 100 and 10,000 Hz. Another mechanical vibrator generating about 250 lb of dynamic force and operating between 15 and 50 Hz was used to obtain the subgrade elastic property.

The vibration energy introduced into the layered system is dissipated primarily as a surface wave. Two accelerometers were located at a known distance apart on the surface of the layered medium. The outputs of these accelerometers were fed into a phase computer and display unit through a dual-channel tracking filter. The phase difference observed was used to compute the phase velocity of the surface wave. The results were plotted as a relation between the phase velocity, v, and the wavelength, Such a relation is called a dispersion curve.

When the experiments were performed in a very short time, a sweep oscillator was used to drive the vibrator through a power amplifier producing a signal of slowly varying frequency. The outputs from the two accelerometers were recorded on a multichannel tape recorder. The data were later reduced by using a high-speed digitizing technique and a Calcomp plotter (4). Figure 1 shows the setup, and Figure 2 shows the apparatus used for obtaining the dispersion curves.

TEST SECTION

The test section consisted of a 10-ft thick processed clay soil of low plasticity (plasticity index = 15) placed at a CBR of 8 to 12, a 6-in. thick compacted gravel base course, and a 12-in. thick surface layer of portland cement concrete with ¾-in. aggregate.

VIBRATION TESTS

High-Frequency Tests

High-frequency vibration tests were performed on this test section. One accelerometer, located 3 in. from the vibrator, was used as a reference. The second accelerometer was placed at various distances from the first in increments of approximately

6 in. The phase difference at a set frequency obtained by the outputs of the two accelerometers was converted to the phase velocity. Several tests were performed at various frequencies, and the dispersion curve was plotted. Figure 3 shows the dispersion curve obtained by the high-frequency vibration tests.

Low-Frequency Tests

Low-frequency vibration tests were performed with a DEGEBO type vibrator (5) using one force level of 250 lb. The reference accelerometer was located at a distance of 1 ft from the center of the vibrator, and the moving accelerometer was located at various distances in increments of approximately 3 ft. Figure 3 also shows the dispersion curve for the low-frequency tests.

INTERPRETATION OF VIBRATION TEST RESULTS

The method of interpreting dispersion curves has been discussed extensively in earlier literature (6, 7). At very high frequencies (very short wavelengths), the dispersion curve gives the properties of the surface layer. The primary mode is the flexure mode; however, it is also possible that the compression mode (8) may be detected in some cases. Thus, it appears according to the theory of Lamb (8) that point A (Fig. 3) would correspond to the Rayleigh wave velocity in concrete. The Rayleigh wave velocity is approximately equal to the shear wave velocity in any material. In concrete, if we assume a Poisson's ratio, ν, of 0.2, the Rayleigh wave velocity, V_r, is related to the shear wave velocity, V_s, by

$$V_r = 0.91\ V_s$$

On the other hand, at very long wavelengths, the dispersion curve would give the properties of the subgrade. Thus, point E on dispersion curve DE would give the shear wave velocity of the subgrade. Region BC of the curve shows a considerable scatter of results.

The assigned values of wave velocities and moduli of elasticity of the various layers were as follows:

1. Rayleigh wave velocity of surface layer, 7,800 ft/sec;
2. Modulus of elasticity of surface layer (assuming $\nu = 0.2$), 5.5×10^6 psi;
3. Shear wave velocity of subgrade material, 880 ft/sec; and
4. Modulus of elasticity of subgrade material (assuming $\nu = 0.45$), 56,000 psi.

The vibration method failed to recognize the presence of the intermediate layer (base course) and to give the information pertaining to Poisson's ratios.

INFLUENCE OF BASE COURSE PROPERTIES

The vibration method is only useful in obtaining the elastic properties of the materials. Because it did not give any information on the properties of the base course, it became necessary to determine the influence of the base course on stresses and displacements. A computer study was thus undertaken to qualitatively assess the relative importance of parameters in a three-layered pavement system. An axisymmetric finite-element program, WIL67 (9), developed at Berkeley was used. A standard problem was conceived. The pavement system contained a 12-in. thick surface course, a 6-in. thick base course, and a 498-in. thick subgrade. A 12-in. diameter area at the center of the slab was assumed to be loaded with a uniform pressure, and the influence of variations of the following parameters was studied: modulus of subgrade layer, E_3; modulus of base course layer, E_2; modulus of surface layer, E_1; Poisson's ratio of subgrade layer, ν_3; Poisson's ratio of base course layer, ν_2; and Poisson's ratio of surface layer, ν_1.

Maximum computed displacements at the center of the loaded area and the radial tensile stresses at a depth of 10.8 in. (inside the surface layer) are given in Table 1.

Table 1 shows that only three parameters (E_1, E_3, and ν_3) are necessary to determine the magnitude of displacement, of which the vibration method could only provide

two. For radial stresses, E_1 and E_3 are the most important parameters. A reasonably good value of Poisson's ratio for the soil can be assumed based on experience (Poisson's ratio varies within a small range from about 0.30 to 0.45 for soils). Because the moisture content was high, the Poisson's ratio assumption of 0.45 for the subgrade seemed justified.

LOAD TESTS AND MEASUREMENT OF DEFLECTION BASIN

Two circular plates, one 6 in. in diameter and one 12 in. in diameter, were used to obtain the deflection basin. The total load applied was 30,000 lb. The test arrangement is shown in Figure 4. The deflections at 11 points on each of the 3 tangential lines at 1, 2, and 3 ft from the center of the loaded area were measured by dial gauges. Also, the deflection of the plate was measured at two points on the plate itself. These deflections were measured from 35-ft long steel beams fixed at one end and supported on rollers at the other end. These beams, as well as the loading frame, spanned the entire cross section of the test section. Average deflections of several loading tests are shown in Figures 5 and 6 for the two plates.

COMPUTED DEFLECTION BASIN

Because Table 1 showed that the base course modulus variation played a very minor role in computed deflections, a modulus of 100,000 psi was selected for the base course. Poisson's ratio was set at 0.3.

The deflection basin was computed with the axisymmetric finite-element program by using the moduli of the three layers along with their assumed values of Poisson's ratio. The only difference between the assumed computation model and the real situation was that the clay layer was taken to be 500 in. thick for purposes of computation, whereas in the test section it was only 120 in. thick and underlaid by an in situ silty sand material. Because the stresses induced by the surface load at depths greater than 120 in. are negligible, the associated displacements are also small, and hence the assumption of the existency of clay in place of silty sand would not cause significant error.

The computed displacements at various points are also shown in Figures 5 and 6. In these figures E_c and E_s are the moduli of the concrete and subgrade respectively.

COMPARISON OF COMPUTED AND MEASURED DEFLECTION BASINS

By studying the agreements between the measured and computed deflection basins (Figs. 5 and 6), one will discover that there are two distinct regions in the displacement field. They are as follows:

1. Region A (high shear strain). The computed deflections are extremely small as compared to measured deflections. Such a region exists directly under the loaded plate or very close to the edge of the plate.
2. Region B (moderate shear strain). The computed deflections are smaller than the measured deflections by approximately one-half to one-third of the measured deflection.

The existence of these regions can be understood by the strain fields in the computations. There is a relatively steep strain gradient at the edge of the plate compared to that at a distance of 3 ft from the plate. The strain gradient decreased as the distance from the center of the plate increases. Such a decrease is rather slow in concrete pavements compared to asphalt pavements. The shear modulus of material like soil depends on the strain level in the material. For instance, the shear modulus obtained by using the pulse technique is much larger than the shear modulus obtained by using the conventional triaxial test. The pulse technique gives the modulus at very small strains, whereas the results of the triaxial test give the modulus at relatively large strains. The moduli obtained vary by several orders of magnitude. Similarly, the strain level in vibratory nondestructive tests is extremely small, whereas the strain level under a loaded plate is relatively large. This is probably the reason why the

Figure 1. Schematic of test setup.

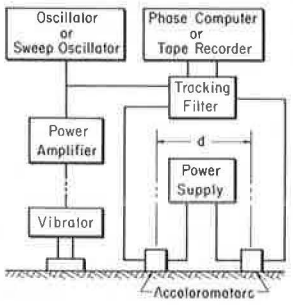

Notes:
1. $\phi°$ = phase difference for distance d
2. One wavelength = 360·d/ϕ
3. Phase velocity = f·360·d/ϕ
4. Frequency, f, is changed to obtain dispersion curves

Figure 2. Vibration test equipment.

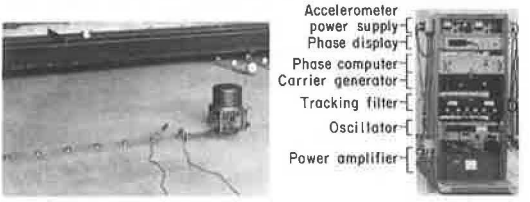

Figure 3. Vibration test results.

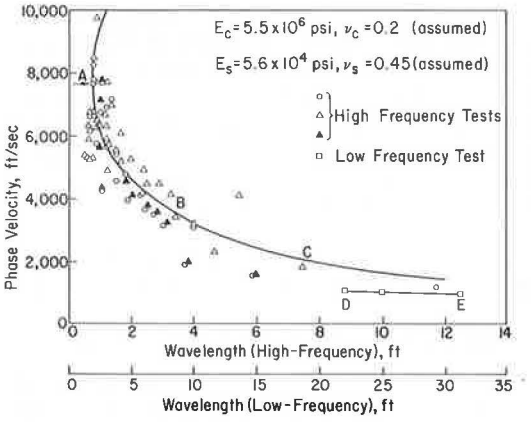

Figure 4. Load test and displacement measurement setup.

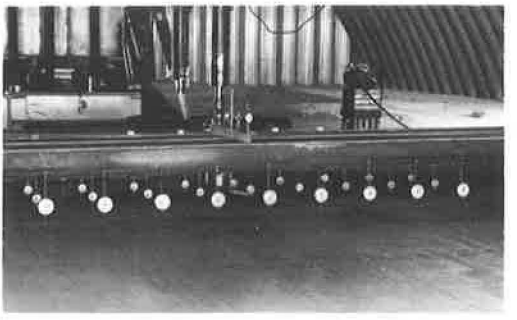

Figure 5. Computed and measured deflection fields (12-in. diameter plate).

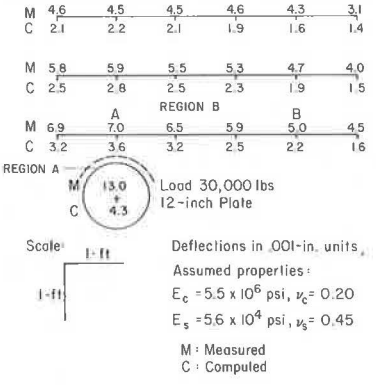

Figure 6. Computed and measured deflection fields (6-in. diameter plate).

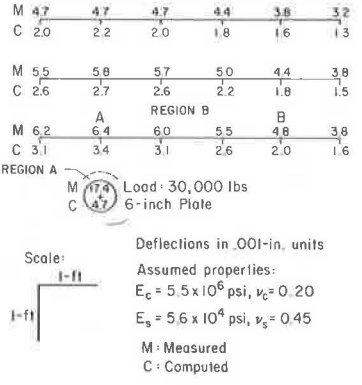

Table 1. Results of parametric study using finite-element model.

Run	System Parameters: Modulus (E), psi	System Parameters: Poisson's Ratio (ν)	Maximum Deflection, in.	Maximum Radial Tensile Stress at 10.8 in., psi	Variable	Remarks
1	$E_1 = 3.5 \times 10^6$ $E_2 = 50{,}000$ E_3 = a) 4,000 b) 40,000 c) 400,000	$\nu_1 = 0.2$ $\nu_2 = 0.3$ $\nu_3 = 0.45$	(a) 0.16383 (b) 0.00486 (c) 0.00210	(a) 157 (b) 130 (c) 99	E_3	Important Parameter
2	$E_1 = 3.5 \times 10^6$ E_2 = a) 2,000 b) 20,000 c) 200,000 $E_3 = 10{,}000$	$\nu_1 = 0.2$ $\nu_2 = 0.3$ $\nu_3 = 0.45$	(a) 0.01109 (b) 0.00957 (c) 0.00892	(a) 161 (b) 155 (c) 131	E_2	Negligible Effect
3	E_1 = a) 10^5 b) 10^6 c) 3.5×10^6 $E_2 = 50{,}000$ $E_3 = 10{,}000$	$\nu_1 = 0.2$ $\nu_2 = 0.3$ $\nu_3 = 0.45$	(a) 0.04790 (b) 0.01699 (c) 0.00935	(a) 28.7 (b) 117 (c) 150	E_1	Important
4	$E_1 = 3.5 \times 10^6$ $E_2 = 50{,}000$ $E_3 = 10{,}000$	$\nu_1 = 0.2$ $\nu_2 = 0.3$ ν_3 = a) 0.15 b) 0.30 c) 0.45	(a) 0.01437 (b) 0.01301 (c) 0.00935	(a) 148 (b) 149 (c) 150	ν_3	Important for Displacement
5	$E_1 = 3.5 \times 10^6$ $E_2 = 50{,}000$ $E_3 = 10{,}000$	ν_1 = a) 0.05 b) 0.20 c) 0.35 $\nu_2 = 0.30$ $\nu_3 = 0.45$	(a) 0.00941 (b) 0.00935 (c) 0.00905	(a) 131 (b) 150 (c) 169	ν_1	Negligible

Figure 7. Computed and measured deflection fields (12-in. diameter plate with modified subgrade modulus).

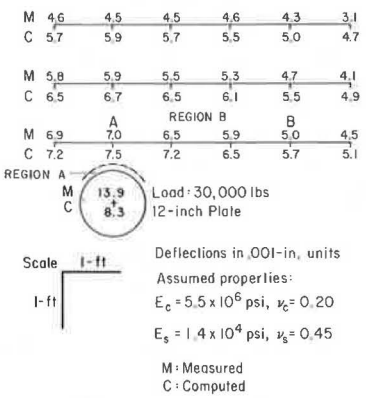

Figure 8. Pure shear stress-strain relation for repeated load tests.

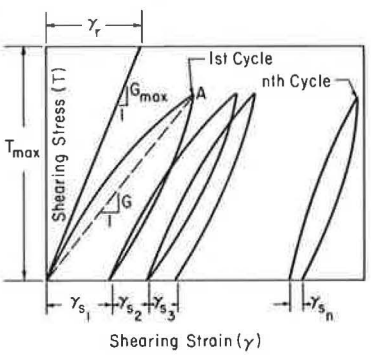

computed displacement fields obtained by using the vibration modulus are much smaller than the measured displacement fields under the loaded plate.

There are two methods for correcting the modulus. One of them is empirical and requires a field test and measurement of the relative deflection between two points. The other utilizes the relation between shear modulus and shear strain on specimens compacted to the same water content and density as in the subgrade.

Method I

The measured relative deflection between points A and B in Figure 5 for the 12-in. diameter plate was 0.0020 in. Similarly, the measured relative deflection between points A and B in Figure 6 for the 6-in. diameter plate was 0.0016 in. These relative deflections occurred under the 30,000-lb load and were easily measured. The computations showed a completely different relative deflection. The computed relative deflection was 0.0014 in. between points A and B for both the 6- and 12-in. diameter plates. Because the deflection is a result of the deformation in the softer subgrade layer, its modulus for purposes of computation may be altered until the computed relative deflection matches exactly the measured deflection basin. Figure 7 shows the results for one of the loaded plate defelction basins by using a modified value of 14,000 psi for the subgrade modulus. The computed relative deflection was 0.0018 in., whereas the measured relative deflection was 0.0020 in. This tends to better match the entire measured deflection basin and the computed deflection basin. This modified modulus value would be more appropriate for computation of the deflection basin under a loaded plate than the modulus obtained by vibration testing. However, this procedure cannot be extrapolated to larger loads.

Method II

This method was developed recently by the University of Kentucky (10). Figure 8 shows the shear stress-strain relation for a continuous constant amplitude loading. Each cycle of loading and unloading is accompanied by a permanent set, γ_{s_n}. The maximum shear modulus obtained at the origin is denoted by G_{max}. For a point A on the loading curve in a load test, one should use G but not G_{max} if linear elastic theories are applied. However, the vibration test results only provide G_{max}. With this fact, a special procedure was developed to correct the modulus (10).

TESTS TO CORRECT ESTIMATED SUBGRADE MODULI

Briefly, the procedure consists of preparing a hollow specimen at the moisture content and density of in situ material and subjecting it, under triaxial conditions, to a torsional type of shear test. The amplitude and rate of loading can be varied. The loading and unloading curves are obtained with an x-y recorder.

A batch of silty clay (used as subgrade material in the test section) was sent to the University of Kentucky, and the results of repeated load tests were published in a recent report (10). Because the subgrade material in the test section had a high moisture content, the data pertaining to high saturation levels were taken from that report and are presented here. Table 2 (taken from another publication, 10) gives the various conditions of the test and the corresponding E values (assuming $\nu = 0.45$).

It is interesting to note that the E_{max} obtained by laboratory tests at the University of Kentucky for the 60 to 90 percent saturation varies between 15 and 20,000 psi. Interpretation of the data from the vibration tests gave an E_{max} of 56,000 psi, which is rather high.

There are three possible reasons for the difference between the E_{max} values obtained by in situ vibration tests and the laboratory tests performed at the University of Kentucky. They are as follows:

1. The presence of the base course in the in situ tests has influenced the interpreted value of the elastic subgrade modulus;
2. The soil in situ could have built a structure because of the time lapse between construction and testing, whereas the tests on the compacted samples were conducted immediately after compaction; and

3. It has been found, by limited experimental data, that E_{max} obtained in the laboratory for stresses below 10^{-6} in./in. remains a constant. If such a statement is not valid for this soil, then the difference in the strain levels on laboratory samples and in in situ tests would account for some of the difference in the E_{max} values.

It is probably because of the first two reasons that a larger E_{max} was produced in the in situ tests. The effect of this difference will diminish when the data are normalized, as will be explained.

The data obtained by the University of Kentucky (10) were plotted in a nondimensional form from the first loading cycle as G/G_{max} versus γ/γ_r (Fig. 9, which is taken from another publication, 10) where γ_r is the reference strain shown in Figure 8. Based on repeated load tests, the best fit curves for samples between 10 and 1,000 cycles of loading and unloading and for first cycles of loading are shown in Figure 9. It was found by these tests that, by dividing the strain, which is already nondimensional, by another reference strain, γ_r (shown in Fig. 8), all data would fall on the two curves shown in Figure 9. The results shown in Figure 9 indicate that the modulus, which varies widely, depends entirely on the strain level. Repeated loads (up to 1,000 cycles) have a tendency to increase the modulus, as shown by the dotted line in Figure 9, until the fatigue effects (which are more pronounced in asphalt pavements) become predominant.

TEST RESULTS TO CORRECT MODULUS

To obtain the deflection basin by nondestructive tests, one must obtain additional information on the variation of shear modulus with the shear strain level. The maximum modulus obtained for the subgrade material by the in situ nondestructive tests will be higher than the value obtained on compacted laboratory samples. One could, therefore, question the applicability of using Figure 9 to correct the in situ modulus. It may be observed from Table 2 that the E_{max} values of the various specimens varied from 5,000 to 20,000 psi. Still, the normalization technique has brought all the results onto one curve shown in Figure 9 (for the first cycle of loading). Hence, the difference in E_{max} values between in situ and compacted laboratory samples will not play a significant role because of the normalization technique used.

Curves similar to Figure 9 are yet to be developed for base course material and for other soil types. The other important study yet to be made is to modify the finite-element programs to accept the modulus variation from point to point. Once these studies are made, an iteration technique may be developed as follows:

1. Based on vibration tests, the maximum moduli values determined by using in situ vibration tests are assumed for each layer, and the strain and deflection fields are obtained by using finite-element programs.
2. Based on data similar to that shown in Figure 9, the modulus of each element is modified depending on its strain level. With the modified modulus value, the new strain and displacement fields are obtained.
3. By iterating several times, the correct deflection profile is obtained for the loaded pavement.

This procedure is under active development at the Civil Engineering Research Facility (CERF), along with the cooperation of several agencies, under the sponsorship of the Air Force Weapons Laboratory (AFWL).

Because this procedure is in the developmental stage, the values given here are assumed to show the validity of the procedure. It is assumed that the properties of each layer will remain constant at each point in the layer but will depend on the average strain level at each layer. With $\gamma/\gamma_r = 1.25$ in the subgrade and $\gamma/\gamma_r = 0$ in the surface layer and base course, the modified moduli values for each layer would be as follows: surface layer, 5.50×10^6 psi; base course, 100,000 psi; and subgrade, $0.25 \times E_{max} =$ 14,000 psi.

Table 2. Data for tests on silty clay.

Test Number	Void Ratio	Saturation (percent)	Chamber Pressure (kg/cm^2)	Initial G_{max} (psi)	Initial[a] E_{max} (psi)
20	0.62	90	0.5	6,770	19,633
21	0.63	91	0.5	5,200	15,080
22	0.74	100	0.5	1,880	5,452
23	0.72	98	0.5	4,360	12,644
24	0.66	96	1.0	4,210	12,200
25	0.74	61	0.5	6,290	18,241

[a]Assuming $\nu = 0.45$.

Figure 9. Normalized loading shear modulus versus normalized strain for silty clay.

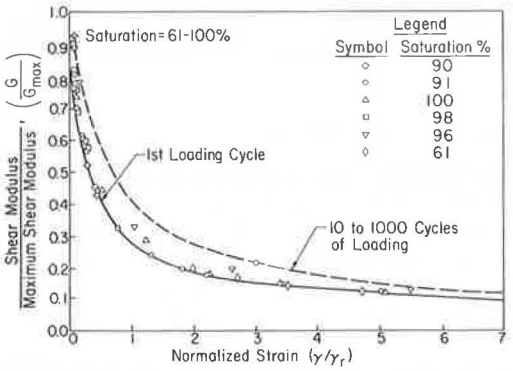

Figure 10. Computed and measured deflection fields (6-in. diameter plate with modified subgrade modulus).

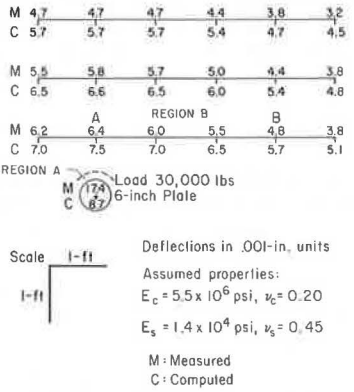

COMPUTED AND MEASURED DISPLACEMENTS WITH MODIFIED SUBGRADE MODULUS

Figure 10 shows a comparison of the measured and computed displacement fields using the modified subgrade modulus and the 6-in. diameter plate. There is closer agreement in the computed and measured displacement fields close to the loaded area, particularly in region B. This study establishes the need for modifying the modulus depending on the strain levels. This procedure can be used not only for evaluation of pavements but also for developing a design technique when laboratory vibration moduli, G_{max} (based on resonant column test or pulse technique), are available for each of the layered materials.

Better agreement between computed and measured deflection at the loaded area itself could be obtained if the finite-element model were developed to accept the change in modulus with strain level at each element.

CONCLUSIONS

Results of the study substantiate the following conclusions:

1. The vibratory method of testing pavement provides information on the maximum modulus of the surface and the deep layer in a three-layered rigid pavement system.
2. The second base course layer plays a minor role in contributing toward the total deflection, and hence any reasonable modulus value may be assumed for this layer.
3. The vibratory method does not provide information on Poisson's ratio.
4. There are two distinct regions in the measured displacement field under thick rigid pavements: regions of high shear strain gradient and regions of moderate shear strain gradient.

5. Two procedures for correcting the modulus of the subgrade have been given. The first matches the relative deflections, and the second uses supplementary laboratory repeated torsion load tests on subgrade soil. The latter procedure is theoretically reasonable; the former procedure is only intuitive.

6. A method has been presented that would make the nondestructive method a practical procedure for estimating the deflection basin under a given load. In the absence of some of the information (like finite-element program accepting of inhomogeneity introduced by different strain levels), an approximate method can be used to predict the deflection basin. This method shows that the predicted deflections agree more closely with the measured deflection in region B when the modulus value for the subgrade is modified.

SUGGESTIONS FOR FUTURE STUDIES

The following suggestions for future studies are offered:

1. The existing finite-element programs should be modified to accept changes in modulus with changes in strain level;
2. Once the capability of predicting the entire deflection field under a loaded area is developed, a distress criterion in terms of strains or stresses should be developed to make the nondestructive procedure practical;
3. More soils should be tested to develop relations between the changes in modulus and the changes in strain level; and
4. This method has been tested on one rigid pavement test section and two flexible pavement test sections (11); however, it should be verified on actual airfields (such investigations are currently in progress).

ACKNOWLEDGMENTS

The research work reported herein was performed under contract F29601-68-C-0009 to AFWL, Kirtland Air Force Base. Appreciation is extended to G. E. Triandafilidis, Manager of Soil and Rock Mechanics at CERF, for guidance at various stages of the work and for review of the manuscript.

REFERENCES

1. Brown, P. P. Airfield Pavement Evaluation Procedures. Jour. of Aerospace Transport Div., Proc. ASCE, Vol. 91, No. AT1, April 1965, pp. 15-31.
2. Finn, F. N., McCullough, B. F., Nair, K., and Hicks, R. G. Plan for Development of a Nondestructive Method for Determination of Load-Carrying Capacity of Airfield Pavements. Materials Research and Development, Inc., Rept. 1062-2(F), Nov. 1966.
3. Jones, R. Surface Wave Techniques for Measuring the Elastic Properties and Thickness of Roads: Theoretical Development. British Jour. of Applied Physics, Vol. 13, 1962.
4. Rao, H. A. B. Nondestructive Evaluation of Airfield Pavements (Phase I). Air Force Weapons Laboratory, Kirtland Air Force Base, Tech. Rept. AFWL-TR-71-75, Dec. 1971.
5. Ramspeck, A., and Schulze, G. A. The Dispersion of Elastic Waves in the Ground. Institute of German Research Association in Soil Mechanics, Technical High School, Berlin, Vol. 14, 1936. (In German.)
6. Jones, R., Thrower, E. N., and Gatfield, E. N. Surface Wave Method. Proc., 2nd Internat. Conf. on Structural Design of Asphalt Pavements, Michigan, Aug. 1967.
7. Vidale, R. F. The Dispersion of Stress Waves in Layered Media Overlaying a Half Space of Lesser Acoustic Rigidity. Univ. of Wisconsin, PhD dissertation, 1964.
8. Lamb, H. On Waves in an Elastic Plate. Proc., Royal Soc. London, Series A, Vol. 93, 1916.

9. Wilson, E. L. Structural Analysis of Axisymmetric Solids. AIAA Jour., Vol. 3, No. 12, Dec. 1965.
10. Hardin, B. O. Constitutive Relations for Airfield Subgrade and Base Course Materials. Univ. of Kentucky, Tech. Rept. UKY32-71-CE5, Soil Mechanics Series 4.
11. Rao, H. A. B. Evaluation of Flexible Pavements by Nondestructive Tests. Proc., 3rd Internat. Conf. on Structural Design of Asphalt Pavements (in publication).

A TECHNIQUE FOR MEASURING THE DISPLACEMENT VECTOR THROUGHOUT THE BODY OF A PAVEMENT STRUCTURE SUBJECTED TO CYCLIC LOADING

William M. Moore and Gilbert Swift, Texas Transportation Institute,
Texas A&M University

•THIS is a progress report on phase 2 of a research study entitled Design and Evaluation of Flexible Pavements, which is being conducted by the Texas Transportation Institute and sponsored by the Texas Highway Department and the Federal Highway Administration. The objective of this phase of the research, as quoted from the study proposal, is "to develop from full-scale testing, a mathematical model estimating the displacement vector at any given point within a pavement structure subjected to Dynaflect loading, given this vector at the surface, the thickness of each layer and a stiffness parameter for each material." Two different models for estimating the vertical component of the displacement vector on a pavement's surface were developed in previous publications (1, 2). The second and more accurate model was used in the development of the flexible pavement design system (3), which is being expanded and implemented in study 123 (4). Use of this model has pointed out several weak points and a pressing need for a still more accurate one.

An accurate model for predicting the displacement vector within any given pavement structure will provide design engineers with a means of calculating strains within the structure and will be an important step in the development of a more realistic approach to pavement design. Thus, it is expected that this study will represent a significant step toward obtaining a more rational pavement design theory.

Several researchers have reported measurements of stresses and strains in situ (5, 6, 7, 8). However, placing stress or strain sensors within a pavement structure tends to destroy the continuity of the material and therefore alters the distribution of the quantities being measured. In contrast, displacement measurements should be substantially unaffected by small perturbations of the system.

Any displacement measurement requires a reference point. As pointed out elsewhere (9), the Dynaflect technique of applying a cyclic force makes it possible to employ an inertial reference point that is not susceptible to measurement errors caused by reference point motion. Other methods of measuring displacement require a physical, tangible reference point that must be sufficiently remote to remain undisturbed during the measurement, at least to the extent set by the desired accuracy of the measurement. Such a point would be quite deep or quite far away if on the surface. Thus, the measurement would require the determination of an extremely small change in a relatively large distance, a requirement that is believed to lead to unacceptably large errors. Accordingly an extention of the Dynaflect measuring technique, employing geophones as displacement sensors, was adopted for this study.

Surface deflections of a pavement structure, as normally measured with the Dynaflect, provide insufficient data to define the response of the entire structure to the loading on its surface. Thus, measurement of the displacement vector field throughout the pavement structure was undertaken in this study to provide data for developing the model required in the study's objective or for verifying existing models such as linear elasticity, linear viscoelasticity, and so forth.

Sponsored by Committee on Pavement Condition Evaluation.

The purpose of this report is to describe the apparatus and technique developed to measure both horizontal and vertical components of the displacement vector. It includes typical measurements obtained as well as the replication errors encountered.

SCOPE OF MEASUREMENTS PROGRAM

The Texas A&M pavement test facility is being used to obtain data for analysis. This facility, located at the University's Research Annex, was constructed for the purpose of providing a means for evaluating nondestructive testing techniques and especially for evaluating testing equipment purporting to furnish information concerning the in situ characteristics of the individual layers in a flexible pavement. It consists of 32, 12- by 40-ft test sections that have different structural characteristics in accordance with the principles of statistical experiment design. The design of the facility is described in detail elsewhere (1). Plan and cross-sectional views of the test facility are shown in Figure 1.

The displacement vector field of a test section is induced by loading the section with a Dynaflect. This instrument, shown in Figure 2, produces a vertical dynamic load of 1,000 lb, oscillating sinusoidally with time at 8 Hz, which is applied to the surface through two steel wheels spaced 20 in. apart. A complete description is given elsewhere (9, 10). Vertical displacement measurements are made on the surface of the pavement by using low-frequency geophones whose output voltage is directly proportional to the amplitude of the sinusoidal motion.

The displacement vector field was determined on a test section by measuring separately the horizontal and vertical components of motion at selected depths and horizontal distances from the points of application of the surface loads. Individual component measurements were made by using a miniature geophone—either one designed for horizontal motion or one designed for vertical motion. The geophone was clamped in place in a small-diameter hole drilled vertically in the pavement section. The measurement depth was altered by clamping the geophone at various depths, while the horizontal distance from the points of application of the surface load was altered by moving the Dynaflect forward on the surface various distances. By utilizing this concept (Fig. 3), we made sufficient measurements to define both the vertical and horizontal component fields in the region from 0 to about 5 ft in depth and from approximately 1 to 18 ft in horizontal distance. Because of the 20-in. spacing of the Dynaflect load wheels, it was not practical to make measurements at horizontal distances less than 10 in.

To date, displacement vector fields have been measured at two locations on each of three test sections. The planned program includes replicate measurements on all 32 of the test sections. Replicate measurements, made on opposite ends of each test section, will permit analysis of overall precision. Replication errors observed on a test section not only reflect the variability of the measuring process but also include the effects of variations in the structural properties of the section. The combined variability will define the limiting prediction accuracy for the displacement model being sought.

MEASURING TECHNIQUE

Basic Technique

Extension of the Dynaflect technique to the measurements of the displacement vector throughout the pavement structure was accomplished by using a pair of suitable geophones—one responsive only to the vertical component of motion, the other responsive only to the horizontal component—and clamping them one at a time at selected depths in a single hole in the structure. With either geophone placed at a given depth, the Dynaflect was positioned at a succession of locations on the surface ranging from directly above the hole up to 18 ft away.

Geophone Emplacement

In order to minimize disturbance to the pavement sections, we obtained miniature geophones, and an assembly that could be emplaced was designed. The assembly was

Figure 1. Pavement test facility.

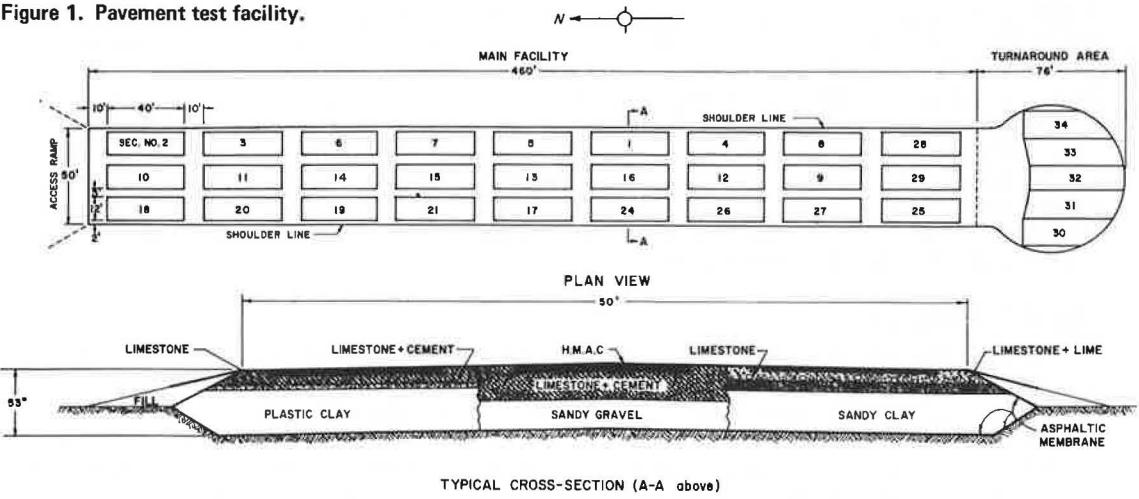

TYPICAL CROSS-SECTION (A-A above)

Figure 2. Dynaflect trailer in normal use with five-geophone array on pavement surface.

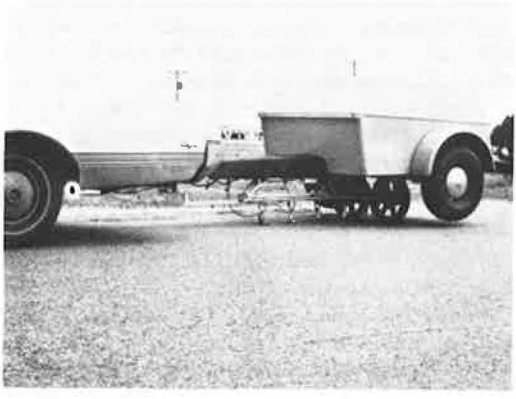

Figure 3. Representation of the technique used to measure vector displacements within a pavement section.

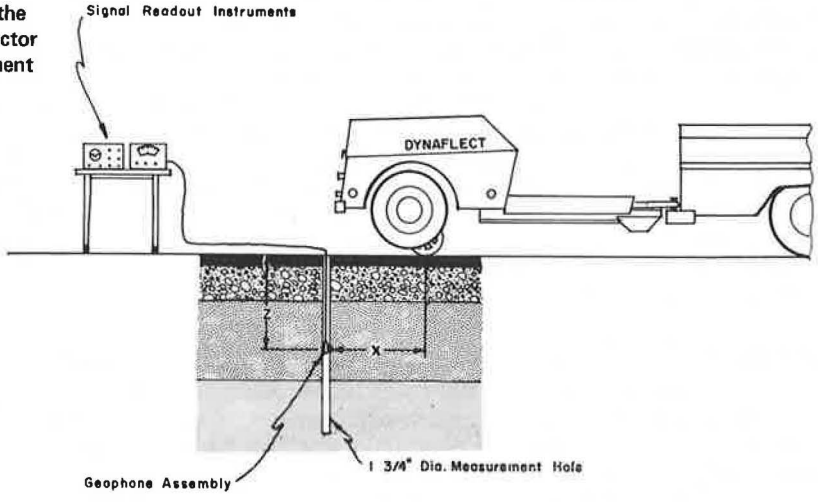

sufficiently small to fit within a $1\frac{3}{4}$-in. diameter hole. The down-hole geophone assembly is shown in Figure 4. It contains a waterproof aluminum housing in which one geophone, either horizontal or vertical, is mounted. Two spring-loaded pistons can be released to expand outward and clamp the device in the hole. Flexible steel cables (fishing leader wire) extend above the surface to permit the release and retraction of the pistons. A removable hollow rod, through which the electrical output cable passes, allows the $1\frac{5}{8}$-in. diameter device to be lowered into the hole with the pistons retracted. At the desired depth, the pistons are released. The rod is then disconnected and removed from the hole, leaving the unit in place with slack wires extending to the surface. The unit is retrieved by reversing this procedure.

Drilling Technique

After disappointing results were obtained with several types of drill rigs and drill bits, a satisfactory combination was found. All of the successful holes, usable for geophone emplacement, have been drilled with a Clipper Core Drill Model D-30-P using a diamond core barrel, $1\frac{3}{4}$ in. in diameter and 14 in. long. This drill is used with a continuous flow of compressed air while penetrating the hot-mix asphaltic concrete surface layer and the limestone base or subbase layers. The same core barrel is employed, without airflow, to penetrate the softer embankment and subgrade materials. Where the material is soft clay, the drill is used without rotation.

It was decided before undertaking this work that air must be employed during drilling because water would alter or damage the pavement sections. In spite of this precaution, water trapped in the embankment material invaded several of the holes during the measurement period within 1 or 2 hours after hole completion. No adverse effects were attributable to this water in those sections in which it was possible to complete the measurement sequence. In one group of sections, however, the hole walls collapsed and prevented emplacement of the geophone. It is planned to drain the excess water from the saturated zones prior to making more measurements on these sections.

Measuring Procedure

The measuring procedure developed for this investigation began with emplacement of the vertical geophone at the greatest chosen depth. The Dynaflect was then positioned on the surface directly over the hole. After it read and recorded the geophone output voltage, the Dynaflect was moved away from the hole to each of a series of preselected distances. The geophone signal was read and recorded at each location. At the end of each such series of measurements, the geophone was retrieved and repositioned at a shallower depth in the hole. On completion of the entire grid of measurements, the preceding procedure was repeated using the horizontal geophone. When using the latter, in addition to recording the magnitude of its output signal, the phase angle was observed to determine whether the horizontal displacement was toward or away from the load.

Ordinarily, one hole and one entire set of vertical and horizontal displacement measurements can be completed within a day. At the end of each set of horizontal or vertical measurements, the geophone used for that set was calibrated by observing its response to a 0.005-in. oscillatory motion provided by the Dynaflect calibrator unit. The calibration factor thus established was utilized to convert the recorded voltage readings to displacements in millionths of an inch. By using a Hewlett Packard Model 502A Wave Analyzer to read the voltages, we measured displacements as small as a millionth of an inch. Thus far, the observed movements have ranged from less than 1 millionth to 2 thousandths of an inch.

Transformation of Measurements to a Single Load Vector Field

As previously mentioned, the Dynaflect applies a 1,000-lb load to the surface through two wheels that are spaced 20 in. apart. Hence, when the Dynaflect is centered over a hole, its two load application points are equidistant at a 10-in. radial (horizontal) distance from the hole. Moving the Dynaflect forward a distance, x, along a straight line increases both of these radial distances while maintaining their equality. The radial distance, r, from the hole to either of the load application points is given by

$$r = \sqrt{x^2 + 10^2}$$

In order to simplify the presentation of the data, we converted the observed measurements to the case of a single 1,000-lb axially symmetrical load acting at a distance, r, from the hole by assuming that the displacement vectors at any depth, z, produced by the two 500-lb loads were of equal magnitude and were vectorially additive.

The vertical displacement components produced by each of the two loads are alike in both magnitude and direction; therefore, the vertical component for a single 500-lb load would be half the measured value, and for a single 1,000-lb load it would be equal to the measured value. This measured value is represented by the symbol w.

The horizontal components of motion produced by each load wheel are alike in magnitude but, unlike the vertical components, are directed along lines parallel to the radial (horizontal) lines on the surface joining the hole with the individual load application points. Hence, when the Dynaflect is centered over the hole, the horizontal components due to each load wheel are in opposite directions. Because this represents a null of horizontal motion, the horizontal measurement is omitted at this position. The horizontal measurement closest to the loads is made with the Dynaflect axle 6 in. away from the hole, and the most remote measurement is made when it is 18 ft (or 216 in.) away. At any given forward distance x (Fig. 5), the horizontal displacement components produced by each load wheel are equal in magnitude but are separated by an angle 2α, where $\alpha = \arctan(10/x)$. Thus the measured horizontal displacement, M_h, is related to the horizontal displacement, u, resulting from a single 1,000-lb load, by

$$u = M_h \sec \alpha$$

as is verified by Figure 5.

Sec α can be regarded as a correction factor that is applied to the measured values of horizontal displacement to transform them to values that would have been obtained in the assumed axially symmetrical case. Figure 6 shows sec α versus x. From this plot, it can be seen that the correction factor approaches unity very quickly as the Dynaflect is moved forward to increase the horizontal distance x. Thus, the principle of Saint-Venant is illustrated in that the correction factor becomes insignificant at values of x exceeding two or three times the 20-in. distance between the load wheels (11).

GEOMETRIC LIMITS OF VECTOR FIELD

Because the existing dimensions of the Dynaflect make it inconvenient to measure vertical displacements at locations closer than x = 0 (or r = 10 in.) from the load application points or horizontal displacements at locations closer than x = 6 in. (or r = 11.7 in.), these dimensions form the close-in limits of the measured displacement fields. The far-out limit of x = 216 in. (or r = 216.2 in.) was selected on consideration of the finite (40 ft) length of the sections and the observed diminution of the displacements with distance and with depth. The depth limit, at $z \approx 65$ in. below the surface, was selected on the basis that the test facility comprises 53 in. of selected materials situated on a reasonably uniform clay foundation that is regarded as extending infinitely downward. In view of the observed displacement behavior, it is believed that the outer limits of the measured fields have been placed amply far to encompass the region of major interest and to permit reasonable extrapolation beyond this region.

Thus, the geometrical limits of the transformed vector fields determined from the measurements are as follows:

1. Field of the component u—11.7 in. $\leq r \leq$ 216.2 in., $0 \leq z \leq 65$ in. (approximately), and
2. Field of the component w—10 in. $\leq r \leq$ 216.2 in., $0 \leq z \leq 65$ in. (approximately).

MEASURED DISPLACEMENTS

Replicate measurements of displacements have been made on three pavement sections and are shown for one section in Figures 7 and 8. Single sets of measurements for the

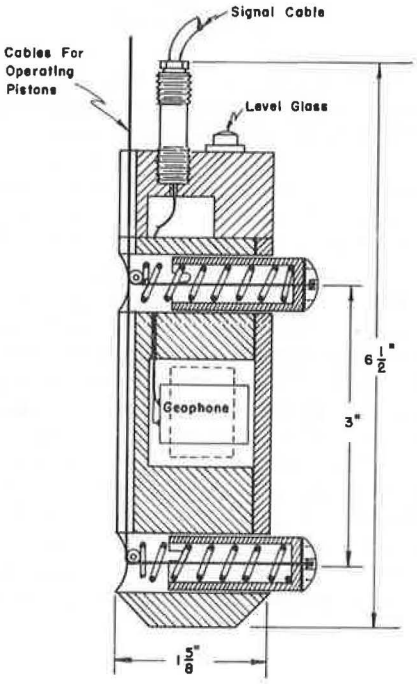

Figure 4. Cross-sectional view of subsurface geophone assembly.

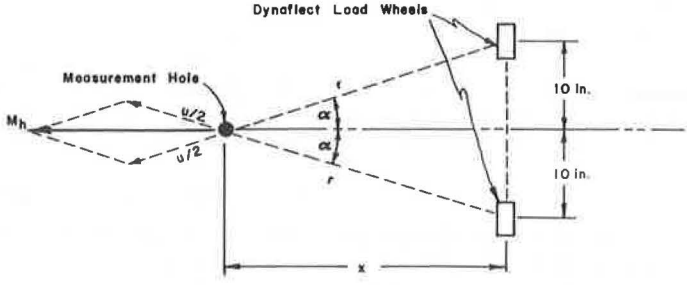

Figure 5. Relation of the horizontal displacement vectors produced by each load wheel and the measured horizontal displacement.

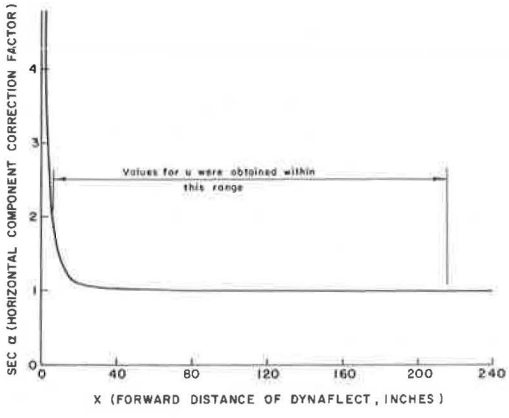

Figure 6. Relation of forward distance of Dynaflect and correction factor applied to the measured horizontal displacement in the transformation to a single load point.

Figure 7. Displacement fields measured in section 25—numerical values on contours denote displacements in microinches.

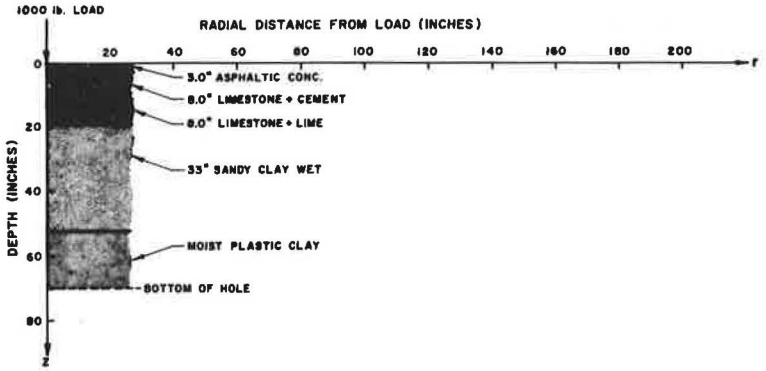

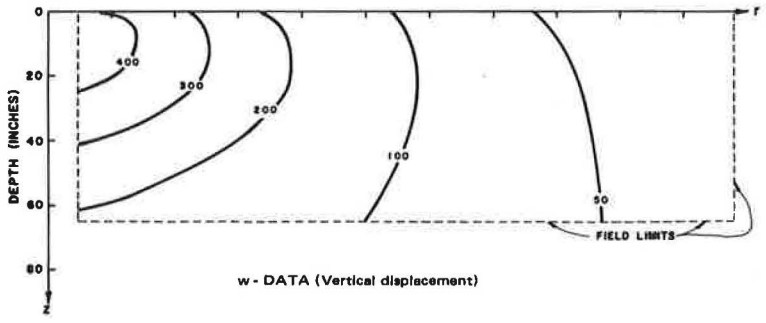

w - DATA (Vertical displacement)

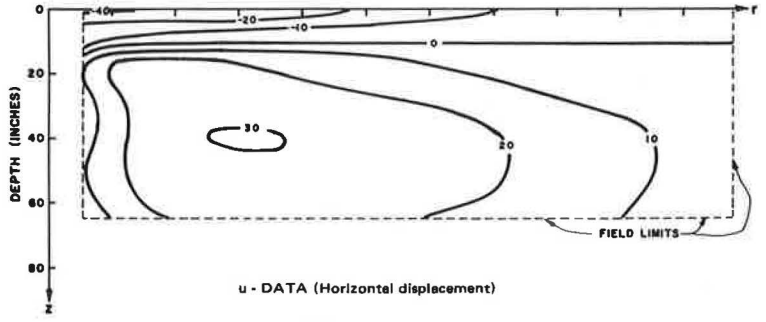

u - DATA (Horizontal displacement)

REPLICATION 1

Figure 8. Replicate measurements of section 25 at a location 40 feet away from the location used for Figure 7.

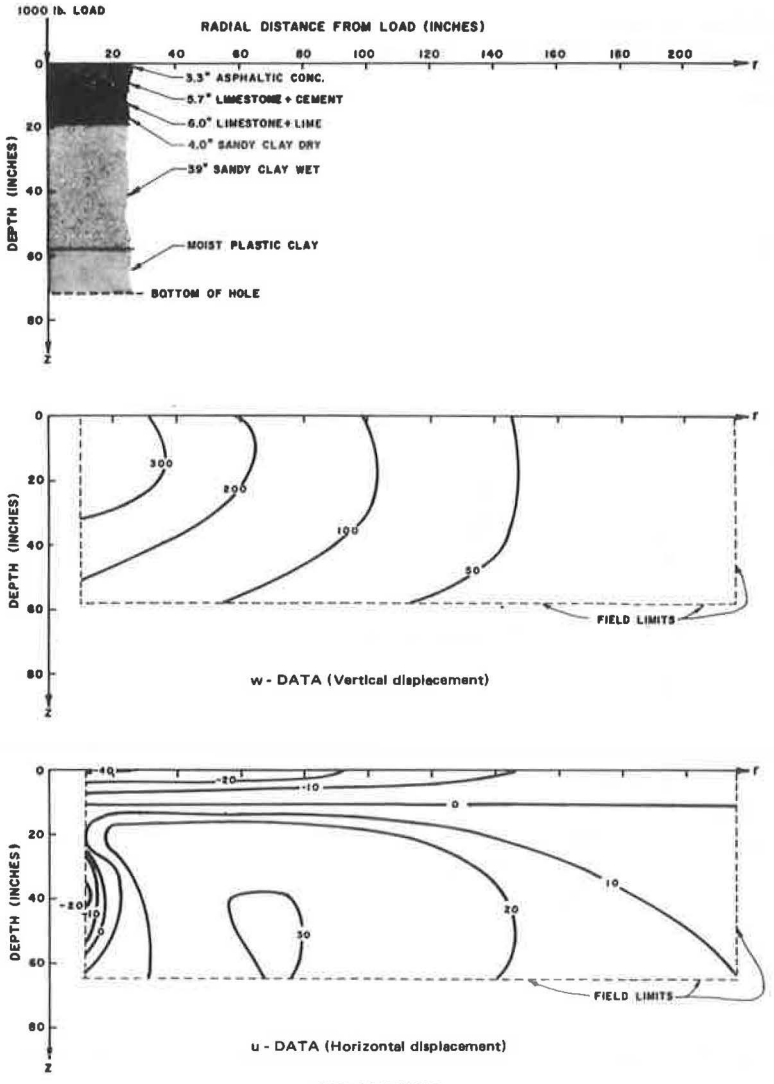

REPLICATION 2

Figure 9. Displacement fields measured in section 31—numerical values on contours denote displacements in microinches.

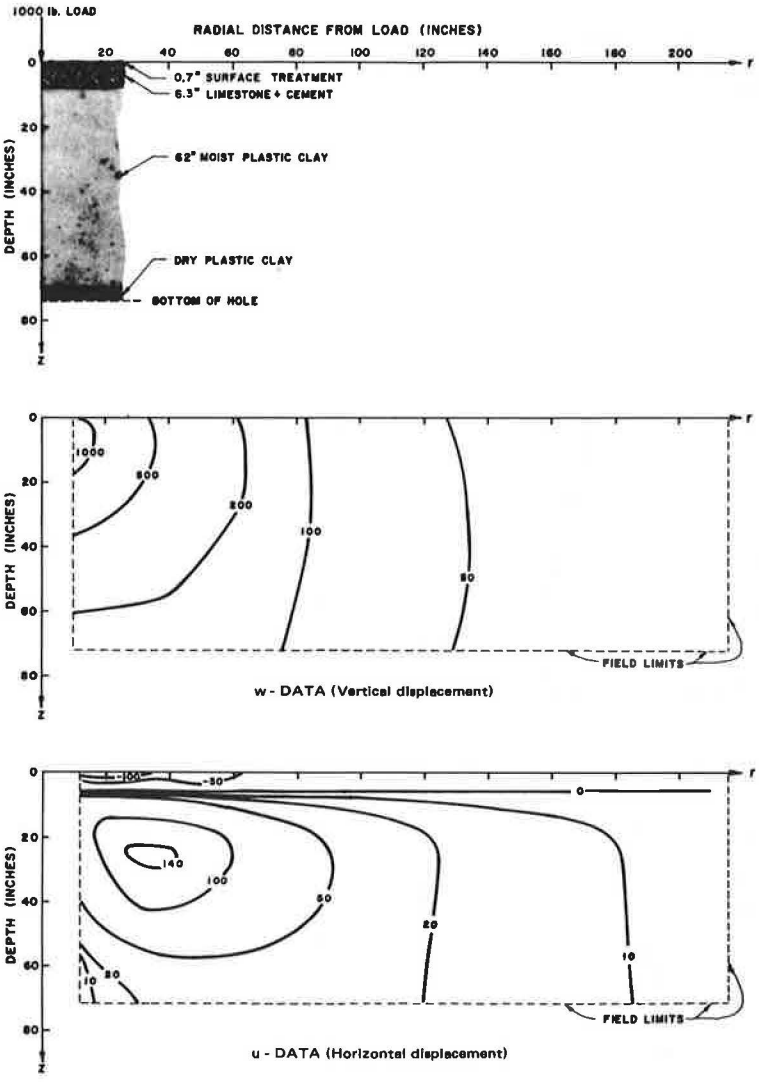

REPLICATION 1

Figure 10. Displacement fields measured in section 32—numerical values on contours denote displacements in microinches.

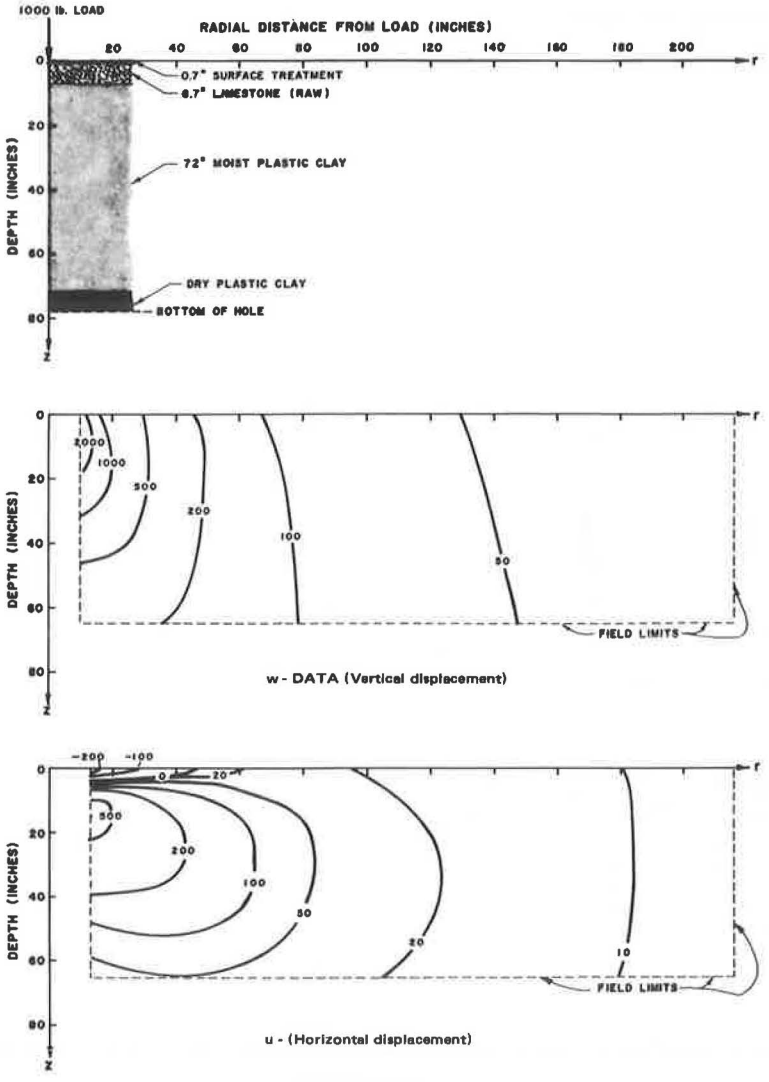

REPLICATION 1

other two sections are shown in Figures 9 and 10. In each of these figures, the layer thicknesses determined in the measurement holes are shown at the top, contours of equal vertical displacement, w, are shown in the center, and contours of equal horizontal displacement, u, are shown at the bottom. Typical data used to prepare these figures are given in the Appendix.

Observed w values are positive everywhere in all plots; thus all points had a component of motion downward. Both positive and negative values were found for u. Positive values indicate a component of motion directed outward from the load axis; negative values indicate motion toward it.

For all three sections, the fields obtained for replication 1 are very similar to those for replication 2. The differences between the replications are quite small in comparison to the differences between sections. The main difference between sections that can be seen in the w fields is in the magnitude near the load. More striking differences between sections appear in the u fields. The general magnitude of the displacements in the three sections shown is clearly related to the designs; that is, the magnitudes are in inverse order of pavement strength.

Figure 11 shows w and u fields for a two-layer elastic system that is composed of a 19-in. thick top layer having an elastic modulus of 600,000 psi above an infinitely thick layer having an elastic modulus of 20,000 psi with Poisson's ratio equal to 0.5 in both layers. The dimension of 19 in. was chosen to match the total design pavement thickness (depth to top of embankment) of section 25. The displacements shown were calculated by using a computer program developed by the Chevron Oil Company (12, 13) using a 1,000-lb load on a circular area having a radius of 1.41 in. This radius approximates that of the contact area of a Dynaflect load wheel (14).

The measurements made on section 25 (Figs. 7 and 8) are somewhat similar to the fields computed for the two-layer elastic system shown in Figure 11. The general shapes of both the u and the w fields are alike, and the position of the zero contour for u in both cases is approximately horizontal and about 10 in. from the pavement surface. Work toward developing elastic-layered system fields to match the observed fields is continuing.

REPLICATION ERRORS

As previously mentioned, replicate measurements were made on opposite ends of a test section, and their differences generally were found to be quite small when compared with differences among sections, as evidenced by Figures 8, 9, and 10. The differences among the measurements made on the same section are due to both the variability of the measuring process and the variability in the structural characteristics of the section at its two ends. In the measurement procedure used, all points were not replicated. Thus, in the determination of the replication errors, only the points that were replicated could be compared.

Plots of the replication errors for section 25 (half the difference between the observations) versus the mean observation (half the sum of the observations) are shown in Figure 12. Also shown on these plots are the percentage-of-error lines that include three-fourths of the replication errors. As can be seen in these figures, the data are somewhat biased as indicated by the sloping trend of the w points. This indicates a consistent difference between the two ends of the section. Nevertheless, when disregarding the reasons for the errors, the errors found in w are very small when compared to the range of the measured values, and the errors found in u are thought to be acceptable. The larger percentage of errors found in u are chiefly due to the fact that the relative magnitude of u changes much more rapidly within the measured field than does the relative magnitude of w. This is evidenced by the crowding of the contour lines in the plots of the u fields (Figs. 7, 8, 9, and 10).

Table 1 gives a summary of the replication measurements. It shows the average, the average absolute, and the range of the mean observations. From these values, one can note that the sections measured were very different. The table also contains the maximum absolute and the root mean square of the replication errors as well as the percentage-of-error values that include half and three-fourths of the errors. Values from the last column for section 25 are shown in Figure 12.

Figure 11. Computed displacement fields for two-layered elastic system—numerical values on contours denote displacements in microinches.

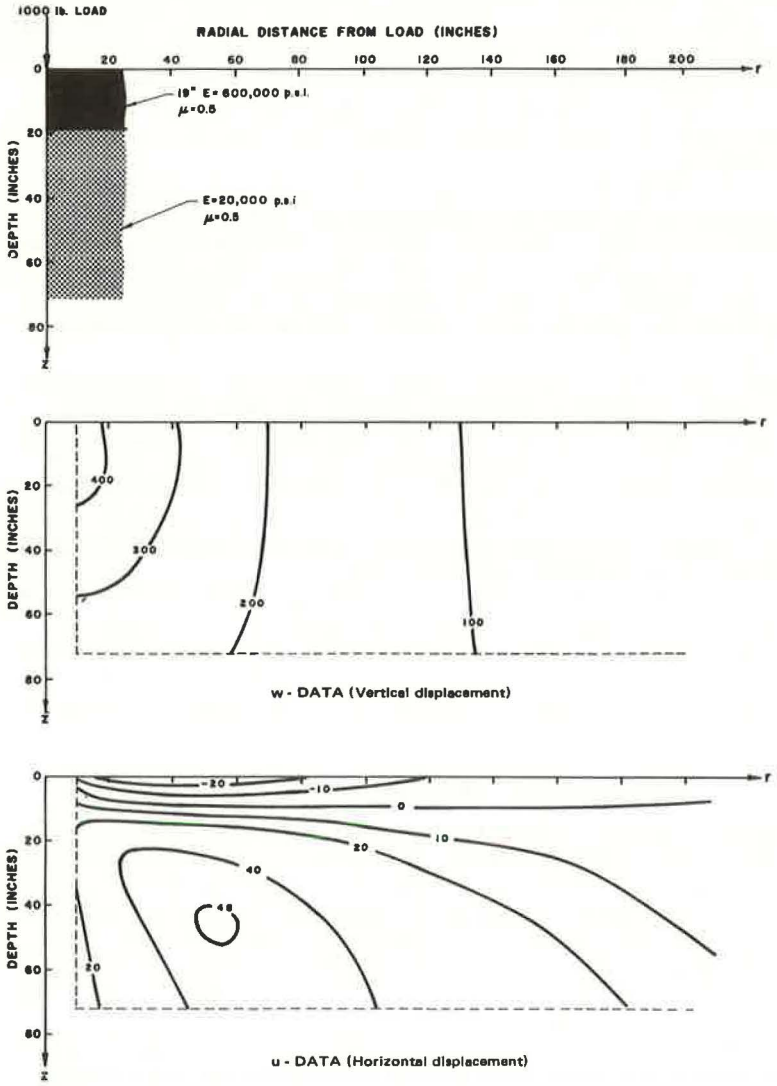

Figure 12. Replication errors for section 25 (half the difference between observations) versus mean observations—scales are in microinches and multiple occurrences of points are indicated by number.

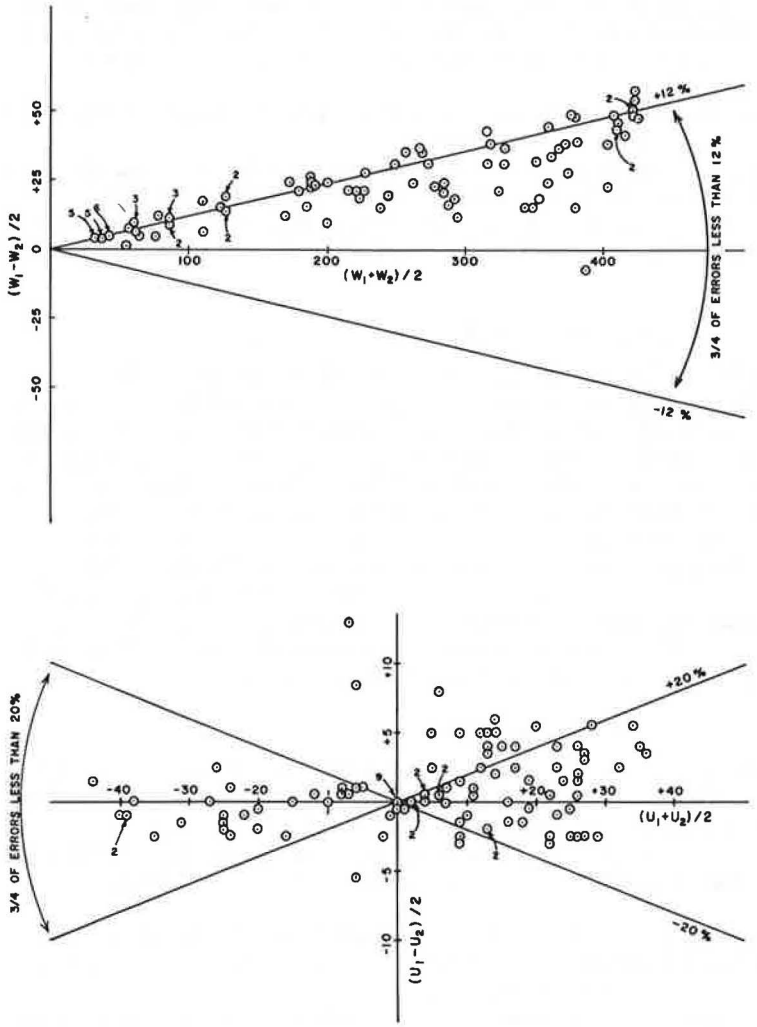

Table 1. Summary of replication measurements.

Section	Variable Measured	Number of Comparisons	Mean Observation[a]			Replication Error[b]		Percentage of Error[c]	
			Average	Average Absolute	Range	Maximum Absolute	Root Mean Square	½ of Errors	¾ of Errors
25	w	98	223.6	223.6	31 to 424	57	26.4	10	12
25	u	104	4.1	15.6	-44 to 36	13	2.9	10	20
31	w	196	301.4	301.4	30 to 1,545	303	52.8	5	8
31	u	182	33.4	51.3	-210 to 166	97	13.6	10	19
32	w	112	433.9	433.9	30 to 2,912	307	60.9	3	6
32	u	89	94.6	123.4	-686 to 556	126	34.0	13	20

[a]Mean of two replicated observations, $(w_1 + w_2)/2$ or $(u_1 + u_2)/2$.
[b]One-half of the difference between two replicated observations, $(w_1 - w_2)/2$ or $(u_1 - u_2)/2$.
[c]Replication error divided by mean observation and expressed as a percentage.

CONCLUSIONS

The results of this study support the following conclusions:

1. A practical fieldworthy measuring technique has been developed for use with the Dynaflect to observe the displacement vector throughout the body of a pavement section;
2. Replication errors observed on a test section are reasonably small compared to variations between sections;
3. The observed vector displacement fields resemble fields computed for a layered elastic system to which an equal static load is applied;
4. It appears feasible to determine for each section a set of elastic layers for which the computed displacement fields will substantially match the observations; and
5. Examination of the data indicates that it should be possible to formulate a useful and practical mathematical model representing the displacement response of the several pavement sections.

ACKNOWLEDGMENTS

The research was done by the Texas Transportation Institute, Texas A&M University, in cooperation with the Texas Highway Department and was sponsored jointly by the Texas Highway Department and the Federal Highway Administration. The authors wish to thank all members of the Institute who assisted in this research. They would like to express special appreciation to Frank H. Scrivner and Lionel J. Milberger. Their help throughout the study has been particularly valuable. Thanks are also due C. H. Michalak for his assistance in the data reduction phase and John Salyer for his assistance during the fabrication and testing phases. The authors are grateful to the Texas Highway Department for its interest and cooperation. They would like to express special gratitude to James L. Brown and Larry J. Buttler of the Highway Design Division for their assistance and support of this research and to the personnel of Districts 8 and 17 for their assistance during the development of the drilling technique.

REFERENCES

1. Scrivner, F. H., and Moore, W. M. Evaluation of the Stiffness of Individual Layers in a Specially Designed Pavement Facility From Surface Deflections. Texas Transportation Institute, Texas A&M Univ., Res. Rept. 32-8, 1966.
2. Scrivner, F. H., and Moore, W. M. An Empirical Equation for Predicting Pavement Deflections. Texas Transportation Institute, Texas A&M Univ., Res. Rept. 32-12, 1968.
3. Scrivner, F. H., Moore, W. M., McFarland, W. F., and Carey, G. R. A Systems Approach to the Flexible Pavement Design Problem. Texas Transportation Institute, Texas A&M Univ., Res. Rept. 32-11, 1968.
4. Hudson, W. R., McCullough B. F., Scrivner, F. H., and Brown, J. L. A Systems Approach Applied to Pavement Design and Research. Texas Transportation Institute, Texas A&M Univ., Res. Rept. 123-1, 1970.
5. Brown, S. F., and Pell, P. S. An Experimental Investigation of the Stresses, Strains, and Deflections in a Layered Pavement Structure Subjected to Dynamic Loads. Proc. 2nd Internat. Conf. on Structural Design of Asphalt Pavements, Univ. of Michigan, Ann Arbor, 1967, pp. 487-504.
6. Busfeldt, K. H., and Dempwolff, K. R. Stress and Strain Measurements in Experimental Road Sections Under Controlled Loading Conditions. Proc. 2nd Internat. Conf. on Structural Design of Asphalt Pavements, Univ. of Michigan, Ann Arbor, 1967, pp. 663-669.
7. Klomp, A. J. G., and Niesman, T. W. Observed and Calculated Strains at Various Depths in Asphalt Pavements. Proc. 2nd Internat. Conf. on Structural Design of Asphalt Pavements, Univ. of Michigan, Ann Arbor, 1967, pp. 671-688.
8. Nijboer, L. W. Testing Flexible Pavements Under Normal Traffic Loadings by Means of Measuring Some Physical Quantities Related to Design Theories. Proc. 2nd Internat. Conf. on Structural Design of Asphalt Pavements, Univ. of Michigan, Ann Arbor, 1967, pp. 689-705.

9. Scrivner, F. H., Swift, G., and Moore, W. M. A New Research Tool for Measuring Pavement Deflection. Highway Research Record 129, 1966, pp. 1-11.
10. Pace, G. M. Evaluation of the Dynaflect for the Non-Destructive Testing of Portland Cement Concrete Pavements. Department of the Army, Ohio Division Laboratories, Corps of Engineers, Cincinnati, Tech. Rept. 4-61, 1967.
11. Timoshenko, S., and Goodier, J. N. Theory of Elasticity. McGraw-Hill Book Co., Inc., 1951, pp. 337-365.
12. Michelow, J. Analysis of Stresses and Displacements in an N-Layered Elastic System Under a Load Uniformly Distributed Over a Circular Area. California Research Corporation, Richmond, Sept. 1963.
13. Warren, H., and Dieckmann, W. L. Numerical Computation of Stresses and Strains in a Multiple-Layered Asphalt Pavement System. California Research Corporation, Richmond, Sept. 1963.
14. Scrivner, F. H., Michalak, C. H., and Moore, W. M. Calculation of the Elastic Moduli of a Two Layer Pavement System From Measured Surface Deflections. Texas Transportation Institute, Texas A&M Univ., Res. Rept. 123-6, 1971.

APPENDIX

TYPICAL REPLICATION DATA

SECTION 25 REPLICATION 1

W - DATA (MICRO-INCHES) FOR SINGLE 1000 LB. LOAD

DEPTH Z (IN.)	**********	RADIAL DISTANCE R (IN.)											**********
	10.0	11.7	15.6	20.6	26.0	37.4	49.0	60.8	72.7	96.5	120.4	144.3	180.3	216.2
0.0	378	424	393	363	357	306	263	209	181	118	81	56	40	33
3.0	469	469	454	424	403	354	303	242	212	145	96	69	48	39
11.0	478	475	454	424	399	345	303	242	212	142	93	66	48	36
15.0	469	469	451	424	403	357	303	248	212	145	96	69	48	39
19.0	451	454	439	409	393	345	303	254	215	142	96	69	48	39
29.0	381	381	369	363	357	309	278	236	199	139	96	66	49	39
41.0	303	299	299	290	284	254	224	196	175	127	90	69	45	36
52.0	230	230	224	218	212	196	178	157	139	109	81	63	45	36
65.0	193	193	187	187	187	175	163	145	133	103	81	63	48	36

U - DATA (MICRO-INCHES) FOR SINGLE 1000 LB. LOAD

DEPTH Z (IN.)	**********	RADIAL DISTANCE R (IN.)											**********
	10.0	11.7	15.6	20.6	26.0	37.4	49.0	60.8	72.7	96.5	120.4	144.3	180.3	216.2
0.0		-42	-38	-40	-39	-39	-37	-32	-26	-20	-14	-10	-7	-5
3.0		-24	-22	-25	-26	-26	-26	-23	-21	-18	-11	-7	-5	-4
11.0		-11	-4	-2	0	0	0	0	0	0	0	0	0	0
15.0		8	13	16	17	19	18	16	14	10	6	4	1	0
19.0		9	18	21	24	26	27	25	22	16	11	7	4	1
29.0		2	10	16	20	27	30	30	29	25	19	15	7	4
41.0		5	13	20	25	33	39	39	39	34	28	20	12	7
52.0		3	10	16	21	28	33	35	35	32	26	21	12	8
65.0		5	6	10	14	18	24	25	26	24	19	15	10	7

FATIGUE CRACK FORMATION AND PROPAGATION IN PAVEMENTS CONTAINING SOIL-CEMENT BASES

P. C. Pretorius, Bruinette, Kruger, Stoffberg and Hugo, Johannesburg, South Africa; and
C. L. Monismith, Institute of Transportation and Traffic Engineering, University of California, Berkeley

In this report an attempt is made to predict the formation and development of fatigue cracks in pavements containing soil-cement bases. It is assumed that transverse shrinkage cracks have already formed. To obtain realistic results, we analyzed a typical pavement section consisting of 3 in. of asphalt concrete and 8 in. of cement-treated base resting on a clayey subgrade. The properties of the cement-treated base were developed from an extensive laboratory investigation, and the fatigue results obtained are reported in some detail. These results confirm previous fatigue studies performed by the Portland Cement Association. To estimate the stresses in a pavement system with transverse shrinkage cracks present and thus to estimate the potential for fatigue cracking, we used a prismatic-space finite-element procedure. The results of the analysis show that the first fatigue crack to develop is perpendicular to the shrinkage crack and in the position of the wheelpath. A crack of this type may propagate fairly rapidly because of stress concentrations at the tip of the crack and lead to the "corner loading" situation bounded by the shrinkage and perpendicular fatigue cracks. This situation can be analyzed approximately by using the Westergaard formula, i.e., transforming the asphalt concrete layer to an equivalent thickness of cement-treated base. The stresses resulting from this analysis indicate the potential for additional load-associated cracking leading to the possibility for the corner to break off. Because this situation can repeat itself with continued load repetitions, the familiar double-ladder crack pattern is established. It is also shown that the presence of a longitudinal shrinkage crack parallel and close to the fatigue crack may give rise to a single-ladder crack pattern. The crack pattern predictions are substantiated to some degree by a field investigation. The propagation of load-associated cracks was traced by periodically photographing an underdesigned pavement containing a cement-treated base over a period of time during which rapid deterioration due to repeated loading occurred.

•IN a previous paper (1) it was shown how the formation and spacing of shrinkage cracks in pavements containing soil-cement bases could be predicted by using laboratory measured material characteristics together with an incremental finite-element solution for a system representative of the pavement structure. Material characteristics included measured values for shrinkage, creep, and strength (both tensile and compressive). Although such an approach may be of interest to the researcher, it may hold less significance for the practicing engineer because the formation of shrinkage cracks in soil cement is generally inevitable (2). Of more significance are the consequences of shrinkage cracking because such cracking may contribute to a rapid deterioration in pavement serviceability under certain circumstances.

Sponsored by Committee on Theory of Pavement Design.

The primary purpose of this paper is to illustrate how load cracks can propagate from a shrinkage crack and includes a discussion of some of the variables that influence the crack pattern and rate of crack propagation. Observations of the performance of an in-service pavement during a 5-month period are included to show the validity of this procedure.

METHOD

The approach used in this investigation involved the selection for analysis of a pavement containing a soil-cement base consisting of 3 in. of asphalt concrete and 8 in. of soil cement resting on a clayey subgrade.

Stiffness characteristics of the asphalt concrete and clayey subgrade were selected on the basis of experience with such materials in previous investigations, recognizing temperature and time of loading effects for the asphalt concrete and stress effects for the subgrade material. Data for the soil cement were the same as reported earlier (1). This material consisted of a partially crushed gravel (gradation shown in Fig. 1) treated with 5.5 percent by weight of cement, which satisfied the wet-dry test of the Portland Cement Association.

Because this aspect of the study was concerned with load-associated cracking of the soil cement, an extensive fatigue investigation was conducted on the cement-treated material, results of which will be detailed in a subsequent section.

To analyze the load-associated stresses in the vicinity of a transverse shrinkage crack, we used the prismatic space finite-element method (3). This analysis procedure is essentially two-dimensional with the third dimension introduced into the idealization by expressing the load as Fourier Series in the third direction. A finite-element discreteness of the structure is shown in Figure 2. A particular structure is solved for every Fourier term necessary to adequately represent the load. The x and y displacements vary cosinusoidally and the stresses sinusoidally in the z direction, which allows a complete stress and strain solution at any desired z position. Unfortunately, the program is time-consuming because a complete finite-element solution is required for every Fourier term required to represent the load. Usually, 10 to 15 such terms produce satisfactory results.

Maximum stresses corresponding to the post-cracked situation can then be compared to the stresses obtained for the internal (uncracked) loading condition (by using either the axisymmetric finite-element approach or the Chevron 5-layer computer program). By comparing fatigue lives corresponding to each loading condition, we can establish the first fatigue crack, and, depending on other influences, a prediction of the pattern of crack propagation may be possible.

FATIGUE INVESTIGATION

Comparatively few data have been reported for soil cement subjected to fatigue loading. Bofinger (4) in a follow-up to an earlier investigation reported for cement-treated soil that a higher cement content increases fatigue life, presoaking drastically reduces fatigue life, and an increase in initial dry density increases fatigue life.

Bofinger prefers direct tension to flexural fatigue testing because the elastic modulus of soil cement in tension differs from that in compression. It should be realized, however, that the fatigue life is sensitive to stress and strain gradients, and results of direct tension fatigue tests (zero stress gradient) can be considered as a lower bound for the fatigue life. In the opinion of the authors, flexural testing is a better simulation of actual field behavior because a stress gradient always exists in cement-treated base subjected to load. By measuring tensile and compressive strains in a laboratory test specimen, we can account for bi-modulus effects. There is also evidence that the standard briquettes (used by Bofinger) are subject to stress concentrations with the result that the stress that actually causes fatigue deterioration is unknown.

The most comprehensive fatigue investigation on soil cement reported to date is that by Larsen and Nussbaum (5). From tests on 3 soil types with 4 beam depths and

4 simulated subgrade moduli as variables, a relation was established as follows:

$$R_c/R = a\,N^{-b}$$

where

R_c = radius of curvature at failure (critical radius of curvatuve),
R = radius of curvature developed for a given load and number of load applications,
a and b = coefficients, and
N = number of load repetitions.

Their test results indicated that the coefficient b, i.e., slope of the line on a semi-logarithmic plot, is dependent only on soil type; subgrade strength had no influence; and the coefficient a decreased with increasing specimen thickness and is independent of soil type.

Some of their measurements may have been influenced by the ratio of span length to beam depth (deep beam action). For small span length-to-depth ratios, the stress and strain distributions are no longer linear, which makes it difficult to compare fatigue results.

Figure 3 shows what can be expected under "deep beam action" and also illustrates the influence of a compression-to-tension modulus ratio that is greater than unity. These results were obtained by means of a plane stress finite-element analysis.

Specimens and Procedures

Specimens for fatigue testing consisted of beams 3 in. by 3 in. in cross section and 18 in. long, prepared by vibratory compaction in three layers perpendicular to the longitudinal axis. After curing overnight in a 100 percent relative humidity environment, the specimens were removed from their molds and the densities were determined; the specimens were then wrapped in polyethelene sheets and returned to the 100 percent relative humidity environment for a curing period of at least 3 months. (A minimum period of 3 months was selected in order to minimize curing effects during testing.)

Average properties for the specimens tested were as follows:

1. Stiffness modulus—2.8×10^6 psi;
2. Compressive strength, 28 days—1,000 psi;
3. Flexural strength (modulus of rupture), 28 days—200 psi; and
4. Direct tensile strength, 28 days—100 psi.

Fatigue tests were conducted in a closed-loop vibration testing system. Repeated loading was applied by using the haversine input function, which is defined by

$$P(\theta) = \tfrac{1}{2}(1 - \cos\theta)$$

Of the available load forms in this type of equipment, the haversine function appears to best represent actual field loading conditions.

Third-point loading at a frequency of 2 cps was utilized for the fatigue tests, and all specimens subjected to fatigue loading were conditioned at a total load of 250 lb (approximately 38 percent of ultimate flexural strength) for at least 500 cycles prior to fatigue testing. Strains were measured by bonded-wire gauges with a gauge length of 2.5 in. cemented to both the top and bottom surfaces of each beam.

Some preliminary studies were conducted to investigate rate of loading effects on material stiffness, which in turn might provide an indirect indication of rate effects on fatigue life. Results of these studies, briefly summarized in Appendix A, indicate that the stiffness characteristics are sensibly independent of rate of loading effects in the frequency range of 0.01 to 10 cps.

Results

A total of 31 specimens was tested in flexural fatigue. Fatigue life as a function of initial maximum flexural strain in tension is shown in Figure 4. As might be expected,

Figure 1. Gradation curve, aggregate for soil cement.

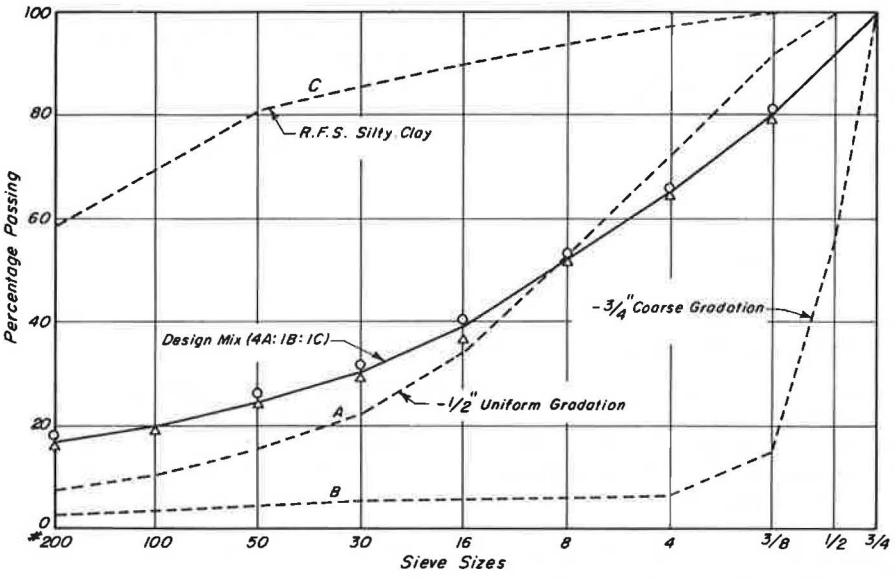

Figure 2. Prismatic-space finite-element representation.

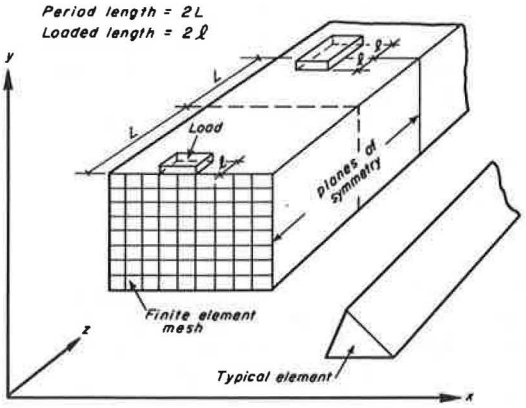

Figure 3. Stress and strain distributions in shallow and deep beams loaded at the one-third points.

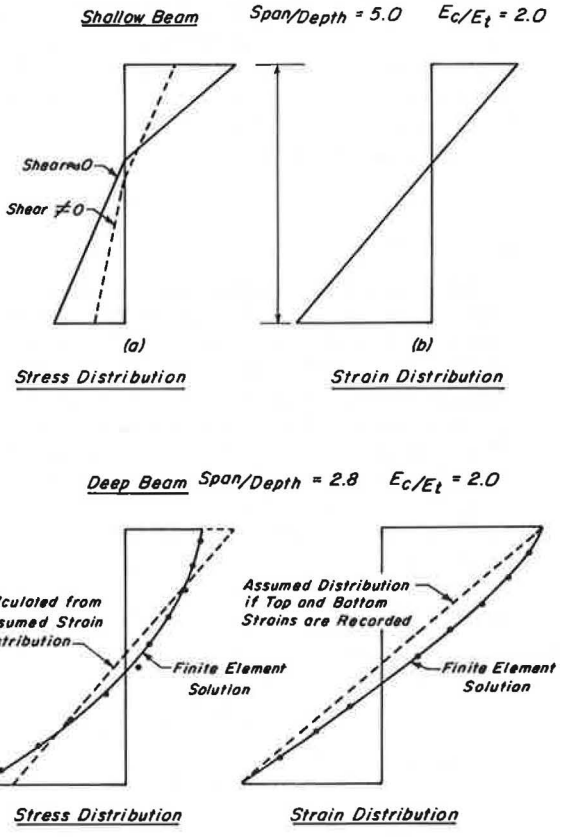

scatter is observed in the test results. Straight-line approximations to this data on semilogarithmic and full-logarithmic plots (using least squares) resulted in the equations shown in Figure 4. The slope of the fatigue curve is quite flat, which indicates considerable sensitivity of fatigue life to small strain variations and may be due, at least in part, to the high flexural stiffness of this material.

Results of this investigation could be compared with those developed by Larsen and Nussbaum (5) because radii of curvature could be obtained directly from the strain measurements, i.e.,

$$R = h/(\epsilon_t + \epsilon_b)$$

where

R = radius of curvature,
h = specimen depth, and
ϵ_t and ϵ_b = top and bottom recorded strains respectively.

A critical radius of curvature, R_c, was obtained by extrapolation of the radius of curvature versus load relation. For this material, R_c was estimated to be 10,000 in.

The resulting data are shown in Figure 5. The data confirm Larsen and Nussbaum's conclusions that the coefficient a in the expression $R_c/R = a\ N^{-b}$ is sensibly independent of soil type, whereas the coefficient b appears to increase as the material becomes more granular.

It has been suggested (6) that a study of strain history in a fatigue test might be of value in assessing the accumulation of fatigue damage. Figure 6 shows some typical flexural tensile strain histories up to failure. It is seen that the strain remains fairly constant over a large portion of the fatigue life after which the rate of change of strain starts to increase. Once the strain starts changing, it does so at an increasing rate until complete rupture is achieved.

An interesting observation in this test series was that specimens that did not fail after 1 million load applications exhibited a constant strain output during the entire test. When these specimens were then failed at a higher stress, the strain history was the same as indicated in Figure 6; also the number of load applications to failure corresponded reasonably well to the fatigue curve, which suggests that the previously induced fatigue damage was comparatively insignificant.

CRACK PROPAGATION

Analytic Study

To evaluate the importance of load transfer across a transverse crack, we obtained results for an interior load condition (i.e., away from the influence of edge effects) by using the Chevron 5-layer axisymmetric computer program. An 18-kip axle load was applied (Fig. 7) to the pavement structure (layer thickness noted earlier) with the cement-treated base assumed to have a stiffness modulus of 2.8×10^6 psi. The maximum flexural stress obtained is indicated in Figure 8; this figure shows the sensitivity of the stress in the cement-treated base to moduli changes in the other layers. The modulus chosen for the asphalt concrete represents a traffic-weighted stiffness modulus (7) corresponding to environmental conditions at Morro-Bay, California (essentially a cool coastal environment).

At a flexural tensile stress of 80 psi (Fig. 8), a fatigue life in excess of 1×10^6 equivalent 18,000-lb axle load applications would be obtained as seen in Figure 9, which contains the fatigue curve of Figure 4 plotted in terms of stress.

Once a transverse crack forms, however, a different set of circumstances exists. Increased stresses may be anticipated because of the loss of continuity (or "load transfer") and the possibility that water infiltration may weaken the subgrade (8). To obtain some estimate of these conditions we analyzed the pavement by using the prismatic-space finite-element method.

This representation of the pavement is shown in Figure 10 with transverse cracks placed at 20-ft intervals. The pavement model is continuous in the z direction, and the free edges are parallel to the z-axis.

Figure 4. Initial strain versus repetitions to fracture, flexural specimens.

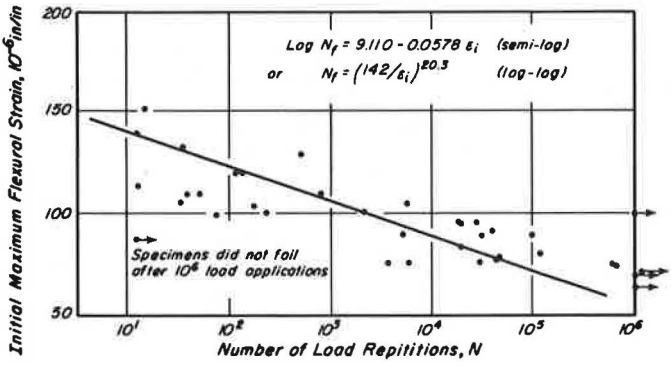

Figure 5. Comparison of fatigue results (Fig. 4) with data developed by Larsen and Nussbaum.

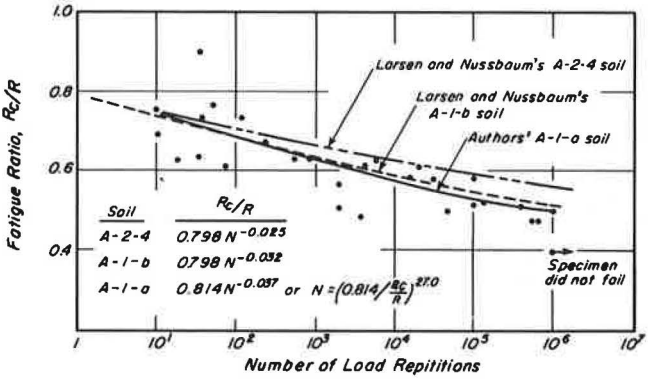

Figure 6. Strain histories of flexural fatigue specimens.

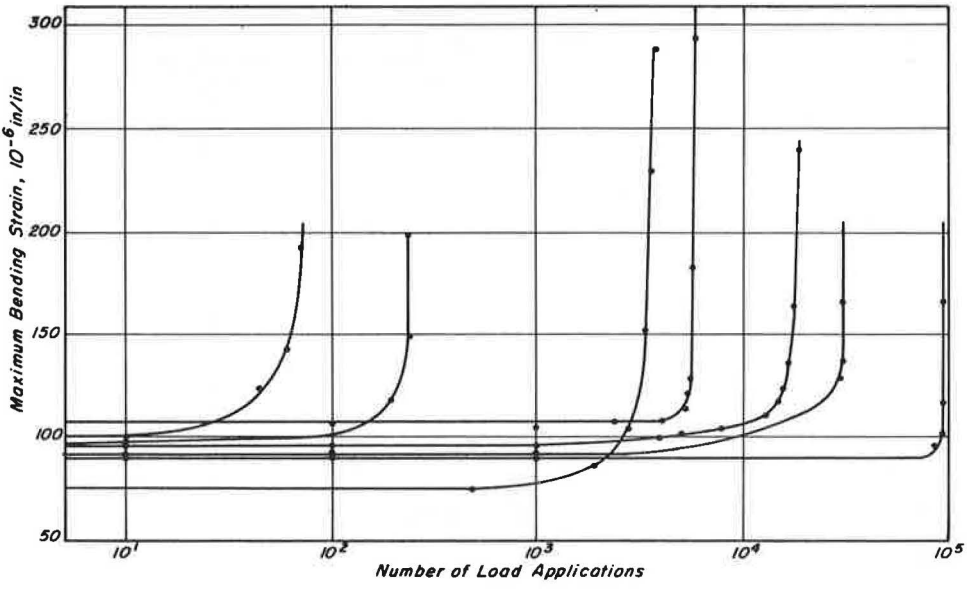

Figure 7. Assumed wheel spacing for 18,000-lb axle load.

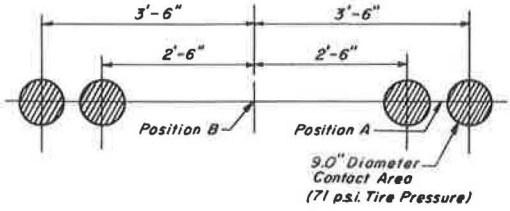

Figure 8. Maximum tensile stress on underside of soil-cement base.

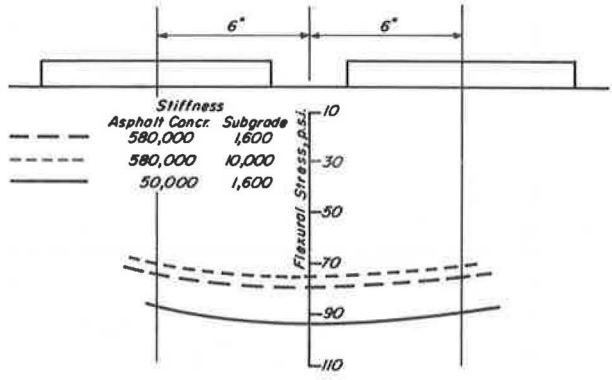

Figure 9. Stress versus repetitions to fracture, flexural specimens.

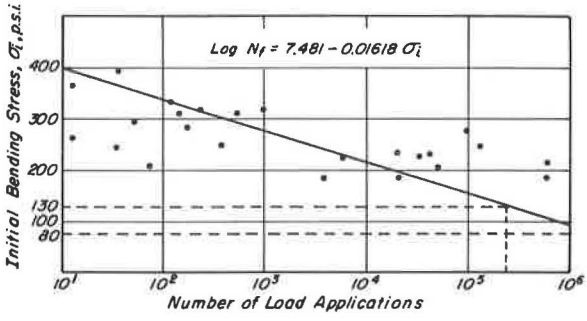

Figure 10. Finite-element mesh for load at an edge.

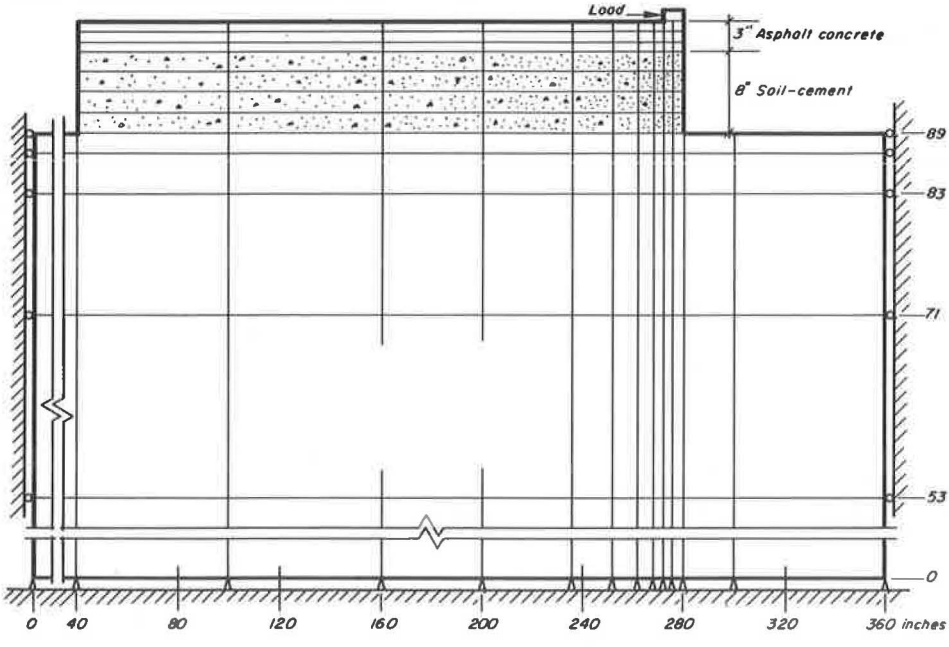

The two loading conditions shown in Figure 11, one at the cracked edge and the other slightly inward from the free edge, were analyzed. Stress contours corresponding to these loadings are shown in Figures 12 and 13. The stresses shown in these figures are not maximum stresses; rather they correspond to the stresses at the center of the upper and lower elements in the finite-element representation of the cement-treated base. The actual stress distributions are shown in Figures 14 and 15. The results indicate that maximum stress is in the z direction at position B for the loading at position BB. This stress, 130 psi, is approximately 60 percent greater than that for the corresponding axisymmetric case, and the fatigue life at this stress (Fig. 9) is considerably less. The results also indicate that fatigue in the asphalt concrete layer is not critical.

As a part of this study, four conditions of subgrade support were investigated (Fig. 21, Appexdix B). Little difference in stress was obtained (Fig. 14), although the surface deflections (Fig. 22, Appendix B) increased with a decrease in subgrade modulus. It was determined that the radius of curvature remained relatively unchanged and is in part attributable to the high modular ratio (approximately 280) of the soil cement to the subgrade, a point also noted by Whiffin and Lister (9).

These results were obtained by assuming complete loss of load transfer across the crack. For very fine cracks, a high percentage of load transfer is still possible, at least initially. However, it is possible, as noted by Colley and Humphrey (10), who measured load transfer for portland cement concrete pavements, that this transfer is reduced with number of load applications as well as with crack width.

CRACK PATTERNS

From the previous discussion, it follows that the first fatigue crack will probably be a longitudinal crack in the center of the wheelpath initiated at the bottom of the cement-treated material.

Once this crack has formed, stress concentrations at the tip of the crack will cause it to penetrate longitudinally and also to the surface. If this crack has progressed far enough, the areas bounded by the fatigue and shrinkage cracks will be subjected to corner loading conditions. Although this problem cannot be handled by the finite-element procedure at the present time, an approximate estimate of stress can be made by using the Westergaard corner loading formula. To use this relation for the asphalt concrete and cement-treated section, we converted the asphalt concrete thickness to an equivalent thickness of soil cement by using the ratio of their moduli (or stiffnesses). For these conditions, a maximum tensile stress of 111 psi was estimated to occur at a distance of about 28 in. from the corner on the diagonal (Fig. 16). As can be seen in Figure 9, this can represent a relatively severe condition for fatigue after the longitudinal crack has formed.

It should be noted that the distance along the corner diagonal is a function of the stiffness of the cement-treated base and will be shorter for more flexible layers. Moreover, load-associated cracks are also possible "normal" to the existing fatigue crack as well as "normal" to the shrinkage and parallel to the first fatigue crack (due to transverse distribution of traffic).

The potential now exists for the corner to break off as shown in Figure 16, and this process will repeat itself with continued load applications to form the familiar double-ladder crack pattern indicated.

It is possible that this crack pattern can be altered if a longitudinal shrinkage crack exists close to the longitudinal fatigue crack as is shown for the right-hand wheelpath in Figure 16. For these circumstances, a longitudinal strip exists that can be analyzed by using the finite-element procedure. For a 2-ft wide strip, for example, a maximum stress of 136 psi adjacent to and in the direction of the longitudinal crack was obtained. As noted earlier, this will lead to early cracking with the result that a single-ladder type crack pattern will now occur (Fig. 16). In all probability, these transverse fatigue cracks will be randomly spaced because the maximum stress occurs directly beneath the wheel load for this loading condition.

Figure 11. Loading positions for edge effect considerations.

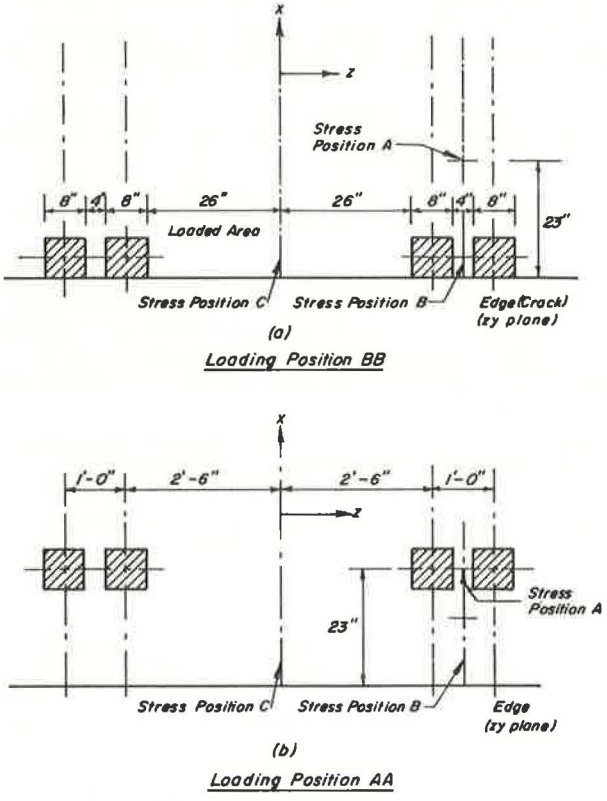

Figure 12. Stress contours for load at position BB.

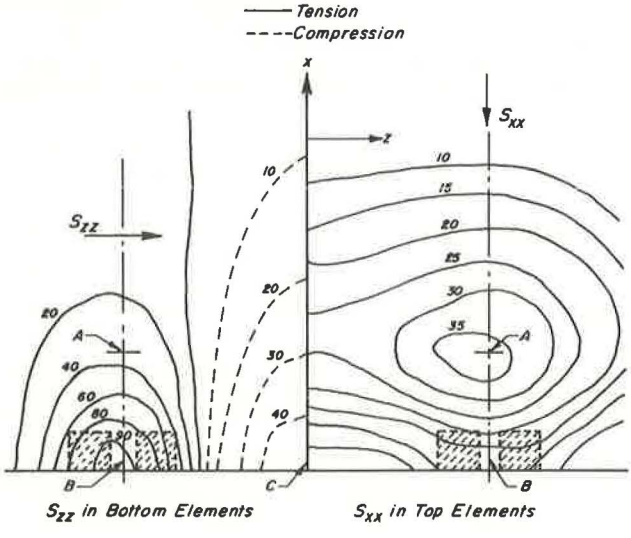

Figure 13. Stress contours for load at position AA.

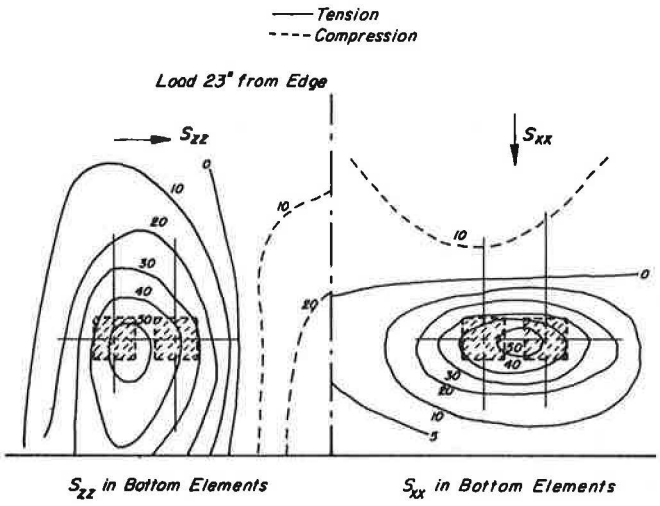

Figure 14. Distribution of stress S_{xx} at position A for loading at positions AA and BB.

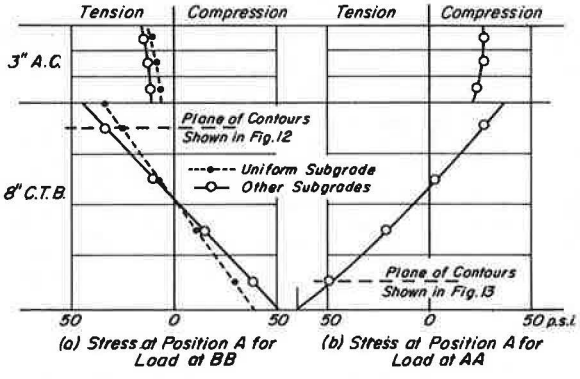

Figure 15. Distributions of stress S_{zz} with depth.

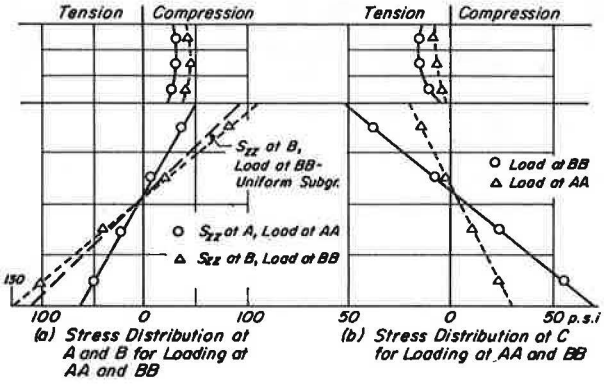

Figure 16. Crack patterns.

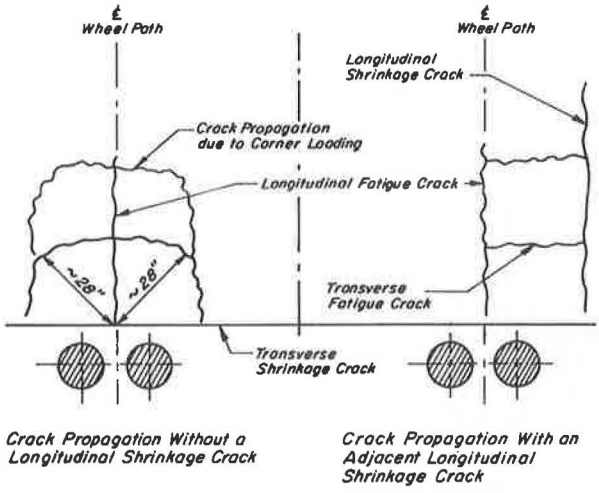

Figure 17. Crack pattern, November 11, 1970.

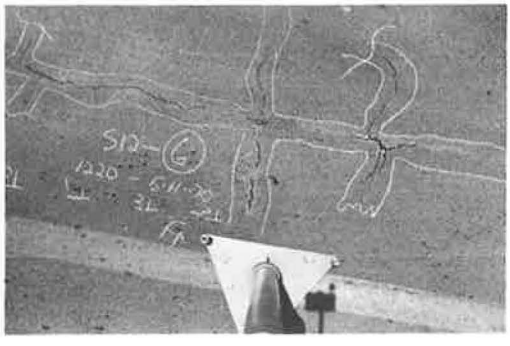

Figure 18. Crack pattern, January 20, 1971.

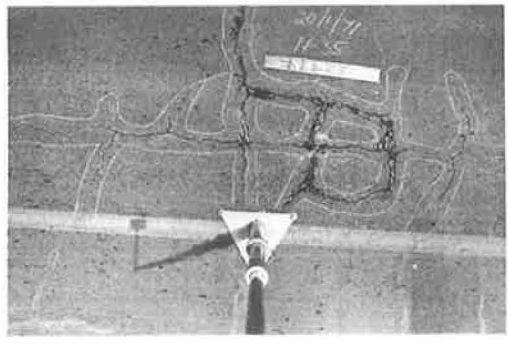

Figure 19. Crack pattern, February 22, 1971.

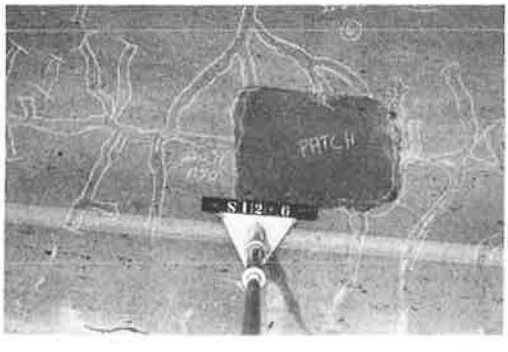

Figure 20. Overall view of pavement showing typical crack pattern.

FIELD STUDY

Subsequent to the analytic study, a recently constructed pavement near Johannesburg, South Africa, containing a soil-cement base, presented an opportunity for a field investigation of the load-associated cracking phenomenon previously described.

On this particular project, the upper 3 layers of the pavement consisted of 1 in. of asphalt concrete, 4 in. of cement-treated base, and 4 in. of compacted gravel. The cement-treated base was a crushed aggregate stabilized with 5 percent cement (by weight). The 28-day cube strength of the cement-stabilized material averaged between 1,000 and 1,500 psi.

The road serves heavy coal traffic, and roadside wheel load measurements indicated that about 10 to 20 percent of the trucks exceeded the legal axle load of 18,000 lb. Areas that showed little fatigue distress were selected, and these areas were photographed monthly by placing the camera at exactly the same position each time.

The crack propagation study, shown in Figures 17-19, covers the 4-month period from November 1970 to March 1971. January was a month of exceptionally high rainfall for the area.

The cement-treated base was laid by a paver in 10-ft wide sections, starting with the section that included the 8-ft wide shoulder. This resulted in a construction joint in the vicinity of the outer wheelpath. Consequently, longitudinal shrinkage cracks at the construction joints appeared simultaneously with transverse shrinkage cracks (spaced between 12 and 20 ft apart). Figure 17 shows these two cracks very distinctly.

This situation differs slightly from the analytic one presented previously in that the longitudinal crack is now also a shrinkage crack instead of a fatigue crack. The result is that fatigue cracks can now develop perpendicularly to either the transverse or longitudinal shrinkage cracks.

Such fatigue cracks, branching off from the longitudinal shrinkage crack, are also shown in Figure 17.

In Figure 18, taken about 10 weeks later, the double-ladder fatigue pattern is well-established. The progressive failure of a corner piece is clearly illustrated.

Figure 19 shows further deterioration after the initial failure area has been repaired.

Figure 20 shows an overall view of a typical crack pattern. It shows a number of closed fatigue cracks as well as a few in the process of closing the loop.

Studies of cracking at various locations on the same route showed the same general pattern; such results would appear to be in general agreement with the crack propagation and patterns predicted previously.

CONCLUSIONS

From the results presented herein, the following conclusions appear warranted:

1. The fatigue results tend to confirm previous research work performed by the Portland Cement Association with the exception of the case for specimens whose span lengths are short relative to their depths ("deep beams"). In this situation, the true fatigue response may differ from that predicted by the PCA results because of "deep-beam" action.
2. For the assumed situation of complete loss of load transfer across a transverse shrinkage crack in the cement-treated base, significantly larger tensile stresses may result adjacent to the crack, which in turn reduces the number of load repetitions that the section can withstand compared to its capabilities in the uncracked condition.
3. By following consecutively the locations of maximum tensile stresses as cracks develop, it is possible to predict crack patterns similar to those observed in in-service pavements as noted from the field observations reported herein.

ACKNOWLEDGMENTS

The assistance of C. K. Chan of the Institute of Transportation and Traffic Engineering in the development, design, and use of the testing equipment is gratefully acknowledged. The authors also wish to acknowledge the South African Council for Scientific and Industrial Research for the research fellowship provided to the first author.

REFERENCES

1. Pretorius, P. C., and Monismith, C. L. The Prediction of Shrinkage Stresses in Pavements Containing Soil-Cement Bases. Highway Research Record 362, 1971, pp. 63-86.
2. Wilson, E. L., and Pretorious, P. C. A Computer Program for the Analysis of Prismatic Soilds. Structural Engineering Lab., Univ. of California, Berkeley, Rept. UC SESM 70-21, 1970.
3. Pretorius, P. C. Design Consideration for Pavements Containing Soil-Cement Bases. Univ. of California, Berkeley, PhD dissertation, 1970.
4. Bofinger, H. E. Further Studies on the Tensile Fatigue of Soil-Cement. Australian Road Research, Vol. 4, No. 1, Sept. 1969.
5. Larsen, T. J., and Nussbaum, P. J. Fatigue of Soil-Cement. Jour. of Portland Cement Association Research and Development Laboratories, Vol. 9, No. 2, May 1967, pp. 37-59.
6. Raithby, K. D., and Whiffin, A. C. Failure of Plain Concrete Under Fatigue Loading—A Review of Current Knowledge. Gt. Brit. Road Research Laboratory, RRL Rept. LR231.
7. Kasianchuk, D. A. Fatigue Considerations in the Design of Asphalt Concrete Pavements. Univ. of California, Berkeley, Phd dissertation, 1968.
8. Williams, A. A. B., and Dehlen, G. L. The Performance of Full-Scale Base and Surfacing Experiments on National Route 3-1, at Key Ridge, After the First Six Years. First Conf. on Asphalt Pavements for Southern Africa, Durban, Aug. 1969.
9. Whiffin, A. C., and Lister, N. W. The Application of Elastic Theory to Flexible Pavements. Internat. Conf. on Structural Design of Asphalt Pavements, Ann Arbor, Mich., 1962.
10. Colley, B. E., and Humphrey, H. A. Aggregate Interlock at Joints in Concrete Pavements. Highway Research Record 189, 1967, pp. 1-18.
11. Papazian, H. S. The Response of Linear Visco-Elastic Materials in the Frequency Domain. Transportation Eng. Center, Eng. Exp. Station, Ohio State Univ., Columbus, Rept. 172-2, 1961.

APPENDIX A

RATE OF LOADING STUDY FOR SOIL CEMENT

In an initial part of the study, surface strains were measured both statically and dynamically on specimens of the soil cement. Linear strain distributions (for all practical purposes) were observed in both types of tests to failure.

Rate of loading effects were observed by defining a complex modulus of the material over a frequency range for loading of 0.01 to 10 cps. The phase angle, ϕ, by which the strain lagged the applied stress was extremely small, indicating essentially elastic response.

The same conclusion was reached from an analysis of the results of short-time creep experiments, which yielded the following results:

$$\text{elastic modulus } E = \frac{\text{initial stress}}{\text{initial strain}} = 2.43 \times 10^6 \text{ psi}$$

$$\text{viscous traction } \lambda = \frac{\text{stress}}{\text{rate of change of strain}} = 7.80 \times 10^9 \text{ psi/sec}$$

$$\text{retardation time } \tau = \lambda/E = 3{,}210 \text{ sec}$$

The phase angle lag can then be estimated from the following (11):

$$\phi = \tan^{-1}(E/\omega\lambda) \tan^{-1}(1/3{,}210\ \omega)$$

where ω = frequency of loading. In the frequency range of 0.01 to 10 cps, it can be seen that ϕ will be quite small, thus substantiating the observations in dynamic loading.

For the range of loading conditions studied herein, the soil cement can, for practical purposes, be considered an "elastic" material.

APPENDIX B

SUBGRADE SUPPORT CONDITIONS

Figure 21.

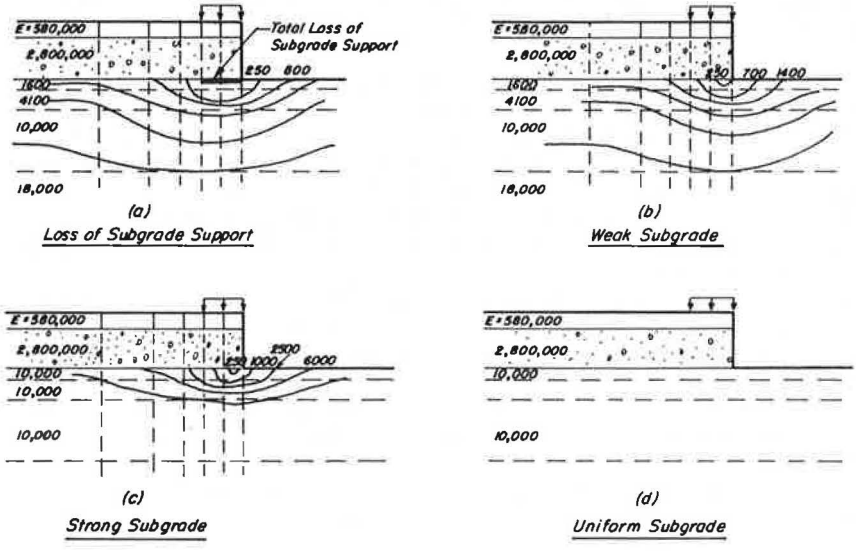

Figure 22.

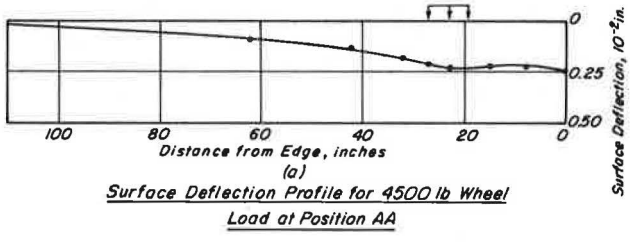

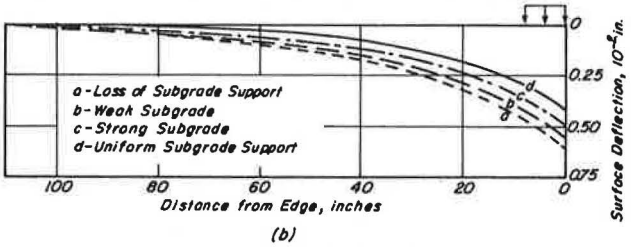

CONCRETE SLAB RESTING ON A STRATIFIED MEDIUM

Michel Fremond, Laboratoire Central des Ponts et Chaussées, Paris

•IT is known experimentally that concrete slabs used in certain highway roads may work themselves partly loose from the base under the action of forces due to temperature variations. This phenemenon happens frequently during the summer and the winter.

The author studied this problem and obtained numerical results that compare favorably with the physical measurements.

In studies made on the calculation of concrete slabs, the ground is generally represented by using Winkler's models or extensions of these models (8, 11, 15, 16, 19). The loosening problem has been studied by Haar, Leonards, Lewis, and Wiseman (8, 11, 12, 20), on the basis of Winkler's model and the plate theory, by solving a differential equation. It has been studied, too, by Hudson and Matlock (9, 10) who use mechanistic models and by Fichera (3) who uses a variational method by assuming the ground to be rigid. To the author's knowledge, this last method (unlike the others) has not resulted in any numerical application.

Equations for the preceding problem are given by the author, in which he assumes that only one elastic slab rests on the soil. To represent the soil, he avoids the use of Winkler's hypothesis and keeps the elastic nature of the soil. The soil is represented by a layered elastic half-space. The contact between the slab and the soil can be bilateral or unilateral. In this case the slab can lose contact with the soil. The actual contact surface is an unknown of the problem as well as the displacements of the slab and the soil.

The equations are solved by using variational methods, i. e., by minimizing the potential energy of the structure. Numerical results and comparisons with physical measurements are also discussed.

MATHEMATICAL MODEL

A roadway forms a complex system. It is represented by a layered half-space, i. e., by a semi-infinite medium covered with a certain number of horizontal layers that may or may not be stuck to one another. A concrete slab rests on this half-space (Fig. 1).

The structure is plotted on a orthonormal system of axes Ox_1, Ox_2, Ox_3. The direction Ox_3 is directed upward. A vector $\vec{u}$ is represented in this system by its components u_1, u_2, u_3; $|\vec{u}|$ is its length. The scalar product of the two vectors $\vec{u}$ and $\vec{v}$ is

$$(\vec{u}\cdot\vec{v}) = \sum_{i=1}^{3} u_i v_i$$

The problem is to compute at any point of the slab (and possibly of the layered half-space) the displacement vector $\vec{u}$ of coordinates u_1, u_2, and u_3, the linear strains due to this displacement,

$$\epsilon_{ij}(\vec{u}) = \tfrac{1}{2}[\partial u_i/\partial x_j) + (\partial u_j/\partial x_i)], \quad i = 1, 2, 3,$$

and the stresses $t_{ij}(\vec{u})$ associated with these strains.

For this purpose, the mechanical properties of the structure are expressed by a certain number of equations, which will make it possible to calculate $\vec{u}$.

Sponsored by Committee on Theory of Pavement Design.

The author assumes that the slab is subjected to a certain number of known forces as follows:

1. Inside Ω, subject to body forces represented by $\vec{f} = [f_1(x_1, x_2, x_3), f_2(x_1, x_2, x_3)$, and $f_3(x_1, x_2, x_3)]$. The vector $\vec{f}$ includes, for example, gravity forces due to shrinkage and swelling of the concrete or to temperature variations.
2. On the surface Γ, subject to superficial forces denoted by $\vec{g} = [g_1(x_1, x_2, x_3), g_2(x_1, x_2, x_3)$, and $g_3(x_1, x_2, x_3)]$. The vector $\vec{g}$ includes, for example, static load forces due to shrinkage and swelling of the concrete or to temperature variations.

Several hypotheses are possible that describe the coupling between the slab and the layered half-space. Two are given here, and a third one will be presented later including a numerical example.

According to one hypothesis, the slab is assumed to be stuck to the layered half-space. This is the case when the bond is of good quality. The stresses and displacements are then continuous at the interface as follows:

$$\vec{u} = \vec{u}' \tag{1}$$

$$\vec{t}(\vec{u}) = \vec{g} - \vec{t}'(\vec{u}') \tag{2}$$

In these relations and in the following ones, the notations bearing accents relate to the half-space and those without accents to the slab. The stresses generated by the displacements $\vec{u}$ and $\vec{u}'$ on the surfaces of the slab and of the half-space are $\vec{t}(\vec{u})$ and $\vec{t}'(\vec{u}')$. They are counted in a positive manner toward the exterior.

According to another hypothesis, the slab may work itself loose on a part Γ_1 of the contact surface while remaining stuck to the Γ_2 other part. The boundary conditions are then as follows:

1. On Γ_1

$$u_3 - u'_3 > 0 \tag{3}$$

$$(u_3 - u'_3)\ |\vec{t}'(\vec{u}')| = 0 \tag{4}$$

$$\vec{t}(\vec{u}) = \vec{g} - \vec{t}'(\vec{u}') \tag{5}$$

2. On Γ_2

$$\vec{u} = \vec{u}',\ \vec{t}(\vec{u}) = \vec{g} - \vec{t}'(\vec{u}')$$

Equation 3 expresses the fact that, if there is a loosening, the slab and half-space do not interpenetrate. Equation 4 expresses the fact that, where a loosening actually takes place $[(u_3 - u'_3) > 0]$, the stress on the layered half-space is zero and, where the stress is not zero, there is no loosening. It should be noted, however, that, in this case, the slab may slide on the half-space ($u_1 \neq u'_1$, $u_2 \neq u'_2$). Equation 5 expresses the fact that, if there is a loosening, $\vec{t}(\vec{u})$ is equal to the exterior forces $\vec{g}$ and that, in the opposite case, the stresses are continuous at the interface between the slab and the half-space. This last hypothesis will be retained throughout the remainder of the report, for it contains the first one ($\Gamma_1 = \phi$).

The author assumes further that the mechanical properties of the materials forming the layered half-space and the slab can be described by the linear-elastic theory. I shall assume in the numerical applications that the materials are homogeneous and isotropic. Hereinafter, this hypothesis is retained; however, it is not essential for the results to be valid. Therefore, the relation that relates strains and stresses is

$$t_{ij}(\vec{u}) = \lambda\ \delta_{ij}\ \mathrm{div}\ \vec{u} + 2\mu\epsilon_{ij}(\vec{u}) \tag{6}$$

where δ_{ij} is the Kronecker's symbol, and λ and μ are the Lamé's parameters. The fundamental relation of dynamics then gives a relation between $\vec{f}$ and $\vec{u}$ in Ω as follows:

$$(\lambda + \mu)\ \text{graddiv}\ \vec{u} + \mu \Delta \vec{u} + \vec{f} = \vec{0} \tag{7}$$

This relation is written symbolically as follows:

$$-\mathfrak{L}\vec{u} = \vec{f} \tag{8}$$

where $\mathfrak{L}$ is the elasticity operator. It is assumed further that the layered half-space is in equilibrium under its own weight in each of its layers and in the semi-infinite medium:

$$-\mathfrak{L}'u' = -\mathfrak{L}''u'' = \ldots = 0 \tag{9}$$

The author assumes here that the layers are stuck on top of one another. Other types of mechanical conditions are of course possible at the interface between two layers. Therefore, the boundary condition at each interface is

$$\vec{u}' = \vec{u}'', \quad \vec{t}'(\vec{u}') + \vec{t}''(\vec{u}'') = 0 \tag{10}$$

All the preceding equations are shown in Figure 2. They form system I.

SOLUTION OF SYSTEM I BY USING A VARIATIONAL METHOD

Elimination of the Layered Half-Space

The autor has avoided the use of Winkler's classical hypothesis, which represents the layered half-space by springs, as well as any extension of this theory (4). He has kept the assumptions about the elastic nature of the layered half-space, and he uses the related results (2, 7, 17) and, in particular, the calculation of the displacements $\vec{u}'_1$, $\vec{u}'_2$, and $\vec{u}'_3$ of the half-space when the latter is subjected to loads $\delta(x_1, x_2)$ (Dirac's Delta) applied to the origin along directions Ox_1, Ox_2, and Ox_3. The three vectors $\vec{u}'_1$, $\vec{u}'_2$, and $\vec{u}'_3$ can be set in a matrix Φ column by column as follows:

$$\Phi = \begin{vmatrix} u'_{1,1} & u'_{2,1} & u'_{3,1} \\ u'_{1,2} & u'_{2,2} & u'_{3,2} \\ u'_{1,3} & u'_{2,3} & u'_{3,3} \end{vmatrix}$$

The matrix Φ is known as Green's matrix for the layered half-space. If $\vec{v}(x_1, x_2)$ is a stress applied to the half-space surface, it can easily be seen that the displacement of the half-space surface is given by $\vec{u}' = \Phi * \vec{v}$ (the convolution product is to be understood with respect to the variables x_1 and x_2); $\vec{u}'$ is the vector with the following coordinates:

$$u'_i = \sum_{j=1}^{3} \Phi_{i,j} * v_j = \sum_{j=1}^{3} u'_{j,i} * v_j$$

The action $\vec{t}'(\vec{u}')$ of the slab on the half-space will henceforth be denoted by $\vec{v}$. By using the relation $\vec{u}' = \Phi * \vec{v}$, one obtains system II (shown in Fig. 3).

The layered half-space (as an unbounded geometric figure) has disappeared. It is symbolized by Φ. As far as the solution of the problem is concerned, $\mathfrak{L}$, Φ, $\vec{f}$, $\vec{g}$, Γ_1, and Γ_2 are known. The unknowns are $\vec{u}$, $\vec{v}$, and that part of Γ_1 in which the slab is actually loose.

Variational Formulation

The author will try to obtain a weak solution to system II or else a solution in terms of energy. He will therefore try to determine the couple $(\vec{u}, \vec{v})$, if it exists, which causes

the potential energy J of the structure to be at a minimum (among the elements of a space W to be defined). The potential energy of the layered half-space is

$$\tfrac{1}{2}\int_{\Gamma_1\cup\Gamma_2}(\vec{v}\cdot\Phi*\vec{v})d\Gamma$$

where $d\Gamma$ stands for the surface element. The potential energy of the slab is

$$\tfrac{1}{2}a(\vec{u},\vec{u}) - \int_{\Omega}(\vec{f}\cdot\vec{u})d\Omega - \int_{\Gamma}(\vec{g}\cdot\vec{u})d\Gamma$$

where $d\Gamma$ is the volume element. The elastic energy is defined by

$$a(\vec{u},\vec{w}) = \int_{\Omega}\sum_{i,j=1}^{3} t_{ij}(\vec{u})\epsilon_{ij}(\vec{w})d\Omega$$

The total potential energy is therefore

$$J(\vec{u},\vec{v}) = \tfrac{1}{2}\{a(\vec{u},\vec{u}) + \int_{\Gamma_1\cup\Gamma_2}(\vec{v}\cdot\Phi*\vec{v})d\Gamma\} - \int_{\Omega}(\vec{f}\cdot\vec{u})d\Omega - \int_{\Gamma}(\vec{g}\cdot\vec{u})d\Gamma$$

The solution (if one exists) to system II results in J over W being a minimum. Conversely, if a component is found in W, which brings J to a minimum, this component is a weak solution. There is a solution to system II only if it is sufficiently regular (i. e., if it is sufficiently differentiable) such that Green's formula can be used (integration by parts). It is in this sense that it can be termed weak.

The space W is the space for displacements $\vec{u}$ and stresses $\vec{v}$ with finite energy ($J < +\infty$). If there exists a part Γ_2 where sticking occurs,

$$W = [H^1(\Omega)]^3 \times [H^{-1/2}(\Gamma_1\cup\Gamma_2)]^3$$

where H^1 and $H^{-1/2}$ are the Sobolev spaces of order 1 and $-\frac{1}{2}$ (13). The displacement $\vec{u}$ belongs to $[H^1(\Omega)]^3$ and the stress $\vec{v}$ to $[H^{-1/2}(\Gamma_1\cup\Gamma_2)]^3$. If a loosening can occur everywhere ($\Gamma_2 = \phi$),

$$W = H^1(\Omega)/P_0 \times H^1(\Omega) \times [H^{-1/2}(\Gamma_1\cup\Gamma_2)]^3$$

where $P_0 = [\vec{u}\,|\,\vec{u} = \vec{a} + \vec{b}\wedge\vec{x};\ a_3 = b_1 = b_2 = 0$; and a_1, a_2, and b_3 are constants$]$. P_0 is the space of horizontal rigid displacements (translations and rotations). It is necessary to introduce a quotient space for the horizontal component of displacement $\vec{u}$ because (since the slab may work itself loose everywhere) it can slide horizontally without expending any energy. Horizontal components of $\vec{f}$ and $\vec{g}$ must then be equivalent to zero in order for a solution to be possible (6). Displacement $\vec{u}$ is therefore defined to within a P_0 component.

The author does not determine the minimum of $J(\vec{u},\vec{v})$ over the entire space W because it is necessary to take into account the relations between $\vec{u}$ and $\vec{v}$ at the interface between the half-space and the slab. Let

$$K = [(\vec{u},\vec{v}) \in W \mid \vec{u} - \Phi*\vec{v} = 0 \text{ on } \Gamma_2;\ u_3 - (\Phi*v)_3 \geq 0 \text{ on } \Gamma_1]$$

K is a closed convex of W formed by displacements $\vec{u}$ and stresses $\vec{v}$, which confirm the geometric boundary conditions.

The variational problem that must be solved is

$$\inf[J(\vec{u},\vec{v}) \mid (\vec{u},\vec{v}) \in K] \tag{11}$$

Existence and Uniqueness of the Solution

In case there is a part Γ_2 in which there is sticking, it is possible to show that Eq. 11 has a solution (5, 6).

If the slab can work itself loose everywhere, an additional hypothesis must be made as follows:

$$\forall(\vec{u}, 0) \in K \cap P_1,\ \vec{u} \neq \vec{0},\ \int_\Omega (\vec{f}\cdot\vec{u})d\Omega + \int_\Gamma (\vec{g}\cdot\vec{u})d\Gamma < 0 \qquad (12)$$

where $P_1 = [(\vec{u}, 0) \in W \mid \vec{u} = \vec{a} + \vec{b}\wedge\vec{x};\ a_1 = a_2 = b_3 = 0$; and a_3, b_1, and b_3 are constants]. P_1 represents the overall rigid displacements of the slab (up to a horizontal rigid displacement). Equation 12 expresses the fact that energy must be expended to lift the slab. This is not true for all solids laid on the ground. System II also describes the equilibrium of an atmospheric balloon placed on the ground. Force $\vec{f}$ is directed upward because Archimedes' pressure is greater than the weight of the balloon. Therefore the following is true:

$$\forall(\vec{u}, 0) \in K \cap P_1,\ \vec{u} \neq 0,\ \int_\Omega (\vec{f}\cdot\vec{u})d\Omega + \int_\Gamma (\vec{g}\cdot\vec{u})d\Gamma > 0$$

The balloon produces energy as it rises. It can be shown that Eq. 11 has no solution under these conditions (6).

Exterior forces $\vec{f}$ and $\vec{g}$ of course confirm Eq. 12. It is then shown, by using Eq. 12, that Eq. 11 has a solution. The uniqueness of the solution results from convexity arguments and from Eq. 12 when the pavement can work itself loose everywhere ($\Gamma_2 = \phi$) (6). The case in which Eq. 12 is replaced by

$$\forall(\vec{u}, 0) \in K \cap P_1,\ \int_\Omega (\vec{f}\cdot\vec{u})d\Omega + \int_\Gamma (\vec{g}\cdot\vec{u})d\Gamma \leq 0$$

is more difficult and is treated in Eq. 6. It is also shown that $\vec{v}$ is orthogonal to Γ_1 on the part where contact occurs.

Solutions to Eq. 11 can be proved to exist by using the results given elsewhere (14) or Galerkin's method (or finite-element method). A brief outline of this latter proof will be given because it justifies the computation made on a computer, which consisted of minimizing J on a subspace W_n of W of finite dimension n. Also it justifies the fact that, if increased accuracy is needed, the dimension n can be increased at the expense of additional work.

Discrete Problem

Let n be an integer that is to increase toward infinity and $\overline{\Omega}_n$ a mesh of Ω (Fig. 4). $\overline{\Omega}_n$ consists, for example, of a certain number of tetrahedrons that constitute a partition of $\overline{\Omega}$. It is assumed that Γ consists of a certain number of plane faces. In each tetrahedron, the displacements $\vec{u}_n$ of W_n are linear functions. The author is aware of the fact that the $\vec{u}_n$ are continuous functions on $\overline{\Omega}$, i.e., that $\vec{u}_n$ is continuous at the vertexes of the network tetrahedrons.

The network $\overline{\Omega}_n$ of Ω induces on Γ a mesh Γ_n consisting of triangles, and on each of these triangles the stress $\vec{v}_n$ of W_n is an affine function. The author also imposes the condition that it is a continuous function on Γ. The continuity of $\vec{v}_n$ at the various vertexes is sufficient to this condition. Therefore, the following is true:

W_n = piecewise linear and continuous displacements in Ω and piecewise linear and continous stresses on Γ

Similarly,

$$K_n = [(\vec{u}_n, \vec{v}_n) \in W_n \mid \vec{u}_n - \Phi^*\vec{v}_n = \vec{0} \text{ on } \Gamma_2;\ (\vec{u}_n - \Phi^*v_n)_3 \geq 0 \text{ on } \Gamma_1]$$

The significance associated with the two conditions defining K_n must be specified. The condition $\vec{u}_n - \Phi^*\vec{v}_n = \vec{0}$ on Γ_2 means that, for any continuous vector $\vec{\phi}_n$ piecewise linear on Γ equal to zero at any vertex of Γ_n not belonging to Γ_2, $\int_{\Gamma_1\cup\Gamma_2} [(\vec{u}_n - \Phi^*\vec{v}_n)\cdot \vec{\phi}_n]d\Gamma = 0$. The condition $(\vec{u}_n - \Phi^*\vec{v}_n)_3 \geq 0$ on Γ_1 means that for any positive, continuous function ψ_n piecewise linear on Γ, zero at any vertex of Γ_n not belonging to Γ_1, $\int_{\Gamma_1\cup\Gamma_2} (\vec{u}_n - \Phi^*\vec{v}_n)_3\ \psi_n\ d\Gamma \geq 0$.

The discrete problem is therefore

$$\inf[J(\vec{u}_n, \vec{v}_n) \mid (\vec{u}_n, \vec{v}_n) \in K_n]$$

It may be written more simply as

$$\inf[x^T Ax - 2f^T x \mid Cx \leq 0] \tag{13}$$

x is the vector formed by components of $(\vec{u}_n, \vec{v}_n)$ in a base of W_n; A is a definite nonnegative matrix ($\forall x$, $x^T Ax \geq 0$). Of course, $Ax = 0$ for $x \neq 0$ when $\vec{u}_n$ is a rigid displacement. The quadratic part of J is $x^T Ax$; $-2f^T x$ is the linear part:

$$x^T Ax = \tfrac{1}{2}[a(\vec{u}_n, \vec{u}_n) + \int_{\Gamma_1 \ \Gamma_2} (\vec{v}_n \cdot \Phi * \vec{v}_n) d\Gamma] - 2f^T x = \tfrac{1}{2}[-2\int_\Omega (\vec{f} \cdot \vec{u}_n) d\Omega - 2\int_\Gamma (\vec{g} \cdot \vec{u}_n) d\Gamma]$$

The condition $Cx \leq 0$ (C is a matrix) expresses the fact that $(\vec{u}_n, \vec{v}_n) \in K_n$. If the slab can work itself loose everywhere ($\Gamma_2 = \phi$), the additional condition $f^T x < 0$ is obtained for $(\vec{u}_n, 0) \in K \cap P$, $\vec{u}_n \neq 0$, which results from Eq. 12. The author shows therefore (6) that Eq. 13 has a single solution $\hat{x}$ or $(\hat{u}_n, \hat{v}_n)$.

Limit Case

The author let $n \to \infty$ and considers the sequence $(\hat{u}_n, \hat{v}_n)$ of the solutions of the various discrete problems. He can show (6) that this sequence is bounded in W and, therefore, that there exists a subsequence that is weakly convergent to $(\hat{u}, \hat{v})$, which is a solution of Eq. 11. Because it is possible to show that $(\hat{u}, \hat{v})$ is unique, the entire sequence $(\hat{u}_n, \hat{v}_n)$ converges to $(\hat{u}, \hat{v})$:

$$J(\hat{u}, \hat{v}) = \inf[J(\vec{u}, \vec{v}) \mid (\vec{u}, \vec{v}) \in K] = \lim_{n \to \infty} J(\hat{u}_n, \hat{v}_n)$$

In the limit case, certain precautions must be taken on the mesh $\overline{\Omega}_n$. The maximum diameter of the tetrahedrons of $\overline{\Omega}_n$ must approach zero, and the angles of the dihedral figures constituting them must remain greater than $\theta_0 > 0$ (1, 21). This means that the tetrahedrons must become progressively smaller without becoming flat.

NUMERICAL EXAMPLE

All data in this example are axisymmetric. The calculations are carried out in a meridian plane in cylindrical coordinates.

The slab is a circular cylinder with height h and radius R. The ground is a homogeneous half-space. The author is working within the theory of linear, homogeneous, and isotropic elasticity for the materials constituting these two solids. Under these conditions

$$\Phi_{33}(r) = (1 - \sigma')/2\pi\mu' \times 1/r$$

where σ' and μ' are the Poisson and Lamé coefficients for the ground.

The conditions at the slab and ground interface are as follows:

$$\text{vertical stress } \vec{v} \ (v_1 = v_2 = 0) \tag{14}$$

and either continuity of vertical displacements

$$u_3 = \Phi_{33} * v_3 \tag{15}$$

or loosening

$$u_3 - \Phi_{33} * v_3 \geq 0 \tag{16}$$

and

$$(u_3 - \Phi_{33} * v_3)v_3 = 0 \qquad (17)$$

The slab therefore slides horizontally on the ground. It is not possible to prescribe continuity of the horizontal displacements because there would then be too many data (a condition has already been prescribed on horizontal stress, which must be zero). As a general rule, at any point of Γ it is not possible to prescribe more than one relation between the displacement and stress vectors. Otherwise, the data would be present in excess, and the problem generally would have no solution.

The forces prescribed are gravity $\vec{f} = (0, 0, f_3)$ and various pressures applied to the slab surface.

To define the mesh $\overline{\Omega}_n$, we divided the radius R into N+1 segments of length R/(N+1), and the height h is divided into M+1 segments of length h/M+1 (Fig. 5). By using these two subdivisions, the author then defines the mesh $\widetilde{\Omega}_n$, which consists of triangles as shown in Figure 5. The mesh Γ_n consists of segments of length R/(N+1) or h/(M+1).

The definition of W_n has been slightly changed to facilitate the computation in polar coordinates. The vertical displacement is indeed in each triangle a linear function of r and z, but the radial displacement is in each triangle of the form $\sqrt{r}(ar + bz + c)$. This radial displacement is indeed zero for r = 0 because of axisymmetry. The vertical stress is such that rv_n is a linear and continuous function of r over the entire part of Γ where contact is possible: $rv_n = ar + b$ over each of the length intervals R/(N+1). The dimension n of W_n is then (M+2)(2N+3) + (N+1).

Slab Stuck to Ground Everywhere

By using the relation Cx = 0, which expresses Eq. 15, we can decrease the dimension of W_n by replacing in the expression of $J(\vec{u}_n, \vec{v}_n)$, at z = 0, u_3 with $\Phi_{33} * v_3$. The dimension n of W_n is then (M+1)(2N+3) + 2N+2. Equation 13 becomes $\inf[x^T Bx - 2f^T x]$ or equivalently Bx = f because B is symmetric.

By using this procedure, we can decrease the dimension of the linear systems that are to be solved, but Eq. 15 is a global condition; i. e., it is a relation between all the components of the vector, which represent u_3 at z = 0 and the components that represent v_3. The matrix B is thus partly "full," which makes computation more difficult. This solution is obtained by using Gauss' tridiagonal block method. The sizes of the blocks are (2N+3)(2N+3). One of these diagonal blocks is almost full for the reason given previously.

The numerical values expressed in the M-K-S system are as follows:

$$\lambda = \mu = 4 \times 10^8 \qquad \sigma = 0.25 \qquad f_3 = -\rho g = -2{,}500 \times 9.81$$
$$\lambda' = \mu' = 4 \times 10^7 \qquad \sigma' = 0.25$$
$$h = 0.1 \text{ or } 1 \qquad R = 1$$

The values for h as well as forces $\vec{f}$ and $\vec{g}$ were chosen in the two following examples so that the results would be close to two types of loads on the layered half-space whose solutions are known.

Constant Displacement of the Ground—The reaction v_3 is then equal to $p/2\sqrt{1-r^2/R^2}$ where p is the average pressure.

In order to obtain a displacement of the ground close to a constant displacement, we take the slab to be very rigid: h = 1. The results of the calculations are shown in Figures 6 and 7 and are in very good agreement with the theoretical results.

Constant Vertical Stress—The displacement of the ground is then $u_3(r) = 2(1 - \sigma')/\Pi\mu$ $v_3 E(r/R)$, where E is the complete second-order elliptical function. The quotient of the vertical displacement at the center by the vertical displacement at the edge is, in particular, equal to $\Pi/2$. An approximation of this solution was obtained by loading with a constant pressure a slab that has a small thickness (h = 0.1). Figures 8 and 9 show again a good agreement between what is expected from the preceding expressions and the

Figure 1. Vertical section of the structure.

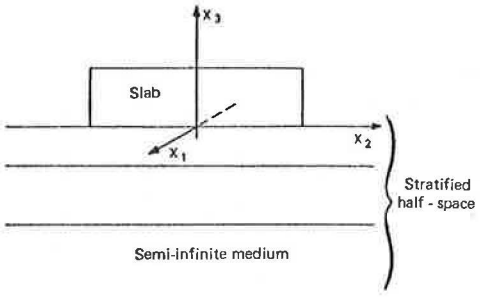

Figure 2. System I.

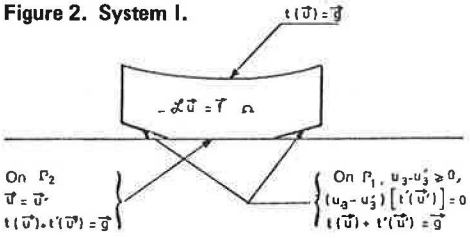

In the stratified half-space : $\mathcal{L}'\vec{u} = \vec{0}$

Figure 3. System II.

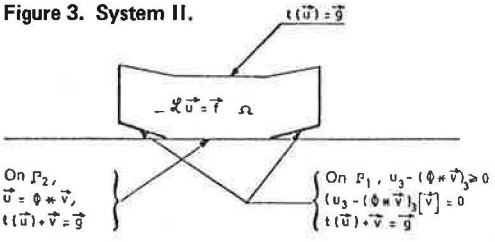

Figure 4. A tetrahedron of the mesh Ω_n and triangles of the mesh Γ_n.

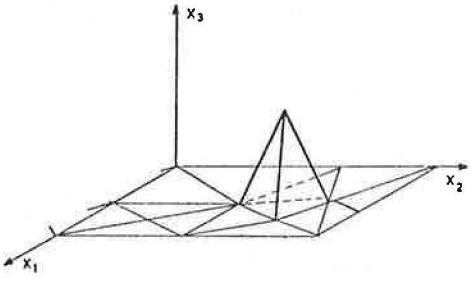

Figure 5. The meshes Ω_n and Γ_n of the meridian plane.

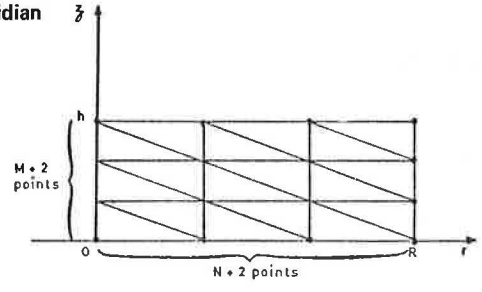

Figure 6. Vertical displacement of the slab, h = 1.

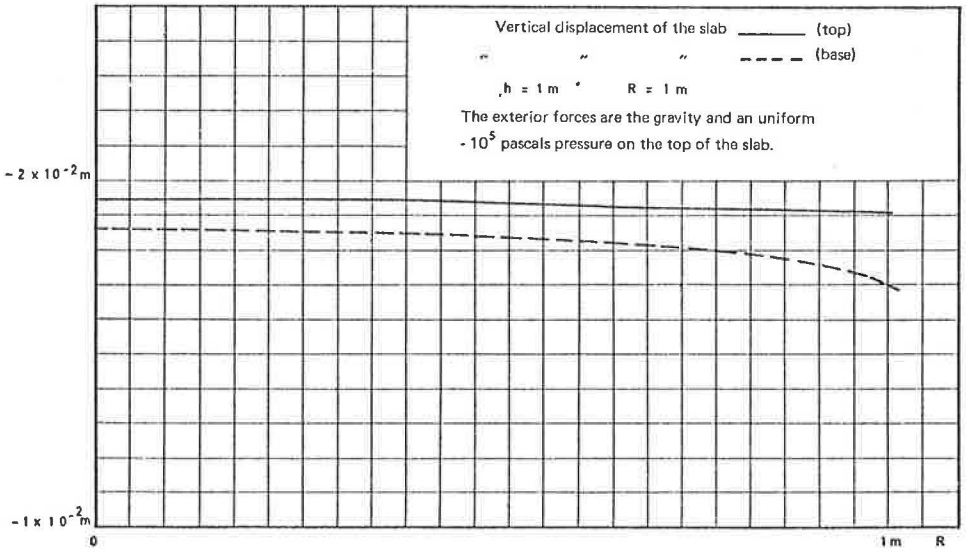

Figure 7. Vertical stress on the ground, h = 1.

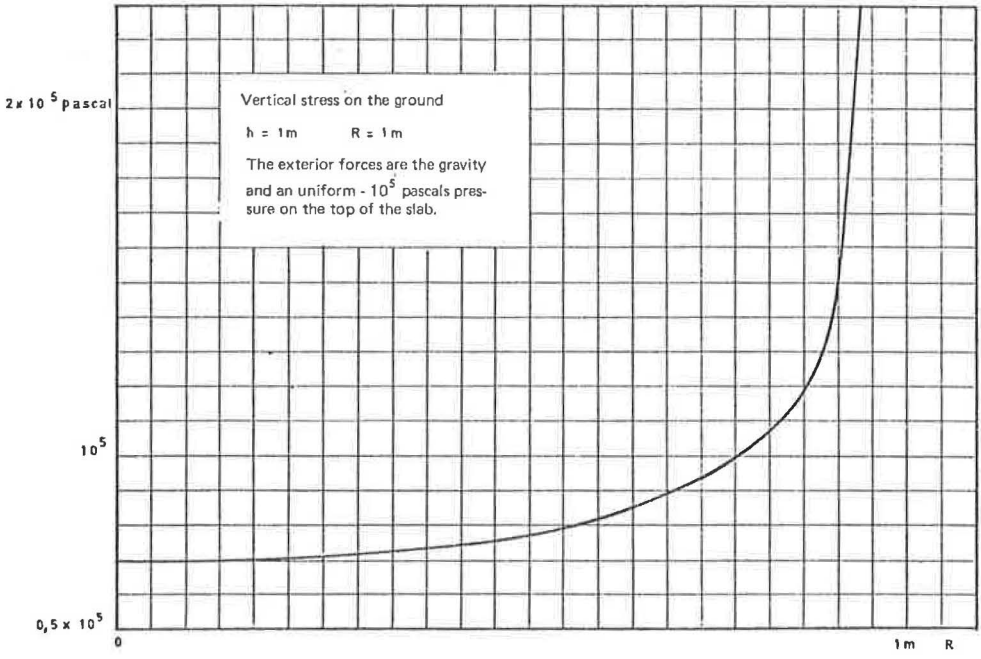

Figure 8. Vertical displacement of the slab, h = 0.1.

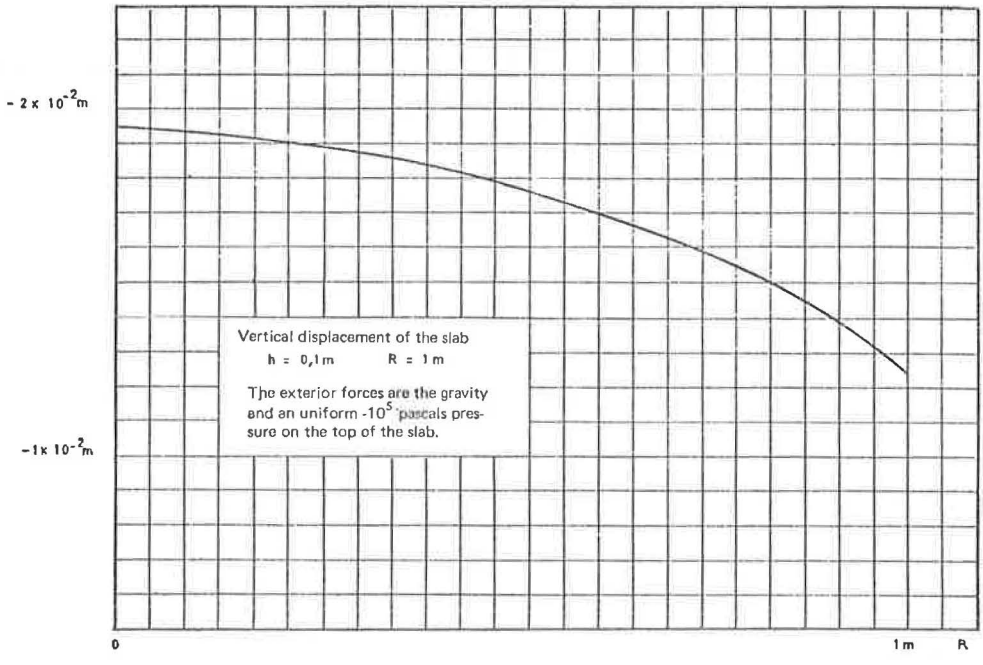

numerical results. The stress v_3 is constant only away from the vicinity of the edge of the slab where it has a singularity. A punching phenomenon is involved here, and the stress v_3 becomes infinite. It is obvious of course that, in this vicinity, the model no longer represents the true situation.

Slab That May Lose Contact Everywhere

The author solves Eq. 13 by replacing it with the following equivalent problem:

$$\max_{\mu \geq 0} \min[x^T Ax - 2f^T x + \mu^T Cx \mid x \in R^n] \tag{18}$$

The complicated condition $Cx \leq 0$ has been replaced with a simple condition $\mu \leq 0$. μ is a vector having as many components as the matrix C has rows.

Equation 18 is solved by using an iterative method (Uzawa's algorithm, 18). (μ_n, x_n) being known, (μ_{n+1}, x_{n+1}) is found using the following method: x_{n+1} is a solution of $\min[x^T Ax - 2f^T x + \mu_n^T Cx \mid f^T x < 0 \text{ if } x \in K_n \cap P_1]$. There is a difficulty in solving this problem because A is not regular. It is known, however, that the slab touches the ground at one point at least. This point must simply be "guessed," which might be the ith, say, and then the relation $(Cx)_i = 0$ is used, leading to the solution of a linear system. If a bad guess is made, all the points must be tried; by using a finite number of trials, we can find a point of contact.

The components of the vector μ_{n+1} are then computed by using the following relation:

$$\mu_{j,\,n+1} = \sup[0,\ \mu_{j,\,n} + \rho(Cx_{n+1})_j]$$

where ρ is a positive parameter that must be suitably chosen so that the process will converge. This choice is not obvious because, if ρ is too small, the convergence is slow, and if ρ is too large, the process diverges. The choice of μ_0 is also important.

The numerical results are shown in Figures 11, 12, and 13 for a slab subjected to its own weight and to forces due to temperature vatiations. In these examples a constant vertical temperature gradient has been assumed. The value of the geometric and mechanical parameters are shown in Figure 10.

In Figures 11 and 12, the temperature gradient is positive (50 C/m) as it is in summer. In Figure 11, a 63,765 N load is applied at the center. This load prevents the slab from losing contact with the half-space at the center. In Figure 12, this load is not applied, and the slab loses contact with the half-space at the center.

In Figure 13, the temperature gradient is negative because it is in winter, and the slab is loaded by the 63,765 N force. The radial displacements are not shown for the preceding examples because they are small.

COMPARISON WITH PHYSICAL MEASUREMENTS

Circular concrete slabs were made at the Laboratoire Régional des Ponts et Chaussées de Rouen. These slabs rest on a very thick sand layer. The author considers it as a semi-infinite medium. The geometric and mechanical characteristics of two structures are shown in Figures 14 and 16. The module E and the Poisson coefficient σ of the slab were measured on a concrete specimen. The module E' of the ground was estimated by using a plate test, and the Poisson coefficient for the sand was chosen to be equal to 0.33. The measured displacements of the two structures are compared with the numerical results shown in Figures 15 and 17. These displacements are in fact the difference between the deflections of the slab subjected to gravity and to the loads and the deflections of the slab subjected to gravity alone. In Figure 15, where no loosening occurs, the displacements computed with the Burmister's model (7, 17) are shown. The difference between the two models can be noticed. In Figure 16, the slab loses contact with the soil.

Agreement between the calculations and physical measurements is good.

Figure 9. Vertical stress on the ground, h = 0.1.

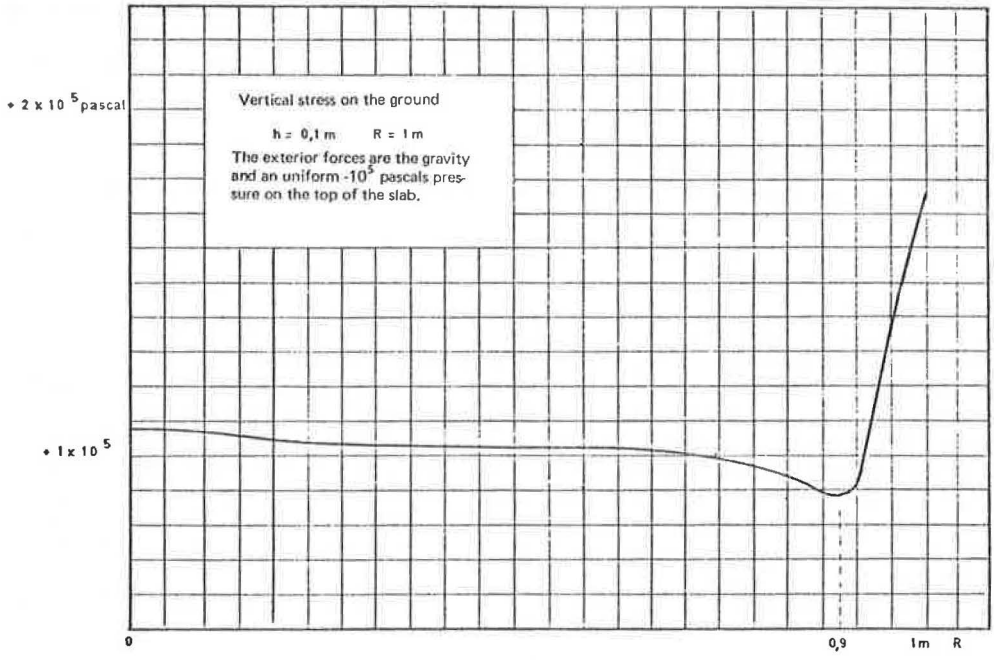

Figure 10. Geometric and mechanical parameters, N = 63,765.

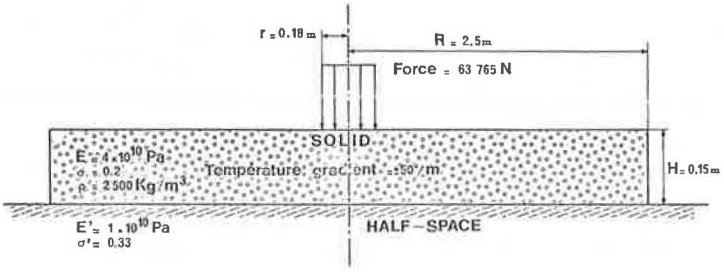

Figure 11. Vertical displacements of the slab and of the half-space—load prevents slab from losing contact with the half-space at the center.

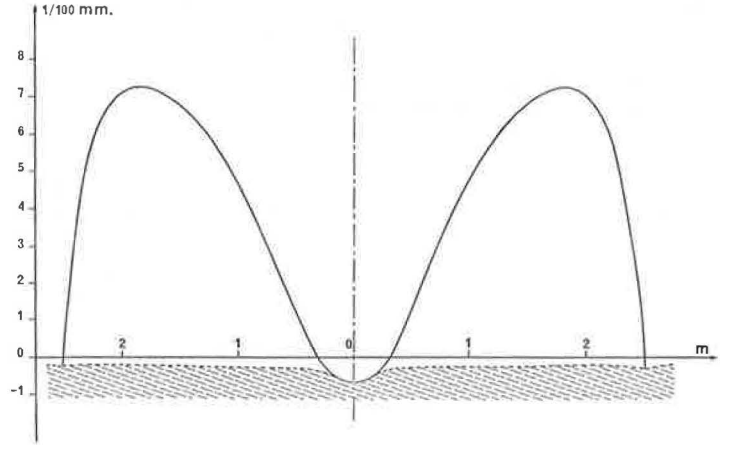

Figure 12. Vertical displacements of the slab and of the half-space—load is not applied and slab loses contact with the half-space at the center.

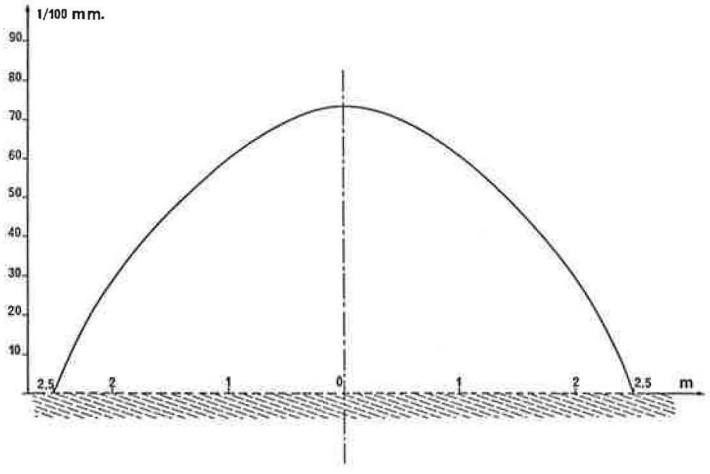

Figure 13. Vertical displacements of the slab and of the half-space—load is applied.

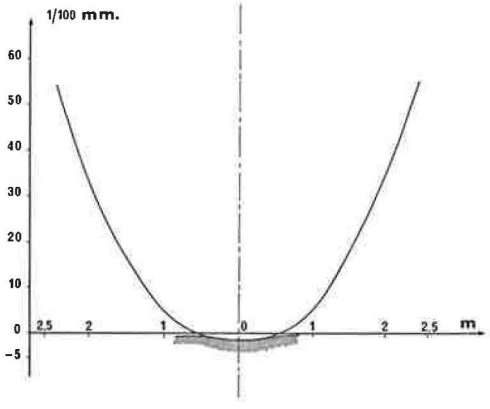

Figure 14. Geometric and mechanical parameters, N = 98,000.

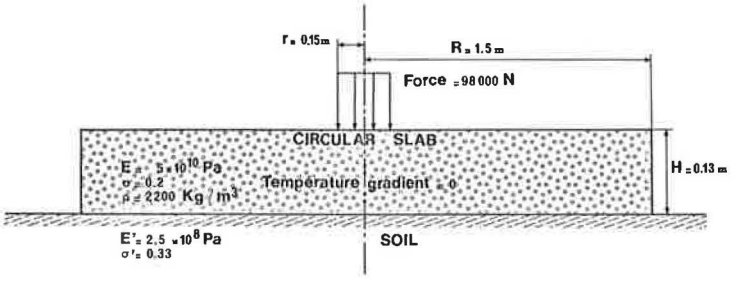

Figure 15. Vertical displacements of the slab (structure of Fig. 14).

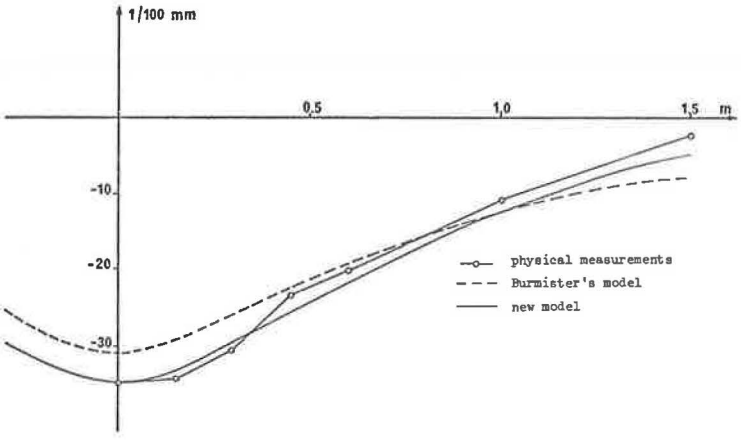

Figure 16. Geometric and mechanical parameters, N = 49,000.

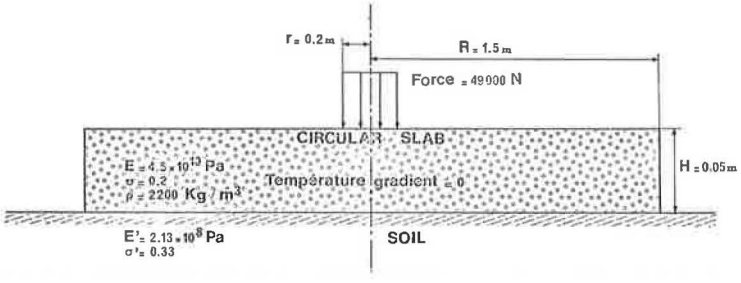

Figure 17. Vertical displacements of the soil and slab (structure of Fig. 16).

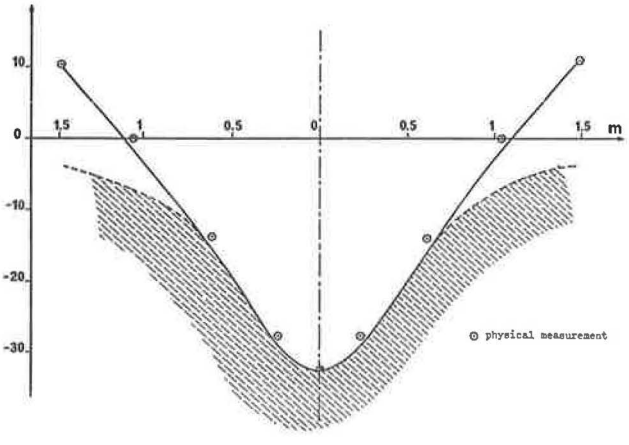

CONCLUSIONS

Measurements are currently being carried out by subjecting the slab to various stresses, in particular, to stresses due to temperature gradients. The first results are satisfactory. In the near future, it will be possible to use a computing program for slabs of any shape and then to come closer to the true situation and to carry out a more rational calculation of concrete slabs for highways.

REFERENCES

1. Ciarlet, P. G., and Wagschal, C. Multipoint Taylor Formulas and Applications to the Finite Element Method. Numer. Math. 17, 1971, pp. 84-100.
2. Ewing, W., Jardetsky, W., and Press, F. Elastic Waves in Layered Media. McGraw-Hill, New York, 1957.
3. Fichera, G. Atti. Acad. Nat. dei Lincei. Memorie 7, No. 1, 1964, pp. 91-40.
4. Fletcher, B. Q., and Hermann, L. R. Elastic Foundation Representation of Continuum. Jour. of Eng. Mechanics Division, Proc. ASCE, Feb. 1971, pp. 96-107.
5. Fremond, M. Solide Posé sur un Sol Élastique. C. R. Acad. Sci. Sér. A t. 271, 14 Paris, Sept. 1970, pp. 508-510.
6. Fremond, M. Etude de Structures Visco-Élastiques Stratifiées Soumises à des Charges Harmoniques et de Solides Élastiques Reposant sur ces Structures. Thesis, Paris, 1971.
7. Fremond, M. Structures Visco-Élastiques Stratifiées Soumises à des Charges Harmoniques. Journal de Mécanique, Vol. 10, No. 1, March 1971.
8. Haar, M. E., and Leonards, G. A. Warping Stresses and Deflections in Concrete Pavements. HRB Proc., Vol. 38, 1959, pp. 286-320.
9. Hudson, W. R., and Matlock, H. Cracked Pavement Slags With Non-Uniform Support. Jour. of Highways, ASCE, Vol. 1, April 1967.
10. Hudson, W. R., and Matlock, H. Discrete-Element Analysis of Discontinuous Plates. Structural Jour., ASCE, Vol. 10, Oct. 1968.
11. Lewis, K. H. Analysis of Concrete Slabs on Grounds and Subject to Warping and Moving Loads. Joint Highway Res. Proj. 16, Purdue University, Lafayette, June 1967.
12. Lewis, K. H., and Haar, M. E. Analysis of Concrete Slabs on Ground Subjected to Warping and Moving Loads. Highway Research Record 291, 1969, pp. 194-211.
13. Lions, J. L., and Magenes, E. Problèmes aux Limites non Homogènes et Applications. Vol. 1, Chap. I, Dunod, Paris, 1968.
14. Lions, J. L., and Stampacchia, G. Variational Inequalities. Comm. Pure Appl. Math., Vol. 20, 1967, pp. 493-519
15. Palatnikov, Z. A. Calcul des Dalles en Béton Pour Aérodromes. Editions Oborongiz, Moscow, 1961.
16. Pasternak, P. L. On a New Method of Analysis of an Elastic Foundation by Means of Two Foundation Constants. Gosudarstvenngo Izdatelstvo Literaturi po Stroitelstou i Arkhitekture, Moscow, 1954.
17. Romain, J. E. Contraintes, Déformations et Déflexions Dans les Systèmes Multicouches Élastiques. Centre de Recherche Routière Belge, Rapport de Recherche No. 151/JER/1969, Feb. 1970.
18. Uzawa, H. Iterative Methods for Concave Programming. In Studies and Non-Linear Programming (Harrow, J. J., Hurwicz, L., and Uzawa, H., eds.), Stanford Univ. Press, 1958.
19. Westergaard, H. M. New Formulas for Stresses in Concrete Pavements of Airfields. Trans. ASCE, Vol. 113, 1948.
20. Wiseman, F., Haar, M. E., and Leonards, G. A. Warping Stresses and Deflections in Concrete Pavements: Part II. HRB Proc., Vol. 39, 1960, pp. 157-172.
21. Zlamal, M. On the Finite Element Method. Numer. Math. 12.5, 1969.

A WORKING SYSTEMS MODEL FOR RIGID PAVEMENT DESIGN

Ramesh K. Kher, W. Ronald Hudson, and B. Frank McCullough,
Center for Highway Research, University of Texas at Austin

In 1971, a conceptual systems analysis was presented at the 50th Annual Meeting of the Highway Research Board by Kher et al. (1). The present paper describes the equations and methods of solution that are required to perform the systems analysis outlined in that paper. A computer program solves the mathematical models by using systems analysis concepts previously described by the authors (1). Analysis techniques, required inputs, and the output obtained are also described. A preliminary system evaluation has been attempted through a sensitivity analysis of important variables affecting rigid pavement design. The computer program is based on a comprehensive economic analysis of various phases of rigid pavement design and management. In general, pavement and overlay type, reinforcement design, joint detailing, subbase and concrete thickness design, and maintenance and overlaying are the important phases that are analyzed to optimize for the best possible design configuration. The program uses 117 different input variables and gives the optimal design and 23 nearly optimal designs in increasing order of total overall cost. The ordered choice provides the designer or the administrator with information needed in making a rational pavement design decision.

•SYSTEMS analysis is a concept by which the generalized form of an ideal model can be defined. The concept as applied to pavement design and management has been presented by several authors in the past (2 - 7). In 1971, a comprehensive systems analysis for rigid pavements (1) was presented, and various subsystems were defined to formulate the overall analysis technique.

The concept of an iterative improvement pattern (8) is one of the important ideas that is implemented through the application of systems analysis to pavement design. This is an approach to which improvements are made with each succeeding cycle of the process. Once a "working" or initial system has been established, it can serve as the first block in a continuing process of improving the design procedure.

The present paper describes an initial working system that is based on the generalized rigid pavement system (1). The required subsystems have been delineated from the best of the current state of the art, and the resulting computer program is called a rigid pavement system (RPS). The version reported here is called RPST2, in which T2 denotes the second University of Texas version of the basic program.

OBJECTIVES AND SCOPE

The computer program was developed with three main objectives:

1. To utilize the best existing state of the art, develop models for any missing links in the system, and evolve an efficient design process;
2. To serve as a first block in the continuing research and to establish priority items for future research by implementation of this system and feedback from such

Sponsored by Committee on Rigid Pavement Design.

an implementation; and

3. To present a simple and generalized design procedure so that future modifications can be incorporated in it with a minimum of effort.

This design procedure has a wide scope of applicability as compared to the prevalent design procedures, which deal primarily with concrete thickness design and use only structural design models. The design procedure makes possible the consideration of a spectrum of influencing variables and provides ordered design output. This in turn helps the administrator to make a more rational design decision and perform long-range planning and budgeting (8) in his district or state.

MATHEMATICAL MODELS OF THE WORKING SYSTEM

The working system RPST2 involves a number of mathematical models. Some of these concern the current state of the art and were developed through experimental test roads, laboratory experiments, and theoretical analyses. Other relations necessary for a rational working system are derived from theory.

Traffic-Related Performance Model

The performance model used originates from the AASHO Road Test data. The AASHO model, which was modified (9), involved the use of observed corner load stresses and their correlation with the design term DT (= D + 1, where D is the thickness of slab). The modified model is as follows:

$$\log W_n = 0.9155\left\{7.35 \log (DT) + 0.05782 + [G/(1) + (16.196 \times 10^6)/(DT)^{8.46}]\right\} \quad (1)$$

$$DT = 183.9/(\sigma\, 690/f_c)^{0.5222} \quad (2)$$

$$G = \log (P_{1n} - P_{2n})/(P_1 - 1.5) \quad (3)$$

$$\sigma = 9.000/D^2\,[1 - (10.11)/(l)] \quad (4)$$

$$l = \sqrt[4]{\frac{ED^3}{11.52K}} \quad (5)$$

where

W_n = number of 18-kip single-axle applications a pavement will sustain in the nth performance period;
D = thickness of concrete, inches;
f_c = allowable flexural strength of concrete, psi;
P_{1n} = initial serviceability index for nth performance period;
P_{2n} = allowable final serviceability index for nth performance period;
J = load transfer characteristic coefficient;
E = modulus of elasticity of concrete, psi; and
K = modulus of subgrade reaction, pci.

The modified model is the best performance model now available, but improvements will be made as additional knowledge is obtained.

Subgrade-Related Performance Model

Subgrade soils exhibit varying behavior with changing physical and environmental conditions. One of the detrimental effects of this behavior on highway pavements is differential vertical movement that decreases the serviceability index of pavements by making them rougher.

The vertical movements of soils can be determined with some degree of success by using complex theoretical and empirical relations, but correlating the resulting differential movements to the decrease in serviceability of the pavement is a very complex

problem. One method for considering such effects is to assume a relation between loss of serviceability and time. The variables in such a relation can then be correlated to certain soil properties by observing pavements over different soils. For the rigid pavement system, the assumed relation is in the form of an exponential curve. The curve is defined by a serviceability index (≤ initial serviceability index) and the rate at which this value will be reached. The mathematical form of the relation, which is derived in terms of a performance loss function, is

$$\Delta_{SI} = (P_I - \lambda)\,(e^{-\theta t_{n-1}} - e^{-\theta t_n}) \tag{6}$$

where

Δ_{SI} = the loss in serviceability index, due to subgrade related factors, in the nth performance period;
P_I = initial serviceability index; and
λ and θ = constants dependent on the soil and site characteristics.

Traffic Projection Model

The AASHO Road Test single-load equation is used for computing equivalency factors for transforming the applications of various loads on a pavement into the equivalent number of 18-kip single-axle applications. The average number of axle loads in both directions per day in each category is the input. A category is defined by the lower and upper values of the loads.

The total equivalent 18-kip axle applications per day W_t is determined by

$$W_t = \sum_{i=1}^{j} E_i W_i \tag{7}$$

where

W_i = the counted number of axles in the ith category, per day;
E_i = the computed equivalency factor for the ith axle load; and
j = the total number of categories of axle loads.

The load used to determine E_i is the average of the lower and upper values of a category.

The total number of equivalent 18-kip axle applications for the entire analysis period W_A is determined by

$$W_A = 365 \times W_t \times D_I \times D_d\,[1 + G_a\,(A_p/2)] \times A_p \tag{8}$$

where

A_p = the length of the analysis period, years;
D_d = the directional distribution factor, $0 < D_d \leq 1$;
D_I = the lane distribution factor, $0 < D_I \leq 1$; and
G_a = the axle growth rate per year, $0 \leq G_a \leq 1$.

The model for the distribution of total 18-kip axles over the analysis period used by the Texas Highway Department is

$$W_n = W_A\,[A(t_n^2 - t_{n-1}^2)/(A_p^2) + B\,(t_n - t_{n-1})/(A_p)] \tag{9}$$

where

W_n = the number of equivalent 18-kip axles experienced by the design facility in the nth performance period;
t_n = time up to the end of the nth performance period, years;
t_{n-1} = time up to the end of n-1th performance period, years;

and A and B are constants:

$$A = A_p \times G_t/A_p \times G_t + 2 \text{ and } B = 2/A_p \times G_t + 2$$

where G_t = the ADT growth factor per year, $0 \leq G_F \leq 1$.

Simultaneous Solution of Equations

Predicting the life of a pavement structure requires simultaneous solution for t_n of Eqs. 1, 6, and 9. The solution is obtained by an iterative procedure using the Newton-Raphson technique, in which the value of t_n is varied until the three equations are satisfied within specified tolerance for P_{2n}.

Foundation Strength Models

The strength of the pavement subgrade appears in the performance equation as a factor K, which is defined by Westergaard (10) as the linear stiffness constant of an assumed bed of springs under the pavement slab. Support for the slab can generally be improved by providing an intermediate layer of material (subbase) between the subgrade and the concrete slab. The improved support value of K increases the performance of a rigid pavement; this increase is considered in light of the economic factors in the program.

The improved value of K is determined by a model developed by using layered elastic theory (program LAYER, 11). A one-layer system resting on a semi-infinite subgrade was analyzed in developing this model. The system was loaded with a 10-psi pressure applied uniformly over a 30-in. diameter circular plate. The value of K at the top of the subbase was determined by using the computed value of deflection under the plate. The values of K at the top of the subbase were computed as a function of the subgrade modulus, the subbase modulus, and the thickness of subbase. A regression analysis was run to develop a prediction model for wide ranges of these three variables, and the model thus developed was used in RPST2 to analyze the increase in pavement performance due to various subbases and subbase thicknesses.

Pavement slabs are always liable to lose foundation support because of traffic and environmental factors such as erosion, pumping, repetitive loading, and freeze and thaw during the lifetime of the pavement. The loss of support is characterized in RPST2 by the term "erodibility factor," which can have any value from 0 to 3. By using numerical solutions (12) for stresses in cracked slabs, we developed a mathematical model that predicts the loss of support and thereby the performance of a pavement having a particular erodibility factor specified for the subbase.

This is the first attempt to predict the effects of subbases and their deterioration during the lifetime of the pavement facility. As additional knowledge is obtained through further research, implementation, and sensitivity analysis, the validity of the approach will be improved, and the models developed will be modified or verified.

Models for Overlay Design

Program RPST2 formulates alternative overlay patterns by predicting the performance of overlayed structures. A new model for the design of asphalt concrete overlays is developed by using layered elastic theory.

It is assumed in this development that a pavement overlay composite structure is equivalent in performance to "an equivalent concrete thickness structure" if both experience the same maximum tensile stresses. The composite pavement structure can then be theoretically replaced by this equivalent concrete thickness and evaluated for performance by the same performance model used to analyze the initial concrete thickness.

The mathematical model for such an equivalent thickness has been developed as a function of existing concrete thickness D_2, asphalt concrete overlay thickness D_1, the modulus of support reaction below the pavement slab K_M, and the modulus value of the asphalt concrete E_1. The details of the model are rather involved and, for simplification, are not included. As an example, the results given by this model are shown in Figure 1.

Portland cement concrete overlays have not been frequently used in the past, and not much is reported in literature about their design. Obviously, a rational design method should consider factors such as fatigue of concrete, volume change stresses, and reflection cracking. The Corps of Engineers (13, 14) has reported an empirical equation for the design of such overlays. The equation is used in RPST2 and is shown in Figure 2. The equation predicts H, which is an equivalent concrete thickness, to be replaced by existing concrete thickness H_2 plus a concrete overlay thickness H_1.

C_D is a coefficient that represents the condition of the existing pavement at the time of the overlay. The value of C_D generally varies between 0.35 for badly cracked slabs and 1.0 for slabs in excellent condition. The coefficient at present can be qualitatively associated with fatigue considerations in concrete pavements and/or engineering judgment.

Models for Reinforcement Design

Reinforcement is designed for controlling crack widths in concrete slabs produced by tensile stresses due to volume changes in horizontal directions. Because the magnitudes of such tensile stresses are dependent on the free length of the slab, among other factors, different models apply for reinforcement design of jointed and continuously reinforced pavements.

In RPST2, longitudinal steel in jointed concrete pavements is designed by the following model (15):

$$A_s = D\, w_c\, L_d\, F_a/24f_s \tag{12}$$

where

A_s = cross-sectional area of steel in square inches per foot of slab width;
D = the thickness of concrete, inches;
w_c = weight of concrete, lb/cu ft;
L_d = distance between free transverse joints, feet;
F_a = average value of coefficient of frictional resistance of foundation; and
f_s = allowable unit stress in reinforcement, psi.

Because the total cost of transverse joints decreases with an increase in the distance between free transverse joints and the required amount of steel, RPST2 optimizes for the area of steel and gives a minimum total cost of transverse joints and the longitudinal reinforcement.

Longitudinal reinforcement for continuously reinforced pavements is designed by considering the pavement as a continuous, restrained member. The model used in RPST2, taken from another publication (16), is

$$A_s = 12D(1.3 - 0.2F_a)T_s/f_s \tag{13}$$

where T_s is the tensile strength of concrete, psi.

Transverse reinforcement in both types of pavement is designed by Eq. 12 with L_d redefined as the free width of the pavement. The area of steel for tie bars across the longitudinal joint used is the area of transverse reinforcement required at that section.

Stochastic Variations in the Material Properties

In RPST2, probability concepts are applied in computing the design values of the flexural strength of concrete, the modulus of subgrade reaction, and the Texas triaxial class of the subgrade.

It is assumed that these properties in large populations of samples have normal probability distributions. Based on standard deviation α of the particular parameter value V_m, the design value V_d is computed as

$$V_d = V_m - \alpha V_c \tag{14}$$

Figure 1. Equivalent concrete thicknesses for different overlay thicknesses over 6-in. PCC pavement.

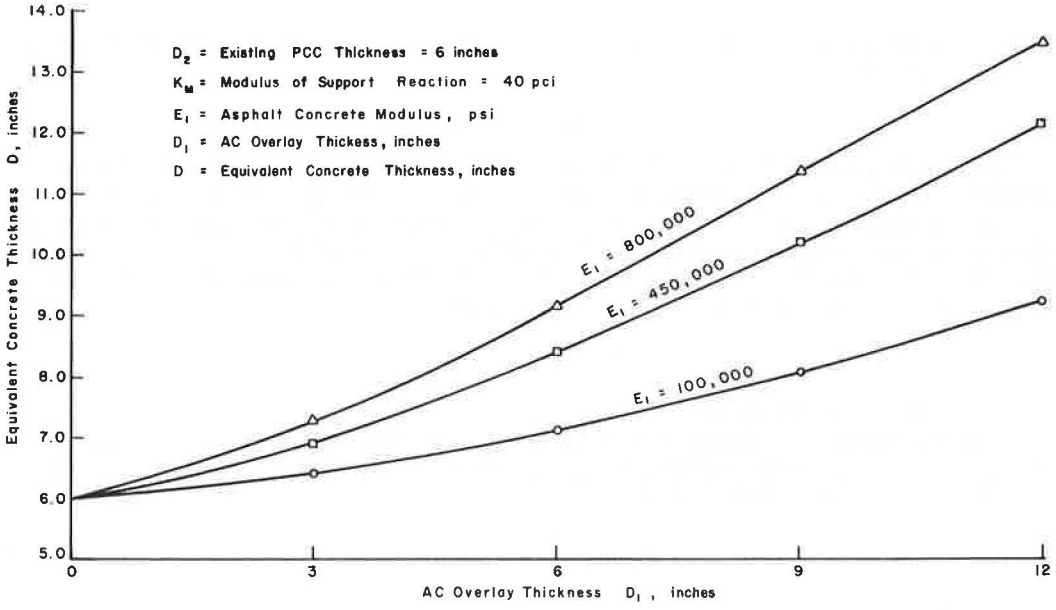

Figure 2. Effective concrete thickness given by Corps of Engineers' model (partially bonded PCC overlays).

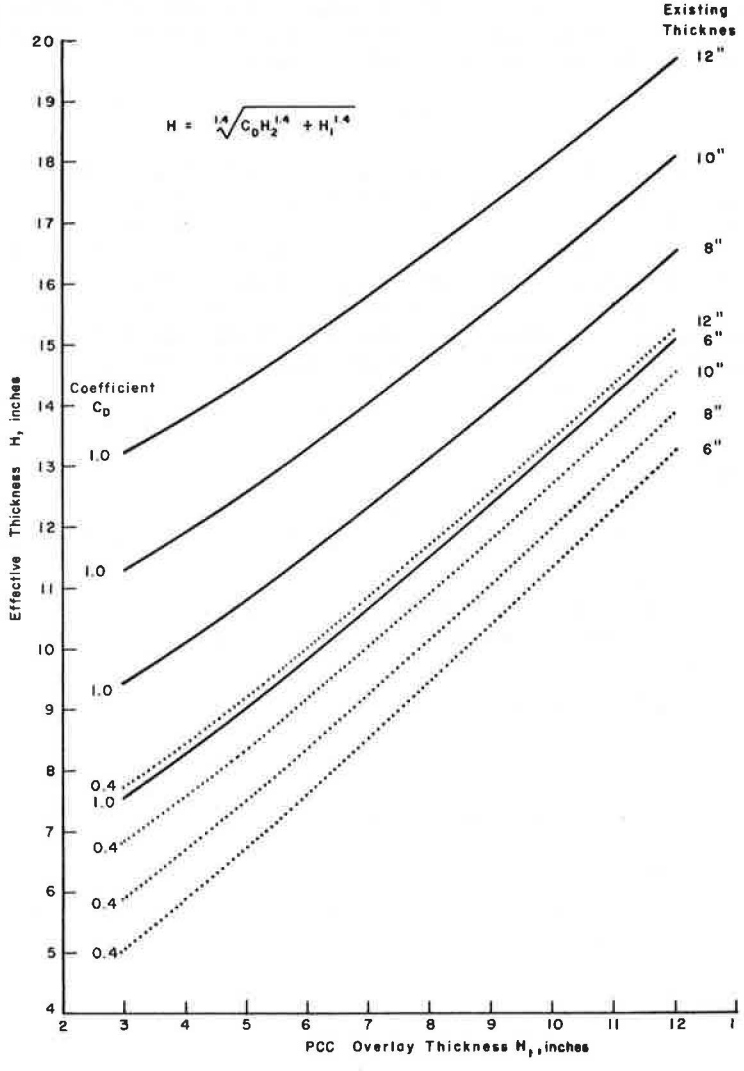

where V_c is determined in the program by using the value of confidence level specified with respect to the parameter.

ECONOMIC MODELS

Design analysis in RPST2 results in alternative strategies that are compared and optimized by the decision criteria of minimum present value of total overall cost. Each strategy consists of a variety of costs incurred at different times during the design life. Relative comparisons are therefore made with future costs discounted back to present values with the interest rate as an input. For example, the present value C_P of a future cost C_F incurred at t years in the future is computed as

$$C_P = C_F/(1 + I_r)^t \tag{15}$$

where I_r is the specified interest rate.

In RPST2, pavement investments are divided into three main categories: initial cost C_i, present value of all future costs C_f, and present value of salvage return C_{sal}.

Total overall cost C_t therefore is given as

$$C_t = C_i + C_f - C_{sal} \tag{16}$$

Initial Costs

Initial cost C_i consists of the expenses for initial construction: cost of subgrade preparation C_g, cost of in-place subbase C_s, cost of in-place concrete C_c, cost of reinforcement C_r, and cost of joints C_j. Thus,

$$C_i = C_g + C_s + C_c + C_r + C_j \tag{17}$$

The cost of subgrade preparation C_g consists of the costs of scarification and mechanical or chemical stabilization of the subgrade surface. The cost of in-place subbase C_s consists of the sum of the costs of subbase material and that of mixing, hauling, and compacting the subbase. The cost of in-place concrete C_c is computed as the sum of the costs of concrete, initial cost of mixing and hauling, and the cost of curing, finishing, and surfacing. The cost of reinforcement C_r is computed as the sum of the costs of longitudinal and transverse reinforcement and that of the tie bars provided in the longitudinal joints. The cost of joints is computed as the sum of the costs of longitudinal and transverse joints.

The costs C_g, C_s, C_c, C_r, and C_j are computed per square yard of the pavements.

Future Costs

The expenses incurred subsequent to the initial construction are accumulated during the analysis period of a strategy. These expenses are as follows:

1. Present value of all the overlays C_o,
2. Present value of the maintenance C_m, and
3. Present value of all the seal coats C_l (only for strategies that have asphalt concrete overlays).

The present value of all future costs C_f is therefore given as

$$C_f = C_o + C_m + C_l \tag{18}$$

C_f, C_o, C_m, and C_l are costs computed per square yard of the pavement.

Overlay Cost

There are two aspects of overlay cost analysis: overlay construction cost C_{oc} and traffic delay cost during overlay operations C_{od}.

Overlay construction cost is the present value of providing all future overlays. This cost is the sum of the costs of materials provided in overlays and the costs of equipment, labor, hauling, curing, and finishing the overlays.

Traffic delay cost during overlay construction deals with the indirect cost that an overlay operation incurs as a result of the disturbances it produces in traffic flow. Traffic speed fluctuations and delays give rise to these indirect costs. The analysis for this cost is taken from the work done by Scrivner et al. (18). The following types of traffic delay costs are considered during the overlay operations:

1. Cost of stopping a certain proportion of hourly traffic outside the overlay zone because of congestion, CO_c;
2. Cost of the remaining hourly traffic to travel at a reduced speed through the overlay zone, CO_s; and
3. Cost of stopping a certain proportion of hourly traffic inside the overlay zone because of the movement of personnel and overlaying equipment, CO_p.

These costs are computed as follows:

$$CO_c = CO_1 + CO_2 + CO_3 \tag{19}$$

$$CO_s = CO_3 + CO_4 \tag{20}$$

$$CO_p = CO_5 + CO_6 \tag{21}$$

where

CO_1 = cost of stopping from and returning to the approach speed,
CO_2 = cost of idling and time loss while stopped outside the overlay zone,
CO_3 = cost of driving at the reduced speed through the overlay zone,
CO_4 = cost of slowing to the reduced speed while in the overlay zone and returning to the approach speed,
CO_5 = cost of stopping from and returning to the reduced speed in the overlay zone, and
CO_6 = cost of idling and time loss while stopped in overlay zone.

The excess time and operating costs of slowing or stopping from different speeds, the costs of traveling at reduced speeds, and the costs of idling are calculated in RPST2 by the built-in tables in the form of data arrays. The tables for these costs are taken from work done by Scrivner et al. (18).

Total traffic delay cost of all overlays discounted to the present value C_d per square yard of pavement is therefore given by

$$C_d = \sum_{n=1}^{N} C_n/(1 + I_r)^{t_n} \tag{22}$$

where

N = number of overlays computed for the design strategy;
I_r = interest rate;
t_n = amount of time to when nth overlay is provided, years; and
C_n = total cost of traffic delay per square yard of pavement during the construction of nth overlay, computed by using Eqs. 19 through 21.

Maintenance Cost

The NCHRP maintenance study (19) has been implemented in this program to quantify the maintenance requirements of various designs.

Each year's maintenance cost is calculated by using this model and is assumed to be paid at the beginning of the year. The total discounted maintenance cost of a strategy is computed as

$$C_m = \sum_{j=1}^{J} \left[\sum_{l=1}^{L_j} \frac{C_{l,j}}{(1 + I_r)^{N_j+l-1}} + \frac{C_{L_j+1,j}}{(1 + I_r)^{N_j+L_j}} (L'_j - L_j) \right] \quad (23)$$

where

$$N_j = \sum_{k=1}^{j} L'_{k-1},$$

$$L'_o = 0.0, \text{ and}$$

$$L'_j = A_p - N_j.$$

The quantities are defined as follows:

- l = year number after initial or overlay construction for which $C_{l,j}$ is calculated;
- $C_{l,j}$ = cost of maintenance for lth year in jth performance period after initial or overlay construction, per square yard of pavement, calculated by using the NCHRP model (19);
- L_j = value of L'_j in jth performance period, rounded to the lower whole number;
- L'_j = life of the jth performance period;
- j = performance period number;
- J = total number of performance periods within the analysis period;
- A_p = analysis period; and
- I_r = interest rate.

Seal Coat Cost

In RPST2, seal coats are provided for strategies for which asphalt concrete overlays are provided. If Q_m number of seal coats are provided in the mth performance period and if the cost per square yard of one seal coat is given by C_{one}, the present worth of all seal coats provided on a strategy will be

$$C_{sc} = \sum_{m=2}^{M} \sum_{q=1}^{Q_m} C_{one}/(1 + I_r)^{t_{qm}} \quad (24)$$

where M is the total number of performance periods for a strategy and t_{qm} is the time when a seal coat is provided after the initial construction.

The number of seal coats and their schedules in a performance period are calculated with the help of the following inputs: the time to the first seal coat after an asphalt concrete overlay, the time between consecutive seal coats within the same performance period, and the cost of one seal coat per lane-mile.

Salvage Returns

Salvage return of a pavement strategy is the value of usable materials at the time when pavement is abandoned.

The present value of salvage returns as calculated in RPST2 is

$$C_{sal} = \frac{C_{cu} \times P_{sc} + C_{su} \times P_{ss} + C_{ou} \times P_{so}}{100 (1 + I_r)^{A_p}} \quad (25)$$

where C_{cu}, C_{su}, and C_{ou} are respectively the costs of portland cement concrete, subbase, and overlay material provided in the pavement strategy. P_{sc}, P_{ss}, and P_{so} are respectively the specified percentage of salvage returns for each of the aforementioned materials.

INPUTS TO THE WORKING SYSTEM MODEL

The design involves the use of a large number of input variables. The program uses 117 different input variables in the broad categories of traffic, environment, performance, materials, costs, dimensions, and constraints. The exact number of pieces of information to be used depends on the individual problem. For example, the exact number of pieces of information used for the example problem reported in the following section is 263. Various inputs to the working system model are shown in Figure 3. The input in this figure is in the same form as when it is echo-printed (for the example problem) by the computer.

THE OPERATION OF THE WORKING SYSTEM MODEL

The computer program RPST2 is written to generate arrays of designs, to estimate their performance and costs, and to store and scan them for optimization. A summary flow chart of the program is shown in Figure 4. There are eight different types of designs that can be analyzed by RPST2. The program can be controlled to design any or all of these designs. Types of designs available for analysis by RPST2 are as follows:

		Reinforcement	
Pavement	Overlay	(mesh)	(bar)
JCP	AC	1	2
	PCC	3	4
CRCP	AC	5	6
	PCC	7	8

The design process of RPST2 is described in the following major steps.

Generating Possible Initial Designs

The thicknesses of the concrete and subbases, starting with their minimum values and increasing to the maximum, produce various combinations of initial designs. These initial designs, when considered with different sets of concrete and subbase properties and for different types of pavements, produce a large number of initial designs. Each initial design thus produced is analyzed for its life and cost.

Selecting Feasible Initial Designs

Each design of the initial design array is further analyzed as follows:

1. Equivalent traffic loads are computed for the design;
2. Improved roadbed support (due to the subbase) is calculated and then reduced for the specified erodibility effect;
3. Initial life of the design is computed;
4. Reinforcement is designed, and joint spacings are determined; and
5. Initial cost of the design is computed.

During this analysis, the initial design is subjected to the following three constraints, the values of which are specified by the designer:

1. Maximum allowable total thickness of initial construction,
2. Minimum time allowed for the first overlay after initial construction, and
3. Maximum allowable cost of initial construction.

If the design under consideration does not satisfy any of these three constraints, it is rejected. All of the designs that do meet these restrictions are feasible initial designs and, except for the designs whose initial lives last the analysis period, are considered for application of overlay strategies.

Developing Overlay Strategies

Every initial design that does not last the analysis period but that meets all other feasibility requirements is overlayed with portland cement concrete or asphalt concrete

Figure 3. Echo-printed input for the example problem.

RIGID PAVEMENT SYSTEM T2 RAMESH KHER MAY 1971
PROB 101 EXAMPLE PROBLEM WITH VARIABLES AT ENGINEERING AVERAGES

TRAFFIC INPUT

LOAD RANGE	AVG. LOAD IN KIPS	AXLE CODE	NO. OF AXLE APPLICATIONS
0 - 3000	1.500	SINGLE	5418
3000 - 6999	4.999	SINGLE	3359
7000 - 7999	7.499	SINGLE	2005
8000 - 11999	9.999	SINGLE	1433
12000 - 15999	14.000	SINGLE	415
16000 - 18000	17.000	SINGLE	71
18001 - 18500	18.250	SINGLE	102
18501 - 20000	19.250	SINGLE	31
20001 - 21999	21.000	SINGLE	11
22000 - 23999	23.000	SINGLE	4
24000 - 25999	25.000	SINGLE	1
26000 - 29999	28.000	SINGLE	1
0 - 6000	3.000	TANDEM	268
6000 - 11999	8.999	TANDEM	4751
12000 - 17999	15.000	TANDEM	2521
18000 - 23999	21.000	TANDEM	1302
24000 - 29999	27.000	TANDEM	306
30000 - 32000	31.000	TANDEM	51
32001 - 32500	32.250	TANDEM	43
32501 - 33999	33.250	TANDEM	24
34000 - 35999	34.999	TANDEM	17
36000 - 37999	36.999	TANDEM	11
38000 - 39999	38.999	TANDEM	7
40000 - 41999	40.999	TANDEM	4
42000 - 43999	42.999	TANDEM	3
44000 - 45999	44.999	TANDEM	2
46000 - 49999	47.999	TANDEM	1

TRAFFIC GROWTH AND DISTRIBUTION

AXLE GROWTH FACTOR	4.00
ADT GROWTH RATE	10.00
DIRECTIONAL DISTRIBUTION FACTOR	50.00
LANE DISTRIBUTION FACTOR	50.00
INITIAL AVERAGE DAILY TRAFFIC	10000.00

RIGID PAVEMENT SYSTEM T2 RAMESH KHER MAY 1971
PROB 101 EXAMPLE PROBLEM WITH VARIABLES AT ENGINEERING AVERAGES

PROGRAM CONTROLS
DESIGNER SPECIFIES

BOTH CRCP AND JCP PAVEMENTS TO BE TRIED
BOTH CC AND AC OVERLAYS TO BE TRIED
BOTH DEFORMED BAR AND WIRE MESH REINFORCEMENT TO BE TRIED
PRINT LONG FORM OF OUTPUT
PRINT FIRST 23 DESIGNS IN INCREASING ORDER OF TOTAL COST

DESIGNERS DECISIONS OR RESTRAINTS

MAXIMUM INITIAL FUNDS AVAILABLE, DOLLARS	6.50
MAX INITIAL THICKNESS, SLAB PLUS SUBBASE, INCHES	20.00
MIN TIME TO FIRST OVERLAY, YEARS	6.00
MIN TIME BETWEEN OVERLAYS, YEARS	6.00
MAX TOTAL AC OVERLAY THICKNESS, INCHES	9.00
MIN AC OVERLAY THICKNESS AT ONE TIME, INCHES	1.50
MAX TOTAL CONC OVERLAY THICKNESS, INCHES	15.00
MIN CONC OVERLAY THICKNESS AT ONE TIME, INCHES	6.00
LENGTH OF ANALYSIS PERIOD, YEARS	20.00

PERFORMANCE VARIABLES

INITIAL SERVICEABILITY INDEX	4.20
TERMINAL SERVICEABILITY INDEX	2.50
SERVICEABILITY INDEX AFTER AN OVERLAY	4.00
LOWER BOUND ON SERV.INDEX,NO TRAFFIC, INFINITE TIME	2.00
SWELLING CLAY EXPONENTIAL DETERIORATION FACTOR, BONE	.02
SWELLING CLAY LINEAR DETERIORATION FACTOR, PHI	0.00

TRAFFIC DELAY COST VARIABLES

DISTANCE OVER WHICH TRAFFIC IS SLOWED,	OV.DIRECTION	.75
	N.OV.DIRECTION	.50
NO. OF OPEN LANES IN RESTRICTED ZONE,	OV.DIRECTION	1
	N.OV.DIRECTION	2
PERCENT VEHICLES STOPPED BY ROAD EQUIP,	OV.DIRECTION	8.00
	N.OV.DIRECTION	4.00
AVG DELAY CAUSED BY ROAD EQUIP, HOURS ,	OV.DIRECTION	.20
	N.OV.DIRECTION	.10
AVG SPEED THROUGH OVERLAY ZONE, MPH ,	OV.DIRECTION	30.00
	N.OV.DIRECTION	40.00
AVERAGE APPROACH SPEED TO OVERLAY AREA		60.00
DETOUR DISTANCE AROUND OVERLAY ZONE		0.00
ADT ARRIVING EACH HOUR OF CONSTRUCTION		7.00
NO. OF HOURS/DAY OVERLAY CONSTRUCTION OCCURS		10.00
TRAFFIC MODEL USED IN THE ANALYSIS		3
ROAD LOCATION		RURAL

RIGID PAVEMENT SYSTEM T2 RAMESH KHER MAY 1971
PROB 101 EXAMPLE PROBLEM WITH VARIABLES AT ENGINEERING AVERAGES

MATERIALS, CONCRETE

	1	2
CONCRETE MIX DESIGN NUMBER	1	2
AGE OF TESTING CONCRETE	28	28
MEASURING POINT	THIRD	THIRD
FLEXURAL STRENGTH,MEAN VALUE	500.00	625.00
FLEXURAL STRENGTH,STD. DEV.	35.00	60.00
FLEX.STR.DESIGN CONF.LEVEL	95.00	95.00
TENSILE STRENGTH	200.00	260.00
ELASTIC MODULUS	2500000	5000000
WEIGHT	140.00	150.00
CONSTRUCTION EQUIPMENT COST	800.00	900.00
COST PER CUBIC YARD	12.00	14.00
COST OF SURFACING CONCRETE	400.00	400.00
SALVAGE PERCENT OF CONCRETE	50.00	60.00

MINIMUM ALLOWABLE CONCRETE THICKNESS	6.00
MAXIMUM ALLOWABLE CONCRETE THICKNESS	10.00
PRACTICAL INCREMENT FOR POURING CONCRETE	.50

MATERIALS, STEEL

	1	2	
BARS			
LONGITUDINAL			
BAR STEEL ASTM DESIG	A-615,GR75	A-432	
TENSILE YIELD PT STR	70000.00	60000.00	
COST/LB OF BAR STEEL	.110	.100	
TRANSVERSE			
BAR STEEL ASTM DESIG	A-15 STR	A-15 INT	
TENSILE YIELD PT STR	33000.00	40000.00	
COST/LB OF BAR STEEL	.070	.080	
BAR NOS. TO BE TRIED	3	4	5
WIRE MESHES			
WIRE MESH ASTM DESIG	ASTM,A-496		
TENSILE YIELD PT STR	70000.00		
COST/LB OF WIRE MESH	.100		
MESH SIZES TO BE TRIED			
LONG. WIRE SPACING	4.00	5.00	6.00
TRAN. WIRE SPACING	12.00	14.00	16.00
TIE BARS USED WITH W. MESH			
TIE BAR ASTM DESIG.	A-615,GR40	A-15 STR	
TENSILE YIELD PT STR	40000.00	33000.00	
COST /LB OF TIE BARS	.080	.070	
TIE BAR NOS TO BE TRIED	3	4	

RIGID PAVEMENT SYSTEM T2 RAMESH KHER MAY 1971
PROB 101 EXAMPLE PROBLEM WITH VARIABLES AT ENGINEERING AVERAGES

MATERIALS, SUBGRADE

SUBGRADE K MEAN VALUE	100.00
SUBGRADE K VALUE, STANDARD DEVIATION	15.00
SUBGRADE K VALUE, DESIGN CONFIDENCE LEVEL	95.00
SUBGRADE FRICTION FACTOR	1.00
SUBGRADE ERODABILITY FACTOR	3.00
COST PER LANE MILE OF SUBGRADE PREPARATION	1350.00

MATERIALS, SUBBASE

SUBBASE TYPE	GRANULAR	C.TREATED
ERODABILITY FACTOR	2.00	0.00
FRICTION FACTOR	1.50	3.00
ELASTIC MODULUS	20000	700000
CONSTR EQUIPMENT COST	300.00	600.00
COST/COMPACTED CU YD	1.50	3.50
SALVAGE PERCENT VALUE	10.00	30.00
MIN ALLOWED THICKNESS	6.00	6.00
MAX ALLOWED THICKNESS	9.00	10.00
INCREMENT FOR SUBBASE	1.00	1.00

OVERLAY

INITIAL COST PER LANE MILE OF EQUIPMENT FOR OVERLAYS	1200.00
COST/CU YD OF IN PLACE COMPACTED ASPHALT CONCRETE	12.00
SALVAGE PERCENT VALUE OF ASPHALT CONCRETE	50.00
ASPHALT CONCRETE MODULUS VALUE	200000
PRODUCTION RATE OF COMPACTED ASPHALT CONCRETE	175.00
CONCRETE PRODUCTION RATE	225.00
CONCRETE COEFFICIENT	.80

SEAL COATS

TIME TO FIRST SEAL COAT AFTER AC OVERLAY	5.00
TIME BETWEEN SEAL COATS	5.00
COST PER LANE MILE OF A SEAL COAT	1100.00

JOINTS

COST/FT OF TRANS. JOINT, SAWING, DOWELS, AND/OR SEALING		1.40
COST/FT OF LONG. JOINT, SEALING		.30
RANGE OF SPACING FOR CONSTRUCTION JOINTS,	LOWER VALUE	15.00
	UPPER VALUE	100.00
NO. OF TRANS. CONST. OR WRAPPING JOINTS/MILE FOR CRCP		0

MAINTENANCE, DIMENSIONS AND MISCELLANEOUS

DAYS OF FREEZING TEMPERATURE PER YEAR	10.00
COMPOSITE LABOR WAGE FOR MAINTENANCE OPERATIONS	2.00
COMPOSITE EQUIPMENT RENTAL RATE FOR MAINT. OPERATION	2.30
COST OF MATERIALS FOR MAINTENANCE OPERATIONS	1.00
WIDTH OF EACH LANE	12.00
TOTAL NUMBER OF LANES IN BOTH DIRECTIONS	4
RATE OF INTEREST OR TIME VALUE OF MONEY	5.00

Figure 4. Summary flow chart for program RPST2.

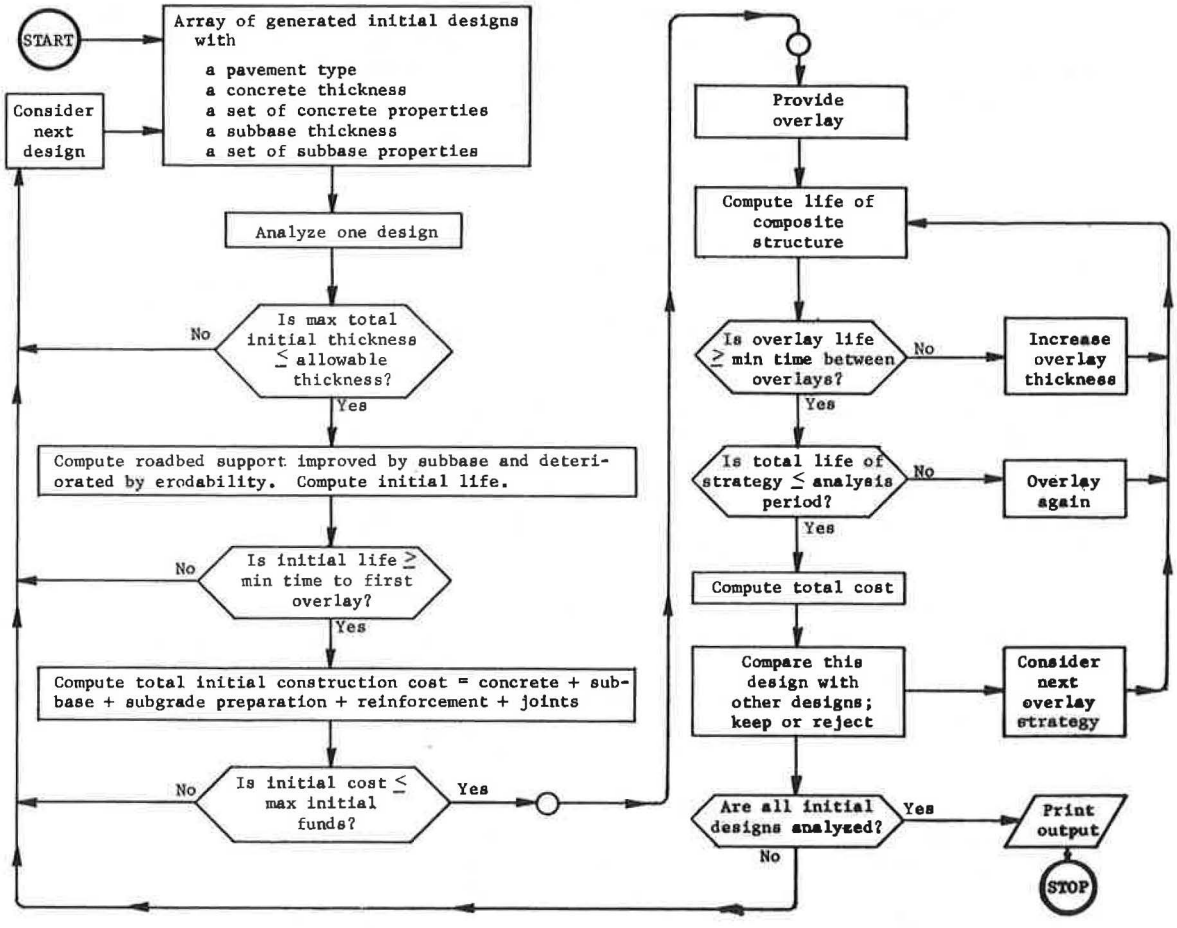

overlays. Minimum thickness of the overlay and maximum combined thickness of all overlays are specified by the program user. As soon as an initial design falls to its terminal serviceability index level, an overlay is provided for, and the composite structure is reanalyzed for its life. Every overlay life is subjected to a constraint specified by the designer. If a strategy requires its next overlay before the minimum specified time between overlays, it is abandoned.

For every successful overlay strategy, the cost of providing the overlay, the cost of traffic delay during the overlay operation, and the cost of maintenance over the life of the overlay are calculated. The total cost for each of these items is computed and stored. If the total life of a pavement strategy, including the life of the overlay, is less than the analysis period, another overlay is provided. If the life exceeds the analysis period, the design is considered a feasible strategy, and the program starts searching for other feasible strategies.

Economic Analysis

For each pavement strategy, the initial design cost and all future expenditures discounted back to the present values are calculated.

Optimization

The program is designed to consider an unlimited number of initial designs and overlay strategies. The optimization process is arranged such that each strategy is

designed completely and its pertinent costs computed up to the end of the analysis period. The strategy is then compared with other strategies previously stored, and it is either rejected or accepted according to the cost-decision criteria built into the program. A minimum possible computer storage is utilized with the method adopted, and the computation and scanning times are kept to a minimum.

OUTPUT OF THE WORKING SYSTEM MODEL

After all of the possible strategies are analyzed, the information that the designer needs for making a rational design decision is printed as output. The output includes the information discussed in the following paragraph.

An optimal design is printed for each combination of pavement and overlay types specified by the designer. If there is one, an optimal initial design that lasts the analysis period without overlay is also printed. A summary table describing as many nearly optimal strategies as specified by the designer is printed. The strategies are arranged in order of increasing total overall cost. Optimization for the summary table includes all designs of every combination tried, including those without overlays. The first design of the summary table, therefore, is the most economical design possible for the given input. The last page of the output contains a summary of the number of possible strategies, the rejected number of strategies due to each constraint specified by the designer, and the total strategies possible for the problem. The output of the example problem (for which the input is shown in Fig. 3) is shown in Figure 5.

PRELIMINARY EVALUATION OF THE WORKING SYSTEM MODEL

Program RPST2 is the first reported version of a particular systematic design procedure for rigid pavements. It links a large number of mathematical models that quantify various aspects of the design. Many of the variables and constraints considered for this design procedure have never been considered in any other rigid pavement procedure. Therefore, an initial evaluation of the method was performed to ascertain the validity of the solutions and the reasonableness of the output and to gain enough initial confidence to implement the system.

Based on engineering practice and judgment, all the input variables of the system were given their typical average values, and with these values a so-called average problem was solved. Ten variables, judged to be important from the standpoint of rigid pavement design, were chosen for study of their effects on RPST2 output. Various problems were solved using each of these variables at its low and high values in practice and all other variables in the system at their average levels. To analyze the effects of these variables on the design system, we examined the optimal solution of each problem for optimal cost and changes in the design strategy. Obviously, the optimal cost changed with a change in the numerical value of any of these variables. Trends of the variations of optimal costs versus the variable values were plotted, and some of these curves are shown in Figure 6.

CONCLUSIONS

The following conclusions are made about the overall rigid pavement research study and the working system presented in this paper:

1. A better design procedure is evolved through the application of systems concepts. The method presented here attempts a more realistic analysis of the problem in that it considers not only the initial design but also subsequent construction, user costs, future maintenance, and overall economics.
2. The computer program RPST2 provides a tool for a feasible consideration of a large spectrum of variables affecting rigid pavement design. It allows use of many kinds of constraints and decision criteria and expands the number of feasible designs by generating a large number of possible alternatives.
3. The initial familiarization and evaluation study has established the reasonableness of the program output and preliminary confidence in its applicability.

Figure 5. Computer output for the example problem.

```
RIGID  PAVEMENT  SYSTEM  T2  RAMESH KHER          MAY  1971
PROB  101      EXAMPLE PROBLEM WITH VARIABLES AT ENGINEERING AVERAGES

     MOST ECONOMICAL JCP PAVEMENT DESIGN WITH  AC OVERLAY,

INITIAL CONSTRUCTION,  LIFE IS  10.046 YEARS

   MATERIALS                                          DESCRIPTION
                                                      MATERIAL    MATERIAL
                                                      NUMBER      NAME

   CONCRETE        10.00 INCHES                          1
   SUBBASE          6.00 INCHES                          2
   LONG.REINF.-MESH SPACING     4.0    5.0    6.0       1        ASTM,A-496
            MESH DIAMETER      .22    .25    .27
   TRAN.REINF.-MESH SPACING    12.0   14.0   16.0       1        ASTM,A-496
            MESH DIAMETER      .32    .34    .37
   TIE BARS       BAR NUMBER     3      4               1        A-615,GR40
                  SPACING      9.5   16.8

                TRANSVERSE JOINT SPACING      35 FEET
                LONGITUDINAL JOINT SPACING    12 FEET


SUBSEQUENT CONSTRUCTION
   1  OVERLAY WITH  1.50 INCHES OF    AC AFTER  10.046 YEARS

     TOTAL OVERLAY THICKNESS   1.50 INCHES     TOTAL LIFE  21.076 YEARS


COST ANALYSIS   DOLLARS PER SQUARE YARD
     INITIAL CONSTRUCTION
        COST OF SUBGRADE PREPARATION                    .192
        COST OF CONCRETE                               3.504
        COST OF SUBBASE                                 .669
        COST OF REINFORCEMENT                           .602
        COST OF JOINTS                                  .472
        COST OF TIE BARS                                .027

     TOTAL INITIAL CONSTRUCTION COST                   5.466
     TOTAL OVERLAY CONSTRUCTION COST                    .411
     TOTAL I.D. COST DURING OV. CONSTRUCTION            .253
     TOTAL MAINTENANCE COST                             .363
     TOTAL SEAL COAT COST AFTER OV. CONSTRUCTION        .075
     SALVAGE RETURNS                                   -.788

    TOTAL OVERALL COST                                 5.779

DESIGN ANALYSIS
   TOTAL 162 INITIAL DESIGNS WERE EXAMINED, OUT OF WHICH,
        108 DESIGNS WERE REJECTED DUE TO USER RESTRAINTS
         54 REMAINING INITIAL DESIGNS PRODUCED  404 OVERLAY STRATEGIES
```

```
RIGID  PAVEMENT  SYSTEM  T2  RAMESH KHER          MAY  1971
PROB  101      EXAMPLE PROBLEM WITH VARIABLES AT ENGINEERING AVERAGES

     MOST ECONOMICAL CRC PAVEMENT DESIGN WITH  CC OVERLAY,

INITIAL CONSTRUCTION,  LIFE IS  8.640 YEARS

   MATERIALS                                          DESCRIPTION
                                                      MATERIAL    MATERIAL
                                                      NUMBER      NAME

   CONCRETE        7.50 INCHES                           1
   SUBBASE         6.00 INCHES                           2
   LONG. REINF.    BAR NO.     3      4                  2          A-432
                   SPACING    3.7    6.5
   TRAN. REINF.    BAR NO.     3      4      5           2        A-15 INT
                   SPACING   12.6   22.4   35.1
   TIE BARS       BAR NUMBER   3      4      5           2        A-15 INT
                  SPACING     12.6   22.4   35.1

                TRANSVERSE JOINT SPACING      0 FEET
                LONGITUDINAL JOINT SPACING    12 FEET


SUBSEQUENT CONSTRUCTION
   1  OVERLAY WITH  6.00 INCHES OF    CC AFTER  8.640 YEARS

     TOTAL OVERLAY THICKNESS   6.00 INCHES     TOTAL LIFE  22.875 YEARS


COST ANALYSIS   DOLLARS PER SQUARE YARD
     INITIAL CONSTRUCTION
        COST OF SUBGRADE PREPARATION                    .192
        COST OF CONCRETE                               2.670
        COST OF SUBBASE                                 .669
        COST OF REINFORCEMENT                          1.360
        COST OF JOINTS                                  .112
        COST OF TIE BARS                                .020

     TOTAL INITIAL CONSTRUCTION COST                   5.023
     TOTAL OVERLAY CONSTRUCTION COST                   1.424
     TOTAL I.D. COST DURING OV. CONSTRUCTION            .206
     TOTAL MAINTENANCE COST                             .360
     SALVAGE RETURNS                                   -.914

    TOTAL OVERALL COST                                 6.093

DESIGN ANALYSIS
   TOTAL 162 INITIAL DESIGNS WERE EXAMINED, OUT OF WHICH,
        62 DESIGNS WERE REJECTED DUE TO USER RESTRAINTS
       100 REMAINING INITIAL DESIGNS PRODUCED  130 OVERLAY STRATEGIES
```

```
RIGID  PAVEMENT  SYSTEM  T2  RAMESH KHER          MAY  1971
PROB  101      EXAMPLE PROBLEM WITH VARIABLES AT ENGINEERING AVERAGES

                SUMMARY OF DESIGNS IN INCREASING ORDER OF TOTAL COST

DESIGN NUMBER                    1       2       3       4       5       6
**********************************************************************
PAVEMENT TYPE                  CRC     CRC     CRC     CRC     JCP     CRC
OVERLAY  TYPE                   AC      AC      AC      AC      AC      AC
REINFORCEMENT TYPE            MESH    BARS    BARS    BARS    MESH    BARS

CONCRETE TYPE                    1       1       1       1       1       1
SUBBASE  TYPE                    1       2       2       2       2       2
**********************************************************************

SLAB THICKNESS                9.00    7.50    7.50    7.50   10.00    7.50
SUBBASE THICKNESS             6.00    7.00    8.00    9.00    6.00    6.00

OVERLAY THICKNESS 1           1.50    2.50    2.00    1.50    1.50    3.50

INITIAL LIFE                  9.84    9.04    9.43    9.82   10.05    8.64

OVERLAY PERF. LIFE 1         20.91   20.20   20.48   20.73   21.08   20.56

TOTAL PERFORMANCE LIFE       20.91   20.20   20.48   20.73   21.08   20.56


SPACING TRANS. JOINTS          .00     .00     .00     .00   35.00     .00
SPACING LONG. JOINTS         12.00   12.00   12.00   12.00   12.00   12.00
**********************************************************************

COST OF SUBG. PREPARATION      .192    .192    .192    .192    .192    .192
COST OF CONCRETE              3.170   2.670   2.670   2.670   3.504   2.670
COST OF SUBBASE                .293    .766    .863    .960    .669    .669
COST OF REINFORCEMENT         1.433   1.360   1.360   1.360    .602   1.360
COST OF JOINTS                 .112    .112    .112    .112    .472    .112
COST OF TIE BARS               .012    .020    .020    .020    .027    .020

INITIAL CONST. COST           5.213   5.120   5.218   5.315   5.466   5.023
OVERLAY CONST. COST            .415    .646    .528    .415    .411    .877
TRAFFIC DELAY COST             .205    .108    .138    .200    .253    .150
MAINTENANCE COST               .361    .355    .357    .360    .363    .360
SALVAGE RETURNS               -.669   -.705   -.685   -.664   -.788   -.757
SEAL COAT COST                 .135    .140    .138    .135    .075    .143

**********************************************************************
TOTAL COST PER SQ YARD        5.660   5.664   5.694   5.761   5.779   5.797
**********************************************************************
```

```
RIGID  PAVEMENT  SYSTEM  T2  RAMESH KHER          MAY  1971
PROB  101      EXAMPLE PROBLEM WITH VARIABLES AT ENGINEERING AVERAGES

                                REINFORCEMENT DESIGN
DESIGN
NUMBER   REINFORCEMENT DESCRIPTION                              MATERIAL  MATERIAL
                                                                NUMBER    NAME

  1   LONG.REINF.-MESH SPACING     4.0    5.0    6.0            1      ASTM,A-496
                   MESH DIAMETER   .43    .48    .52
      TRAN.REINF.-MESH SPACING    12.0   14.0   14.0            1      ASTM,A-496
                   MESH DIAMETER   .21    .23    .25
      TIE BARS       BAR NUMBER     3      4                   1      A-615,GR40
                     SPACING     21.0   37.4

  2   LONG. REINF.     BAR NO.      3      4                   2        A-432
                       SPACING     3.7    6.5
      TRAN. REINF.     BAR NO.      3      4      5            2      A-15 INT
                       SPACING    12.6   22.4   35.1
      TIE BARS       BAR NUMBER     3      4      5           2      A-15 INT
                     SPACING      12.6   22.4   35.1

  3   LONG. REINF.     BAR NO.      3      4                   2        A-432
                       SPACING     3.7    6.5
      TRAN. REINF.     BAR NO.      3      4      5           2      A-15 INT
                       SPACING    12.6   22.4   35.1
      TIE BARS       BAR NUMBER     3      4      5           2      A-15 INT
                     SPACING      12.6   22.4   35.1

  4   LONG. REINF.     BAR NO.      3      4                   2        A-432
                       SPACING     3.7    6.5
      TRAN. REINF.     BAR NO.      3      4      5           2      A-15 INT
                       SPACING    12.6   22.4   35.1
      TIE BARS       BAR NUMBER     3      4      5           2      A-15 INT
                     SPACING      12.6   22.4   35.1

  5   LONG.REINF.-MESH SPACING     4.0    5.0    6.0            1      ASTM,A-496
                   MESH DIAMETER   .22    .25    .27
      TRAN.REINF.-MESH SPACING    12.0   14.0   16.0            1      ASTM,A-496
                   MESH DIAMETER   .32    .34    .37
      TIE BARS       BAR NUMBER     3      4                   1      A-615,GR40
                     SPACING      9.5   16.8

  6   LONG. REINF.     BAR NO.      3      4                   2        A-432
                       SPACING     3.7    6.5
      TRAN. REINF.     BAR NO.      3      4      5           2      A-15 INT
                       SPACING    12.6   22.4   35.1
      TIE BARS       BAR NUMBER     3      4      5           2      A-15 INT
                     SPACING      12.6   22.4   35.1


DESIGN                    SEAL COAT SCHEDULE
NUMBER
   1     14.84  19.84
   2     14.04  19.04
   3     14.43  19.43
   4     14.82  19.82
   5     15.05
   6     13.64  18.64
```

Figure 6. Cost of optimal design versus variable level.

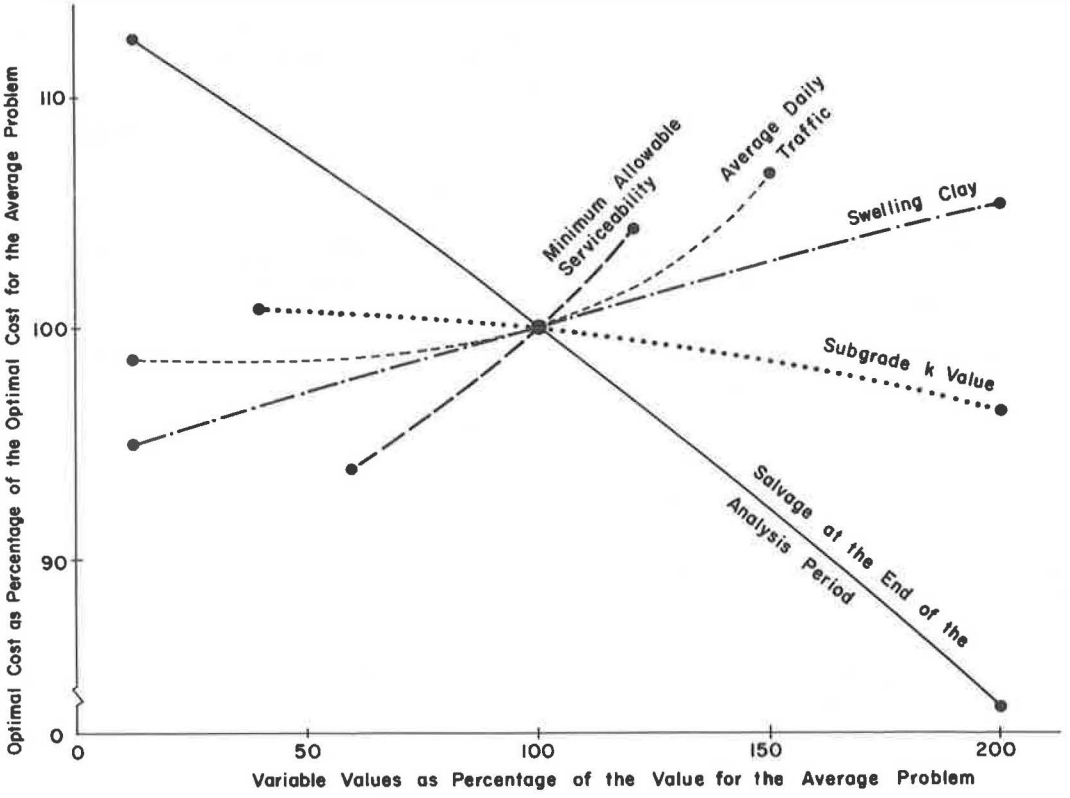

4. The design procedure has wide applicability for an administrator in long-range budgeting and manpower planning.
5. Sensitivity analysis and implementation of this system will provide a framework for outlining areas of future research.
6. The design procedure, which is a computer program, will be relatively easy to modify as the results of future research become available.

ACKNOWLEDGMENTS

This investigation was conducted at the Center for Highway Research, University of Texas at Austin. The authors wish to thank the sponsors, the Texas Highway Department and the Federal Highway Administration. Special thanks are due the co-investigators, Frank Scrivner and James L. Brown. The opinions, findings, and conclusions expressed in this publication are those of the authors and not necessarily those of the Federal Highway Administration.

REFERENCES

1. Kher, R. K., Hudson, W. R., and McCullough, B. F. Comprehensive Systems Analysis for Rigid Pavements. Highway Research Record 362, 1971, pp. 9-20.
2. Hudson, W. R., Finn, F. N., McCullough, B. F., Nair, K., and Vallerga, B. A. Systems Approach to Pavement Design—Implementation Phase. Materials Research and Development, Inc., Interim Rept., NCHRP Project 1-10A, March 1968.
3. Hutchinson, B. G., and Haas, R. C. G. A Systems Analysis of the Highway Pavement Design Process. Highway Research Record 239, 1968, pp. 1-24.
4. Hudson, W. R., McCullough, B. F., Scrivner, F. H., and Brown, J. L. A Systems Approach Applied to Pavement Design and Research. Published jointly by

Texas Highway Dept.; Texas Transportation Institute, Texas A&M Univ.; and Center for Highway Research, Univ. of Texas at Austin, Res. Rept. 123-1, March 1970.

5. Haas, R. C. G., and Hutchinson, B. G. A Management System for Highway Pavements. Prepared for presentation to the Australian Road Research Board, Sept. 1970.
6. Lemer, A. C., and Moavenzadah, F. The Analysis of Highway Pavement Systems. M.I.T., Professional Paper P69-12, Sept. 1969.
7. Pister, K. S. Some Remarks on Research for Structural Design of Asphalt Concrete Pavement Systems. HRB Spec. Rept. 126, 1971, pp. 63-76.
8. Hudson, W. R., Kher, R. K., and McCullough, B. F. Automation in Pavement Design and Management Systems. HRB Spec. Rept. 128, 1972, pp. 40-53.
9. Hudson, W. R., and McCullough, B. F. An Extension of Rigid Pavement Design Methods. Highway Research Record 60, 1964, pp. 1-14.
10. Westergaard, H. M. Stresses in Concrete Pavements Computed by Theoretical Analysis. Public Roads, Vol. 7, No. 2, 1926.
11. Warren, H., and Duckmann, W. L. Numerical Computation of Stresses and Strains on a Multiple-Layered Asphalt Pavement System. California Research Corp., Richmond, Sept. 24, 1963.
12. Panak, J. J., and Matlock, H. A Discrete-Element Method of Analysis for Orthogonal Slab and Grid Bridge Floor Systems. Center for Highway Research, Univ. of Texas at Austin, Res. Rept. 56-25, Aug. 1971.
13. Airfield Pavement Design Engineering and Design—Rigid Pavements. Air Force Manual 88-6.
14. Engineering and Design—Rigid Airfield Pavements. Corps of Engineers' Manual EM 1110-45-303, 1958.
15. Kelley, E. F. Applications of the Results of Research to the Structural Design of Concrete Pavements. Public Roads, Vol. 2, No. 5 and No. 6, 1939.
16. McCullough, B. F., et al. Evaluation of AASHO Interim Guides for Design of Pavement Structures. Materials Research and Development, Inc., draft of final report of NCHRP Project 1-11, 1968.
17. McCullough, B. F. Design Manual for Continuously Reinforced Concrete Pavement. United States Steel Corp., Pittsburgh, 1968.
18. Scrivner, F. H., Moore, W. M., McFarland, W. F., and Carey, G. R. A Systems Approach to the Flexible Pavement Design Problem. Texas Transportation Institute, Texas A&M Univ., Res. Rept. 32-11, 1968.
19. Bertram D. Tallamy Associates. Interstate Highway Maintenance Requirements and Unit Maintenance Expenditure Index. NCHRP Rept. 42, 1967, 144 pp.
20. Kher, R. K., Hudson, W. R., and McCullough, B. F. A Systems Analysis of Rigid Pavement Design. Published jointly by Texas Highway Dept.; Texas Transportation Institute, Texas A&M Univ.; and Center for Highway Research, Univ. of Texas at Austin, Res. Rept. 123-5, Jan. 1971.

RELIABILITY CONCEPTS APPLIED TO THE TEXAS FLEXIBLE PAVEMENT SYSTEM

Michael I. Darter and B. Frank McCullough, Center of Highway Research, University of Texas at Austin; and
James L. Brown, Texas Highway Department

The flexible pavement system (FPS) is a working pavement design system in trial use by the Texas Highway Department. FPS utilizes a systems approach to the pavement design process by considering all phases of design, construction, and in-service performance to arrive at an acceptable pavement design. The working system is computerized and uses more than 50 inputs. The output is an array of possible pavement design strategies based on total overall cost. Trial implementation of FPS in the Texas Highway Department has shown a definite need to consider the stochastic nature of many of the variables used in pavement design. This paper describes how the uncertainty of estimation of variables like traffic or the highly variable deflections along a highway pavement can be considered in a comprehensive design procedure to make it possible to determine design reliability. Reliability is defined as the probability that the pavement will have an adequate serviceability level for a specified design performance period. Considered in this reliability analysis are variability associated within a project such as material properties, thicknesses, and strengths; variability between assumed design values and those actually constructed or under which the pavement will be subjected during its design life (traffic and environment); and variability due to lack of fit of the empirical equations used in the structural subsystem. Significant sources of error were found associated with along-the-roadway variation as measured by deflection and with the lack-of-fit error of the structural design equations. Significant error was found to be associated with the variations in initial serviceability index and estimated traffic loadings.

•PAVEMENT design engineers have been plagued in the past by the large random variability of almost every measurable parameter associated with pavement design, construction, and performance. This variability has made it difficult to control material quality and has made it extremely difficult to formulate a rational pavement design procedure. Most design procedures have, therefore, been empirical in nature (i.e., equations derived from regression and/or experience) (13).

This paper deals with the application of reliability concepts to the flexible pavement system (FPS). Reliability theory takes into account the stochastic (random) nature of many variables such as traffic loadings, deflections, and temperature. Reliability of a pavement design is the probability that the pavement will have an adequate serviceability level for the design performance period. The pavement designer is provided in this paper with the necessary theory and with a working method of applying reliability concepts to the FPS as used in Texas (1). FPS is the result of 7 years of applying the AASHO Road Test results to Texas conditions. This study (1), which terminated in 1968, resulted in the computerized FPS, which has more than 50 physical inputs. The output consists of an array of recommended pavement design strategies based on the net present worth of the lowest total cost.

Sponsored by Committee on Flexible Pavement Design.

The current method of design using FPS is deterministic in nature (i.e., utilizes exact inputs and outputs). The truly variable nature of each of the factors used in FPS, such as strength coefficients, traffic loadings, thickness of pavement layers, and temperature parameter, are not considered, and average values are input. Trial implementation of FPS by the Texas Highway Department has shown a definite need to consider the stochastic nature of the design inputs and other variabilities associated with the pavement design process. The results obtained show the need to take into account the stochastic nature of the variables associated with the FPS pavement design procedure. A significant increase in pavement thickness is required for reasonable reliability levels greater than the 50 percent level that is now used.

Stochastic concepts are discussed, and the theory of reliability of pavement design is developed. The FPS design procedure is then discussed, and an error analysis associated with the design inputs and design equations (lack-of-fit error) is given. The theory is then illustrated by a pavement design example using FPS.

STOCHASTIC CONCEPTS

General

Almost every measurable variable associated with the pavement design process tends to vary in a stochastic (random) manner. For example, the deflection of a highway pavement from one end of a project to the other usually varies considerably along the roadway rather than holding at a constant magnitude. The result of a series of values is a population of values: $x_1, x_2, x_3, x_4, \ldots, x_n$.

When these values are plotted on a graph as magnitude versus frequency, a distribution is found that may be approximated by a normal, log normal, gamma, and so forth. Many highway design parameters have been shown to be approximately normal or log normal. Thus, these variables may be described by a mean value μ_x and standard deviation σ_x as follows (2): (μ_x, σ_x).

Design variables in FPS are related by mathematical equations. Because each variable is a random variable, the design process involves functional relations among random variables. For example, the number of load applications a pavement can carry is a function in FPS of the following:

$$N = f(Q, \alpha, S)$$

where

- Q = function of serviceability loss,
- α = temperature parameter, and
- S = surface curvature index of pavement.

Q, α, and S are all random variables. Therefore, N, the number of load applications a highway pavement may carry to failure, is a random variable. The theory developed in this paper makes it possible to consider the variable nature of these parameters.

The importance of applying a probabilistic approach to the design of pavement structures was pointed out elsewhere (3, 12). This topic was listed as one of the ten most important areas of needed research.

There are essentially three types of variations associated with the pavement design process and construction:

1. Variability associated within a project such as in the materials used in construction, which in turn cause variation in stiffness and strengths of the pavement components including the foundation;
2. Variability between the assumed design values and those actually constructed or under which the pavement will be subjected during its design life, such as traffic loadings and environment; and
3. Variability due to lack of fit of the empirical equations used in the design procedures.

Reliability

Reliability is a measure of the adequacy of a design and is defined as follows:

$$\text{Reliability } (R) = 1 - \text{failure probability}$$

Reliability in terms of pavements is the probability that the pavement will have an adequate serviceability level for the design performance period. The reliability of a pavement structure is determined from the basic concept that a no-failure probability exists when the number of load repetitions that a given pavement section can withstand to terminal serviceability, N, is not exceeded by the number of load applications applied, n.

Failure as used in this paper refers to a condition of the pavement when the serviceability index drops below its terminal level. When a pavement reaches the terminal serviceability index, repair maintenance or replacement is needed.

The number of load applications a pavement can withstand, N, is a random variable because of the random nature of the factors on which it depends. Its distribution may be visualized by considering a long highway pavement divided into many short sections and by observing the distribution of the number of load repetitions of a given wheel load that the sections can withstand before failure. The distribution of N to failure is assumed log normal. That is, the logarithm of all N's is approximately normally distributed. This result was verified in part from the results of the AASHO Road Test (4) and laboratory fatigue tests (5) on asphalt concrete.

The number of load applications that will travel over a given pavement is of course an exact number. However, this number is not known until after the service life of the pavement has passed. The n must be estimated for design purposes, and herein lies the uncertainty of n. Some pavements have shown premature failure because of unforeseen traffic loadings. On the other hand, some pavements have lasted longer than expected because of an overestimation of the traffic loadings. It is assumed that the ability to predict the number of traffic load applications (equivalent number of 18-kip single-axle loads) is log normally distributed.

These two random variables may be defined therefore as follows:

N ≡ number of load applications that a section of pavement can withstand before failure, and
n ≡ number of load applications that are applied to a section of pavement.

As has been previously assumed, N and n are log normally distributed.

Reliability is the probability that N exceeds n, or

$$P(\log N - \log n > 0) = R$$

$$P(D > 0) = R$$

where

$$D = \log N - \log n$$

f(D) is defined as the difference density function of log N and log n. Because log N and log n are normally distributed, D is normally distributed, as is shown in Figure 1.

$$\overline{D} = \overline{\log N} - \overline{\log n}$$

$$S_D = \sqrt{S_{\log N}^2 + S_{\log n}^2}$$

where S_D = estimated standard deviation of D. As shown in Figure 1, reliability is given by the area to the right of 0.

$$R = P(0 < \log N - \log n < \infty) = P(0 < D < \infty) \qquad (1)$$

The transformation that relates D and the standardized normal variable Z is

$$Z = (D - \overline{D})/s_D \tag{2}$$

When D = 0, $Z = -\overline{D}/s_D$; and when $D = \infty$, $Z = \infty$. Therefore, the expression for reliability may be rewritten as

$$R = P(-\overline{D}/s_D < Z < \infty) \tag{3}$$

The reliability may now be determined very easily by means of the normal distribution table. The area under the normal distribution curve between the limits of

$$Z = -\left[(\overline{\log N} - \overline{\log n})/\sqrt{s_{\log N}^2 + s_{\log n}^2}\right] \tag{4}$$

and $Z = \infty$ gives the reliability of design. Equation 4 is called a "coupling" equation because it probabilistically relates the applied and allowable traffic loadings (2).

An example calculation of reliability will be given. Assume $(\overline{\log N}, s_{\log N}) = (7.000, 0.500)$, and $(\overline{\log n}, s_{\log n}) = (6.477, 0.200)$.

$$Z = -\left[(7.000 - 6.477)/\sqrt{(0.5)^2 + (0.2)^2}\right] = -0.968$$

From normal distribution tables the area from -0.968 to ∞ is 0.83. Therefore, the reliability, R, is 83 percent.

APPLICATION TO FLEXIBLE PAVEMENT SYSTEM

The entire FPS procedure is computerized to provide an output of feasible pavement designs, sorted by increasing total cost. The primary purpose of FPS is to provide the designer with a means for investigating a large variety of pavement design options in a systematic and efficient manner (11).

The mathematical models developed for FPS are based on the established objectives of providing from available materials a pavement capable of being maintained above a specific level of serviceability over a specified period of time, at a minimum overall cost (1).

The inputs consist of a large number of factors that make it possible to use as many variables as necessary. The inputs include program controls, unit costs, material properties, environmental factors, serviceability index values, seal coat schedules, constraints, traffic demand inputs, traffic controls, and miscellaneous inputs.

The mathematical models can be broken down into four types: physical, economical, optimization, and interaction, as explained elsewhere (6). Only the physical models will be considered directly for implementation of stochastic input. However, the costs of materials cannot be exactly estimated; therefore, they are random variables and should eventually be considered as such in the future. The physical models break down into deflection, performance, and traffic models.

There are basically three types of variations that will be considered in this reliability analysis. These were listed in a previous section and will now be analyzed in detail.

Lack-of-Fit Variability

The deflection equation predicts the surface curvature index measured by the Dynaflect if pavement layer thicknesses, strength coefficients, and the subgrade strength coefficient are known.

> The equation was derived in two basic steps: (1) a mathematical model of the deflection phenomenon, containing certain undetermined coefficients was developed, and (2) the coefficients were evaluated by fitting the model to Dynaflect deflection data gathered on a set of special test sections constructed in accordance with statistical principles of experiment design (7).

The deflection equation is explained in detail elsewhere (7).

If the actual measured S is plotted versus the predicted S from the deflection equation, a scatter of data is found indicating some error associated with the deflection equation.

The scatter about the line of equality is a result of the (a) lack of fit of the equation and (b) some replication or pure error due to inherent differences among strength coefficients of sections with the same materials. Each data point is an average of five measurements within a test section. This averaging reduces the testing or within-section variation so that the remaining variation consists mainly of lack-of-fit and pure error.

Because there were no replicate sections, an estimate of pure error cannot be made. Therefore, all scatter about the line of equality will be assumed to be lack-of-fit error. The total residual is found by the following method:

$$\text{Sums of squares (total residual)} = \sum_{i=1}^{i=26} (S_i - \hat{S}_i)^2$$

where S_i = measured S, $\hat{S}_i$ = predicted S from deflection equation, SS(total residual) = 0.0360, and mean square (total residual) = 0.0360/26 = 0.001385. The coefficient of variation for predicting S is

$$CV_s = s_s/\overline{S} = 0.0372/0.1415 = 0.26$$

The performance equation predicts behavior of the pavement based on the current serviceability index concept developed at the AASHO Road Test. The loss in serviceability of a pavement depends on deflection of the pavement structure, the number of load applications, temperature, and foundation movements due to swelling clays. The effect of swelling clay will not be considered in this analysis. The performance equation developed for FPS is as follows:

$$N = Q\alpha 10^6/KS^2 \qquad (5)$$

where

- N = number of equivalent 18-kip single-axle load applications;
- Q = $\sqrt{5 - P_2} - \sqrt{5 - P_1}$, function of serviceability loss;
- P_2 = terminal serviceability;
- P_1 = initial serviceability index;
- K = regression coefficient = 53.6 (or 0.134 if the "partial deflection" produced by any given axle load is used for S, and the number of applications of that load is used for N);
- S = SCI of pavement structure, as measured by the Dynaflect in inches $\times 10^{-3}$; and
- α = temperature statistic depending on maximum and minimum daily temperature for a given locality as described elsewhere (1).

This equation was derived by using data from the AASHO Road Test as explained elsewhere (8). By using the logarithm of each side, we derive the following:

$$\log_{10}N = (\log Q) + (\log \alpha) - (\log K) - (2 \log S) + (6.0) \qquad (6)$$

There is a certain error associated with this prediction equation. The error may be determined by direct comparison of the actual number of load applications an AASHO test pavement carried until it dropped out of service to the number of load applications predicted by Eq. 6. There were ten performance periods used to develop data for Eqs. 5 and 6. These periods were characterized by constant α and constant S. Therefore, the N predicted for a given test section was calculated and summed for each period that the section was in service.

For example, test section 315 lasted six performance periods, and the predicted N was calculated as follows:

$\hat{N}_{315} = \hat{N}_{period\ 1} + \hat{N}_{period\ 2} + \ldots \hat{N}_{period\ 6}$;
$\hat{N}_{315}$ = 268,600 load applications; and
N_{315} = 247,700 actual load applications.

The N versus $\hat{N}$ results from 83 test sections are shown in Figure 2. The data show about equal scatter bands from 3,500 to 550,000 load applications. The data also show approximately log normal distribution of points within groups. The sections that went out of test at the same time may be considered replicates because the N actual is equal for all of them. Therefore, a replicate or pure error may be calculated.

The error (due to lack of fit) of Eq. 6 was calculated as follows:

Sums of squares (total residual) = SS (lack of fit) + SS (replicate or pure error)

$$SS\ (\text{total residual}) = \sum_{i=1}^{83} \left(\log N_i - \log \hat{N}_i\right)^2 = 6.6245$$

$$SS\ (pe) = \sum_{1}^{g} \sum_{1}^{r} \left(\log \hat{N}_i - \log \bar{\hat{N}}_i\right)^2 = 5.1278$$

where

r = number of data points within a replicate group (example: period 1 with N = 3,500, r = 9), and
g = 8 (number of groups with replicate data points).

The following tabulation gives an AOV breakdown of expected mean squares:

Source of Variation	df	SS	MS	Expected MS
Total residual	83	6.6245	—	—
Lack of fit	10	1.4967	0.1497	$\sigma_{pe}^2 + \sigma_{lof}^2$
Pure	73	5.1278	0.0702	σ_{pe}^2

Therefore, the component of variation due to lack of fit only is estimated to be as follows:

$$s_{lof}^2 = 0.1497 - 0.0702 = 0.0795$$

The mean absolute residual ($|\log N - \log \hat{N}|$) for the 83 sections was 0.21. This value is less than the mean absolute residual obtained from the equations derived in the AASHO Road Test report (4) of 0.23.

The error to be included in the lack of fit of Eq. 6 is $s^2 = 0.0795$. This variance (due to lack of fit) occurs mainly because the performance model does not contain all necessary terms and/or is not the correct combination of terms. It is assumed that this error does not include any variance due to P_1, P_2, α, or S. These components of variance, which existed at the AASHO Road Test, are contained in the pure error variance. The additional variance that these factors create in a new design project will be added in separately. The magnitude of each will be derived from in-service projects. The total variation associated with estimating N from Eq. 6 depends on the variations of S, α, and Q and the lack-of-fit variance s_{lof}^2. Statistically, the variances add up as follows (assuming independence):

$$s_{\log N}^2 = s_{\log Q}^2 + s_{\log \alpha}^2 + s_{\log s}^2 + s_{lof}^2 \qquad (7)$$

Estimates of the variations of Q, α, and S are derived in the following sections based on in-service projects.

Figure 1. Difference distribution: D = log N - log n.

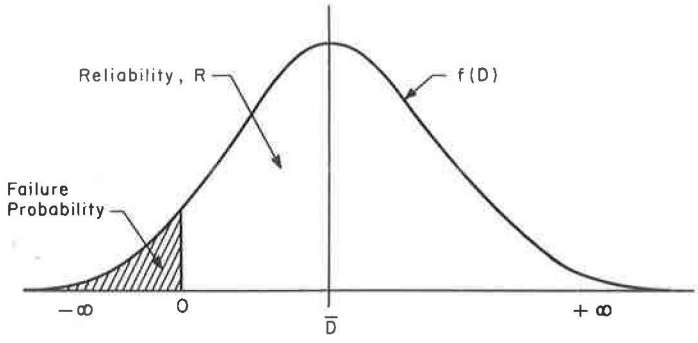

Figure 2. Observed N versus predicted $\hat{N}$ (each point represents a test section).

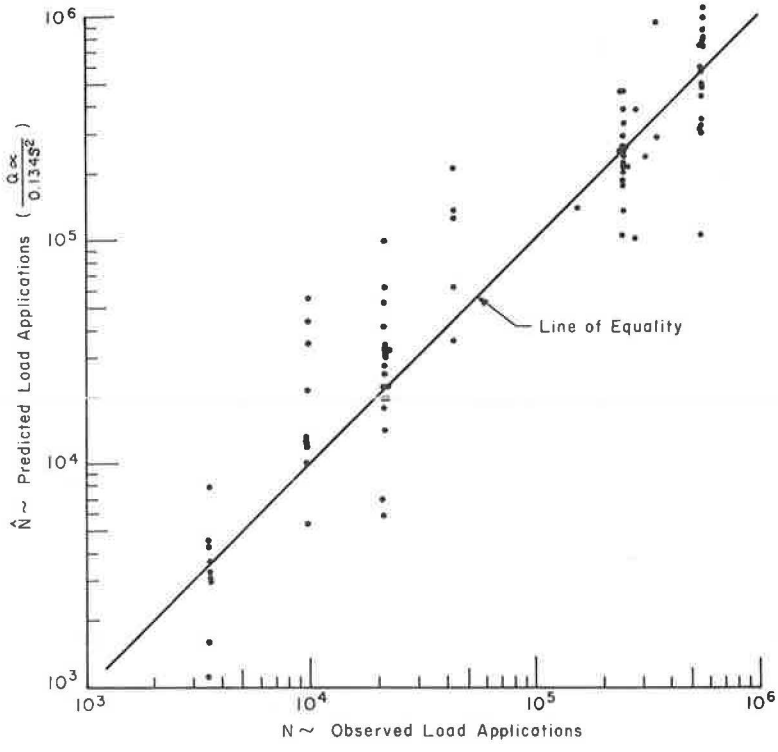

Within-Project Variability

The variability that occurs within a project is associated with such factors as the strength coefficients and thicknesses of the various pavement layers. This type of variability has been lumped into a single factor, the surface curvature index of the pavement. It is assumed that the variability in the strength coefficients and thicknesses will be reflected in the S along the pavement. Future improvements of this method would include the specific variations of the strength coefficients and thicknesses.

Considerable variability in S is found along most highway in-service pavements. This variation is due to variations in subgrade strength, thickness of pavement layers, and strength of pavement layers. To estimate this variability, we measured the S on 119 in-service projects in Texas, which were all more than 0.5 mile in length. Measurements were usually taken 0.1 mile apart on each project in the outer wheelpath. The mean $\overline{S}$ and standard deviation s_s for each project was calculated.

A plot of $\overline{S}$ versus s_s shows considerable scatter in the data, but the overall trend shows that the greater is the mean $\overline{S}$, the greater is the s_s. This nonhomogeneity of variance is common for many measurable parameters.

A straight line was fitted with zero intercept, and the slope was found to be 0.34. This value will be used as the overall coefficient of variation for S along an in-service pavement. This variation must be considered in computing the overall error of the performance equation. The total variation in S, which must be considered for use in the performance equation, is the sum of the deflection equation lack-of-fit variance and the along-the-roadway variance.

$$s_s^2 = (0.26)^2 \overline{S}^2 + (0.34)^2 \overline{S}^2 = 0.1832 \overline{S}^2 \tag{8}$$

The overall coefficient of variation of S is therefore 0.428. The variance of the 2 log S must be derived for use in the overall summation given in Eq. 7. This may be accomplished by using statistical theory. If g is a function of x [$g = f(x)$], then the variance of g is approximated by (2)

$$s_g^2 \approx \sum_{j=1}^{j} \left(\frac{\partial g}{\partial x_j}\right)^2 s_{x_j}^2 \tag{9}$$

Therefore, the variance of 2 log S is

$$s_{2 \log S}^2 \approx \left[\partial(2 \log S)/\partial S\right]^2 s_s^2 = 0.755\, s_s^2/\overline{S}^2 = 0.755(CV_s)^2$$

Design and Actual Variability

Pavement design usually requires estimates of such factors as traffic, initial serviceability index, and climate several years in advance of construction. There may be considerable difference between the as-built or actual values and those estimated during design. The serviceability loss function Q, temperature constant α, and traffic loadings are three design factors used in FPS, which fall into this type of variability category.

Serviceability Loss Function—All newly constructed pavements are not constructed with the same smoothness; consequently, there is variation in their initial serviceability index. The distribution of initial serviceability indexes is assumed normal. The following estimates of the standard error associated with initial serviceability index have been found:

Source	$\overline{P}_i$	s_p	n
AASHO Road Test (4)	4.2	0.39	24
Utah State Department of Highways (10)	3.9	0.35	82
Texas Highway Department (8)	4.3	0.40	16

Pavements are also overlayed or reconstructed at variable terminal serviceability indexes, which depend mostly on available funding. No estimate of this variability is available.

The best estimate of variance available is to assume that the coefficient of variation is about 10 percent for initial and terminal serviceability indexes.

For Texas, $CV_p = (0.40 \times 100)/4.3 \approx 10$ percent and also for AASHO and Utah estimates.

The $s^2_{\log Q}$ must now be derived:

$$g = \log\left(\sqrt{5 - P_2} - \sqrt{5 - P_1}\right)$$

$$s_g^2 \approx \left\{\left[\partial \log\left(\sqrt{5 - P_2} - \sqrt{5 - P_1}\right)/\partial P_2\right]\right\}^2 s_{P_2}^2 + \left\{\left[\partial \log\left(\sqrt{5 - P_2} - \sqrt{5 - P_1}\right)/\partial P_1\right]^2 s_{P_1}^2\right\}$$

$$s^2_{\log Q} \approx (4.71 \times 10^{-2})/\overline{Q}^2 \{[(s^2_{P_2}/(5 - \overline{P}_2)] + [s^2_{P_1}/(5 - \overline{P}_1)]\} \quad (10)$$

Temperature Constant—An average temperature constant α has been estimated for each highway department district headquarters in Texas, as described elsewhere (11). The range in α over the state is from 9 to 38. Because the temperature constant was determined for each district headquarters over a 10-year period, it may be a fairly good estimate with regard to long time periods at a district headquarters, but it varies somewhat around a given district. An estimate of the maximum amount of variability may be found by taking the difference in temperature constant α between each district headquarters and those surrounding the district and by calculating the variance as follows:

$$s_\alpha^2 = \left(\sum_{i=1}^{q}\sum_{j=1}^{b} D_{ij}^2\right)\Big/(h - 1) \quad (11)$$

where

D_{ij} = difference between the α for district i and an abutting district j,
q = 25 (number of districts in Texas),
b = number of districts abutting a given district i,
h = total number of abutting districts, and
s_α^2 = 18.

The $s^2_{\log \alpha}$ is derived as follows:

$$g = \log \alpha$$

$$s^2_{\log \alpha} \approx (\partial g/\partial \alpha)^2 s_\alpha^2 = 0.189 s_\alpha^2/\overline{\alpha}^2 \quad (12)$$

Traffic Estimate—The FPS requires an estimate of the number of equivalent 18,000-lb axle loads that the pavement will carry throughout its design analysis period. There are many uncertainties associated with predicting the total 18-kip axle load applications during the design analysis period. Basically, these uncertainties may be grouped into three types:

1. Estimation of total number of axles that will pass over the pavement during the period,
2. Estimation of axle weight distribution, and
3. Method of conversion of mixed traffic to 18-kip equivalent axle loads.

The total number of axles for the entire design period for a highway is determined by the Texas Highway Department as follows (for trucks only):

$$a = (ADT_d)(A)(L)(T) \tag{13}$$

where

a = total number of axles for design period;
ADT_d = design ADT, $(ADT_i + ADT_f)/2$;
ADT_i = initial ADT at beginning of design period;
ADT_f = final ADT at end of design period;
A = average number of axles per truck;
T = percent trucks of ADT; and
L = number of days in design period.

The total equivalent 18-kip single-axle loads may be calculated as follows:

$$n = \left(\sum_{i=1}^{i=k} P_i EF_i \right) a \tag{14}$$

where

P_i = percentage of axles in ith load group;
EF_i = AASHO load equivalence factor for given axle group pavement structural number, terminal serviceability, etc.; and
k = number of load groups.

By taking the logarithm of each side of Eq. 14, we obtain the following equation:

$$\log n = \log \left(\sum_{i=1}^{k} P_i EF_i \right) + (\log ADT_d) + (\log A) + (\log L) + (\log T) \tag{15}$$

Each of the terms in Eq. 15 (with the exception of L, the number of days in the design analysis period) has some uncertainty or variability associated with it. The total variance associated with log n (due to the variance of the factors in Eq. 15) will be the sum of the variances of each term, assuming they are independent factors (2):

$$s^2_{\log n} = s^2_{\log (\Sigma P_i EF_i)} + (s^2_{\log ADT_d}) + (s^2_{\log A}) + (s^2_{\log T}) \tag{16}$$

The first two types of variations are contained in Eq. 16.

Also, there is a possible error that is the result of the overall method of calculating the total equivalent 18-kip axle loads (s^2_{method}). Therefore, the problem of determining the overall error associated with estimating the log n becomes one of determining the magnitude of each of the variance terms given in Eq. 16 and then summing them.

Approximate estimates of these variances have been made elsewhere (16). Only a brief outline of the results will be given here because of space limitations, but complete details will be published in a future report.

An estimate of the error in predicting an axle weight distribution for a given highway location in Texas was obtained from the work of Heathington and Tutt (15).

$$s^2_{\log (\Sigma P_i EF_i)} \approx 0.0179$$

They calculated the 20-year equivalent 18-kip axle applications at loadometer stations by using estimated axle load distributions and also the actual axle load distributions determined at the loadometer stations. Three different methods of grouping traffic were used. The average residual mean square of the difference in the logarithm of the predicted and actual was found to be 0.0179. This value probably underestim s

the actual error variance because a change in the distribution of axles with time has not been considered.

The variability associated with predicting the ADT_d depends on the ADT_1 and G. The equation for variance was derived by using the method of partial derivatives as given in Eq. 9.

$$s^2_{\log ADT_d} \approx 0.189/ADT_1^2 \{s^2_{ADT_1} + (ADT_1^2\, m^2\, s_G^2)/4[1 + (Gm/2)]^2\}$$

where

G = average growth rate = $(ADT_f - ADT_1)/ADT_1 m$, and
m = number of years in analysis period.

Heathington and Tutt (15) found a very good linear correlation between the number of trucks and number of axles passing a given point. An average value of 2.75 axles per truck was obtained with a small coefficient of variation of about 5 percent. The method of partial derivatives (Eq. 9) was used to obtain the approximate relation.

$$s^2_{\log A} \approx 0.189(\text{coefficient of variation of A})^2$$

The percentage of trucks is a difficult value to estimate because it must be valid throughout the design period. A coefficient of variation must be assumed.

$$s^2_{\log T} \approx 0.189(\text{coefficient of variation of T})^2$$

The following error results mainly from the application of incorrect equivalency factors and other errors such as load groupings that are too wide.

$$s^2_{(method)} \approx 0$$

The equivalency factor depends on such factors as the structural number of the pavement and terminal serviceability. By assuming a zero variance, the engineer will use the correct method of converting mixed traffic to equivalent axle loads. McCullough et al. (17) outline the correct procedures to use to minimize the possible errors.

Summary of Variances

The total variance associated with the number of load applications to failure was given in Eq. 7. An estimate of the variances of the design factors has been made. Equation 7 may now be rewritten as follows:

$$s^2_{\log N} \approx (4.71 \times 10^{-2})/\overline{Q}^2 \{[(s^2_{P_2})/(5 - \overline{P}_2)] + [s^2_{P_1}/(5 - P_1)]\}$$
$$+ (0.189 s^2_\alpha/\bar{\alpha}^2) + 0.755(CV_s) + 0.0795 \quad (17)$$

The total variance associated with the predicted number of load applications was given in Eq. 16.

$$s^2_{\log n} \approx 0.0179 + 0.189/ADT_1^2 \{s^2_{ADT_1} + (ADT_1^2\, m^2\, s_G^2)/4[1 + (Gm/2)]^2\}$$
$$+ 0.189\ (\text{CV of A})^2 + 0.189\ (\text{CV of T})^2 \quad (18)$$

These results will now be used in a pavement design example.

FPS DESIGN EXAMPLE

The application of reliability concepts to FPS can best be illustrated by an example problem. Figure 3 summarizes the inputs required for a typical design problem. Using these inputs, the FPS program outputs an array of designs shown in Figure 4.

Figure 3. Example problem.

THE CONSTRUCTION MATERIALS UNDER CONSIDERATION ARE

LAYER	MATERIALS CODE	NAME	COST PER CY	STR. COEFF.	MIN. DEPTH	MAX. DEPTH	SALVAGE PCT.
1	A	ASPHALTIC CONCRETE	10.00	.96	1.00	12.00	50.00
2	B	BASE MATERIAL	5.00	.47	6.00	6.00	75.00
		SUBGRADE	0.00	.23	0.00	0.00	0.00

NUMBER OF OUTPUT PAGES DESIRED(4 DESIGNS/PAGE)	3
TOTAL NUMBER OF INPUT MATERIALS,EXCLUDING SUBGRADE	2
LENGTH OF THE ANALYSIS PERIOD (YEARS)	20.0
WIDTH OF EACH LANE (FEET)	12.0
RELIABILITY OF PAVEMENT DESIGN	50 and 95%
DISTRICT TEMPERATURE CONSTANT	20.0
SERVICEABILITY INDEX OF THE INITIAL STRUCTURE	4.2
SERVICEABILITY INDEX P1 AFTER AN OVERLAY	4.2
MINIMUM SERVICEABILITY INDEX P2	3.0
SWELLING CLAY PARAMETERS -- P2 PRIME	4.20
B1	0.0000
ONE-DIRECTION ADT AT BEGINNING OF ANALYSIS PERIOD (VEHICLES/DAY)	4000
ONE-DIRECTION ADT AT END OF ANALYSIS PERIOD (VEHICLES/DAY)	8000
ONE-DIRECTION 20-YR ACCUMULATED NO. OF EQUIVALENT 18-KIP AXLES	3000000
PROPORTION OF ADT ARRIVING EACH HOUR OF CONSTRUCTION (PERCENT)	6.0
THE ROAD IS IN AN URBAN AREA.	
MINIMUM TIME TO FIRST OVERLAY (YEARS)	10.0
MINIMUM TIME BETWEEN OVERLAYS (YEARS)	5.0
TIME TO FIRST SEAL COAT AFTER INITIAL OR OVERLAY CONST.(YEARS)	2.0
TIME BETWEEN SEAL COATS (YEARS)	5.0
MAX FUNDS AVAILABLE PER SQ.YD. FOR INITIAL DESIGN (DOLLARS)	10.00
MAXIMUM ALLOWED THICKNESS OF INITIAL CONSTRUCTION (INCHES)	20.0
MINIMUM OVERLAY THICKNESS (INCHES)	1.0
ACCUMULATED MAXIMUM DEPTH OF ALL OVERLAYS (INCHES)	5.0
ASPHALTIC CONCRETE PRODUCTION RATE (TONS/HOUR)	75.0
ASPHALTIC CONCRETE COMPACTED DENSITY (TONS/C.Y.)	1.80
C.L. DISTANCE OVER WHICH TRAFFIC IS SLOWED IN THE O.D. (MILES)	1.00
C.L. DISTANCE OVER WHICH TRAFFIC IS SLOWED IN THE N.O.D. (MILES)	0.00
DETOUR DISTANCE AROUND THE OVERLAY ZONE (MILES)	0.00
OVERLAY CONSTRUCTION TIME (HOURS/DAY)	8.0
NUMBER OF OPEN LANES IN RESTRICTED ZONE IN O.D.	1
NUMBER OF OPEN LANES IN RESTRICTED ZONE IN N.O.D.	2
PROPORTION OF VEHICLES STOPPED BY ROAD EQUIPMENT IN O.D. (PERCENT)	0.00
PROPORTION OF VEHICLES STOPPED BY ROAD EQUIPMENT IN N.O.D. (PERCENT)	0.00
AVERAGE TIME STOPPED BY ROAD EQUIPMENT IN O.D. (HOURS)	0.000
AVERAGE TIME STOPPED BY ROAD EQUIPMENT IN N.O.D. (HOURS)	0.000
AVERAGE APPROACH SPEED TO THE OVERLAY ZONE (MPH)	70.0
AVERAGE SPEED THROUGH OVERLAY ZONE IN O.D. (MPH)	50.0
AVERAGE SPEED THROUGH OVERLAY ZONE IN N.O.D. (MPH)	70.0
TRAFFIC MODEL USED IN THE ANALYSIS	3
FIRST YEAR COST OF ROUTINE MAINTENANCE (DOLLARS/LANE MILE)	50.00
INCREMENTAL INCREASE IN MAINT. COST PER YEAR (DOLLARS/LANE MILE)	20.00
COST OF A SEAL COAT (DOLLARS/LANE MILE)	900.00
INTEREST RATE OR TIME VALUE OF MONEY (PERCENT)	5.0

Figure 4. Best design strategies in order of increasing total cost (reliability = 50 percent).

	1	2	3	4	5	6	7	8
MATERIAL ARRANGEMENT	AB	A	AB	AB	A	A	AB	AB
INIT. CONST. COST	2.222	2.153	2.292	2.361	2.222	2.292	2.569	2.431
OVERLAY CONST. COST	.325	.325	.295	.281	.295	.267	0.000	.255
USER COST	.007	.007	.006	.006	.006	.006	0.000	.006
SEAL COAT COST	.328	.328	.388	.337	.388	.334	.334	.331
ROUTINE MAINT. COST	.250	.250	.268	.280	.268	.294	.387	.309
SALVAGE VALUE	-.550	-.458	-.563	-.576	-.471	-.484	-.563	-.589
TOTAL COST*	2.582	2.604	2.689	2.688	2.707	2.708	2.727	2.743
NUMBER OF LAYERS	2	1	2	2	1	1	2	2
LAYER DEPTH (INCHES)								
D(1)	5.00	7.75	5.25	5.50	8.00	8.25	6.25	5.75
D(2)	6.00		6.00	6.00			6.00	6.00
NO.OF PERF.PERIODS	2	2	2	2	2	2	1	2
PERF. TIME (YEARS)								
T(1)	10.9	11.1	12.6	14.4	12.7	14.5	21.0	16.4
T(2)	25.2	25.5	28.4	31.8	28.7	32.1		35.5
OVERLAY POLICY(INCH) (INCLUDING LEVEL-UP)								
O(1)	2.0	2.0	2.0	2.0	2.0	2.0		2.0
NUMBER OF SEAL COATS	4	4	5	4	5	4	4	4
SEAL COAT SCHEDULE (YEARS)								
SC 1)	2.0	2.0	2.0	2.0	2.0	2.0	2.0	2.0
SC 2)	7.0	7.0	7.0	7.0	7.0	7.0	7.0	7.0
SC 3)	12.9	13.1	12.0	12.0	12.0	12.0	12.0	12.0
SC 4)	17.9	18.1	14.6	16.4	14.7	16.5	17.0	18.4
SC 5)			19.6		19.7			

* All costs in dollars per square yard of pavement.

This figure gives only eight of the many possible designs (sorted by increasing total costs) that meet all of the design criteria. Figure 4 shows data from the current FPS, which does not consider the stochastic nature of the input factors, and consequently the reliability of the design is only 50 percent. This means that, because average regression equations and average inputs are used, there is only a 50 percent probability that the pavement will withstand the applied traffic loads before the overall serviceability level drops below terminal before the predicted time to overlay. This result was supported by feedback from the implementation of FPS in the Texas Highway Department by means of opinions of experienced field engineers.

Therefore, it was realized that FPS must be capable of accounting for the highly variable nature of the pavement design process. A higher level of reliability than 50 percent must be "designed" into a pavement structure for satisfactory performance.

By using the concepts and equations explained in this paper, we modified the FPS program such that any desired level of reliability could be used for the design. The output results from FPS for a reliability level of 95 percent is shown in Figure 5 for the first eight designs. The thickness of the gravel base layer was restricted to 6 in. in both Figures 4 and 5 so that a direct comparison between asphalt concrete thickness could be made. The minimum time to the first overlay was set at 10 years. The designs may be compared by observing design number 1 from Figure 4 with design number 1 from Figure 5. Both have two layers with a base thickness of 6 in. and similar overlay strategies. The design at R = 50 percent shows 5 in. of asphalt concrete over 6 in. of base, whereas the design at R = 95 percent shows 8.5 in. of asphalt concrete over 6 in. of base. The overall cost difference in the optimum design is $2.58 per square yard for the 50 percent level and $3.37 per square yard for the 95 percent level.

A diagram of the concepts needed for design when using FPS at a desired reliability R is shown in Figure 6. The three general sources of variation in the pavement design and performance process are shown with the corresponding FPS inputs that measure these variations. The conceptual procedures for determining reliability are shown across the top of the figure. The N_R is the value of 18-kip equivalent single-axle loads. The pavement should be designed such that there will be a probability of R that the serviceability index will not fall below terminal throughout each design period.

The calculations needed for design at a given reliability level will be briefly summarized with actual inputs from Figure 3:

1. Determine reliability level: R = 95 percent.
2. Determine $s^2_{\log n}$: The average number of 18-kip equivalent wheel loads estimated by the Planning Survey Division was 3,000,000. The variance of this estimate may be calculated by using Eq. 18 (assuming that the coefficient of variation of G, ADT_1, and T is 15 percent):

$$s^2_{\log n} = 0.0273$$

3. Determine $s^2_{\log N}$: Eq. 17 summarizes the components of variance (for $\bar{\alpha} = 20$):

$$s^2_{\log N} = s^2_{2\ \log s} + s^2_{\log \alpha} + s^2_{\log Q} + s^2_{lof}$$

$$= 0.1383 + 0.0085 + 0.0464 + 0.0795 = 0.2727$$

4. Determine N to design for 95 percent reliability: By rearranging Eq. 4 (Z = 1.64 for R = 0.95), we get

$$\log \bar{N}_{95} = \log \bar{n} + Z \sqrt{s^2_{\log N} + s^2_{\log n}}$$

$$\log \bar{N}_{95} = \log (3 \times 10^6) + 1.64 \sqrt{0.2727 + 0.0273}$$

$$= 6.4771 + 0.8987 = 7.3758$$

Figure 5. Best design strategies in order of increasing total cost (reliability = 95 percent).

	1	2	3	4	5	6	7	8
MATERIAL ARRANGEMENT	AB	A	AB	AB	A	A	AB	A
INIT. CONST. COST	3.194	3.125	3.333	3.264	3.264	3.194	3.403	3.333
OVERLAY CONST. COST	.325	.325	.281	.309	.281	.309	.267	.267
USER COST	.007	.007	.006	.007	.006	.007	.006	.006
SEAL COAT COST	.328	.328	.337	.393	.337	.393	.334	.334
ROUTINE MAINT. COST	.250	.250	.280	.258	.280	.258	.294	.294
SALVAGE VALUE	-.733	-.641	-.759	-.746	-.667	-.654	-.772	-.680
TOTAL COST	3.371	3.393	3.477	3.485	3.500	3.507	3.531	3.554
NUMBER OF LAYERS	2	1	2	2	1		2	1
LAYER DEPTH (INCHES)								
D(1)	8.50	11.25	9.00	8.75	11.75	11.50	9.25	12.00
D(2)	6.00		6.00	6.00			6.00	
NO.OF PERF.PERIODS	2	2	2	2	2	2	2	2
PERF. TIME (YEARS)								
T(1)	11.1	11.1	13.8	12.4	13.9	12.5	15.4	15.4
T(2)	24.1	24.1	28.9	26.4	28.9	26.4	31.6	31.6
OVERLAY POLICY(INCH) (INCLUDING LEVEL-UP)								
O(1)	2.0	2.0	2.0	2.0	2.0	2.0	2.0	2.0
NUMBER OF SEAL COATS	4	4	4	5	4	5	4	4
SEAL COAT SCHEDULE (YEARS)								
SC 1)	2.0	2.0	2.0	2.0	2.0	2.0	2.0	2.0
SC 2)	7.0	7.0	7.0	7.0	7.0	7.0	7.0	7.0
SC 3)	13.1	13.1	12.0	12.0	12.0	12.0	12.0	12.0
SC 4)	18.1	18.1	15.8	14.4	15.9	14.5	17.4	17.4
SC 5)				19.4		19.5		

* All costs in dollars per square yard of pavement.

Figure 6. FPS pavement design for desired reliability R.

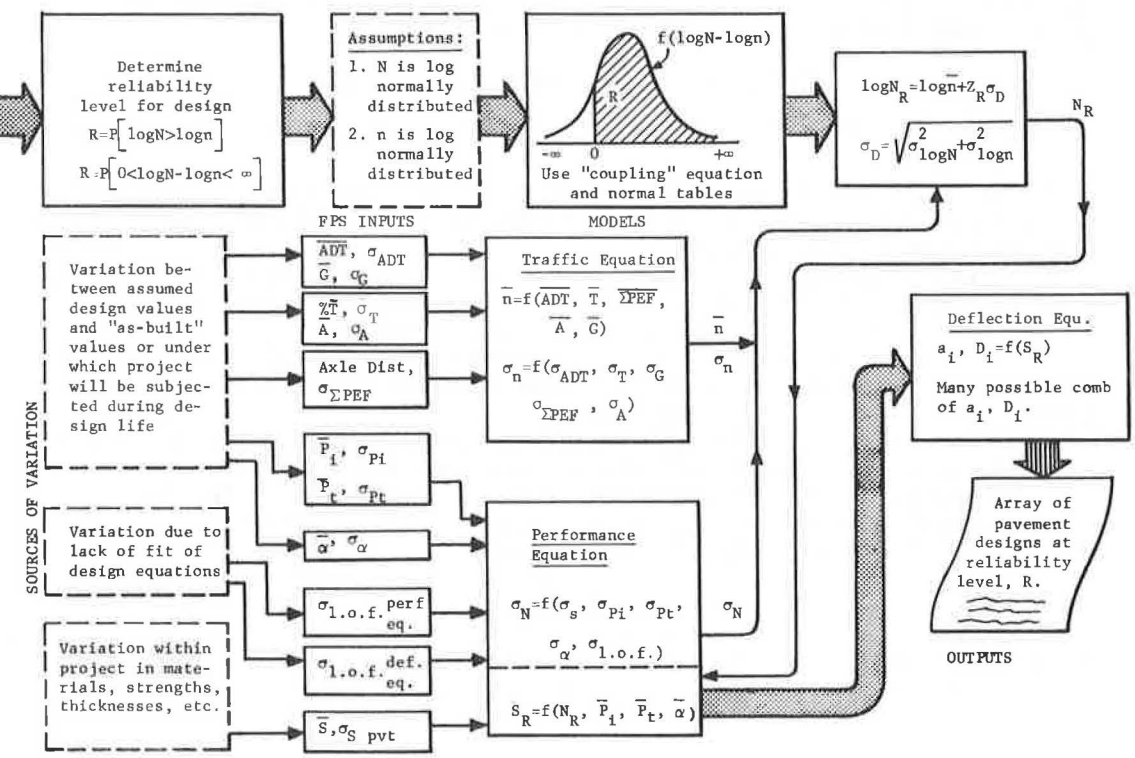

5. Determine the design thickness required using N_{95}: By using the performance, deflection, and traffic equations, we get a pavement design that gives 8.5 in. of asphalt concrete and 6 in. of gravel base for an initial life of 11.1 years. The pavement design for 50 percent reliability showed 5.0 in. of asphalt concrete and 6 in. of gravel base.

It is of importance to note the percentages of magnitude of the components of variance used in Eq. 4.

Source of Variance	Percentage of Total Variance
Lack of fit of performance equation	27
Lack of fit of deflection equation	17
S along pavement	29
Temperature statistic α	3
Initial and terminal serviceability index	15
Traffic estimate n	9
Total	100

The magnitude of these variances could be reduced in several ways. The variance in S along a pavement could be reduced by varying the design thickness of a pavement. Because this is the highest source of variation, this procedure, where practical from a construction standpoint, would greatly reduce the variance of S and should prove economical. The variance in initial serviceability index might be reduced by better construction control of pavement smoothness (this could force bid prices to increase also). The procedure for estimating traffic could be improved, thereby reducing the variance. The lack-of-fit variation of the performance and deflection equations could be reduced by replacing the structural subsection of FPS with an improved subsystem with a lower lack-of-fit error when it becomes available. Because this total variance amounts to 44 percent, a need for a more rational structural subsystem is evident. Work is progressing rapidly in this direction at the present time (14).

CONCLUSIONS AND RECOMMENDATIONS

The following conclusions and recommendations seem appropriate from the results of this analysis:

1. The design risk may be quantified by using reliability concepts. The designer may now consider the percentage of pavement that may "fail" during the analysis period in arriving at a design reliability.
2. A pavement designer may design at any specific level of reliability within certain economical and practical restraints. Various types of highways may be designed for different reliability levels, thereby achieving design uniformity.
3. Assistance in formulating research priorities may be obtained. The magnitude of variations associated with the design factors and equations may be examined and research initiated to reduce these uncertainties.
4. With regard to conclusion 3, the importance of quality control during construction is obvious, and furthermore its influence may be computed directly.
5. The basic concepts presented herein are applicable to any pavement design method, provided the lack-of-fit errors of the design equations and the variance and distribution of the design factors can be determined.
6. The analysis presented in this paper represents a first-order approximation of applying reliability concepts to a comprehensive pavement design system (because there are several sources of uncertainty that were not considered). The reliability level defined here applied only to the performance of a pavement as measured by the serviceability index. Other factors, such as costs and skid resistance, are not directly considered. Future work will provide these refinements of the method.

ACKNOWLEDGMENTS

This investigation was conducted at the Center for Highway Research, University of Texas at Austin. The authors wish to thank the sponsors, the Texas Highway Department and the Federal Highway Administration. Special thanks are due Joseph A. Kozuh and Frank H. Scrivner for their invaluable assistance on this project. The opinions, findings, and conclusions expressed in this publication are those of the authors and not necessarily those of the Federal Highway Administration.

REFERENCES

1. Scrivner, F. H., Moore, W. M., and Carey, G. R. A Systems Approach to the Flexible Pavement Design Problem. Texas Transportation Institute, Texas A&M Univ., College Station, Res. Rept. 32-11, 1968.
2. Haugen, E. B. Probabilistic Approaches to Design. John Wiley and Sons, 1968.
3. Structural Design of Asphalt Concrete Pavement Systems. HRB Spec. Rept. 126, 1971, 207 pp.
4. The AASHO Road Test: Report 5—Pavement Research. HRB Spec. Rept. 61E, 1962, 352 pp.
5. Moore, R. K., and Kennedy, T. W. Tensile Behavior of Stabilized Subbase Materials Under Repetitive Loading. Center for Highway Research, Univ. of Texas at Austin, Res. Rept. 98-12, Aug. 1971.
6. Hudson, W. R., McCullough, B. F., Scrivner, F. H., and Brown, J. L. A Systems Approach Applied to Pavement Design and Research. Center for Highway Research, Univ. of Texas at Austin, Res. Rept. 123-1, March 1970.
7. Scrivner, F. H., and Moore, W. M. An Empirical Equation for Predicting Pavement Deflections. Texas Transportation Institute, Texas A&M Univ., College Station, Res. Rept. 32-12, 1968.
8. Scrivner, F. H., and Michalak, C. H. Flexible Pavement Performance Related to Deflections, Axle Applications, Temperature and Foundation Measurements. Texas Transportation Institute, Texas A&M Univ., College Station, Res. Rept. 32-13, 1969.
9. AASHO Interim Guide for the Design of Flexible Pavements. American Association of State Highway Officials, Oct. 1961.
10. Liddle, W. J. Evaluation of Pavement Serviceability on Utah Highways. Utah State Department of Highways, Interim Rept., 1969.
11. Brown, J. L., Buttler, L. J., and Orellana, H. E. A Recommended Texas Highway Department Pavement Design Systems User's Manual. Texas Highway Department; Texas Transportation Institute, Texas A&M Univ.; and Center for Highway Research, Univ. of Texas at Austin, Res. Rept. 123-2, March 1970.
12. Hudson, W. R., and McCullough, B. F. Translating AASHO Road Test Findings—Basic Properties of Pavement Components. Materials Research and Development, Inc., Final Rept., Dec. 1970.
13. Sherman, G. B. In Situ Materials Variability. HRB Spec. Rept. 126, 1971, pp. 180-190.
14. Jain, S. P. Flexible Pavement System—Second Generation Incorporating Fatigue and Stochastic Concepts. Univ. of Texas at Austin, PhD dissertation, in progress.
15. Heathington, K. W., and Tutt, P. R. Estimating the Distribution of Axle Weights for Selected Parameters. Highway Research Record 189, 1967, pp. 1-18.
16. Darter, M. I. Applying Reliability Concepts to Pavement Design Systems. Univ. of Texas at Austin, PhD dissertation, in progress.
17. McCullough, B. F., Van Til, C. J., Vallerga, B. A., and Hicks, R. G. Evaluation of AASHO Interim Guides for Design of Pavement Structures. Materials Research and Development, Inc., Final Rept., Dec. 1968.

DEVELOPING A PAVEMENT FEEDBACK DATA SYSTEM

R. C. G. Haas, University of Waterloo, Canada;
W. Ronald Hudson and B. F. McCullough, University of Texas at Austin; and
James L. Brown, Texas Highway Department

One of the key phases of pavement design and management is performance evaluation. This activity is vital to the successful improvement and updating of any design and management working system, such as that developed for the Texas Highway Department. A feedback data system, which involves the systematic collection, storage, and retrieval of data, is in turn the major component of performance evaluation. This paper describes the initial planning and development of such a system that is part of the overall design and management system. The role of a pavement feedback data system within the area of pavement management is discussed. Its relation to other data files in the highway department is considered, and the functional requirements are discussed. A component format for the data system, involving a number of variables within a suggested classification of data files, is described. Some implementation requirements in terms of data flows and software development are considered.

•A COMPREHENSIVE pavement design and management working system has been developed for the Texas Highway Department (1, 2, 3) and has been implemented in selected areas. This working system is based on systems engineering principles and makes extensive use of the computer.

The underlying philosophy was that a working system should be developed and implemented now, based on the best existing technology and knowledge. Current information was organized and coordinated, and the system was designed such that new knowledge could be efficiently incorporated as it became available. It was felt that continued updating and improvement of a working system offered a better approach than did waiting for the ultimate, ideal method.

Because of this approach of continued updating and improving, it was necessary to plan for the systematic collection, storage, and retrieval of data on pavements designed by the working system. Consequently, the development and implementation of a pavement feedback data system were undertaken in 1970 (4).

This paper describes the initial development of the data system. In particular, attention is focused on the general principles involved, the requirements of the data system, the coordination with other highway department data files, and the structure of the pavement data system.

GENERAL PRINCIPLES OF DATA SYSTEM DEVELOPMENT

Function of a Data System

The basic function of a data system is to provide information efficiently, quickly, and cheaply for planning, design, and operational needs. In scope, the following aspects are involved: (a) proposed use of the data, (b) collecting data, (c) organizing and processing data, (d) storing data, (e) retrieving data, and (f) analyzing data.

Some sort of automated means is usually required for these functions. However, it is very easy to underestimate the effort required to institute and maintain a data system.

Sponsored by Committee on Theory of Pavement Design.

Overall Highway Data System

Highway departments usually maintain data files (some of which are automated) on practically all aspects of their operations, but the establishment of an overall, automated, and integrated data system for the entire department is a complex and comprehensive task. Nevertheless, the Wisconsin Department of Transportation is establishing a comprehensive highway network data and information system (5). As well, the Texas Highway Department has reported its efforts toward analyzing and automating where possible a major portion of its planning information (6).

A pavement data system should be developed within the context of such a broad highway data system. The major considerations involved include the following: (a) relation of data system to planning, (b) basic design and use criteria, and (c) indexing, control, and coordination.

Most highway departments are concerned with resource allocation over some time span. The effectiveness of the decision to allocate resources is directly related to the level of support information available on economic, physical, and social factors. A properly designed data system can provide this support base.

The basic design and use criteria involve the storage of data in a single-element manner, although a number of individuals or sections of the department may need the data at various times. Obviously, it is desirable to institute common controls so that data can be requested from individual systems.

Proper indexing, control, and coordination are the keys to satisfying these criteria. A common locational index is probably the best method for accomplishing this [i.e., route location and number, geographical coordinates (7), or project number].

The development of a data management system on a widespread basis requires the inclusion of a very large number of comprehensive data files. Wisconsin (5) has emphasized that this requires many years and that staged implementation is a necessity.

Type of Data System Required

The type of data system required depends on a number of factors. One of the most important is the previously mentioned need for common indexing and access to all data files. This is best satisfied by an integrated computer system (4), especially in view of the computer hardware available to most highway departments.

Role of the Data System in Pavement Management

Pavement management consists of a large number of interrelated activities in the planning, design, construction, maintenance, performance evaluation, and research of pavements. Figure 1 shows these major management phases. The role of the data system as a major component of the performance evaluation phase is indicated.

The design and implementation of an overall performance evaluation scheme have been discussed by Haas and Hudson (4, 8). They have pointed out that the following are involved:

1. Preliminary planning, including inventories of current practices and data collection resources, a review of other systems in use, a statement of objectives and constraints, a preliminary schedule, and a preliminary estimate of costs;
2. Identification and classification of all factors (climatic, materials, load, construction, maintenance, costs, etc.), including an initial selection of key factors;
3. Selection and/or development of techniques and/or units for quantitatively measuring the performance factors;
4. Development of a coding, indexing, and data aquisition format for the various factors;
5. Development of a sampling plan, including operational manuals, on the various evaluation segments of the paved network;
6. Testing and implementation of the sampling plan;
7. Design and implementation of the data bank itself, including software development for data storage and retrieval; and

Figure 1. Role of the data system in the pavement management system.

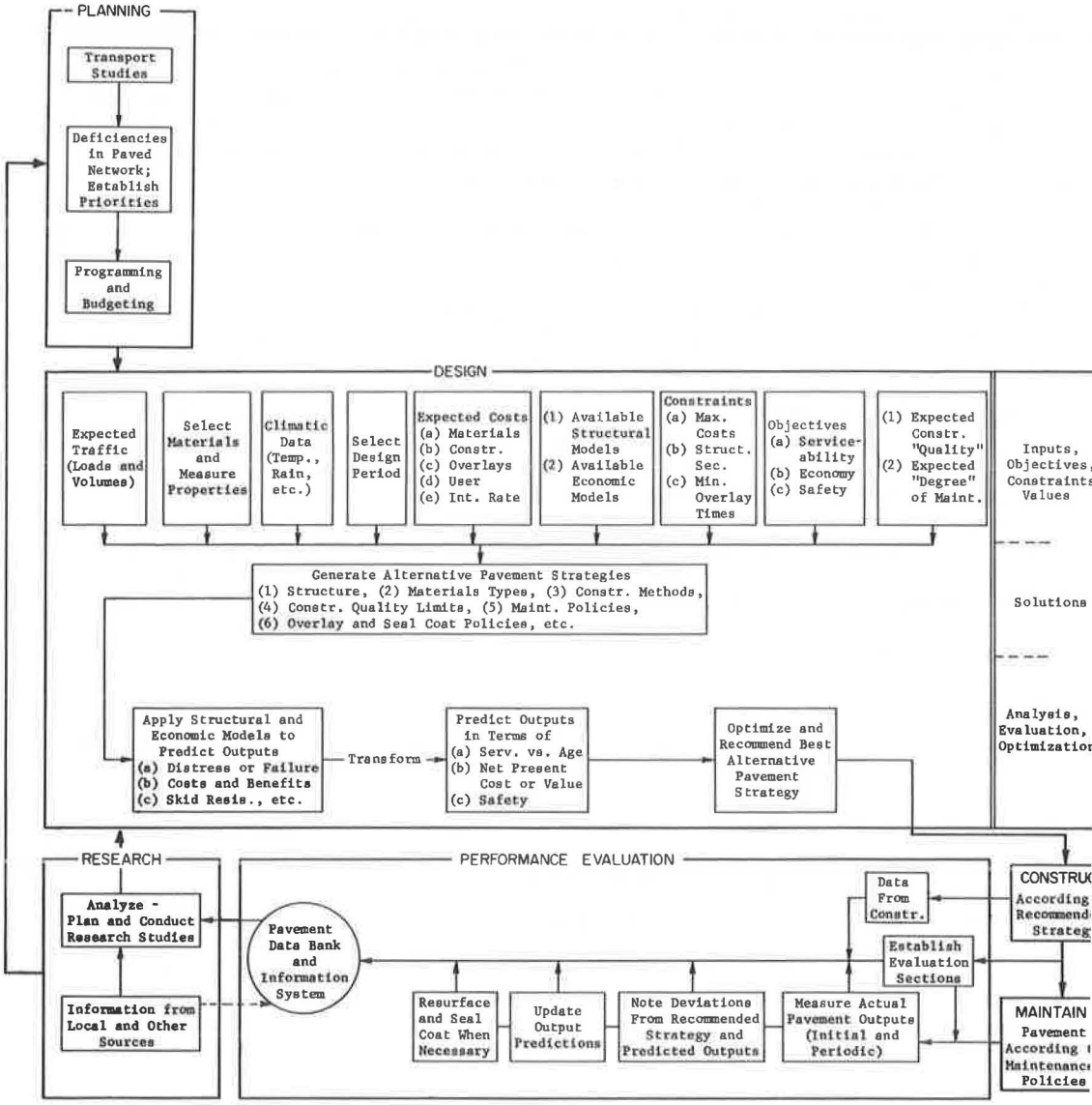

8. Development of analysis techniques on stored data for checking and updating models, establishing sensitivity of performance factors, evaluating maintenance strategies, and updating terminal serviceability predictions for programming and budgeting purposes.

EXISTING DATA FILES IN THE HIGHWAY DEPARTMENT

The Texas Highway Department has 16 headquarters' divisions, 25 districts, and the Houston Urban Project, which all acquire and use data of various forms. There are a very large number of data files in existence, and it would be a massive task to document and integrate all of these. However, the Planning and Survey Division (D-10) provides much of the documentation relevant to the pavement design and management system and is the principal repository for a large amount of information. A complete listing and description of this documentation is given elsewhere (6). A list of data files directly relevant to the pavement data system can be found in another publication (4).

An example data file from D-10 is shown in Figure 2. It shows the inputs, operations, and outputs associated with the state roadway file. Also shown in the diagram are some of the output reports that are currently being produced from this file.

FUNCTIONAL REQUIREMENTS FOR THE PAVEMENT DATA SYSTEM

General Requirements

The pavement data system was to be an explicit part of the overall pavement design and management system. However, the following basic questions had to be faced in the planning phase: Should the entire paved network be included in the data system, or should only certain, selected evaluation segments be included?

Although programming and budgeting require data on the whole network, it was decided (on the basis of available resources) that the second approach was more feasible for the initial data system.

Nevertheless, a general requirement was to provide in the data system flexibility for expansion to include any number of additional portions of the network. In this way, for example, a particular district could collect widespread information on one or more specific data items (e.g., skid resistance, present serviceability index, etc.) with no change in format.

Another obvious requirement was to include the data system factors that related to the physical and economic models in the flexible and rigid pavement design system.

Finally, a major requirement was the provision for accessing other data files, such as that previously described. It has been pointed out that this can be accomplished by proper indexing, control, and coordination.

Figure 3 shows the overall requirements for the pavement data system. It points out that there is both a supplier and a user of data, which in many cases may be the same person, section, division, or district.

Specific Requirements

The successful implementation of a pavement data system depends on prior and specific consideration of the general, major requirements. This may be done by first listing the classes in which they fit and then by considering these classes in more detail:

1. Existing channels of communication in the highway department's administrative structure should be used to acquire and transmit data;
2. The data system should be implemented on a progressive or staged basis, including trial and testing work; and
3. A means for determining the usefulness or value of the data system should be established.

Communication of data requires the following: (a) computer programs for processing input data, updating files, processing output data requests, and accessing other data files; (b) availability of equipment (field, laboratory, and computer hardware); (c) delineation of the highway department's organizational structure, particularly relating

Figure 2. Inputs, operations, and outputs for the state roadway file (RI-2) (taken from Kher et al., 3).

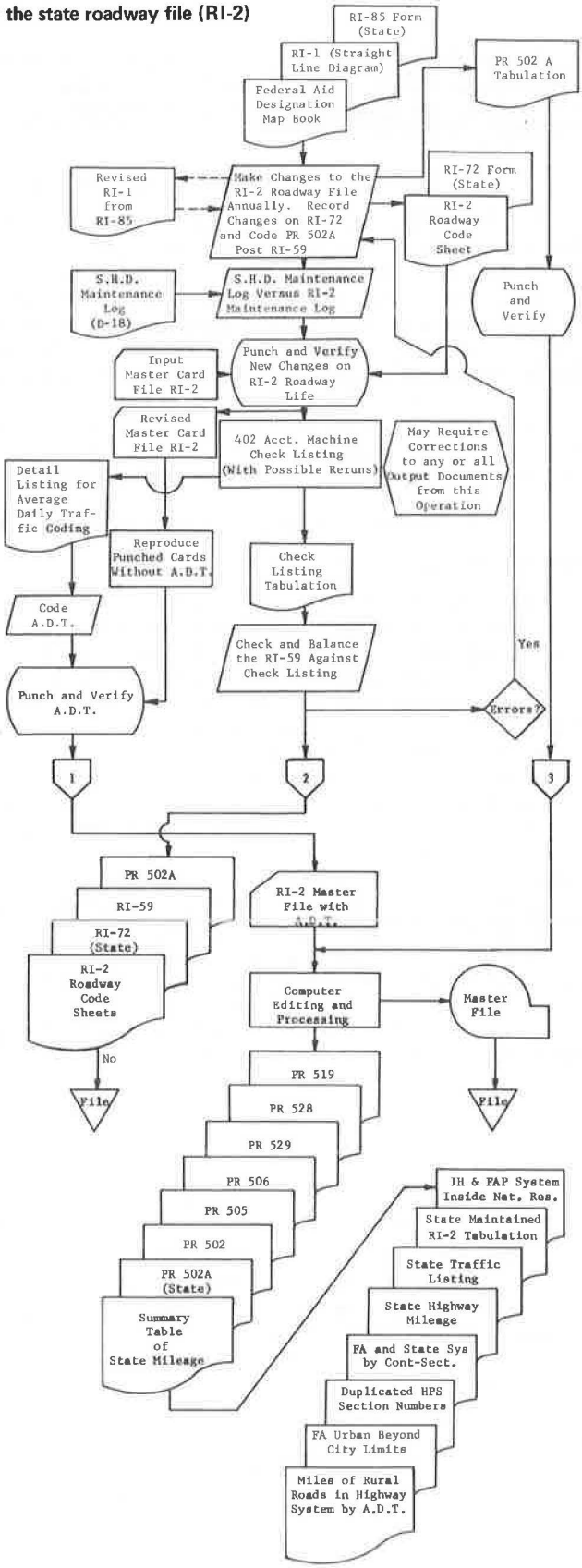

to pavement management information flows; (d) operational guides and sampling plans for field staff engaged in acquiring and forwarding raw data; (e) description, for distribution, of the standard retrieval output reports available; and (f) no constraints within the data system itself on the amount of information that can be handled.

Progressive implementation is a logical and more feasible approach that can incorporate improvements on a stepwise basis. The following are required for such a staged implementation:

1. Selection of one or more short, representative evaluation segments on each section designed by the working system—this provides an orderly annual addition to the total inventory covered by the data system;
2. Output reports having an initial, finite, and standard form—this recognizes the major task of software development; and
3. Provision for adding future, new data fields—this recognizes initial resource limitations on acquiring data and allows for the possibility of currently "unimportant" factors changing in status.

Determining the usefulness of the system is necessary in order to avoid continued collection of useless data while perhaps neglecting the addition of new, important data fields. The following standards of comparison have been adopted for the overall project (discussed more extensively elsewhere, 1, 4) and are applicable to the pavement data system: operationality, rationality, acceptability, and reviseability.

DEVELOPING THE COMPONENT FORMAT OF THE DATA SYSTEM

Planned Operating State

The data system was planned on an integrated basis, within the overall development and application scheme shown in Figure 1. The planned operating state of such an integrated, computer-based, pavement data system is shown in Figure 4.

Identification of Factors and Classification for Data Files

The identification and classification of factors are iterative processes requiring considerable judgment, some of which is perhaps arbitrary. Because of the extremely large variety of factors possibly relevant to pavements, we selected as a starting point the variables used in the models in the flexible and rigid pavement working design systems.

A number of classification schemes were considered, along with the many variables. Table 1 gives the final classification scheme that was selected. It is in the form of various data files, similar in concept to the data files used by the Planning and Survey Division (D-10). The "123" number relates to the original project number and provides sufficient "open" numbers for any D-10 increase of road inventory files. A listing of the actual factors in each of the data files given in Table 1 and a detailed description of each file are contained elsewhere (4). The following discussion is a brief summary of some of these descriptions.

The master file (RI-123) essentially contains data on the initial as-built pavement, which primarily relate to the dimensions of the pavement structure, the materials used, and the cost of the materials. It is therefore a file of initial information, as contrasted with the subfiles that contain provision for future changes or additions and for periodic data acquisition. The locational identifiers for RI-123 and for all the subfiles correspond to those used by D-10. As well, the pavement data system files provide for a beginning and ending mile point for each evaluation segment (in addition to provision for point, lane, and wheelpath location if desired) within a state highway department section number. This in effect makes possible the development of variable length records within each section. A number of factors in RI-123 and in the subfiles are in coded form for efficiency and convenience. The development of the appropriate codes is facilitated by the design of coding sheets. An example is given in the next section.

The performance data subfile (RI-123-01) has been designed for periodic measurements of the pavement surface in order to assess the level of service provided by the

Figure 3. General functional format for a pavement data system.

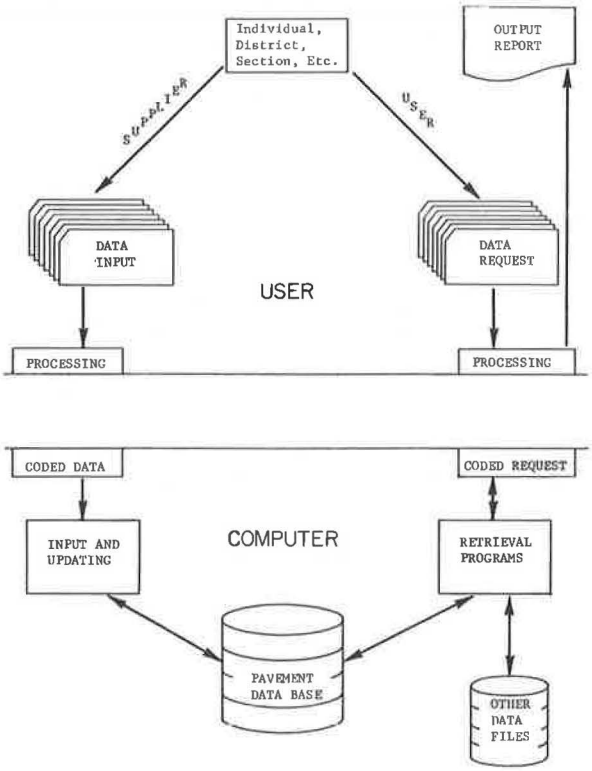

Figure 4. General operating state of an integrated, computer-based pavement data system for Project 123.

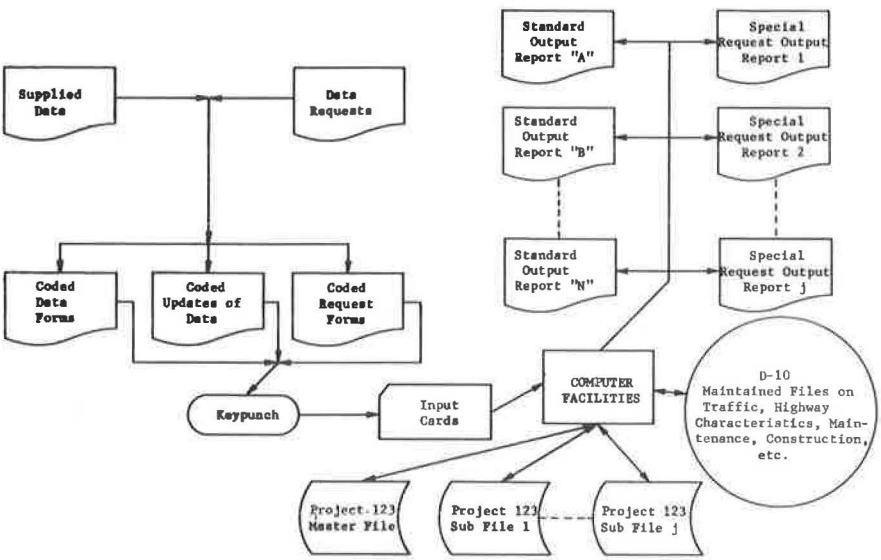

Table 1. Classification of Project 123 pavement data files.

File Number	File Name	Remark
RI-123	Master file	Contains as-built data on dimensions of pavement structure, construction and materials costs, etc.
RI-123-01	Performance data subfile	Contains periodic performance data on roughness, pavement deterioration, skid resistance, etc.
RI-123-02	Structure capacity subfile	Contains periodic structural capacity measurements for deflection.
RI-123-03	Maintenance, resurfacing, and seal coats subfile	Contains periodic data on maintenance, resurfacing, and seal coats types and costs.
RI-123-04	Environment subfile	Contains periodic data on rainfall, temperature, moisture variations, freezing, etc.
RI-123-05	Materials data subfile	Contains as-built and periodic data on physical and chemical properties of pavement component materials.
RI-123-06	Traffic data subfile	Contains initial and periodic data on traffic volumes, truck percentages, weights, etc. (access to D-10 traffic data file).

Figure 5. Coding sheets for the performance data subfile (RI-123-01).

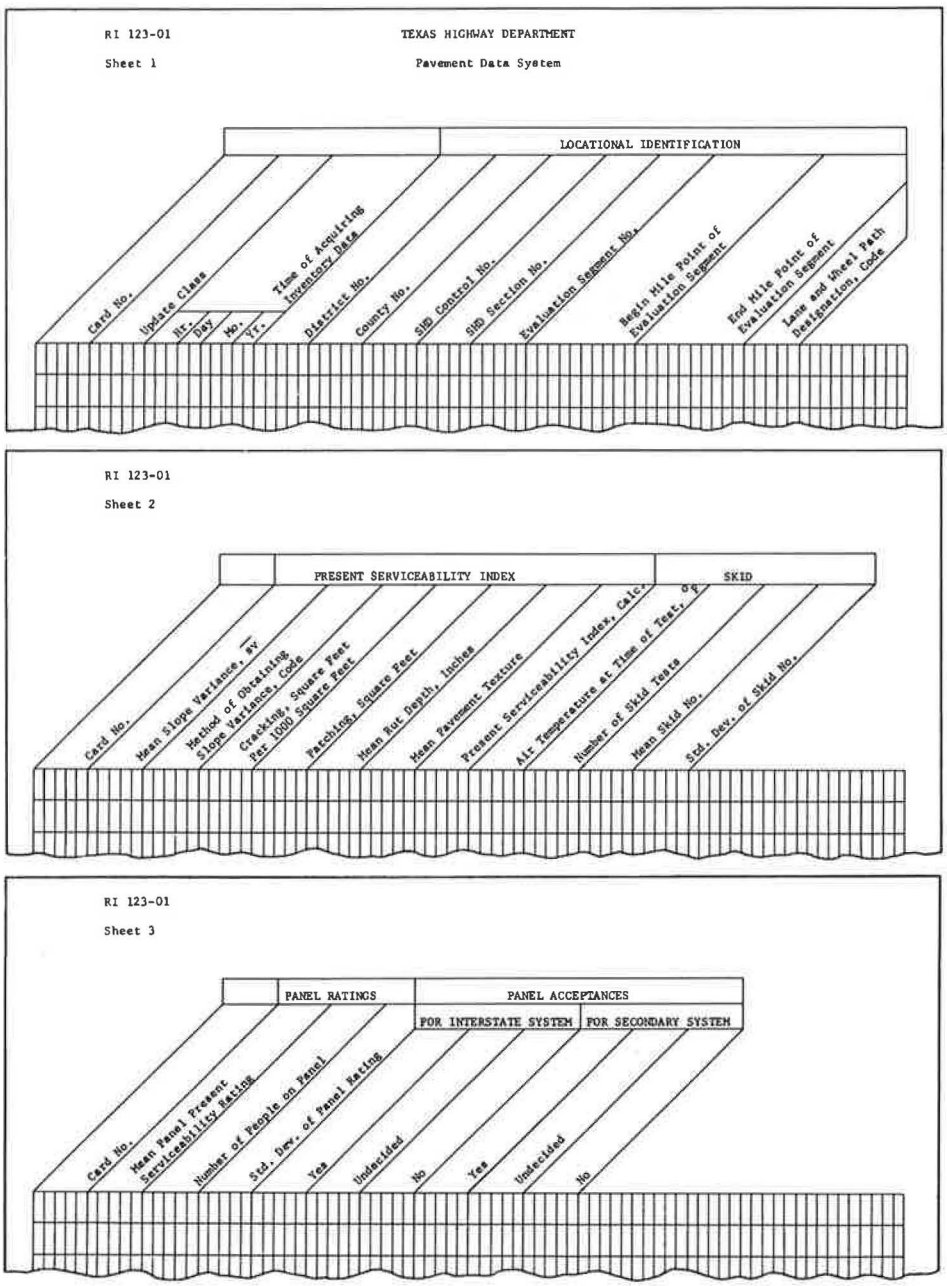

Figure 6. General communication and data flow channels for the Project 123 pavement data system.

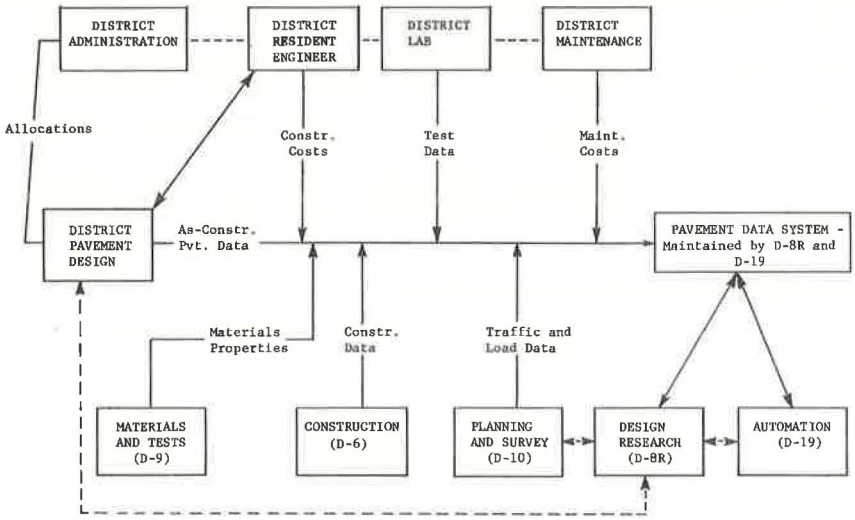

Figure 7. Example retrieval from the Project 123 pavement data system.

TEXAS HIGHWAY DEPARTMENT

PAVEMENT DATA SYSTEM - DATA RETRIEVAL

INVENTORY OF PAVEMENT EVALUATION SEGMENTS DESIGNED BY FPS AND RPS

FILES ACCESSED- RI-123
RI-123-01
RI-123-06

HWY	CONTL	SEC NO	EVAL SEG NO	BEG MI PT	END MI PT	DATE PVT COMPL	PVT SURF TYPE	BASE TYPE	SUBB TYPE	SUBGR SOIL TYPE	TOT PVT DEPTH	INITIAL PSI	INITIAL ADT
IH35	15	7	3	24.610	25.083	30AUG68	2	0	1	A-7-5	9	4.5	25000
IH35	15	8	3	34.700	35.173	11SEP68	2	0	1	A-7-5	9	4.5	25000
IH35	15	9	3	43.240	43.713	010CT68	2	0	1	A-7-5	9	4.5	25000
IH35	15	10	4	52.115	52.588	170CT68	2	0	1	A-7-6	9	4.5	25000
US77	371	3	1	18.210	18.683	10FEB69	1	2	1	A-2-7	12	4.3	15000
US77	371	4	2	22.450	22.923	12FEB69	1	2	1	A-2-7	12	4.4	15000
SH103	336	5	1	15.335	15.808	25APR69	1	2	4	A-4	13	4.2	12000
SH103	336	6	2	25.650	26.123	30APR69	1	2	4	A-5	13	4.2	12000
SH103	336	7	3	33.825	34.298	02MAY69	1	2	4	A-3	13	4.0	12000
SH103	336	8	4	41.220	41.693	05MAY69	1	2	4	A-4	13	4.4	12000
US377	80	2	1	40.400	40.873	01JUN70	1	2	1	A-7-5	12	4.4	16000
US377	80	3	2	45.265	45.738	06JUN70	1	2	1	A-7-6	12	4.5	16000

pavement. The most important of these performance indicators, in terms of current technology, are the present serviceability index (PSI) and the skid resistance factor. The RI-123-01 file also contains data items for panel ratings. This is an example of data that may be collected only at infrequent intervals, such as part of a special study. An example of the coding sheets used for this subfile is shown in Figure 5. Coding sheets for the other files have been designed in a similar manner.

The structure capacity subfile (RI-123-02) has also been designed for periodic measurements, primarily using Dynaflect measurement data because they are used by the working design system for flexible pavements. The RI-123-02 file also contains data items for structural parameters of the layers used in elastic "n-layer" analyses.

The maintenance, resurfacing, and seal coats subfile (RI-123-03) provides data not only useful for modifying the design models per se but also useful for periodically updating the original design predictions. The data collected primarily relate to periodic costs incurred.

The environment subfile (RI-123-04) is primarily used for recording climatic data. It is also designed to include some general topographic and drainage information as well as temperature and moisture data through the pavement depth.

The materials data subfile (RI-123-05) has been held to slightly more than a hundred items. This may seem extreme, but several hundred variables could quite easily be included. As well, the final sampling plan will contain only certain key items from this list for routine measurement. The others are included, as for other data files, to provide flexibility for expansion and for special studies.

The traffic data subfile (RI-124-06) is designated as a distinct part of the pavement data system but will initially operate only on the basis of accessing the Planning and Survey Division's data files.

IMPLEMENTATION

Sampling Plan and Data Flows

A sampling plan and operational guides are currently being developed. Because the major amount of data will come from district staffs, the resources available in the district are carefully considered in selecting the number of evaluation segments and the intensity or frequency of sampling.

The data flows involved are shown in Figure 6. Although pavement design is separated from district resident engineer, these coincide in a number of cases.

Because the primary initial purpose of the data system is for checking and updating design models, the Research Section of the Design Division (D-8R) will have responsibility for its maintenance. The Automation Division (D-19) will handle data processing and storage.

Software Development

One of the major developmental tasks that is needed before full implementation can be realized involves writing a variety of data retrieval programs. There are, of course, a large number of possible types of retrieval that may be desired. Figure 7 is an example output showing some data as they would be "stored" in the system. Other forms of output might include varying degrees of analysis and/or correlation.

There are two basic types of retrieval programs: (a) periodic, "standard" outputs, primarily for trend analyses; and (b) special outputs, for research purposes.

CONCLUSIONS

Pavement design and management incorporate a variety of interrelated activities, most of which function better with an adequate data base. This paper has demonstrated that a feedback data system is vital to the efficient, continued updating and improvement of pavement management activities.

The initial planning and development of a pavement data system for the Texas Highway Department have been outlined in the paper. Other data files in the highway department have been considered in designing the component format. A classification scheme

for the pavement data files has been described. Finally some suggestions have been set forth for data flow and software development requirements.

ACKNOWLEDGMENTS

This investigation was conducted at the Center for Highway Research, University of Texas at Austin. The authors wish to thank the sponsors, the Texas Highway Department and the Federal Highway Administration. The opinions, findings, and conclusions expressed in this publication are those of the authors and not necessarily those of the Federal Highway Administration.

REFERENCES

1. Hudson, W. R., McCullough, B. F., Scrivner, F. H., and Brown J. L. A Systems Approach Applied to Pavement Design and Research. Published jointly by Texas Highway Department; Texas Transportation Institute, Texas A&M Univ.; Center for Highway Research, Univ. of Texas at Austin, Res. Rept. 123-1, March 1970.
2. Brown, J. L., Buttler, L. J., and Orellana, H. E. A Recommended Texas Highway Department Pavement Design System User's Manual. Published jointly by Texas Highway Department; Texas Transportation Institute, Texas A&M Univ.; Center for Highway Research, Univ. of Texas at Austin, Res. Rept. 123-2, March 1970.
3. Kher, R. K., Hudson, W. R., and McCullough, B. F. Automation in Pavement Design and Management Systems. HRB Spec. Rept. 128, 1972, pp. 40-53.
4. Haas, R. C. G. Developing a Pavement Feedback Data System. Published jointly by Texas Highway Department; Texas Transportation Institute, Texas A&M Univ.; Center for Highway Research, Univ. of Texas at Austin, Res. Rept. 123-4, Feb. 1971.
5. Hart, T. J. The Highway Network Data and Information System. Highway Research Record 326, 1970, pp. 33-41.
6. Systems Analysis of the Planning Survey Division. Texas Highway Department, Staff Report, Vol. 2, June 1, 1968.
7. Vance, J. A. Geographical Data Coding Grid. Proc. Canadian Good Roads Assn., 1966.
8. Haas, R. G. C., and Hudson, W. R. The Importance of Rational and Compatible Pavement Performance Evaluation. HRB Spec. Rept. 116, 1971, pp. 92-111.

PAVEMENT INVESTMENT DECISION-MAKING AND MANAGEMENT SYSTEM

W. A. Phang and R. Slocum, Ontario Department of Transportation and Communications

•IN recent years, a great deal of effort has been spent on organizing pavement management practices into a systems framework. In 1968, Wilkins (1) reported on this matter to the Canadian Good Roads Association [now Roads and Transportation Association of Canada (RTAC)]. Figure 1, taken from his report, shows the relations among design, performance, and costs of pavements. Also in 1968, Hutchinson presented research results that dealt at some length with the elements of design, performance, and costs and with optimization and use of the computer. It also contained some of the fundamentals of a pavement management system.

In 1970, Hudson et al. (3) outlined an ideal pavement management system and developed a working pavement system. The pavement design method is based on a specially developed model that utilizes pavement deflections measured with the Dynaflect.

In 1971, Hejal, Buick, and Oppenlander (4) reported on a computerized method of selecting the pavement component arrangement to minimize the total cost of the pavement's structure selected to fulfill the design requirements.

In all of these efforts, the decision criteria were based on lowest costs in one form or another. Costs used for optimization of pavement components are construction costs. Costs used for comparison of various pavement strategies are annual costs on a present worth basis. This is shown in Figure 2 where the net present values (NPV) of a series of different pavement strategies are compared.

In 1971, Millard and Lister (5) described the methods developed for a rating system in which the condition of roads is measured quantitatively for deflection, riding quality, and resistance to skidding so that maintenance programs can be defined objectively.

In this report, the elements of economic costing, pavement design, and pavement strategy are examined with a view toward providing improved information from which a management decision can be more readily determined. Figure 3 shows the flow path of information necessary for the decision-making process.

The authors of the report recommend the establishment of a pavement monitoring system to serve as feedback to confirm, adjust, or amend the models used in the decision-making process.

ECONOMIC MODEL

The economic analysis of pavement designs is relatively straightforward. The economist is interested in measuring the cost of providing a given benefit, namely pavement service. Such cost comparisons are valid for specific pavement investments that serve specific traffic needs.

The following factors are essential to the proper indentification of economic costs:

1. Present and future construction and maintenance costs,
2. Range of estimated service life expected from the pavement,
3. Discount rate to be used to bring future costs back to their present value, and
4. Analysis period over which the costs of various pavement designs can be compared.

These four elements are combined in a formula to provide the economic cost of any pavement strategy, as shown in Figure 4.

Sponsored by Committee on Theory of Pavement Design.

Figure 1. Pavement management system (after Wilkins, 1).

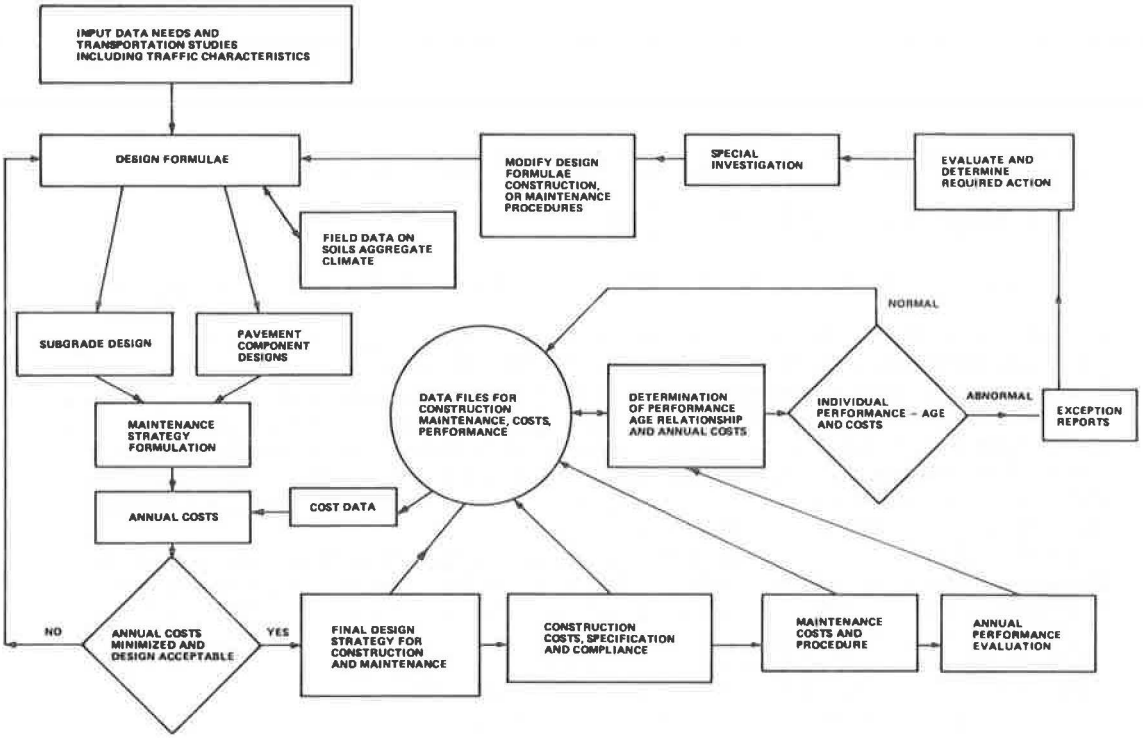

Figure 2. Performance and value implications of gross output of a pavement system (Haas and Hudson, 5).

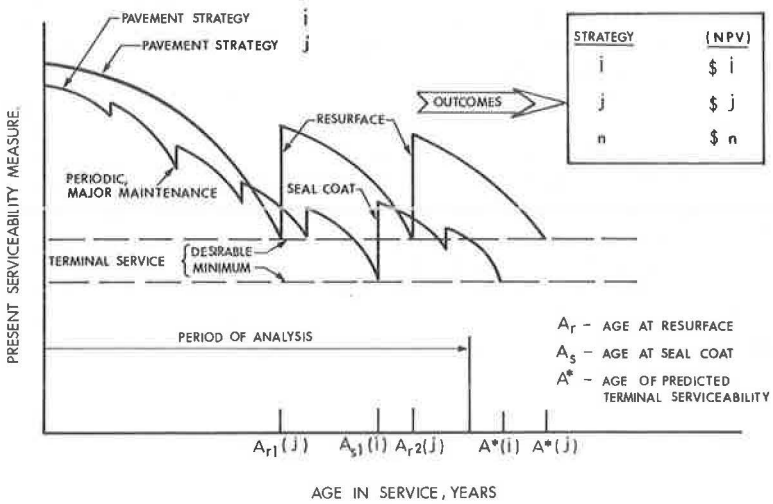

Figure 3. Pavement decision chart.

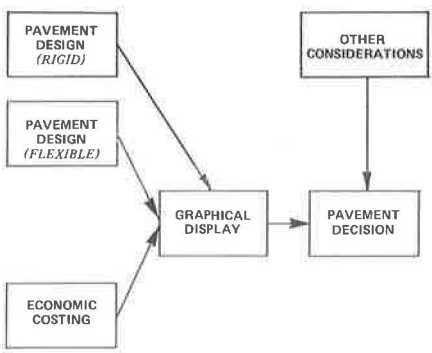

Figure 4. Economic model chart.

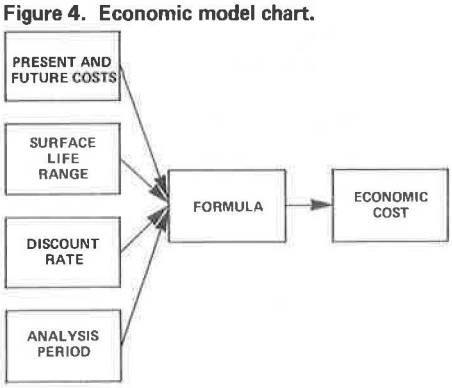

Other methods of economic costing are compared with this approach in later sections. The economic costing model is used later to provide economic cost comparisons of various pavement strategies.

Present and Future Construction and Maintenance Costs

All costs associated with pavement type should be included in the economic analysis, whereas costs that are common to all types may be excluded.

Present construction costs should include the cost of materials and labor for surfacing, base, subbase, and shoulders. Engineering, administration, and grading and traffic delays are excluded as common costs.

Future construction costs include not only the materials and labor cost of resurfacing but also engineering, administration, and grading and traffic delay costs. Because future construction needs are determined by the original pavement design strategy, these additional costs should be included as being characteristic of the pavement type.

No attempt is made in this presentation to specify traffic delay costs associated with resurfacing and maintenance, nor have engineering and administrative costs been discussed. An example of the substantial research effort in the development of traffic delay costs is given elsewhere (6).

Maintenance costs are difficult to estimate because of inadequate data on the independent effects of pavement type, thickness, age, and traffic. For this report, maintenance costs are assumed to increase with pavement age, and some rough estimates were used in the examples illustrating the development of economic costs.

Real resource costs are reflected by using constant dollars rather than inflated dollars. Where relative price changes are predictable, they should be included in the analysis.

Estimated Service Life

Life expectancy for a pavement can range over a number of years (Fig. 5); hence, the economic model must accommodate pavement life as a variable over a range of years. For example, the estimate for the service life of a 2-in. hot-mix on a 10-in. granular base may be 10 to 13 years. The model will identify the effect of these different life expectancies on economic cost.

Discount Rate

The debate among economists still continues regarding an appropriate rate for the discounting of public investment streams. There is no question that future values should be discounted. Delayed benefits are not so attractive as present benefits, and present costs are not so attractive as delayed costs. Hence, the discounting process reduces both future benefits and future costs.

The rate of discount should reflect society's time preference for early benefits versus late benefits. Education could be cited as an investment requiring a very low discount rate, reflecting society's willingness to receive benefits far in the future. The average Provincial borrowing rate for Ontario (approximately 6 percent) is suggested as an appropriate discount rate for pavement investment.

Analysis Period

The analysis period should correspond to the functional design life of the alignment. Because geometric standards change, reflecting advancing technology, and highways typically require rebuilding, in many instances, in less than 30 years, longer analysis periods seem unrealistic. The periods used in the examples vary from 15 to 30 years.

The establishment of an analysis period allows cost comparison between pavement designs that yield equal benefits (pavement service) during the analysis time period. For example, pavement type A may last the entire analysis period without need for a resurfacing, whereas type B may require one or two resurfacings during the analysis period. By comparing the present value of costs for A and B over the same analysis period, we have a meaningful measure of the costs of providing the same benefit.

The Formula

The economic model is represented by the following formula, which calculates the total costs of a pavement strategy during an analysis period. It uses the input on costs, service lives, discount rate, and analysis period previously outlined.

$$TC = C_c + \frac{C_{r1}}{(1+i)^s} + \frac{C_{r2}}{(1+i)^{s+t}} + \frac{C_{r3}}{(1+i)^{s+2t}} + \ldots$$

$$+ \frac{C_r m}{(1+i)^{s+(m-1)t}} - \left(1 - \frac{Y}{t}\right) \frac{C_r m}{(1+i)^n} + \sum_{a=1}^{n} \frac{Ma}{(1+i)^a}$$

where

C_c = initial construction cost,
C_r = resurfacing construction cost (including engineering, administration costs, and traffic delay costs),
i = rate of discount,
m = number of resurfacings during the analysis period,
n = analysis period,
s = life of initial surface,
t = life of subsequent surface,
Y = number of years between the time of last resurfacing and the end of the analysis period,

$\left(1 - \frac{Y}{t}\right)$ = residual-value coefficient, and

Ma = annual maintenance cost.

Where a resurfacing occurs near the end of the analysis period, its residual value is deducted from total costs; this allows an adjustment for the discontinuous (lumpy) nature of the investment function.

Other Approaches

Another method of analysis is to compute the annuity or equivalent annual cost. This has been the practice of the Department of Transportation and Communications (DTC) (7). Baldock (8) presents a formulation of the annual cost derived by multiplying the present value of total cost by the capital recovery factor. The annuity method is advantageous when comparing the economic cost over different analysis periods. Because our model has a common analysis period, the present value of total cost is employed as the unit of economic value.

PAVEMENT DESIGN MODEL

In 1965, the RTAC issued a publication (9) in which, for flexible pavements, the model is based on pavement deflections and on traffic loading. The criterion for design purposes recommended in this guide (9) is that for "flexible pavements which will, within 10 years after construction, have ADT volumes per lane of 1,000 or more vehicles, including 10 percent or more trucks and buses, be designed for a maximum spring Benkelman beam rebound value ($\bar{x} + 2\sigma$) of between 0.030 and 0.050 in."

Because the DTC supplied considerable data to the committee that compiled the guide, the recommendations are applicable to the Ontario environment.

The pavement design model developed herein extends the deflection criterion recommended in the guide to include a range of traffic volumes, and develops thickness-deflection design curves on the basis of experience and research that complement these deflection criteria.

The current policies of the DTC with respect to the types and thicknesses of asphalt surfacings are given in Table 1. Experience gained by the DTC on total pavement thickness over the last 10 years has been recorded and organized in the format given in Table 2. The proposed design model utilizes this experience in thickness design.

Figure 5. Mileage-age distribution of 3½-in. asphalt pavements (Ontario, 1971).

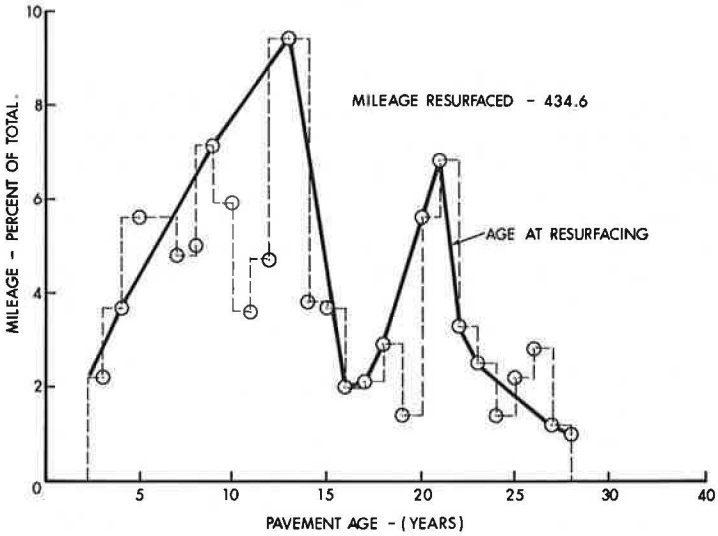

Table 1. Surface standards for rural Ontario roads.

AADT at Time of Construction	Type of Surface[a]
Less than 200[b]	Gravel, prime and single or double surface treatment[c]
200 to 1,000[b]	Prime and single or double surface treatment[c], road mixed mulch 1½ in. of hot mix
1,000 to 2,000	For lower volumes in range—1½ in. of hot mix; for higher volumes in range—2½ in. of hot mix
More than 2,000	3½ to 5½ in. of hot mix

[a]The grade on which the surface type is to be applied must be structurally adequate.
[b]Apply prime and surface treatment 1 ft wider than lane width; e.g., for 10-ft lane width, apply 11 ft wide.
[c]Selection of surface type to be based on economy and performance. Gravel in the less-than-200 range and prime and double surface treatment in the 200 to 1,000 range are usually adequate and the most economical.

Table 2. Current flexible pavement design thickness guidelines (1971).

Road	Subgrade Material	Granular Type Material Suitable as Granular Borrow (in.)	Silt <40; Very Fine Sand and Silt <45 (in.)	Silt 40 to 50; Fine Sand and Silt 45 to 60 (in.)	Silt >50; Very Fine Sand and Silt >60 (in.)	Lacustrine Clays (in.)	Varved and Leda Clays (in.)
Kings' highways							
Multilane	HM	5½	5½	5½	5½	5½	5½
	B	6 to 9	6	6	6	6	6
	SB	—	12 to 18	18 to 24	24 to 30	18	18 to 42
	GBE	17 to 20	25 to 29	29 to 33	35 to 37	29	29 to 45
2 lanes, more than 2,000 AADT	HM	4½	4½	4½	4½	4½	4½
	B	6 to 9	6	6	6	6	6
	SB	—	12 to 18	18 to 24	24 to 30	18	18 to 42
	GBE	15 to 18	23 to 27	27 to 31	33 to 35	27	27 to 43
2 lanes, less than 2,000 AADT	HM	3½	3½	3½	3½	3½	3½
	B	6	6	6	6	6	6
	SB	—	12	12 to 18	18 to 24	12 to 18	18 to 30
	GBE	13	21	21 to 35	25 to 29	21 to 25	25 to 33
Secondary							
Paved, more than 1,000 AADT	HM	1½	1½	1½	1½	1½	1½
	B	6	6	6	6	6	6
	SB	—	6 to 12	12	18 to 24	12 to 18	18 to 30
	GBE	9	13 to 17	17	21 to 27	17 to 21	21 to 29
Unpaved, less than 1,000 AADT	HM	—	—	—	—	—	—
	B	6	6	6	6	6	6
	SB	—	6	6 to 12	18	12	18
	GBE	6	10	10 to 14	18	14	18
Township							
Paved, more than 200 AADT	HM	1½	1½	1½	1½	1½	1½
	B	4 to 6	6	6	6	6	6
	SB	—	6	6	6 to 12	6 to 12	12 to 18
	GBE	7 to 9	13	13	13 to 17	13 to 17	17 to 21
Unpaved, less than 200 AADT	HM	—	—	—	—	—	—
	B	4 to 6	6	6	6	6	6
	SB	—	6	6 to 12	12 to 18	12	12 to 18
	GBE	4 to 6	10	10 to 14	14 to 18	14	14 to 18
Mining and access	HM	—	—	—	—	—	—
	B	4 to 6	6	6	6	6	6
	SB	—	6	6	6 to 12	6 to 12	12 to 18
	GBE	4 to 6	10	10	10 to 14	10 to 14	14 to 18

Note: The range in total thickness shown in table is dependent on the moisture content of the subgrade. HM = hot-mix asphalt thickness; B = base thickness; SB = subbase thickness; and GBE = granular base equivalency thickness (1 in. HM = 2 in. B = 3 in. SB).

Figure 6 shows the flexible pavement design model.

Only three inputs are required for pavement design: the loading expected to travel over the highway expressed as the design traffic number (DTN) or the daily number of passages of equivalent 18-kip single-axle loads in the design lane; the selected design life alternatives in years; and the nature and moisture condition of the subgrade soil.

The first two items, traffic loading and selected design life, are used as input data in the deflection criteria charts shown in Figure 7 to obtain one value of deflection for each alternative combination of traffic and selected design age. These deflection criteria are then used with the third input, the nature and moisture condition of the subgrade soil, by entering the deflections in the thickness design charts shown in Figure 8 and by using the curve that represents our experience with the particular soil to arrive at the required thickness of pavement for each alternative, expressed in terms of equivalent gravel.

An array of thicknesses and design alternatives can then be obtained by using suitable equivalency values for the various layer materials. In this report, the equivalency values used are 1 in. of hot-mix asphalt to 2 in. of granular A base material to 3 in. of granular subbase. These equivalency values lie within the range of equivalencies found for the materials at the Brampton test road (12, 15) and are therefore considered applicable for use in the pavement design model (Table 3).

Basis of Design

The basis of the method of design described in the RTAC guide is that

$$P = f(P_o, S_s, A, L)$$

where

- P = PPR at age A,
- P_o = initial as-constructed PPR,
- S_s = surface strength of flexible pavement (as determined by the Benkelman beam rebound procedure),
- A = age of pavement in years, and
- L = traffic loading (volumes and axle weights).

This relation is shown in Figure 7.

In his analysis of the AASHO test road data, Painter (10) used a general model for the present serviceability index (PSI) with respect to the number of load applications; this is shown in Figure 8. A comparison of this curve with the RTAC curve indicates that, for a linear performance scale, the RTAC plot curves downward with age, whereas the Painter plots curve downward sharply and then drop more slowly with accumulated axle loads. The RTAC plots cover a large number of different pavements over prolonged periods of time, whereas the Painter model is based on a large number of loads over a very short period of time in one locality.

A present performance rating (PPR) model with respect to accumulated equivalent 18-kip single-axle load repetitions is proposed, which is dependent on the strength of the pavement surface as measured by the Benkelman beam rebound procedure. The model is based on the principle that the difference in PPR at any time for any two sections of a given strength difference is constant and on the assumption that the RTAC deflection criterion mentioned previously was based on a PPR of 4.5 after 0.5 million applications of an 18-kip axle for a pavement with an $(\bar{x} + 2\sigma)$ deflection of 0.050 in. The model assumes that the PPR versus log of accumulated 18-kip axle load plots follow basically a straight line but are adjusted for change in deflection with increasing values for accumulated axle loads. This change in deflection with load applications has been determined by Millard and Lister (11) and is shown in Figure 9.

The principle that the PPR of two pavements at any time is inversely proportional to their initial peak $(\bar{x} + 2\sigma)$ deflection has been demonstrated by Phang (12) and is shown in Figure 10. This figure shows a straight-line correlation of the PPR of the sections of pavement measured in June 1970 against the initial peak Benkelman beam rebound measurements obtained in the spring of 1966; i.e., the difference in perfor-

Figure 6. Flexible pavement design model chart.

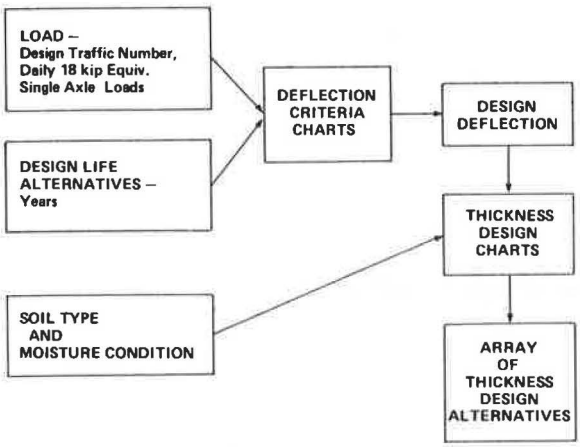

Figure 7. Relation among PPR, age, and Benkelman beam rebound for flexible pavements carrying 1,000 vehicles per lane per day (9).

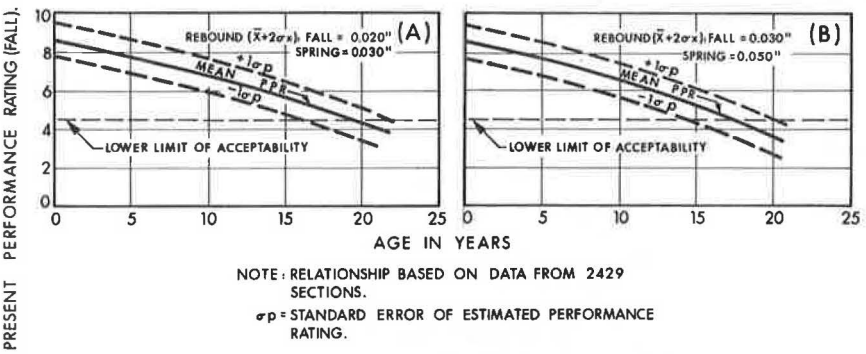

Figure 8. Basic performance relations (Painter, 10).

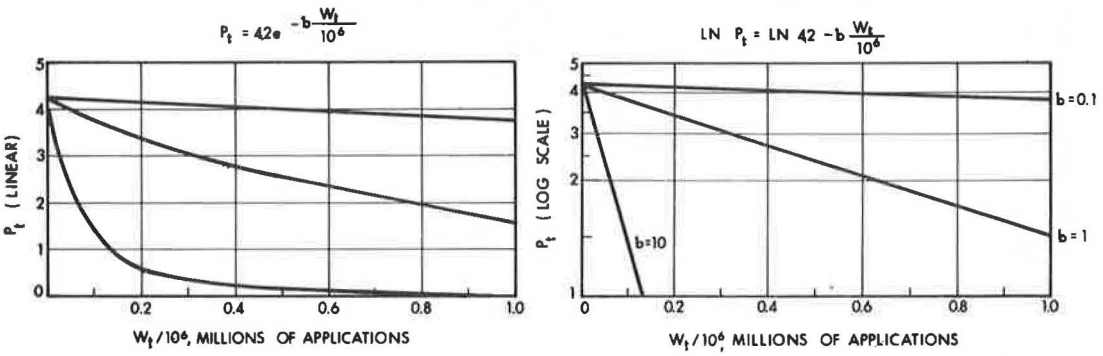

Table 3. Gravel equivalencies (Brampton test road).

Type of Base	Equivalence in Inches of Crushed Gravel[a]				
	1966	1967	1968	1969	1970
1 in. of cement-treated base	3.8	3.50	2.0	1.89	3.0
1 in. of asphalt concrete	1.79	1.75	1.14	2.12	2.8
1 in. of bituminous-stabilized base	1.3	1.08	1.00	0.95	1.05
1 in. of crushed rock	1.06	0.75	0.73	0.90	0.98
1 in. of sand subbase	0.59	0.52	0.54	0.62	0.73

[a]For a 0.050-in. deflection.

Figure 9. Critical life of pavements with rolled-asphalt bases (Millard and Lister, 11).

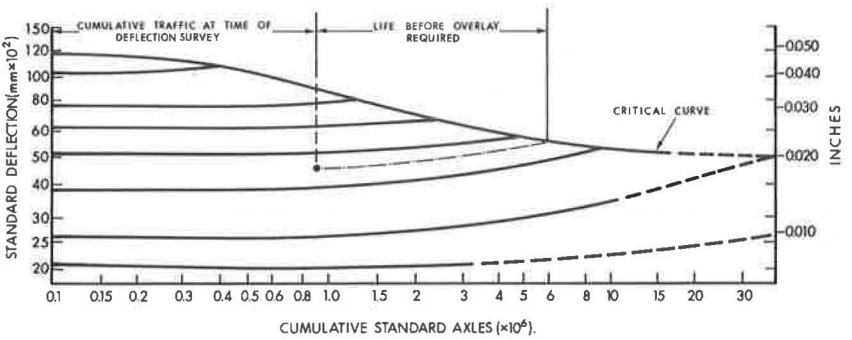

Figure 10. Pavement deflection as a predictor of performance.

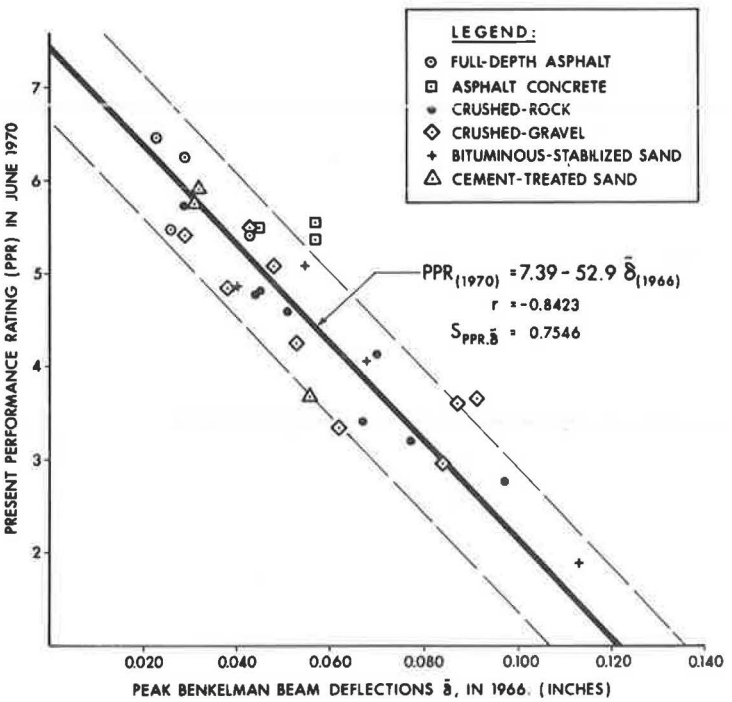

mance in June 1970 for any two sections of a given strength difference is constant. For example, the difference in performance for two pavements whose deflections are 0.020 and 0.040 in. is equal to approximately 1.05 PPR units, which is the same as for pavements of deflections of 0.040 and 0.060 in.

Figure 11 was constructed by drawing a straight line from the initial PPR of 8.5 of the pavement slightly downward and by increasing its downward curvature as the distance along the horizontal axis (log scale) increased. The line is drawn to pass through a point representing the RTAC criterion, i.e., a PPR of 4.5 at 0.5 million load repetitions. At a value of 300,000 load repetitions, the estimated number of load repetitions over the Brampton test road up to June 1970 and the predicted PPR values of pavements of deflections (0.02, 0.04, 0.05, 0.06, 0.08 and 0.10 in.—taken from the regression of Fig. 10) are plotted on a vertical line. It can be observed that the predicted PPR value of 4.8 for a pavement of 0.05-in. deflection taken from Figure 10 falls on the curved line drawn previously. Starting at an initial PPR of 8.5, other similarly shaped curves are constructed through the PPR points plotted on the vertical line. These curves are so constructed that, at any value of accumulated load, the PPR intercepts between the 0.02-, 0.04-, 0.06-, 0.08-, and 0.10-in. curves are always equal. It is noteworthy that the curve extrapolated to represent a pavement of zero deflection shows there is a progressive loss of PPR, and this is considered as representing the loss due to the environment.

Terminal Performance Ratings

Two criteria lines for terminal performance ratings have been proposed: The first is a desirable terminal PPR, and the second is a minimum PPR at which time the riding quality is so bad as to substantially affect the normal operation of passenger cars.

The desirable terminal PPR was fixed on two points, a PPR of 4.5 for a pavement with a deflection of 0.050 in. and a PPR of 3.5 for a pavement with a deflection of 0.100 in. A straight line through these two points determines the desirable terminal PPR's for any other deflection.

The minimum terminal PPR of 3.0 was picked for a pavement with a deflection of 0.100 in. and a parallel line to the desirable PPR line drawn to represent the other minimum terminal PPR's. This gives a minimum terminal PPR of 4.0 for a pavement with a deflection of 0.050 in., which is not unreasonable.

The desirable and minimum terminal PPR's for a pavement with a 0.02-in. deflection are about 5.4 and 5.2 respectively.

The differences in terminal PPR for different strengths of pavement really reflect the purpose that roads of different strengths serve. A very strong pavement is needed for major highways where speeds are quite high, and many of the weaker pavements are used for low-volume roads.

Deflection Criteria

The accumulated axle-load repetitions at desirable terminal performance ratings for a pavement of any given deflection can be converted into a DTN or number of equivalent 18-kip single-axle loads per day in the design lane for any time, in years. For this purpose, the accumulated loads were made equal to 285 DTN times the number of years (285 is taken as the number of days per year during which the design traffic occurs). At this time, no traffic growth rate has been included in the calculations, but this is easily arranged. By using the accumulated axle loads for a series of different pavement strengths, we calculated DTN's for lives of 10, 15, and 20 years and the calculated points shown in Figure 12. The deflection criteria determined in this way, as shown by the straight lines in this figure, agreed very closely with pavement deflection criteria determined by the DTC previously (13). In view of the assumptions made in setting up this method, the slight discrepancies between calculated deflection criteria and criteria previously developed are of little consequence at this time and can be amended after further experience with the method.

Kingham (14) compiled beam deflection criteria, which are shown in Figure 13 with the calculated criteria superimposed. The reasonableness of the calculated criteria is clearly demonstrated.

Figure 11. Estimated current performance of pavements of different deflections (maximum annual).

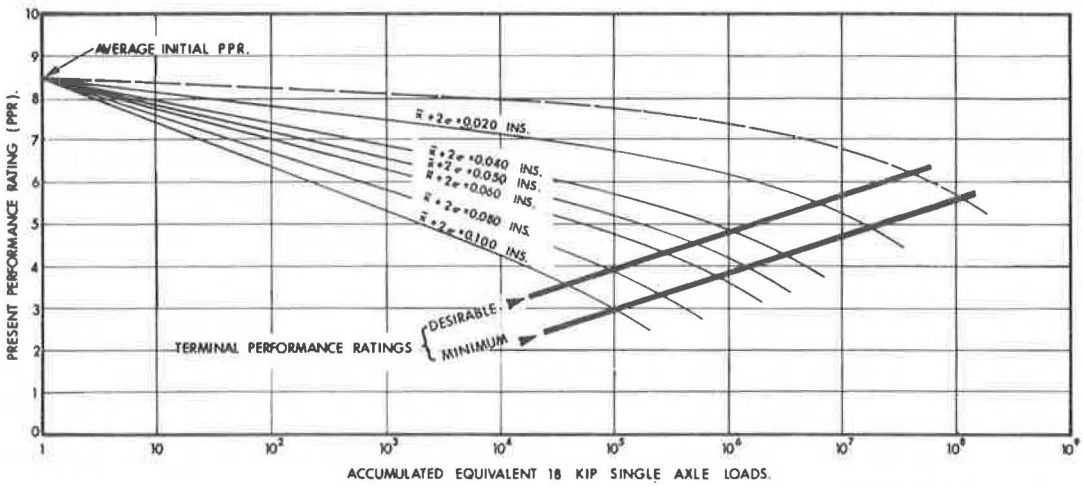

Figure 12. Deflection criteria.

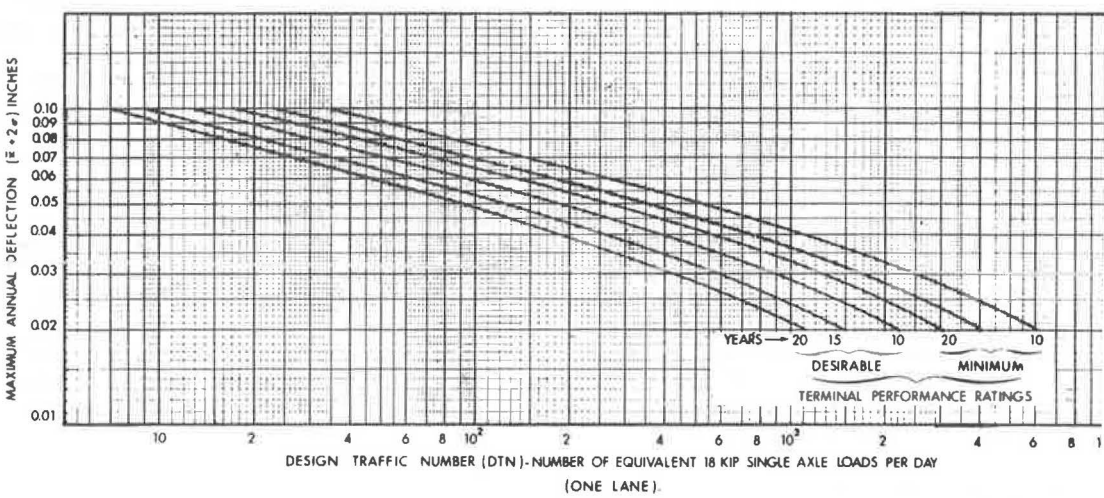

Figure 13. Compilation of beam deflection experience (Kingham, 14).

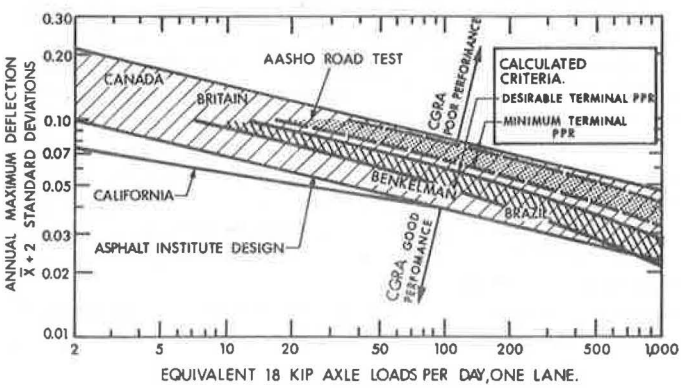

Thickness-Deflection Design Curves

The experience gained by the DTC with pavements having various types of subgrade provides a means for developing thickness-deflection design curves. In Table 2, all of the designs have been reduced to an equivalent gravel thickness by the use of strength equivalencies of 1 in. of hot-mix to 2 in. of base to 3 in. of subbase.

Also, from the Brampton test road experiment, thickness-deflection curves for each year's deflection measurements were calculated and were all found to conform to the general equation

$$\bar{x}(t' + a) = K$$

where

$\bar{x}$ = peak deflection, and
t' = inches of equivalent gravel a and K are constants.

Figure 14 shows these curves for the years 1966 and 1970, and it is noted that the 1970 curves have shifted to the right and upward. It is assumed that thickness-deflection curves derived from the data given in Table 2 will follow the form of this same general equation.

To develop the thickness-deflection design curves, we made one further assumption or rather an arbitrary assignment of DTN's to represent the various traffic classifications and the various types of roads. These DTN's were estimated on the basis of 10 percent truck volumes using truck factors that vary with the traffic volume. These truck factors are still under development but represent the best knowledge of the situation at this time (16).

From the DTN's assigned to each design or class of road, the appropriate peak Benkelman beam rebound ($\bar{x} + 2\sigma$) was selected from the deflection criteria curve. The 15-year curve was selected because this represents the average pavement life recorded. The DTN's used and their corresponding deflections are as follows:

DTN	Deflection (in.)
1,150	0.030
600	0.038
380	0.043
190	0.052
10	0.100
50	0.070
10	0.100

Correlations were carried out by using the mean values in the range of granular base equivalency for each design against the peak Benkelman beam deflection. The regression model used was the same as the deflection-thickness equation determined for the Brampton test road test sections. The results of the correlations for all six categories of subgrade material are given in Table 4; correlation coefficients for all of the regressions were in all cases greater than 0.953. Because of the wide range in thicknesses for varved and leda clays, a seventh regression was carried out for the upper limits of the ranges for gravel equivalencies in each design. The regression equations are shown in Figure 15.

The elements of the pavement design model are now complete, and Figure 6 shows the steps to be taken in flexible pavement thickness design.

Pavement Design Procedures

The required inputs to the design model are (a) load, in terms of daily 18-kip equivalent single-axle load repetitions, or DTN; (b) desired design life in years; and (c) soil type and moisture condition, as determined from soil surveys.

The first two inputs, load and design life, are entered in the deflection criteria chart (Fig. 12), and a deflection is obtained. This deflection, together with the third input,

soil type and moisture, is then entered in the deflection-thickness design curves shown in Figure 15, and an appropriate granular base equivalency thickness design is determined.

By using the minimum thickness of asphalt surfacing given in Table 1 and the equivalency factors used in Table 2, we can find a number of design thickness alternatives. The experience at the Brampton test road suggests that, for full-depth asphalt pavements, the 1 in. of hot-mix equals 2 in. of crushed gravel equivalency should be increased. Because this is based on very limited experience, it is at the designer's discretion to adopt what he considers a suitable equivalency value to use in converting the total granular base equivalency to full-depth asphalt thickness.

Because these designs were obtained on the basis of a desired terminal performance rating, whereas in-service pavements may be allowed to drop to a minimum terminal performance rating, the data shown in Figure 11 may be used to calculate the increase in life of any pavement allowed to fall to the minimum terminal performance rating.

Life of Overlays

For purposes of developing optimum pavement strategies, it is necessary to develop a methodology for determining the required thickness of an overlay as well as its probable life span.

Observations made by Millard and Lister (11) indicate that pavement deflections increase as the accumulated number of axle loads increases (Fig. 9). The critical curve shown in Figure 9 appears to conform to a terminal PPR of about 5.2.

Because of the large seasonal strength variation of pavements experienced in Ontario, this increase in deflection is extremely difficult to detect but undoubtedly exists here (Fig. 14). Figure 9 shows that very strong pavements can increase in deflection by 100 percent before terminal serviceability is reached, whereas weaker pavements increase by as little as 10 percent in deflection before reaching terminal serviceability. Differences in deflection increase appear to be governed by the rapidity with which the terminal serviceability is reached.

Figure 9 is used as the basis for Figure 16, which consists of an extrapolation of the curves of Millard and Lister as well as the addition of curves of higher deflection than are shown therein. The critical curve of Millard and Lister has been replaced by another curve that represents the desirable terminal performance ratings taken from Figure 11.

The increase in deflection with increasing applications of equivalent 18-kip axle loads is a result of several factors: subgrade condition attaining an equilibrium in high moisture conditions, deterioration in the strength of the pavement components caused by aggregate degradation, changes in the asphalt binder characteristics, stripping of the asphalt, fatigue (17), and other causes.

The strengthening of the pavement through the addition of an overlay will not change the state of these deteriorated materials; thus, it can be expected that, after placement of the overlay, the increase in deflection with increase in traffic will continue at approximately the same rate as before.

Figure 17 can therefore be used to estimate the life of overlays, as shown by the example. When a pavement has reached desirable terminal serviceability and has been strengthened by an overlay, the overlaid pavement will continue to increase in deflection with traffic until terminal serviceability is again reached. The number of load repetitions between these two occasions represents the life of the overlay, and the life in years can be found by dividing this number of load repetitions by 285 DTN. A range in life of the overlay can be determined by using two different rates of deterioration, one corresponding to the deterioration rate of the original pavement, the other corresponding to the deterioration rate of a pavement equal in strength to the overlaid pavement.

The thickness of overlay required to reduce the pavement deflection to the desired level is found from overlay design charts published by the RTAC and extended by Chong and Stott (13); these overlay design charts are shown in Figure 18. As an alternative, the overlay design charts published by The Asphalt Institute (18) may be used for this purpose.

Figure 14. Deflection versus thickness.

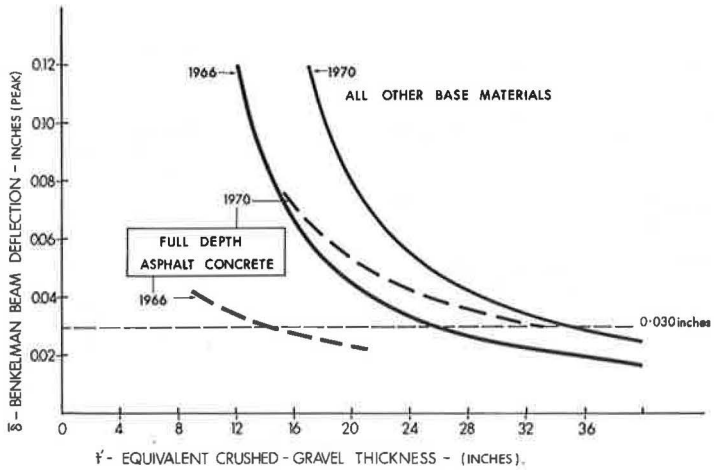

Table 4. Deflection-thickness relations derived from design thickness guidelines.

Subgrade Material	Regression Equation*, $\bar{\delta}(t' + a) = K$	Correlation Coefficient
Granular type materials suitable as granular borrow	$\bar{\delta}(t' + 1.4) = 0.6363$	0.9780
Silt <40; very fine sand and silt <45	$\bar{\delta}(t' - 1.6) = 0.8113$	0.9853
Silt 40 to 50; very fine sand and silt 45 to 60	$\bar{\delta}(t' - 0.5) = 0.9871$	0.9631
Silt >50; very fine sand and silt >60	$\bar{\delta}(t' - 4.4) = 1.0190$	0.9530
Lacustrine clays	$\bar{\delta}(t' - 5.9) = 0.7314$	0.9814
Varved and leda clays	$\bar{\delta}(t' - 6.5) = 0.9797$	0.9800
Varved and leda clays (wet)	$\bar{\delta}(t' - 3.8) = 1.3249$	0.9780

*t' = thickness in equivalent inches of granular base.

Figure 15. Thickness design curves.

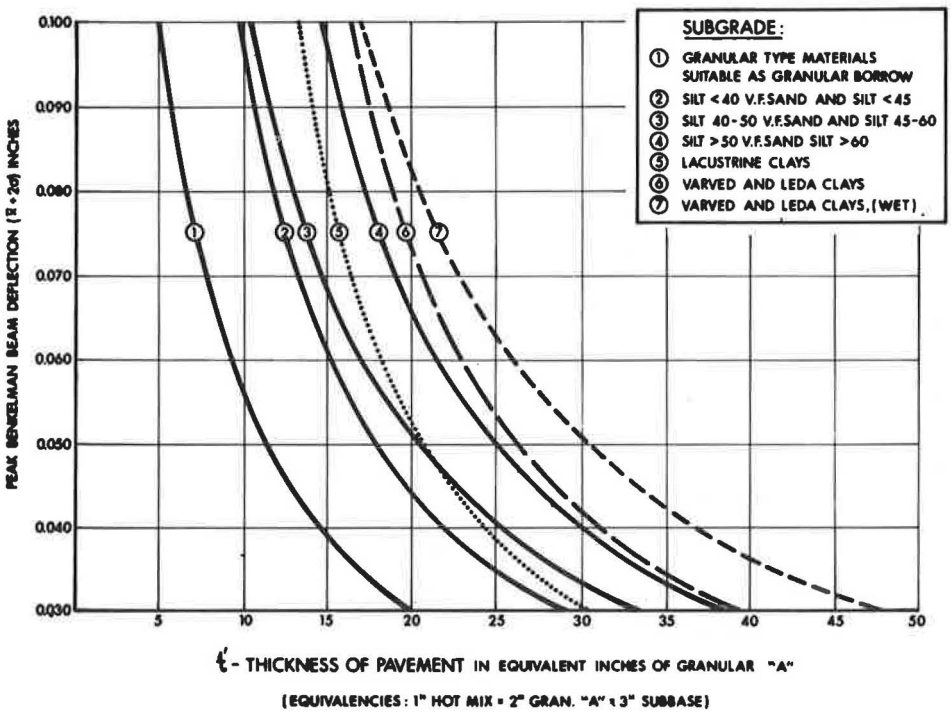

Figure 16. Estimating life of pavement overlays.

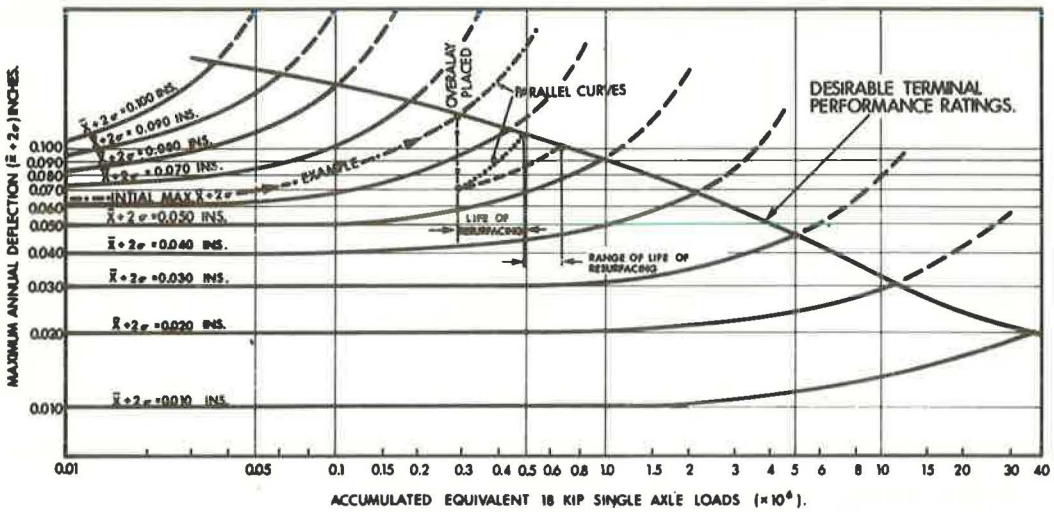

Figure 17. Graphic method of comparing costs of alternative pavement designs.

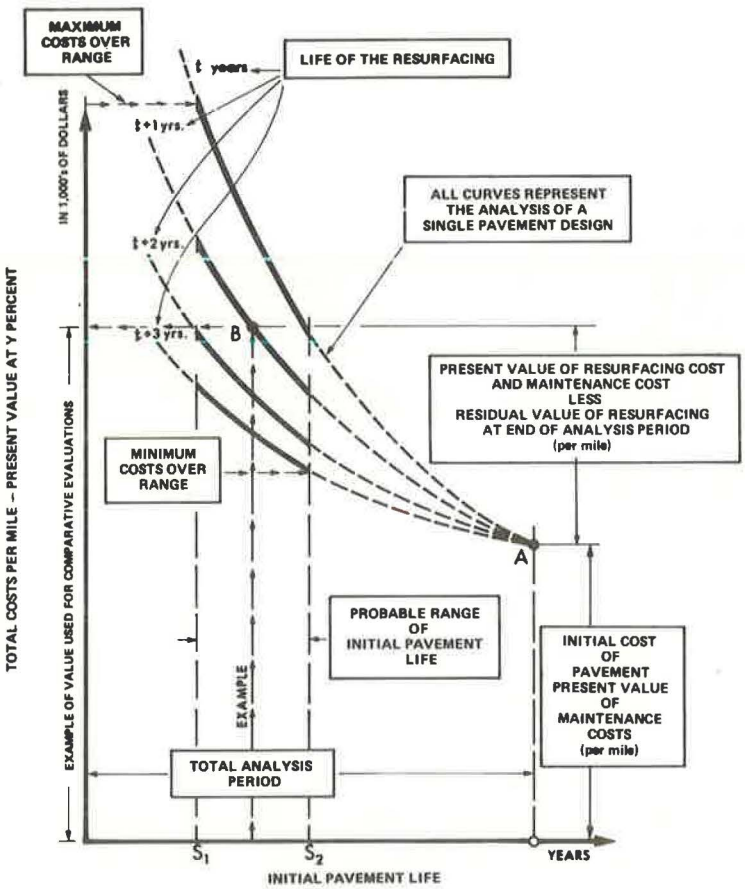

GRAPHIC EXPOSITION

Figure 19 (using the total cost formula) shows the variability of total cost (TC) resulting from changes in initial surface life (s). (Life of subsequent surfaces is held constant.) The negative slope shown in Figure 19 indicates the cost-reducing effect of longer pavement life.

Total economic costs would also be lowered by a longer life (t) from any given resurfacing. Figure 20 shows a family of curves depicting the effect on total cost of variable life expectancy for the original and subsequent surfaces.

The cost curves converge at a single point, where the original pavement provides acceptable service for the entire analysis period, and no resurfacing cost is incurred. For a more detailed exposition, see Figures 17 and 21.

Figure 17 shows a family of curves within the range of initial life of S_1 and S_2 years; each of the individual curves represents the total cost when the life of the resurfacing is t years, (t + 1) years, (t + 2) years, etc. In the example shown, if the initial pavement life and the resurfacing life are known, it is a simple matter to select the total cost of this pavement strategy. The pavement strategies examined automatically by this method of graphic exposition are shown in Figure 21. For each pavement strategy in this three-dimensional figure, the initial service life is expressed as the time in years during which the performance rating remains above the desirable terminal performance rating. Subsequent resurfacings can also have a range of resurfacing lives. Further, subsequent resurfacings after the first, taking place when the present performance has dropped to the terminal rating, ensure that pavement serviceability during the entire analysis period never falls below the desired terminal serviceability levels. Thus, the total cost comparisons for each strategy take into account the provision at all times of a minimum riding quality or serviceability of the pavement.

PAVEMENT DECISION

So far, the economic model and the flexible pavement models have been discussed, and it has been shown how the graphic exposition combines these two models to arrive at comparative total cost figures to use as the basis for the pavement decision (Fig. 3). However, there are other factors (19) that also affect the decision, which are as follows: traffic; soils characteristics; weather; performance of similar pavements in the area; economics or cost comparisons; adjacent existing pavements; stage construction; depressed, surface, or elevated design; highway system; conservation of aggregates; stimulation of competition; construction considerations; municipal preference and recognition of local industry; traffic safety; and availability and adaptations of local materials or of local commercially produced paving mixes.

EXAMPLES

Example 1

The AADT of the pavement to be designed is now 6,000 vehicles per day, of which 12 percent is trucks and buses. The average growth rate of traffic is 4 percent. A four-lane undivided highway is determined to be suitable for this situation. Paved width is to be 48 ft with 10-ft shoulders (+2 ft rounding). If the design life is taken to be 15 years, then the AADT at that time would be about 10,800 vehicles per day. With 80 percent in the design lane, this results in 518 trucks per day. If we use a truck factor of 0.50, the DTN is 259. For a DTN of 259 on the deflection criteria chart, the design deflection for a desirable terminal performance rating is found to be 0.047 in. If the design life is taken as 20 years, the DTN would be 267 and the design deflection 0.043 in.

Soils information indicates that thickness design curve number 4 (silt > 50, very fine sand silt > 60) is the correct design curve for this highway. For the 0.043-in. deflection, an equivalent gravel thickness of 29 in. is required, whereas for the 0.047-in. deflection the equivalent gravel thickness is 26 in. The asphalt surfacing thickness in each case is taken to be a minimum of $5\frac{1}{2}$ in. For the purposes of this example, only two alternatives will be considered for each design. For the design deflection of

Figure 18. Overlay design charts (Chong and Stott, 13).

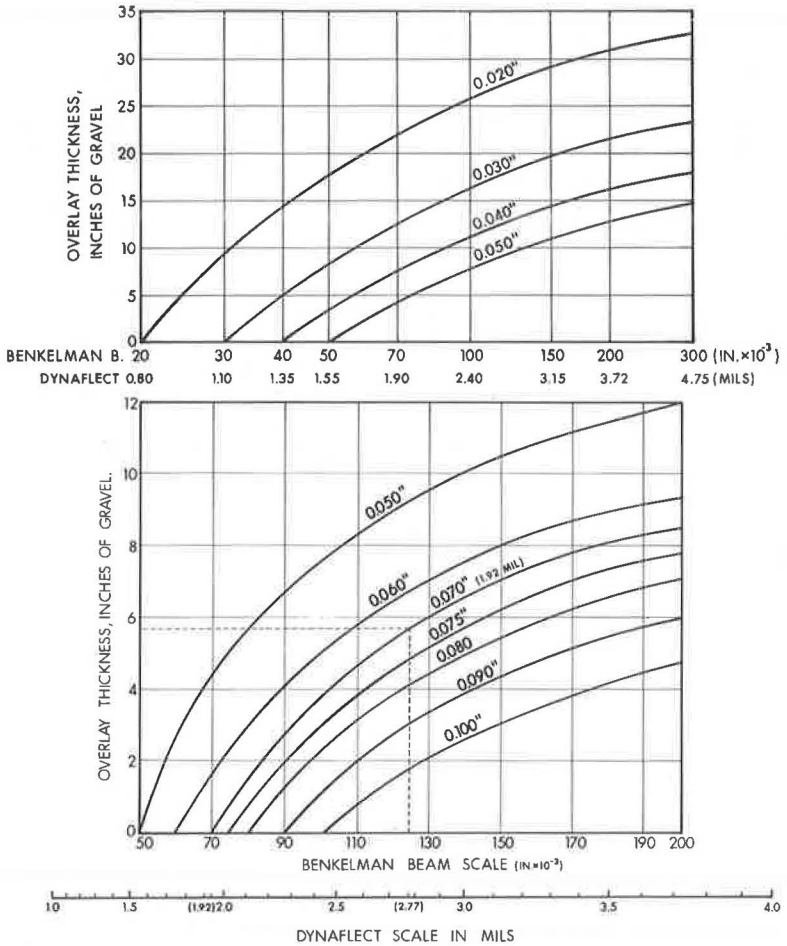

Figure 19. Initial surface life plot.

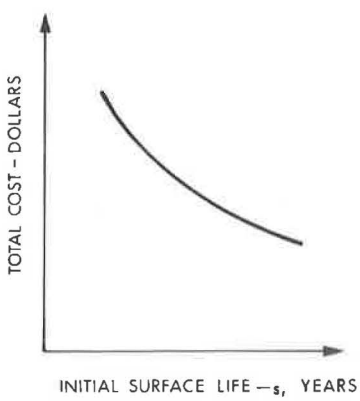

Figure 20. Initial surface life (analysis period).

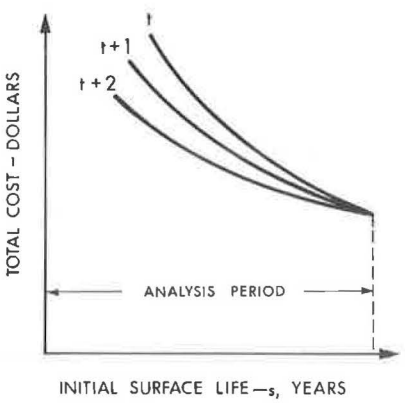

Figure 21. Pavement strategies in cost analysis.

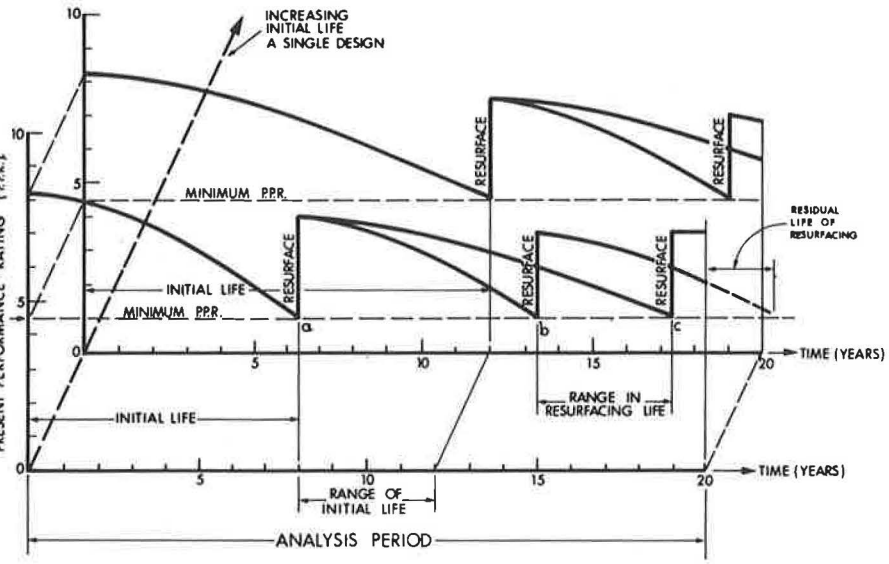

Figure 22. Data printout.

```
*********5.5AC 6B 13.5SB ******
  1    1    0     79.00      1.13      0.0       1.00     74.00     0.50      0.0       1.86      0.0    59938.54
  9    1    0     48.00    632.00      0.05     35.18      0.0      0.0       0.0       5.5C      0.C    69640.06
 13    1    0     20.00    665.00      0.0       1.86      0.0      0.0       0.0       C.0       0.C     6594.25
  8    0    1     48.00     80.00      0.07     35.18      0.0      0.0       0.0       5.55      0.C     5213.04
  9    0    1     48.00    112.00      0.05     35.18      0.0      0.0       0.0       5.5C      C.C    18552.68
 13    0    1     20.00    248.00      0.0       1.86      0.0      0.0       0.0       0.0       0.C     2703.10

OTAL CONST. COST IS $ 136172.81

OTAL RESURF.COST IS $  30866.82
NAME
I=          1,CONST=  136172.81     ,MINS=          13,MAXS=          17,CRSF=  30866.816     ,MINT=           4,MAXT=           8,LI=
         5,CC1=  300.00000     ,CC2=  900.00000     ,N=          30
END
NIT.SURFACE LIFE    13YRS.,RESURFACE LIFE     4YRS, DISCOUNTED TOTAL COST IS 185255.31
NIT.SURFACE LIFE    14YRS.,RESURFACE LIFE     4YRS, DISCOUNTED TOTAL COST IS 181288.50
NIT.SURFACE LIFE    15YRS.,RESURFACE LIFE     4YRS, DISCOUNTED TOTAL COST IS 177774.25
NIT.SURFACE LIFE    16YRS.,RESURFACE LIFE     4YRS, DISCOUNTED TOTAL COST IS 174383.00
NIT.SURFACE LIFE    17YRS.,RESURFACE LIFE     4YRS, DISCOUNTED TOTAL COST IS 171107.56
NIT.SURFACE LIFE    13YRS.,RESURFACE LIFE     5YRS, DISCOUNTED TOTAL COST IS 177724.56
NIT.SURFACE LIFE    14YRS.,RESURFACE LIFE     5YRS, DISCOUNTED TOTAL COST IS 174498.31
NIT.SURFACE LIFE    15YRS.,RESURFACE LIFE     5YRS, DISCOUNTED TOTAL COST IS 171393.81
NIT.SURFACE LIFE    16YRS.,RESURFACE LIFE     5YRS, DISCOUNTED TOTAL COST IS 168675.63
NIT.SURFACE LIFE    17YRS.,RESURFACE LIFE     5YRS, DISCOUNTED TOTAL COST IS 166083.31
NIT.SURFACE LIFE    13YRS.,RESURFACE LIFE     6YRS, DISCOUNTED TOTAL COST IS 172618.88
NIT.SURFACE LIFE    14YRS.,RESURFACE LIFE     6YRS, DISCOUNTED TOTAL COST IS 169959.75
NIT.SURFACE LIFE    15YRS.,RESURFACE LIFE     6YRS, DISCOUNTED TOTAL COST IS 167433.31
NIT.SURFACE LIFE    16YRS.,RESURFACE LIFE     6YRS, DISCOUNTED TOTAL COST IS 164999.19
NIT.SURFACE LIFE    17YRS.,RESURFACE LIFE     6YRS, DISCOUNTED TOTAL COST IS 162652.06
NIT.SURFACE LIFE    13YRS.,RESURFACE LIFE     7YRS, DISCOUNTED TOTAL COST IS 169138.25
NIT.SURFACE LIFE    14YRS.,RESURFACE LIFE     7YRS, DISCOUNTED TOTAL COST IS 166713.88
NIT.SURFACE LIFE    15YRS.,RESURFACE LIFE     7YRS, DISCOUNTED TOTAL COST IS 164383.19
NIT.SURFACE LIFE    16YRS.,RESURFACE LIFE     7YRS, DISCOUNTED TOTAL COST IS 162141.00
NIT.SURFACE LIFE    17YRS.,RESURFACE LIFE     7YRS, DISCOUNTED TOTAL COST IS 160253.69
NIT.SURFACE LIFE    13YRS.,RESURFACE LIFE     8YRS, DISCOUNTED TOTAL COST IS 166345.94
NIT.SURFACE LIFE    14YRS.,RESURFACE LIFE     8YRS, DISCOUNTED TOTAL COST IS 164083.25
NIT.SURFACE LIFE    15YRS.,RESURFACE LIFE     8YRS, DISCOUNTED TOTAL COST IS 162141.94
NIT.SURFACE LIFE    16YRS.,RESURFACE LIFE     8YRS, DISCOUNTED TOTAL COST IS 160350.25
NIT.SURFACE LIFE    17YRS.,RESURFACE LIFE     8YRS, DISCOUNTED TOTAL COST IS 158584.13
```

0.043 in., the first alternative is 5½ in. of asphalt surfacing, 6 in. of granular base, and 18 in. of subbase; the second alternative is 10 in. of asphalt surfacing and 13½ in. of subbase. For the design deflection of 0.047 in. the first alternative is 5½ in. of asphalt surfacing, 6 in. of granular base, and 13½ in. of subbase; the second alternative is 10 in. of asphalt surfacing and 9 in. of subbase.

The initial surface-life ranges assumed would be ±2 years of the design lives, i.e., 13 to 17 years for the 0.047-in. deflection design and 18 to 22 years for the 0.043-in. deflection design. A discount rate of 6 percent is to be used with an analysis period of 30 years.

Resurfacings are expected to consist of ¾ in. of SAB, plus a 1½-in. lift of HL-4. These surfacings will reduce the increased pavement deflections at their terminal serviceabilities from about 0.084 in. to about 0.055 in. for the 15-year design and from about 0.075 in. to about 0.050 in. for the 20-year design. The range in life of the resurfacings is worked out from the additional accumulated loads before terminal serviceability is again reached, making allowance for the 4 percent annual traffic increase. For the 15-year design, the resurfacing life range is 4 to 8 years, whereas for the 20-year design the resurfacing life range is 6 to 9 years.

The maintenance costs of the two designs are not expected to differ substantially, and a value of $300 per mile for the first 5 years, increasing to $500 per mile thereafter, appears to be a reasonable assumption.

Unit prices to be used should vary with the quantities and other factors but, for the purposes of this analysis, will be kept the same for each of the alternatives. The price for asphalt concrete is assumed to be $5.90 per ton, $5.55 per ton for sand asphalt, $1.86 per ton for granular base and shouldering material, $1.00 per ton for subbase materials, and $35.18 per ton for asphalt cement.

All of the information needed to fill in the computer input forms has now been assembled and can be entered in the appropriate spaces in the forms. A users' manual has been prepared to explain how to enter the data on the forms. The data are then run through the computer, and the output is in the form of a printout of the computed total costs together with a graphic display of the computations. (See Fig. 22 for a typical computer printout.) The economic cost data are now at the stage where, together with the knowledge of funds available for construction and other factors, they can be used as the basis for the pavement decision.

In Figure 23, the conventional designs with 5½ in. of asphalt surfacings have a lower total cost than the deep strength designs. The 20-year designs have a narrower spread in range of total cost and a lower slope or sensitivity to age than the 15-year designs. Unless there is a highly abnormal or skewed age distribution for the 15-year design, the 20-year designs appear more suitable.

In the example, just sufficient data have been processed to permit understanding of the principles involved. By setting up a more extensive array of alternatives, it is possible not only to examine various pavement strategies but also to examine each design for sensitivity to cost variations by utilizing a range of unit prices.

Example 2

One of the counties in Ontario recently supplied the authors with surface cost data and pavement life estimates. Economic comparisons were made between various pavement designs displaying a range of unit costs and lives.

Because one county's experience cannot be generalized, the cost details are not presented. The computer graph is presented as an interesting application of the model (Fig. 24).

PAVEMENT MANAGEMENT SYSTEM

The pavement design model together with the economic model forms the nucleus of a pavement management decision tool. To these models must be added the overlay design model plus unit price determinations, maintenance costs, and information on the available funds and other data before the pavement decision can actually be made. To round out the decision-making process, we must periodically review the design models with

Figure 23. Costs of conventional and deep strength designs.

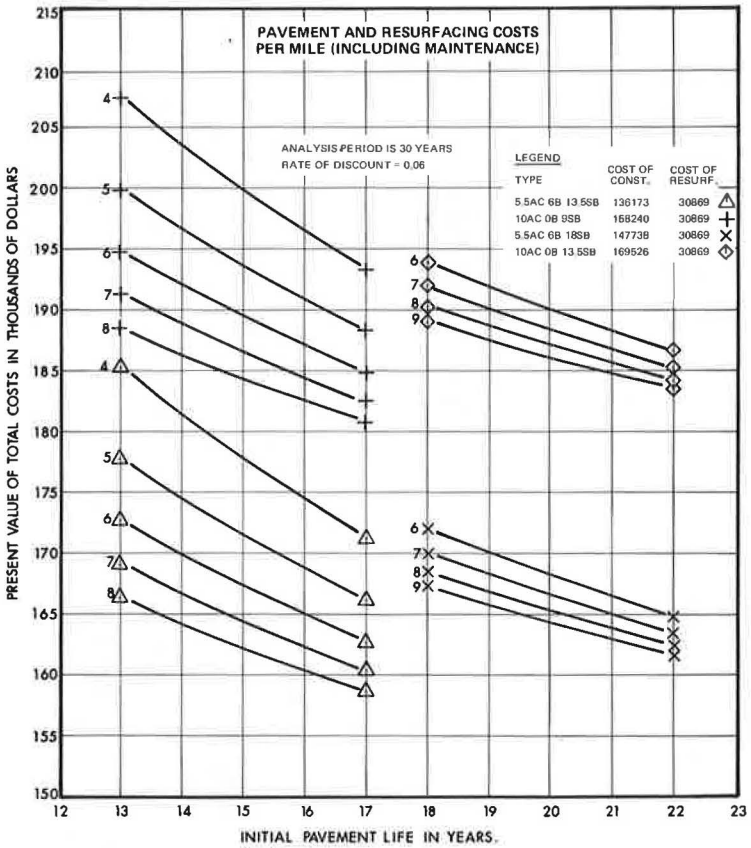

Figure 24. Total cost analysis.

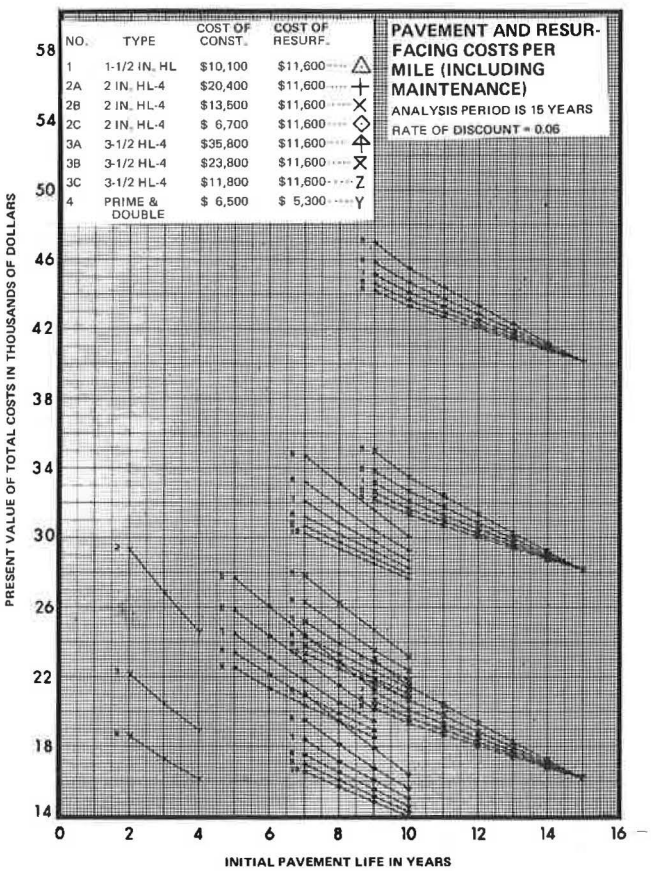

Figure 25. Pavement management system chart.

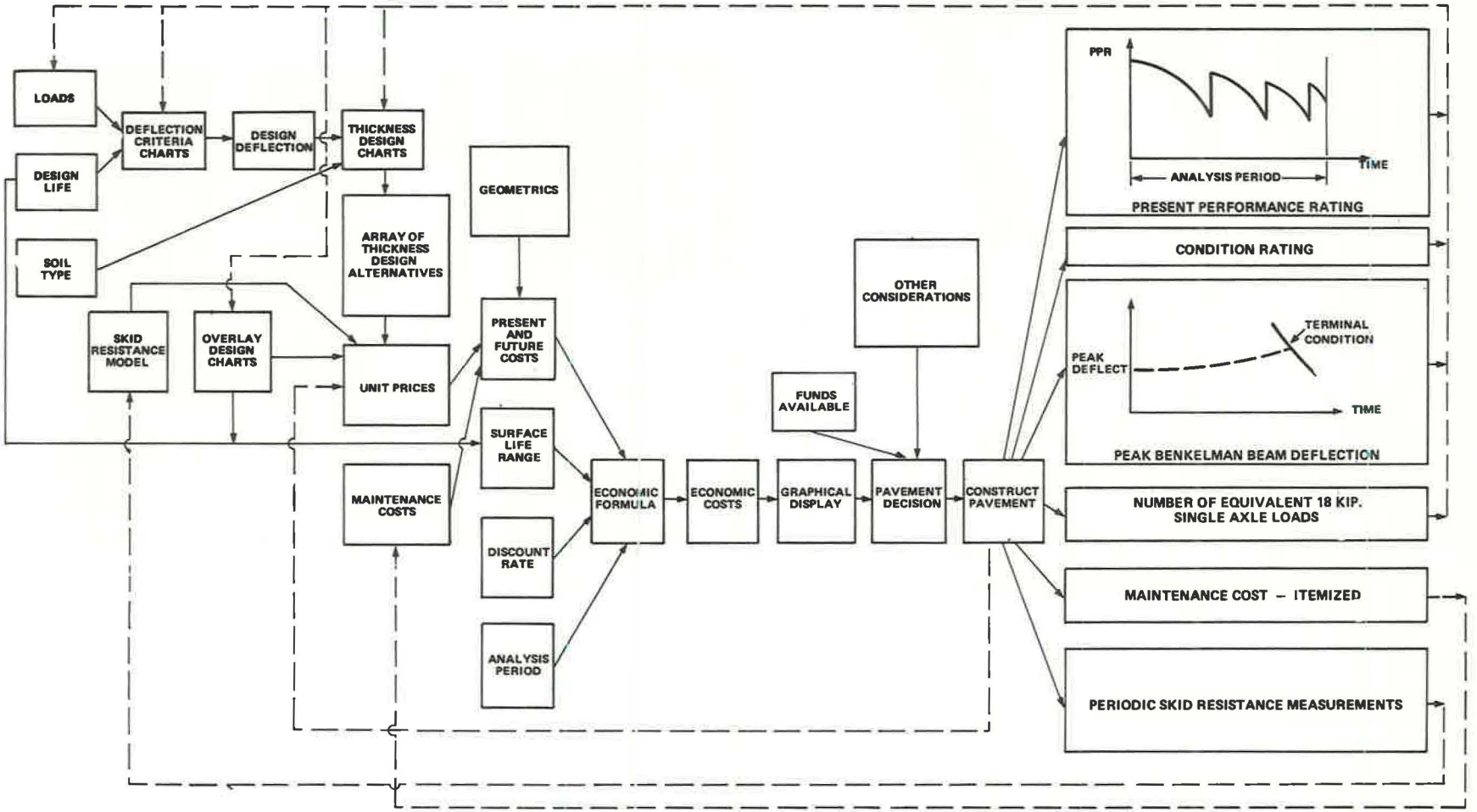

reference to their actual field performance. Therefore, constructed pavements will undergo systematic observations or monitorings of all the elements that affect the design models. This monitoring involves measurement of present performance ratings, annual spring Benkelman beam rebound and skid resistance, numbers and magnitudes of axle loads, and the costs of maintenance. The skid resistance model at this time is simply the estimated time various types of surfacings last without becoming too slippery.

Figure 25 shows how the various design models are interconnected to result in a pavement decision and the subsequent monitoring of the constructed pavement to serve as feedback to the design models. In practice, the figure will need amendment to correspond with actual information flows within the DTC. Current practice in arriving at the pavement decision is quite similar to that shown in the figure, but the feedback needed to adjust the design models has been based on subjective ratings and opinions and should now be replaced with objective measurements.

CONCLUSIONS

There are two main phases to this report. The first phase is dealt with quite extensively and is concerned with the development of investment cost data used in comparing alternative flexible pavement designs. An economic cost model that uses the present value of total costs over an analysis or service period is the basis for a technique of graphic presentation of total costs of a design over a range of initial lives and with different surfacing lives. A pavement design model together with an overlay design model provides the background by which comparable design strategies can be worked out to provide pavements that will remain above selected serviceability limits over the service or analysis period. The pavement design and overlay models utilize Benkelman beam annual maximum rebound measurements, and serviceability levels of the pavement are represented by PPR. Thickness-deflection curves for the different subgrade conditions encountered in the Province are developed from extensive field experience. Figures are presented that indicate the information flows needed to produce the investment data on which a pavement decision can be based.

The second phase of the report considers the other information flows that are needed to supplement the first phase. These consist of highway geometrics, unit prices determinations, maintenance costs, and constraints due to skid resistance, funds available, and other considerations. For a management system to be fully operative, the pavement must be monitored after it is constructed to determine whether its subsequent behavior agrees with the prescribed pavement strategy. Such monitoring is important because the information gathered can then be used to adjust the design models so that future decisions would be based on more accurate predictions. A pavement management system flow chart shows how the two phases are interconnected.

This approach to decision-making and pavement management offers a means of rationalizing policies that affect Kings' highways and Municipal and Regional highways and a framework on which effective long-term planning and programming may be based.

The system is at present only applicable to flexible pavements, but it is arranged such that rigid pavements can also be considered as soon as a suitable design model is prepared. The economic model is applicable to both flexible and rigid pavement designs.

REFERENCES

1. Wilkins, E. B. Outline of a Proposed Management System for the CGRA Pavement Design and Evaluation Committee. Proc., Canadian Good Roads Assn. Convention, 1968, pp. 363-371.
2. Hutchinson, B. G. A Design Framework for Highway Pavements. Ontario Joint Highway Research Program, Dept. of Highways Rept. RR127, 1968.
3. Hudson, W. R., McCullough, B. F., Scrivner, F. H., and Brown, J. L. A Systems Approach Applied to Pavement Design and Research. Texas Highway Dept.; Texas A&M Univ.; and Univ. of Texas at Austin, Res. Rept. 123-1.
4. Hejal, S. S., Buick, T. R., and Oppenlander, J. C. Optimal Selection of Flexible Pavement Components. Proc. ASCE, Transportation Engineering Jour., Feb. 1971.

5. Haas, R. C. G., and Hudson, W. R. The Importance of Rational and Compatible Pavement Performance Evaluation. HRB Spec. Rept. 116, 1971, pp. 92-110.
6. The Cost of Constructing and Maintaining Flexible and Concrete Pavements Over 50 Years. Road Research Laboratory, Crowthorne, RRL Rept. 256, 1969.
7. Farren, D. W., and Kip, A. A Method of Evaluating the Cost of Granular Base Courses and Pavement Types of Major Highways. Dept. of Highways, Ontario, Road Design Division Rept., June 1970 (unpublished).
8. Baldock, R. H. The Annual Cost of Highways. Highway Research Record 12, 1963, pp. 91-111.
9. A Guide to the Structural Design of Flexible and Rigid Pavements in Canada. Pavement Design and Evaluation Committee, Canadian Good Roads Assn., Ottawa, Ontario.
10. Painter, L. G. Analysis of AASHO Road Test Data by the Asphalt Institute. Proc., Internat. Conf. on Structural Design of Asphalt Pavements, Univ. of Michigan, 1962.
11. Millard, R. S., and Lister, N. W. The Assessment of Maintenance Needs for Road Pavements. Proc., Institution of Civil Engineers, Vol. 48, Feb. 1971, pp. 223-244.
12. Phang, W. A. The Effects of Seasonal Strength Variation on the Performance of Selected Base Materials. Dept. of Highways, Ontario, Rept. IR39, April 1971.
13. Chong, G. J., and Stott, G. M. A Design for Low Traffic Volume Municipal Roads. Dept. of Highways, Ontario, Rept. RR156, Feb. 1970.
14. Kingham, R. I. Development of the Asphalt Institute's Deflection Method for Designing Asphalt Concrete Overlays for Asphalt Pavements. The Asphalt Institute, Res. Rept. 69-3, 1969.
15. Phang, W. A. Four Years' Experience at the Brampton Test Road. Highway Research Record 311, 1970, pp. 68-90.
16. Chong, G. J., and Stott, G. M. Evaluation of the Dynaflect and Pavement Design Procedures. Dept. of Transportation and Communications, Ontario, Rept. IR42.
17. Kallas, B. Flexural Fatigue Tests on Asphalt Paving Mixtures. ASTM Symposium, 1971.
18. Asphalt Overlays and Pavement Rehabilitation. The Asphalt Institute, Manual Series 17, Nov. 1969, p. 51.
19. An Informational Guide on Project Procedures. AASHO, Nov. 26, 1960; revised March 1963, pp. 49-50.

SPONSORSHIP OF THIS RECORD

GROUP 2—DESIGN AND CONSTRUCTION OF TRANSPORTATION FACILITIES
John L. Beaton, California Division of Highways, chairman

PAVEMENT DESIGN SECTION
John E. Burke, Illinois Department of Transportation, chairman

Committee on Rigid Pavement Design
B. F. McCullough, University of Texas at Austin, chairman
Henry Aaron, Kenneth J. Boedecker, Jr., Philip P. Brown, John E. Burke, W. Herman Carter, Bert E. Colley, Donald K. Emery, Jr., W. J. Liddle, Phillip L. Melville, Lionel T. Murray, L. Frank Pace, R. G. Packard, Thomas J. Pasko, Jr., Frank H. Scrivner, M. D. Shelby, Don L. Spellmann, W. T. Spencer, T. C. Paul Teng, William Van Breeman

Committee on Flexible Pavement Design
Stuart Williams, Federal Highway Administration, chairman
J. A. Bishop, W. H. Campen, Robert A. Crawford, James M. Desmond, W. B. Drake, Charles R. Foster, John M. Griffith, Frank B. Hennion, John W. Hewett, William S. Housel, R. V. LeClerc, W. J. Liddle, R. E. Livingston, Alfred W. Maner, Chester McDowell, Carl L. Monismith, William M. Moore, Frank P. Nichols, Jr., Donald R. Schwartz, George B. Sherman, Eugene L. Skok, Jr., Richard Lonnie Stewart, B. A. Vallerga, Anwar E. Z. Wissa

Committee on Pavement Condition Evaluation
Karl H. Dunn, Wisconsin Department of Transportation, chairman
Frederick Roger Allen, Frederick E. Behn, W. B. Drake, Malcolm D. Graham, Leroy D. Graves, Ralph C. G. Haas, William S. Housel, W. Ronald Hudson, C. S. Hughes, III, J. W. Lyon, Jr., Alfred W. Maner, K. H. McGhee, Phillip L. Melville, Alfred B. Moe, Bayard E. Quinn, G. Y. Sebastyan, Foster A. Smiley, Lawrence L. Smith, Elson B. Spangler, W. E. Teske, Allan P. Whittemore, Eldon J. Yoder

Committee on Theory of Pavement Design
W. Ronald Hudson, University of Texas at Austin, chairman
Richard G. Ahlvin, Ernest J. Barenberg, Richard D. Barksdale, Santiago Corro Cabellero, Ralph C. G. Haas, Eugene Y. Huang, William J. Kenis, Fred Moavenzadeh, Carl L. Monismith, Thomas D. Moreland, R. G. Packard, W. H. Perloff, Dale E. Peterson, Robert L. Schiffman, G. Y. Sebastyan, James F. Shook, Roberto Sosa Garrido, Aleksandar S. Vesic, E. B. Wilkins, Loren M. Womack, Nai C. Yang

Committee on Strength and Deformation Characteristics of Pavement Sections
John A. Deacon, University of Kentucky, chairman
Richard D. Barksdale, Bert E. Colley, Hsai-Yang Fang, Frank L. Holman, W. Ronald Hudson, Melvin H. Johnson, Bernard F. Kallas, William J. Kenis, Wolfgang G. Knauss, Milan Krukar, H. Gordon Larew, Fred Moavenzadeh, Carl L. Monismith, William M. Moore, Keshavan Nair, Eugene L. Skok, Jr., Ronald L. Terrel

Lawrence F. Spaine and John W. Guinnee, Highway Research Board staff

The sponsoring committee is identified by a footnote on the first page of each report.